Development of transfer functions for partial differential equations with propulsion systems appl...
Sarantopoulos, Athanasios D
ProQuest Dissertations and Theses; 1994; ProQuest Dissertations & Theses Full Text
pg. n/a

INFORMATION TO USERS

This manuscript has been reproduced from the microfilm master. UMI films the text directly from the original or copy submitted. Thus, some thesis and dissertation copies are in typewriter face, while others may be from any type of computer printer.

The quality of this reproduction is dependent upon the quality of the copy submitted. Broken or indistinct print, colored or poor quality illustrations and photographs, print bleedthrough, substandard margins, and improper alignment can adversely affect reproduction.

In the unlikely event that the author did not send UMI a complete manuscript and there are missing pages, these will be noted. Also, if unauthorized copyright material had to be removed, a note will indicate the deletion.

Oversize materials (e.g., maps, drawings, charts) are reproduced by sectioning the original, beginning at the upper left-hand corner and continuing from left to right in equal sections with small overlaps. Each original is also photographed in one exposure and is included in reduced form at the back of the book.

Photographs included in the original manuscript have been reproduced xerographically in this copy. Higher quality 6" x 9" black and white photographic prints are available for any photographs or illustrations appearing in this copy for an additional charge. Contact UMI directly to order.

U·M·I

University Microfilms International
A Bell & Howell Information Company
300 North Zeeb Road, Ann Arbor, MI 48106-1346 USA
313/761-4700 800/521-0600

Reproduced with permission of the copyright owner. Further reproduction prohibited without permission.

Order Number 9505927

Development of transfer functions for partial differential equations with propulsion systems applications

Sarantopoulos, Athanasios D., Ph.D.

The University of Akron, 1994

Copyright ©1994 by Sarantopoulos, Athanasios D. All rights reserved.

U·M·I
300 N. Zeeb Rd.
Ann Arbor, MI 48106

Reproduced with permission of the copyright owner. Further reproduction prohibited without permission.

DEVELOPMENT OF TRANSFER FUNCTIONS FOR PARTIAL DIFFERENTIAL EQUATIONS WITH PROPULSION SYSTEMS APPLICATIONS

A Dissertation

Presented to

The Graduate Faculty of the University of Akron

In Partial Fulfillment

of the Requirements for the Degree

Doctor of Philosophy

Athanasios D. Sarantopoulos

August 1994

Reproduced with permission of the copyright owner. Further reproduction prohibited without permission.

© 1994

ATHANASIOS D. SARANTOPOULOS

ALL RIGHTS RESERVED

Reproduced with permission of the copyright owner. Further reproduction prohibited without permission.

DEVELOPMENT OF TRANSFER FUNCTIONS FOR PARTIAL DIFFERENTIAL EQUATIONS WITH PROPULSION SYSTEMS APPLICATIONS

Athanasios D. Sarantopoulos

Dissertation

Approved:

Tom T. Hartley
Advisor

Celal Batur
Committee Member

Glenn K. Hartman
Committee Member

Committee Member

S. I. Hariharan.
Committee Member

Accepted:

Department Head

Dean of the College

Dean of the Graduate School

03 August 1994
Date

Reproduced with permission of the copyright owner. Further reproduction prohibited without permission.

ABSTRACT

This dissertation is concerned with finding spatially-distributed models for internal flow propulsion systems and is part of ongoing research being conducted at the Electrical Engineering Department of the University of Akron under the support of the Advanced Control Technology Branch of NASA Lewis Research Center. The derived models retain important structural properties of internal flow systems and are very useful for control system studies.

The central objective of this dissertation is to develop exact transfer function solutions for linearized systems of hyperbolic partial differential equations that describe a variety of practical "air-in-a-pipe" problems. Mathematical models of several internal flow system configurations are developed in the complex frequency-space domain.

The describing partial differential equations for linearized inviscid compressible flow are solved exactly using Laplace transform theory. In the past, approximate solutions were tried by replacing time delay terms with Padé functions. A novel technique for analyzing multiple-channel flows with internal inputs is presented, based on the Green's function of the non-static flow problem. Finally, an exact closed-form solution for flows in channels with exponentially varying cross-sectional areas is developed.

Reproduced with permission of the copyright owner. Further reproduction prohibited without permission.

A plethora of transfer function models for some typical internal flow propulsion systems is generated. Frequency responses computed for the NASA Lewis Mach 2.5 inlet models developed using the new approach are in excellent agreement with previously published data. The derived models offer essential intuition and quick insight about a flow system. They are expandable and reconfigurable for different upstream or downstream inflow or outflow boundary conditions and are very important for control system analysis and design.

Reproduced with permission of the copyright owner. Further reproduction prohibited without permission.

"Αἰέν ἀριστεύειν καί ὑπείροχον ἔμμεναι ἄλλων"

ΟΜΗΡΟΣ

"Always be best and preeminent"

HOMER

Reproduced with permission of the copyright owner. Further reproduction prohibited without permission.

ACKNOWLEDGEMENTS

I dedicate this dissertation to my parents Georgia and Dimitrios Sarantopoulos, and my sisters Anastasia, Eleni, and Daria, whose unconditional love, strong moral and financial support and encouragement enabled me to complete my doctoral studies at the University of Akron.

I would like to express my most sincere thanks to all the faculty members who have helped in completing this project. I would especially like to thank Dr. Tom T. Hartley, the head of my Student Advisory Committee. His excellent guidance, patience, continuing support and encouragement along with his deep knowledge, strong intuition, clear sense of direction, great organizational and teaching skills and nice personality enabled me to complete this dissertation that at times seemed it had no end. I would also like to thank him for his suggestions concerning the actual writing of the document.

Sincere thanks to Dr. Max Willis for reviewing this dissertation. Dr. Celal Batur, Dr. Jose Alexis De Abreu-Garcia, Dr. Subramaniya Hariharan, and Dr. Glenn Heitman, all members of my Doctoral Commitee, are acknowledged for their very useful feedback during the defense. In particular, Dr. Hariharan is thanked for his useful comments regarding many of the practical issues of the problem.

Reproduced with permission of the copyright owner. Further reproduction prohibited without permission.

The Electrical Engineering Department, the School of Engineering, the Graduate School, and NASA Lewis Research Center, Advanced Control Technology Branch are acknowledged for their general financial support that I have received during my entire course of study.

Many other individuals and organizations have supported me morally and financially over the years and I would like to acknowledge them: Costas and Soula Collias, Dr. Athanasios and Eleni Kasamias, Dr. Costas and Pauline Sarantopoulos and family, Dr. De Abreu, Dr. Hartley, The Hellenic Club, The AHEPA Educational Foundation of Washington, DC, The Anthony D. Retikas Memorial Fund of Akron, The Nick Cost Scholarship Fund, The George Leber Scholarship Fund, The Hellenic University Club of Northeastern Ohio Scholarship Fund, Mr. Walter Fluharty and the Norton Chemical Process Products Corporation, Dr. Lambros Katafygiotis, Dr. John Kamvouris, Dr. Gus Mavrigian, Mr. Nikos Diamantides, Dr. Stavros Constantinou, Dr. John Demos and family, the Annunciation Greek Orthodox Church of Akron, and the Goodfriendship # 63 and Lincoln # 89 Chapters of the Order of AHEPA.

Special thanks are also due to all my friends--too many to be mentioned here--for their support and encouragement during my stay in this very hospitable country.

Reproduced with permission of the copyright owner. Further reproduction prohibited without permission.

TABLE OF CONTENTS

PAGE

LIST OF TABLES xiii

LIST OF FIGURES xiv

CHAPTER

I. INTRODUCTION 1

II. PROBLEM DEFINITION 5

2.1 Introduction 5

2.2 The Equations of Motion 9

2.3 Quasi-Linear Formulation of Euler Equations 15

2.4 Quasi-One Dimensional Flow 20

2.5 Boundary Conditions 22

2.6 Concluding Remarks 34

III. A REVIEW OF INLET MODELING TECHNIQUES 35

3.1 Introduction 35

Reproduced with permission of the copyright owner. Further reproduction prohibited without permission.

3.2 A Classification of Modeling of High Speed Propulsion Systems 36

3.3 Low Order Linear Models 36

3.3.1 Model Reduction Methods 37

3.3.2 Model Reduction of Models Obtained Using the Split Flux Approach 39

3.3.3 LOL Inlet Models Obtained Using the Physical Lumping Technique 40

3.3.4 LOL Inlet Models Obtained Using Input/Output Identification 41

3.3.5 Reduction of Meromorphic Transfer Functions 43

3.3.6 The Cole-Willoh Approach 45

3.3.7 Equivalent Circuit Modeling 47

3.3.8 Hydraulic Analogies 49

3.3.9 A Schwarz-Christoffel Transformation Technique 49

3.3.10 Supersonic Inlet/Engine Combinations 50

3.3.11 Bond Graphs 51

3.3.12 The Barry Model 54

3.4 High Order Linear Models 56

3.5 High Order Nonlinear Inlet Models 58

Reproduced with permission of the copyright owner. Further reproduction prohibited without permission.

3.6 Low Order Nonlinear Inlet Models 60

3.7 Concluding Remarks..... 62

IV. NEW APPROACHES TO MODELING FLOW PROBLEMS..... 64

4.1 Introduction..... 64

4.2 The Free-Space Problem..... 71

4.3 The Bounded Problem 88

4.4 The Two-Channel Free-Space Problem..... 100

4.5 The N-Channel Free-Space Problem..... 102

4.6 The Two-Channel Bounded Problem..... 107

4.7 The N-Channel Bounded Problem..... 110

4.8 The Two-Channel with Internal Input Free-Space Problem..... 116

4.9 The N-Channel with Internal Inputs Free-Space Problem..... 121

4.10 The Two-Channel with Internal Input Bounded Problem..... 126

4.11 The N-Channel with Internal Inputs Bounded Problem..... 148

4.12 The Green's Function Problem..... 154

4.13 A Channel with Exponential Cross-Sectional Area..... 171

Reproduced with permission of the copyright owner. Further reproduction prohibited without permission.

4.14 Concluding Remarks 178

V. MODELING INTERNAL FLOWS 180

5.1 Introduction 180

5.2 Key Technologies for Air-Breathing Propulsion 181

5.3 Modes of Operation in Compressible Flow 184

5.4 Input and Outputs 187

5.5 An Illustrative Example 198

5.6 Simulations 206

5.7 Qualitative Guidelines for Choosing Model Parameters 215

5.8 Concluding Remarks 216

VI. SUMMARY AND FUTURE WORK 218

6.1 Summary 218

6.2 Directions for future Research 221

REFERENCES 224

APPENDICES 233

A. GLOSSARY OF TERMS 234

Reproduced with permission of the copyright owner. Further reproduction prohibited without permission.

B. NASA LEWIS MACH 2.5 40-60 INLET DATA 243

C. PROGRAM LISTINGS 247

D. FREQUENCY RESPONSES 292

Reproduced with permission of the copyright owner. Further reproduction prohibited without permission.

LIST OF TABLES

TABLE		PAGE
3.1	Equivalence between bond graph variables and flow variables	52
4.1	Outline of research	70
4.2	Characteristics of a three-wave bounded system	97
4.3	Notation list for 2- & 3-wave systems	161
5.1	Modes of operation in a three-wave system	185

Reproduced with permission of the copyright owner. Further reproduction prohibited without permission.

LIST OF FIGURES

FIGURE		PAGE
2.1	A converging-diverging channel	5
2.2	A mixed-compression inlet	6
2.3	A typical stream tube	20
2.4	A series junction	31
2.5	A branching system	33
3.1	A second-order bond graph of a long fluid line	53
4.1	A stream tube	66
4.2	The free-space problem	71
4.3	The bounded problem	88
4.4	A supersonic inlet model	89
4.5	A two-wave bounded inlet system	90
4.6	Boundary conditions for the three-wave problem	96

Reproduced with permission of the copyright owner. Further reproduction prohibited without permission.

4.7 The two-channel problem 100

4.8 The N-channel problem 103

4.9 An alternative way of computing the system transfer function in combinational flows 106

4.10 The two-channel bounded problem 107

4.11 The N-channel bounded problem 111

4.12 A block diagram of a N-channel bounded inlet system 113

4.13 A two-channel system with an internal input 117

4.14 Block diagram describing the flow in Channel 2 of a two-channel with internal input flow system 119

4.15 The N-channel with internal inputs free-space problem 121

4.16 The two-channel with internal input bounded problem 126

4.17 Boundary conditions for the two-channel with internal input bounded problem (2-wave) 127

4.18 Boundary conditions for the three-wave problem 145

4.19 The N-channel with internal inputs bounded problem 149

4.20 The Green's function problem 154

4.21 Boundary conditions for the two-wave problem 159

4.22 Boundary conditions for the three-wave problem 162

4.23 A channel with exponentially varying cross-sectional area ... 172

Reproduced with permission of the copyright owner. Further reproduction prohibited without permission.

5.1 How to describe the speed 181

5.2 Cross section of a typical inlet 182

5.3 Cross section of a ramjet 183

5.4 Cross section of a simplified supersonic combustion ramjet..... 183

5.5 Exit boundary with a pressure input 190

5.6 An inlet system 198

5.7 Normalized magnitude response of shock position due to downstream pressure perturbations (NASP Report)..... 209

5.8 Normalized phase response of shock position due to downstream pressure perturbations (NASP Report)..... 209

5.9 Normalized magnitude response of of X_s (CASE A)..... 211

5.10 Normalized phase response of of X_s (CASE A)..... 211

5.11 Normalized magnitude response of shock position due to downstream pressure perturbations (Cases C and D)..... 212

5.12 Normalized phase response of shock position due to downstream pressure perturbations (Cases C and D)..... 213

5.13 Normalized magnitude response of X_s (Case E) 214

5.14 Normalized phase response of of X_s (Case E) 214

Reproduced with permission of the copyright owner. Further reproduction prohibited without permission.

CHAPTER I

INTRODUCTION

Technological advances in the area of computers have received a lot of attention from engineers, applied mathematicians, and scientists over the recent years. Thus, an increasing number of people use the digital computer to simulate the behavior of simple as well as complex dynamical systems in order to save time and obtain more accurate results for their problems. There is no doubt that the power and user-friendliness of this amazing machine, called personal computer, has helped us solve many difficult problems that were impractical to solve in the past. The influence of the computer is so strong that in many engineering problems, the traditional methods that were used in the past, and which were based on advanced mathematics, have been threatened to become extinct as they are now replaced by iterative computer-based techniques. An example of this trend is found in the area of fluid dynamics, in which powerful computational fluid dynamic (CFD) techniques have put aside transform techniques characteristically used in the past. In many internal flow applications accurate numbers may be a desirable and practical form of a problem's solution. However, a mere examination of a set of numbers, such as those obtained from a CFD-based algorithm, cannot give the engineer the information that a closed-form solution, obtained using

Reproduced with permission of the copyright owner. Further reproduction prohibited without permission.

advanced mathematical techniques, can provide. Thus, essential intuition about a problem could be lost. This is particularly true in the control system area where structural properties of a system are more important than specific responses.

In internal propulsion systems as well as in other systems, it is important that fast and accurate mathematical models of all the components of the system under study be available. Thus, a good system model is a powerful tool that a control engineer can use in order to assess the control needs of a given system and develop an effective control strategy which corrects any unwanted behavior of the integrated system with a minimum of control effort.

In this study, the area of internal propulsion systems will be revisited and several "air-in-a-pipe" modeling problems will be posed. The main objective is to develop transfer functions for linearized systems of hyperbolic partial differential equations that describe a variety of practical "air-in-a-pipe" problems. Thus, accurate mathematical models of some general internal propulsion systems, useful for control systems studies, will be developed.

Some of the contributions of this research will be developing exact solutions of the free-space flow problem, solving the Green's function problem for non-static flows, providing solution to the two-wave flow problem in a channel with exponentially varying cross-sectional area, and extending the Cole-Willoh approach. Also, solving additional theoretical

Reproduced with permission of the copyright owner. Further reproduction prohibited without permission.

and practical problems arising from modeling of supersonic inlets, ramjets, and scramjets.

An outline of this dissertation is as follows. After the brief introduction given above, next, in Chapter 2, the inlet modeling problem is introduced. First, the geometry of a typical internal flow system is given and the governing equations of fluid flow are presented in several forms. Finally, some typical boundary conditions are discussed.

In Chapter 3, all relevant previous work in propulsion system modeling is presented. Existing inlet modeling methods are classified into various categories, according to the system order of the resulting model, high or low, and the type of the resulting model, linear or nonlinear. Models in each category are then studied and various features of each modeling technique are pointed out.

Following this, is Chapter 4 which is the main chapter of this dissertation. It contains several sections describing the analytical solutions of many important practical and theoretical original problems of varying degrees of complexity. Special emphasis is given to problems arising from supersonic inlet applications. The first four sections of Chapter 4 are extremely important as they form the basis of this research. The latter sections of Chapter 4 contain solutions to problems which can arise from combinations and/or generalizations of the basic problems studied in the former sections of the chapter.

Reproduced with permission of the copyright owner. Further reproduction prohibited without permission.

Chapter 5, on the other hand, provides the reader with some supplementary pieces of information that would be needed to apply the theory developed in Chapter 4 to any practical flow scenario. In particular, the techniques developed in Chapter 4 are applied to a specific inlet system which consists of a supersonic/subsonic channel combination and incorporates the Cole-Willoh shock conditions in its interior boundary. Resulting models are then validated using available data for the NASA Lewis Mach 2.5 40-60 inlet.

Finally, in Chapter 6 a brief summary of the dissertation is given and conclusions are drawn. Also, some suggestions for further work are presented.

A complete bibliographical list on the inlet modeling problem is presented after the main body of this dissertation. For a more thorough knowledge of the subject under study, it is strongly suggested that the interested reader consult as many of the references found in the bibliography section as possible.

Lastly, this study concludes with four appendices. The first one contains a glossary of terms and is intended to assist the reader in understanding the most common terminology used in the area of gas dynamics. The second appendix contains actual data for the NASA Lewis Mach 2.5 40-60 inlet. The third appendix contains all software code used to implement the models of Chapters 4 and 5. Finally, the last appendix contains frequency responses corresponding to key problems of Chapters 4 and 5.

Reproduced with permission of the copyright owner. Further reproduction prohibited without permission.

CHAPTER II

PROBLEM DEFINITION

2.1 Introduction

One of the essential components of an internal propulsion system is a supersonic inlet. An inlet is basically a diffuser that consists of a converging and a diverging section as Figure 2.1 illustrates. The minimum-area portion of the inlet is called the throat of the inlet.

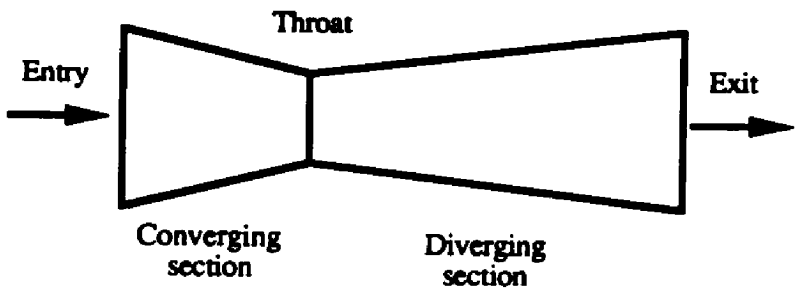


Figure 2.1 A converging-diverging channel

The main function of the inlet is to decelerate the incoming supersonic air stream to velocities suitable for the engine, which is attached to the exit portion of the inlet through a relatively long pipe called a duct. Typically the flow in the duct is subsonic, hence the term subsonic duct. A

Reproduced with permission of the copyright owner. Further reproduction prohibited without permission.

cross section of an idealized mixed compression inlet is shown on Figure 2.2. Furthermore, the inlet converts part of the free stream kinetic energy to internal energy and flow energy. An inlet achieves its objective by varying the flow area. In doing so, an internal discontinuity in the flow, termed a normal shock, is formed.

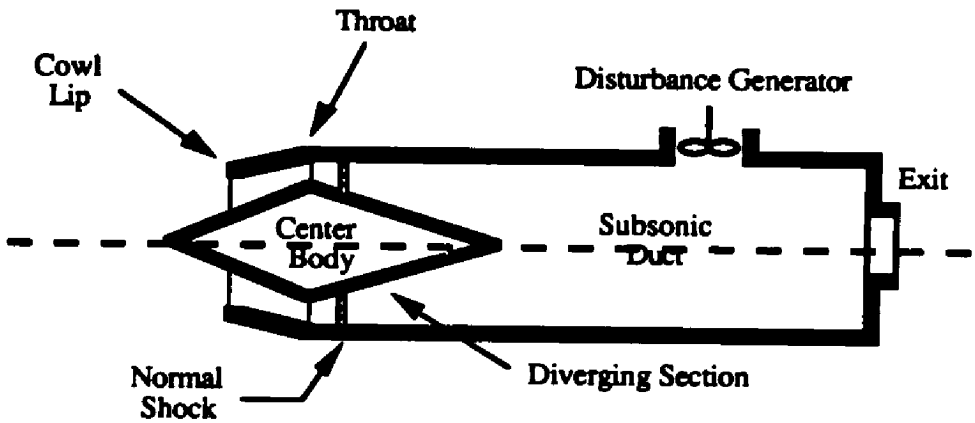


Figure 2.2 A mixed-compression inlet

Across a normal shock there is a fall in the flow velocity and a rise in static pressure. As the flow goes through the diverging section of the inlet, it continues to slow down while the static pressure as well as the temperature continue to increase.

For maximum overall inlet efficiency it is desirable that the normal shock be positioned as close to the throat of the inlet as possible [LZ72]. In this case, the engine weight flow and thrust are at their maximum. However, as the inlet moves through its different points of operation,

Reproduced with permission of the copyright owner. Further reproduction prohibited without permission.

inevitably, the shock position will change. Flow field perturbations such as those caused by atmospheric turbulence may cause drastic changes in the engine operation and produce very undesirable effects such as engine unstart and buzz [BAR73]. During an unstart a shock wave sweeps out of the throat and a strong shock wave forms ahead of the inlet. Therefore, for a stable and efficient system operation, it is imperative that all undesirable effects be avoided by proper control of the normal shock position.

One way of controlling the shock position is by using a bypass door located alongside the duct. The controller must command the actuator to open the bypass door when an upstream movement of the normal shock is detected and close it when the shock starts moving downstream [COL77]. By opening the bypass door, the excessive air may exit the duct thus causing a decrease in pressure. Alternatively, a small disturbance generator, similar to that shown on Figure 2.2, may be used to inject air into or take air out of the duct, as the control algorithm requires, in order to stabilize the shock position. In either of these cases, the controller must estimate the normal shock position from pressure measurements at various points in the inlet, produce an appropriate error signal, and command the actuators to act so as to drive the error signal to zero.

It must be noted at this point that it is more difficult to control the shock position in a variable geometry inlet. This type of inlet can operate over a wider range of disturbances than a conventional fixed-geometry

Reproduced with permission of the copyright owner. Further reproduction prohibited without permission.

inlet. In a typical flight scenario, the controller commands the actuator to move the translating centerbody forward or backward. Usually, a forward movement of the translating centerbody will cause the throat area of the inlet to increase and vice versa. A translation of the centerbody can also change the normal shock position and potentially cause catastrophic results for the entire system. Thus, the geometry of the inlet is not allowed to change in an arbitrary fashion. Instead, changes in the geometric characteristics of the inlet usually occur at prescheduled time intervals along the flight trajectory and never used to actively control the normal shock position.

Undoubtedly, in order to design an efficient control system for the inlet system, it is essential that the designer have a clear understanding of the dynamics of the system which include the shock dynamics, the gas dynamics for the duct, and the inlet exit conditions.

In the following sections of this chapter, the nonlinear equations governing the dynamics of a compressible flow through an inlet will be presented in some detail. Also, simpler quasi-one dimensional models will be presented. Furthermore, a classification of general second-order operators and systems of partial differential equations will be given.

Finally, this chapter will end with a discussion of shock dynamics and some realistic boundary conditions imposed on typical inlet modeling problems.

Reproduced with permission of the copyright owner. Further reproduction prohibited without permission.

2.2 The Equations of Motion

Incompressible and isentropic flow may be sufficiently represented by an equation derived from the balance of linear momentum. On the other hand, isentropic flow may be sufficiently described by the two equations derived from the law of conservation of mass and the balance of linear momentum. Finally, in compressible flow, as in the case of air-breathing propulsion systems, the addition of a third unknown is required. It is well known from thermodynamics that for a homogeneous gas, any two state properties are sufficient to determine all the rest. Therefore, a third equation derived from the conservation of energy may be used.

The addition of a third equation results in a system of inviscid conservation laws, called Euler equations. These equations in their integral form are as follows [HIR90],

Continuity equation

$$\frac{\partial}{\partial t}\iiint_{\Omega} \rho \, d\Omega + \oiint_{S} \rho \vec{v} \, d\vec{S} = 0 \qquad (2.1)$$

Momentum equation

$$\frac{\partial}{\partial t}\iiint_{\Omega} \rho \vec{v} \, d\Omega + \oiint_{S} (\rho \vec{v} \cdot \vec{v} + p) \, d\vec{S} = \iiint_{\Omega} \rho \, \vec{f}_e \, d\Omega \qquad (2.2)$$

Energy equation

$$\frac{\partial}{\partial t}\iiint_{\Omega} \rho E \, d\Omega + \oiint_{S} \rho \, H \vec{v} \, d\vec{S} = \iiint_{\Omega} \rho \, \vec{f}_e \vec{v} \, d\Omega \qquad (2.3)$$

Reproduced with permission of the copyright owner. Further reproduction prohibited without permission.

where,

ρ = density,

$\vec{v}$ = velocity vector,

p = pressure,

$\vec{f}_e$ = external forces,

E = total energy per unit mass of the moving fluid = $e + \frac{1}{2}(\vec{v},\vec{v})$,

e = internal energy per unit mass,

H = stagnation (total) enthalpy per unit mass = $E + \frac{p}{\rho}$,

$\vec{S}$ = surface vector,

Ω = volume.

All in all, Euler equations simply represent the conservation laws for a three-dimensional flow through a volume Ω, enclosed by the surface S.

In fact, the continuity equation is a mathematical formulation of the physical principle which states that mass can be neither created nor destroyed. This equation states that the net mass flow into the control volume must equal the rate of increase of mass inside the same control volume.

On the other hand, the momentum equation states that the time rate of change of momentum of a body must equal the net force (i.e., body

Reproduced with permission of the copyright owner. Further reproduction prohibited without permission.

force + surface force) exerted on it. This equation is the integral formulation of Newton's second law applied to inviscid fluid flows, namely those in which viscosity, thermal conduction and diffusion are ignored.

Finally, the energy equation states the conservation of energy principle. In other words, energy can be neither created nor destroyed, although it can change in form.

Parenthetically, the energy equation can be also put into the following form [AND82],

$$\iiint_{\Omega} \rho\,(\vec{f}_e \cdot \vec{v})\,d\Omega - \oiint_{S} \rho\,\vec{v}\,d\vec{S} = \iiint_{\Omega} \frac{\partial}{\partial t}(\rho E)\,d\Omega + \oiint_{S} \rho E\,\vec{v}\cdot d\vec{S}. \qquad (2.4)$$

Next, returning to equations (2.1)-(2.3), it should be clear that they can also be written in a *compact form* as follows,

$$\frac{\partial}{\partial t}\iiint_{\Omega} U\,d\Omega + \oiint_{S} \vec{F}\cdot d\vec{S} = \iiint_{\Omega} Q\cdot d\Omega \qquad (2.5)$$

where the vectors U, $\vec{F}$, and Q are given by,

Reproduced with permission of the copyright owner. Further reproduction prohibited without permission.

$$U=\begin{bmatrix}\rho\\ \rho\vec{v}\\ \rho E\end{bmatrix}\qquad \vec{F}=\begin{bmatrix}\rho\vec{v}\\ \rho\vec{v}\cdot\vec{v}+p\,I_3\\ \rho\vec{v}H\end{bmatrix}\qquad Q=\begin{bmatrix}0\\ \rho\vec{f}_e\\ \rho\vec{f}_e\cdot\vec{v}\end{bmatrix}. \tag{2.6}$$

Alternatively, Euler equations (2.1)-(2.3) may also be expressed using the following *divergence form*,

$$\frac{\partial\rho}{\partial t}+\vec{\nabla}\cdot(\rho\vec{v})=0 \tag{2.7}$$

$$\frac{\partial(\rho\vec{v})}{\partial t}+\vec{\nabla}\cdot(\rho\vec{v}\cdot\vec{v}+p\,I_3)=\rho\vec{f}_e \tag{2.8}$$

$$\frac{\partial(\rho E)}{\partial t}+\vec{\nabla}\cdot(\rho\vec{v}H)=\rho\vec{f}_e\cdot\vec{v}. \tag{2.9}$$

Moreover, further use of vector notation allows equations (2.7)-(2.9) to be condensed as follows,

$$\frac{\partial U}{\partial t}+\vec{\nabla}\cdot\vec{F}=Q \tag{2.10}$$

where, in Cartesian coordinates the conservation variable U, the source vector Q, and the flux vector-tensor $\vec{F}$ can be written explicitly as follows,

$$U=\begin{bmatrix}\rho\\ \rho u\\ \rho v\\ \rho w\\ \rho E\end{bmatrix}\qquad Q=\begin{bmatrix}0\\ f_{ex}\\ f_{ey}\\ f_{ez}\\ w_f\end{bmatrix}\qquad \vec{F}=f\,\vec{i}+g\,\vec{j}+h\,\vec{k} \tag{2.11}$$

where,

$$\vec{v}=u\,\vec{i}+v\,\vec{j}+w\,\vec{k} \tag{2.12}$$

Reproduced with permission of the copyright owner. Further reproduction prohibited without permission.

$$\vec{f_e} = f_{ex}\,\vec{i} + f_{ey}\,\vec{j} + f_{ez}\,\vec{k} \qquad (2.13)$$

and,

$$f = \begin{bmatrix} \rho u \\ \rho u^2 + p \\ \rho u v \\ \rho u w \\ \rho u H \end{bmatrix} \quad g = \begin{bmatrix} \rho v \\ \rho u v \\ \rho v^2 + p \\ \rho v w \\ \rho v H \end{bmatrix} \quad h = \begin{bmatrix} \rho w \\ \rho u w \\ \rho v w \\ \rho w^2 + p \\ \rho w H \end{bmatrix}. \qquad (2.14)$$

Therefore, the condensed equation (2.10) can be put into the following *Cartesian form*,

$$\frac{\partial U}{\partial t} + \frac{\partial f}{\partial x} + \frac{\partial g}{\partial y} + \frac{\partial h}{\partial z} = Q \qquad (2.15)$$

where, (2.15) is written explicitly as follows,

$$\frac{\partial}{\partial t}\begin{bmatrix} \rho \\ \rho u \\ \rho v \\ \rho w \\ \rho E \end{bmatrix} + \frac{\partial}{\partial x}\begin{bmatrix} \rho u \\ \rho u^2 + p \\ \rho u v \\ \rho u w \\ \rho u H \end{bmatrix} + \frac{\partial}{\partial y}\begin{bmatrix} \rho v \\ \rho v u \\ \rho v^2 + p \\ \rho v w \\ \rho v H \end{bmatrix} + \frac{\partial}{\partial z}\begin{bmatrix} \rho w \\ \rho w u \\ \rho w v \\ \rho w^2 + p \\ \rho w H \end{bmatrix} = \begin{bmatrix} 0 \\ f_{ex} \\ f_{ey} \\ f_{ez} \\ W_f \end{bmatrix}. \qquad (2.16)$$

At this point it should be pointed out that in (2.16) there are five equations and seven unknowns: ρ, u, v, w, E, p, and H. Thus, in order to specify the unknown quantities uniquely some additional equations are needed. An additional constraining equation can be found if one recalls that H is related to E, p, and ρ, in the following manner

$$H = E + \frac{p}{\rho} \qquad (2.17)$$

Reproduced with permission of the copyright owner. Further reproduction prohibited without permission.

where, the total energy per unit mass E is given by the sum of the specific internal energy and the specific kinetic energy in all three space dimensions:

$$E = e + \frac{1}{2}(u^2+v^2+w^2). \qquad (2.18)$$

Hence, augmenting the system of (2.16) with equations (2.17) and (2.18) increases the number of equations to seven. However, an eighth unknown, e is also introduced and now an additional eighth equation is required. This constraint usually comes from the equation of state which in its general form is as follows,

$$p = p(\rho,E).$$

However, for a perfect gas the above equation becomes

$$p = (\gamma - 1)\left[E - \frac{1}{2}\rho\, u^2\right] \qquad (2.19)$$

where, γ is the specific heat ratio, given by

$$\gamma = \gamma(T) = \frac{C_p(T)}{C_v(T)} = \frac{\text{specific heat at constant pressure}}{\text{specific heat at constant volume}} \qquad (2.20)$$

and is a measure of the internal complexity of the molecules [PL91].

There is no general method of solution to equations (2.16)-(2.19) that will satisfy an arbitrary set of initial and boundary conditions. Therefore, approximate methods must be used to solve complicated problems. According to Shih-I Pai and Shijun Luo some of the most

Reproduced with permission of the copyright owner. Further reproduction prohibited without permission.

important approximate methods used to solve compressible flow problems are the following [PL91],

1. Method of small perturbations,
2. Method of characteristics,
3. Rayleigh-Janzen method,
4. Hodograph method,
5. Variational method, and
6. Computational fluid dynamics methods.

It must be made clear at this point that it is beyond the scope of this study to analyze each method given above. Nevertheless, the most popular of these techniques will be dealt with in some detail in the following chapter. On the other hand, good discussions of the rest of the methods can be found in advanced engineering mathematics textbooks.

In the following section, quasi-linear formulations of the Euler equations are presented.

2.3 Quasi-Linear Formulation of Euler Equations

The system of equation (2.15) or (2.16) of the previous section is a set of nonlinear differential equations. However, it can be put into a more useful quasi-linear form.

In general, a partial differential equation is said to be *quasi-linear* if it is true only that no products or powers of the partial derivatives of highest order are present [HIL76]. For example, the most general quasi-

Reproduced with permission of the copyright owner. Further reproduction prohibited without permission.

linear partial differential equation of first-order can be written in the form,

$$A(x,t,U(x,t))\frac{\partial U(x,t)}{\partial t} + B(x,t,U(x,t))\frac{\partial U(x,t)}{\partial x} = Q(x,t,U(x,t)) \qquad (2.21)$$

where, x, t are the independent variables and U(x,t) is the dependent variable.

To obtain the quasi-linear form of (2.15), assuming that all sources are ignored (that is, Q=0), one preceeds as follows

$$\frac{\partial U}{\partial t} + \frac{\partial f}{\partial x} + \frac{\partial g}{\partial y} + \frac{\partial h}{\partial z} = 0$$

$$\Rightarrow \frac{\partial U}{\partial t} + \frac{\partial f}{\partial U}\frac{\partial U}{\partial x} + \frac{\partial g}{\partial U}\frac{\partial U}{\partial y} + \frac{\partial h}{\partial U}\frac{\partial U}{\partial z} = 0.$$

Therefore, the homogeneous system becomes,

$$\frac{\partial U}{\partial t} + J_f\frac{\partial U}{\partial x} + J_g\frac{\partial U}{\partial y} + J_h\frac{\partial U}{\partial z} = 0 \qquad (2.22)$$

where, the Jacobian matrices J_f, J_g, and J_h are defined as follows,

$$J_f = \frac{\partial f}{\partial U}, \qquad J_g = \frac{\partial g}{\partial U}, \qquad J_h = \frac{\partial h}{\partial U}$$

and,

$$J_k = \left[\frac{\partial k}{\partial \rho}, \frac{\partial k}{\partial (\rho u)}, \frac{\partial k}{\partial (\rho v)}, \frac{\partial k}{\partial (\rho w)}, \frac{\partial k}{\partial (\rho E)}\right], \forall k \in \{f, g, h\}. \qquad (2.23)$$

Reproduced with permission of the copyright owner. Further reproduction prohibited without permission.

With the aid of the perfect gas equation of state (2.19), the Jacobian matrices J_f, J_g, and J_h are given by [HIR90],

$$J_f = \begin{bmatrix} 0 & 1 & 0 & 0 & 0 \\ -u^2+\frac{\gamma-1}{2}(\vec{v},\vec{v}) & (3-\gamma)u & -(\gamma-1)v & -(\gamma-1)w & \gamma-1 \\ -uv & v & u & 0 & 0 \\ -uw & w & 0 & u & 0 \\ -u[\gamma E-(\gamma-1)(\vec{v},\vec{v})] & \gamma E-\frac{\gamma-1}{2}((\vec{v},\vec{v})+2u^2) & -(\gamma-1)uv & -(\gamma-1)uw & \gamma u \end{bmatrix} \qquad (2.24)$$

$$J_g = \begin{bmatrix} 0 & 0 & 1 & 0 & 0 \\ -uv & v & u & 0 & 0 \\ -v^2+\frac{\gamma-1}{2}(\vec{v},\vec{v}) & -(\gamma-1)u & (3-\gamma)v & -(\gamma-1)w & \gamma-1 \\ -uw & 0 & w & v & 0 \\ -v[\gamma E-(\gamma-1)(\vec{v},\vec{v})] & -(\gamma-1)uv & \gamma E-\frac{\gamma-1}{2}((\vec{v},\vec{v})+2v^2) & -(\gamma-1)vw & \gamma v \end{bmatrix} \qquad (2.25)$$

and,

$$J_h = \begin{bmatrix} 0 & 0 & 0 & 1 & 0 \\ -uw & w & 0 & u & 0 \\ -vw & 0 & w & v & 0 \\ -w^2+\frac{\gamma-1}{2}(\vec{v},\vec{v}) & -(\gamma-1)u & -(\gamma-1)v & (3-\gamma)w & \gamma-1 \\ -w[\gamma E-(\gamma-1)(\vec{v},\vec{v})] & -(\gamma-1)uw & -(\gamma-1)vw & \gamma E-\frac{\gamma-1}{2}((\vec{v},\vec{v})+2w^2) & \gamma w \end{bmatrix}. \qquad (2.26)$$

Reproduced with permission of the copyright owner. Further reproduction prohibited without permission.

In *two-dimensional space*,

$$U=\begin{bmatrix}\rho\\ \rho u\\ \rho v\\ \rho E\end{bmatrix} \qquad f=\begin{bmatrix}\rho u\\ \rho u^2+p\\ \rho u v\\ \rho u H\end{bmatrix} \qquad g=\begin{bmatrix}\rho v\\ \rho u v\\ \rho v^2+p\\ \rho v H\end{bmatrix} \qquad h=0 \tag{2.27}$$

and equation (2.22) then becomes,

$$\frac{\partial U}{\partial t}+J_f\frac{\partial U}{\partial x}+J_g\frac{\partial U}{\partial y}=0 \tag{2.28}$$

where the two nonzero Jacobians J_f and J_g are as follows

$$J_f=\begin{bmatrix}0 & 1 & 0 & 0\\ -u^2+\frac{\gamma-1}{2}(\vec{v},\vec{v}) & (3-\gamma)u & -(\gamma-1)v & \gamma-1\\ -uv & v & u & 0\\ -u\left[\gamma E-(\gamma-1)(\vec{v},\vec{v})\right] & \gamma E-\frac{\gamma-1}{2}((\vec{v},\vec{v})+2u^2) & -(\gamma-1)uv & \gamma u\end{bmatrix} \tag{2.29}$$

and,

$$J_g=\begin{bmatrix}0 & 0 & 1 & 0\\ -uv & v & u & 0\\ -v^2+\frac{\gamma-1}{2}(\vec{v},\vec{v}) & -(\gamma-1)u & (3-\gamma)v & \gamma-1\\ -v\left[\gamma E-(\gamma-1)(\vec{v},\vec{v})\right] & -(\gamma-1)uv & \gamma E-\frac{\gamma-1}{2}((\vec{v},\vec{v})+2v^2) & \gamma v\end{bmatrix}. \tag{2.30}$$

Finally, in the *one-dimensional case*,

$$U=\begin{bmatrix}\rho\\ \rho u\\ \rho E\end{bmatrix} \qquad f=\begin{bmatrix}\rho u\\ \rho u^2+p\\ \rho u H\end{bmatrix} \qquad g=0 \qquad h=0 \tag{2.31}$$

and thus (2.21) becomes,

Reproduced with permission of the copyright owner. Further reproduction prohibited without permission.

$$\frac{\partial U}{\partial t} + J_f \frac{\partial U}{\partial x} = 0 \qquad (2.32)$$

where the nonzero Jacobian matrix J_f is

$$J_f = \begin{bmatrix} 0 & 1 & 0 \\ \frac{(\gamma-3)}{2}u^2 & (3-\gamma)u & \gamma-1 \\ (\gamma-1)u^3-\gamma uE & \gamma E-\frac{\gamma-1}{2}(3u^2) & \gamma u \end{bmatrix}. \qquad (2.33)$$

The eigenvalues of J_f give the speed of signal propagation and are as follows,

$$\lambda_1 = u\,, \qquad \lambda_2 = u + a, \qquad \lambda_3 = u - a \qquad (2.34)$$

where, a is the local speed of sound and u is the fluid velocity [WIL68]. The first eigenvalue, λ_1, corresponds to a wave that travels with the fluid at the fluid velocity. The second eigenvalue, λ_2, corresponds to a wave which travels downstream at a velocity equal to the sum of the fluid velocity and the local speed of sound. Lastly, λ_3 corresponds to a wave which travels upstream at a velocity equal to the speed of sound less the flow velocity.

In this section, the quasi-linear formulation of Euler equations was discussed. The following section deals with a very practical concept, that of quasi-one dimensional flow.

Reproduced with permission of the copyright owner. Further reproduction prohibited without permission.

2.4 Quasi-One Dimensional Flow

Quasi-one dimensional flow is the flow that occurs in a channel with a small rate of change of cross section or between nearly parallel streamlines.

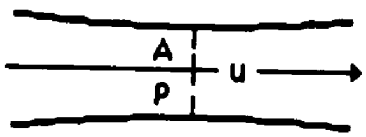


Figure 2.3 A typical stream tube

In the quasi-linear case, the velocity components normal to the mean flow direction are small compared to the components parallel to the flow direction. From reference [MVA84], the quasi-one dimensional form of Euler equations is as follows,

Continuity Equation

$$\frac{\partial(\rho A)}{\partial t} + \frac{\partial(\rho u A)}{\partial x} = M_s \qquad (2.35)$$

Conservation of Momentum Equation

$$\frac{\partial(\rho u A)}{\partial t} + \frac{\partial[A(p + \rho u^2)]}{\partial x} = p\frac{\partial A}{\partial x} + F_s \qquad (2.36)$$

Reproduced with permission of the copyright owner. Further reproduction prohibited without permission.

Conservation of Energy Equation

$$\frac{\partial(E\,A)}{\partial t} + \frac{\partial[A\,u\,(E+p)]}{\partial x} = -p\,\frac{\partial A}{\partial t} + Q_s \qquad (2.37)$$

where,

ρ = density,

$A = A(x, t)$ = channel cross section area,

u = velocity vector,

p = pressure,

$E = \rho\left(C_v T + \frac{1}{2}u^2\right)$ = stagnation (total) energy per unit mass,

M_S = mass bleed term,

F_S = friction term + mass bleed momentum term,

Q_S = heat transfer term + mass bleed energy term.

The above system of equations (2.35)-(2.37) is a nonlinear system of equations and can be linearized about some convenient operating point. Furthermore, in the same system the cross-sectional area, A, can be both a function of time t and the position x. A realistic profile for $A(x,t)$ in a snapshot of time, t_o, can be as follows. In the converging section of the converging-diverging inlet, as x increases, $A(x,t_o)$ decreases monotonically and finally attains its minimum value at the throat of the inlet. From that point on, as x increases, $A(x,t_o)$ also increases until the point where the

Reproduced with permission of the copyright owner. Further reproduction prohibited without permission.

subsonic duct begins. From that point on, since the subsonic duct section closely resembles a cylindrical pipe, the cross-sectional area of the channel remains, for all practical purposes, constant.

On the other hand, the cross-sectional area is usually time-varying only if there is a boundary layer present in the flow system which varies with time or when variable geometry inlets are used. However, it is not in the scope of this study to model the boundary layer effects. Thus, in the foregoing it will be assumed that in the worst case scenario, A is strictly a function of x.

In many practical cases the assumptions for quasi-one dimensional flow are very nearly fulfilled. Thus, in conclusion, quasi-one dimensional inlet models are useful.

2.5 Boundary Conditions

No system would be completely specified unless the proper boundary conditions are applied. Thus, for the inlet modeling problem it is of utmost importance to constrain the problem by introducing appropriate boundary conditions.

Some common boundary conditions applied to typical inlet modeling problems are the following.

Reproduced with permission of the copyright owner. Further reproduction prohibited without permission.

A. Reflective Boundary Condition

This type of boundary condition requires that the flow vector reflected back from a physical system boundary, S, be simply a scaled version of the incident flow vector. Mathematically, this notion is expressed in the frequency domain as follows

$$Q_{-}(s) = R(s)\, Q_{+}(s) + Q_{in}(s)$$

where,

$Q_{-}(s)$ = reflected flow vector at boundary S,

$Q_{+}(s)$ = incident flow vector at boundary S,

$R(s)$ = reflection coefficient,

$Q_{in}(s)$ = external input at boundary S.

In the case that the reflection coefficient R is a constant function of the Laplace Transform variable s, then the boundary condition will be called *simply reflective*. Furthermore, if an external input is also absent, then this condition implies that the flow vector is only scaled in amplitude at the boundary. An example of a reflective boundary condition for a two wave system is as follows

$$\rho_{ds} = R\, u_{ds} + f_{ds}$$

where,

ρ_{ds} = downstream flow density (reflected quantity),

Reproduced with permission of the copyright owner. Further reproduction prohibited without permission.

R = reflection coefficient,

u_{ds} = downstream flow velocity (incident quantity),

f_{ds} = external input at downstream boundary.

Finally, if a dynamic system, such as an engine, is attached to a flow channel, then the reflection parameter will typically be a transfer function, representing the engine dynamics. In this case, $Q_{in}(s)$ can be used to model any losses or mismatches occuring at the boundary, external inputs, compressor or combustor signals as well as perturbations in the free stream atmosphere.

B. Choked Flow

In many practical fluid flow scenarios it is desirable that a special type of boundary condition be applied to the problem under study. This is the case of choked flow or thermal choking. Under this constraint, the flow is restricted to have a Mach number of unity at the boundary and thus sonic flow occurs locally.

Choked flow is an exit boundary condition typically used when an inlet is to be connected to an engine. Thermal choking is usually accomplished by terminating the inlet with a choked orifice.

Finally, the equation describing choked flow at the exit of the inlet is [WIL68],

Reproduced with permission of the copyright owner. Further reproduction prohibited without permission.

$$\dot{W}_E = A_E \sqrt{\frac{\gamma}{R}} \frac{P_{T,E}}{\sqrt{\Theta_{T,E}}} \frac{M}{(1 + 0.2\,M^2)^3}$$

where,

$\dot{W}_E$ = weight flow at orifice

A_E = cross-sectional area at orifice,

γ = ratio of specific heats,

R = universal gas constant,

$P_{T,E}$ = total pressure at orifice,

$\Theta_{T,E}$ = absolute temperature at orifice,

M = Mach number = 1.0.

C. Shock Dynamics

Occasionally, flow discontinuities occur in a flow system. These anomalies in the airflow result in formation of shocks. It is usually necessary to treat a shock as a moving boundary condition. This can be the case in an upstream boundary of an inlet system where a typical upstream boundary condition can be expressed mathematically as follows

$$Q_1(s) = Z(s)\, Q_2(s) + Q_{in}(s)$$

where,

Reproduced with permission of the copyright owner. Further reproduction prohibited without permission.

$Q_1(s)$ = flow vector upstream of the shock,

$Q_2(s)$ = flow vector downstream of the shock,

$Z(s)$ = vector containing the shock transfer function,

$Q_{in}(s)$ = external input at boundary S.

Usually, in order to determine the flow variables immediately upstream of a shock, the Rankine-Hugoniot conditions are used. Furthermore, for control system applications, it is possible to describe a shock using its input/output characteristics also known as shock transfer function, shock dynamics, or simply the shock model. The shock model is a dynamic model for the moving normal shock that separates the supersonic and subsonic flow regions of an inlet. Specifically, it relates the flow variables just upstream of the normal shock to the flow variables just downstream of the normal shock.

The effect of small downstream pressure disturbances on the position of a normal shock in a duct with varying cross-sectional area was studied by Hurrel in [HUR57]. In this analysis the author neglects the boundary layer and assumes that the flow in the duct is quasi-one dimensional. He then derives an expression for normal shock position changes in terms of downstream disturbances in pressure. The relationship he derived is the following first-order lag expression,

$$\frac{\Delta x(s)}{\Delta p(s)} = \frac{K}{1 + \tau s}.$$

Reproduced with permission of the copyright owner. Further reproduction prohibited without permission.

The time constant τ and the gain K of this lag are expressed in terms of a dimensionless time constant, which depends only on the steady-state Mach number of the shock.

For most isentropic applications, the first-order lag relationship given above will adequately describe the situation, if the parameters K and τ are chosen accurately. Although higher order shock models could be used, the complexity of the problem is also expected to increase drastically. An example of this type of boundary condition for a two wave system is as follows

$$u = Z(s)\,\rho + f_e$$

where,

u = flow velocity upstream of the shock,

$Z(s)$ = shock transfer function,

ρ = flow density downstream of the shock,

f_e = external input at downstream boundary.

Finally, this type of boundary condition is commonly used in a supersonic inlet system and is very useful for control system applications. The dynamics of the system can be studied and the sensitivity of the overall performance to normal shock parameter changes can be analyzed so that the best control strategy possible in any given situation is used.

Reproduced with permission of the copyright owner. Further reproduction prohibited without permission.

D. Cole-Willoh Boundary Conditions

This set of boundary conditions is discussed in [WIL68] and [CW75]. Basically, the Cole-Willoh constraints describe the dynamic relations for perturbations upstream and downstream of the normal shock, which is located near the throat of a converging-diverging channel. Using matrix notation, the Cole-Willoh boundary conditions are written in the Laplace domain as follows,

$$\begin{bmatrix} \tilde{P}_2(s) \\ \tilde{\dot{W}}_2(s) \\ \tilde{S}_2(s) \end{bmatrix} = \begin{bmatrix} C_4 & \frac{C_1}{C_r} & \frac{C_1}{7} \\ 0 & 1 & 0 \\ \frac{6}{7} C_1 & -\frac{C_1}{C_r} & C_5 \end{bmatrix} \begin{bmatrix} \tilde{P}_1(s) \\ \tilde{\dot{W}}_1(s) \\ \tilde{S}_1(s) \end{bmatrix} + \begin{bmatrix} -C_1 \left(R_c \frac{A'}{A} + C_2 s \right) \\ C_r C_3 s \\ C_1 \left(R_c \frac{A'}{A} - C_3 s \right) \end{bmatrix} \tilde{X}_s(s)$$

where,

$\tilde{P}_2(s)$ = Laplace transform of pressure just aft of normal shock,

$\tilde{\dot{W}}_2(s)$ = Laplace transform of weight flow just aft of normal shock,

$\tilde{S}_2(s)$ = Laplace transform of entropy just aft of normal shock,

$\tilde{P}_1(s)$ = Laplace transform of pressure ahead of normal shock,

$\tilde{\dot{W}}_1(s)$ = Laplace transform of weight flow ahead of normal shock,

$\tilde{S}_1(s)$ = Laplace transform of entropy ahead of normal shock,

$\tilde{X}_s(s)$ = Laplace transform of the shock position,

Reproduced with permission of the copyright owner. Further reproduction prohibited without permission.

C_1, C_4, C_5 = dimensionless coefficients,

C_2, C_3 = coefficients,

C_r = ratio of airflow rates just ahead of normal shock to most upstream station,

R_C = radius of inlet cowl measured at cowl-lip station,

$A = A(x)$ = duct cross-sectional area,

$A' = \frac{dA(x)}{dx}$ = rate of change of duct cross-sectional area along duct,

s = Laplace transform variable,

$\sim$ = indicates a nondimensional small perturbation variable.

It must be noted that the above set of equations must be modified if provisions are made for bleed flow near the normal shock operating point. If this is the case, then the coefficient of $\tilde{X}_s(s)$ in the weight flow equation is increased by the stability bleed coefficient, C_B. Furthermore, in the absence of upstream perturbations the set simplifies to the following constraints, referred to as the Willoh boundary conditions [WIL68],

$$\begin{bmatrix} \tilde{P}_2(s) \\ \tilde{W}_2(s) \\ \tilde{S}_2(s) \end{bmatrix} = \begin{bmatrix} -C_1\left(L_T \frac{A'}{A} + C_2 s\right) \\ C_3 s \\ C_1\left(L_T \frac{A'}{A} - C_3 s\right) \end{bmatrix} \tilde{X}_s(s)$$

Reproduced with permission of the copyright owner. Further reproduction prohibited without permission.

where,

$\tilde{P}_2(s)$ = Laplace transform of pressure just aft of normal shock,

$\tilde{W}_2(s)$ = Laplace transform of weight flow just aft of normal shock,

$\tilde{S}_2(s)$ = Laplace transform of entropy just aft of normal shock,

$\tilde{X}_s(s)$ = Laplace transform of the shock position,

C_1 = nondimensional coefficient,

C_2, C_3 = coefficients,

L_T = duct lenght from normal shock to exit station,

$A = A(x)$ = cross-sectional area,

$A' = \frac{dA(x)}{dx}$ = rate of change of duct cross-sectional area along duct,

s = Laplace transform variable,

~ = indicates a nondimensional small perturbation variable.

E. Other Boundary Conditions

Additional boundary conditions, which may be used in special flow system configurations, can be found in the literature. For instance, in Chapter 8 of reference [CHA79], one can find the boundary conditions applied to flow discontinuity, series junctions, and branching systems. The

Reproduced with permission of the copyright owner. Further reproduction prohibited without permission.

development of the boundary conditions is done in the Laplace domain and is based on the following three types of transfer matrices:

- Field transfer matrix,
- Point transfer matrix,
- Overall transfer matrix.

A *field transfer matrix* relates the state vectors at two adjacent sections of a flow channel. A *point matrix* relates the state vectors just to the left and to the right of a discontinuity. Finally, the *overall transfer matrix* simply relates the state vector at one end of a system to that at the other end. Thus, to relate two adjacent points within a flow channel, a field transfer matrix should be used. On the other hand, to relate state vectors at either side of a series junction, i.e., a flow discontinuity, a point matrix must be used. At last, to relate the flow between the upstream end of a flow channel to the downstream end of the same channel, the overall transfer matrix must be used. As an example, consider the boundary conditions of the series juction of Figure 2.4.

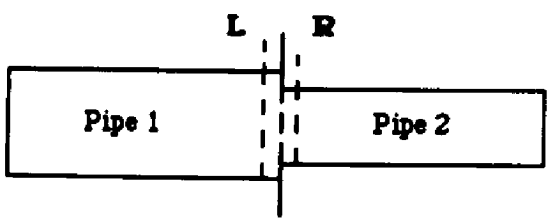


Figure 2.4 A series junction

Reproduced with permission of the copyright owner. Further reproduction prohibited without permission.

The boundary conditions of this system are as follows,

$$Q_2^R = P_s\, Q_2^L + Q_{IN}$$

where,

Q_2^R = Flow vector just to the right of the discontinuity,

Q_2^L = Flow vector just to the left of the discontinuity,

Q_{IN} = Input vector at discontinuity,

P_s = Point transfer matrix for a series junction.

This set of boundary conditions, if applied correctly, is very practical to control engineers since several scenarios involving compound flows can be examined. Finally, many practical as well as theoretical problems, which will be discussed later, can be studied.

Additional boundary conditions, which can be used in compound flow systems, are found in reference [RIC86]. Specific boundary conditions for two-wave series and parallel flow systems are given and transmission-line formalism is used to express the boundary conditions in the following compact form,

$$\begin{bmatrix}\text{UPSTREAM} \\ \text{VECTOR}\end{bmatrix} = \begin{bmatrix}\text{ABCD} \\ \text{MATRIX}\end{bmatrix}\begin{bmatrix}\text{DOWNSTREAM} \\ \text{VECTOR}\end{bmatrix}$$

Reproduced with permission of the copyright owner. Further reproduction prohibited without permission.

In reality the ABCD matrix is like the overall transfer matrix for the system under study. For example, in a two-wave system, if pressure and volume are the independent variables, the boundary conditions for the branching system of Figure 2.5 are,

$$\begin{bmatrix} P \\ V \end{bmatrix}_{UPSTREAM} = \begin{bmatrix} 1 & 0 \\ \frac{1}{Z_1} + \frac{1}{Z_2} + \frac{1}{Z_3} + \cdots & 1 \end{bmatrix} \begin{bmatrix} P \\ V \end{bmatrix}_{DOWNSTREAM}$$

where,

$P = P(s)$ = Pressure,

$V = V(s)$ = Volume,

$Z_i = Z_i(s) = \frac{P_i(s)}{V_i(s)}$ = Input impedance to i_{th} branch.

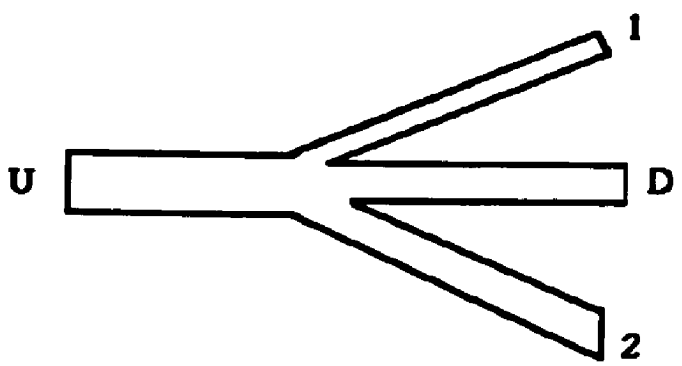


Figure 2.5 A branching system

Reproduced with permission of the copyright owner. Further reproduction prohibited without permission.

Also, the subscripts *UPSTREAM* and *DOWNSTREAM* describe the flow vector just upstream and downstream of the discontinuity, respectively. Finally, the numbers 1,2,3,... describe the entrance to the side branches.

2.6 Concluding Remarks

In this chapter, a general introduction of the inlet modeling problem was presented.

First, the objectives of an inlet system were given and then the geometry of a typical mixed compression inlet was described. Next, various nonlinear, quasi-linear, and linearized versions of the governing equations of the flow inside the inlet were shown. Also, some brief theory on the classification of linear operators and sets of linear partial differential equations was given. The chapter ended with a presentation of boundary conditions typically used in the inlet modeling problem.

The following chapter contains a more specific literature search on the inlet modeling problem.

Reproduced with permission of the copyright owner. Further reproduction prohibited without permission.

CHAPTER III

A REVIEW OF INLET MODELING TECHNIQUES

3.1 Introduction

This chapter covers the results of a comprehensive literature search on the inlet modeling problem. The survey covers many low order and high order linear and nonlinear inlet models.

The objectives of this search are as follows:

First, by studying and analyzing the various approches of solution of the inlet modeling problem, the control engineer can select the most suitable model for a specific application.

Secondly, by performing a critical analysis of inlet modeling techniques, the control engineer will be capable of modifying and improving existing algorithms, thus making a contribution to the knowledge.

In the following sections of this chapter, each inlet modeling method is discussed briefly and, when deemed necessary, related supporting theory is presented. In order to gain a better understanding of the method under consideration, the interested reader is referred to the many references given in each section.

Reproduced with permission of the copyright owner. Further reproduction prohibited without permission.

3.2 A Classification of Modeling of High Speed Propulsion Systems

A comprehensive study of inlet modeling techniques was presented by Hartley in [HAR86]. More recently, a skeleton of existing inlet modeling techniques is given in [HAR91]. Furthermore, in a more thorough fashion, reference [HD91] presents a hierarchy for modeling high speed propulsion systems typified by supersonic inlets, ramjets, nozzles, and scramjets. All methods examined are based on the assumption of quasi-one dimensional, inviscid, compressible flow which is governed by Euler's equations.

Inlet models are grouped into linear and nonlinear models. Linear and nonlinear models are further divided into four major categories: low order linear models (LOL), high order linear models (HOL), low order nonlinear models (LON), and high order nonlinear models (HON).

The classification of modeling techniques presented in [HD91] is very practical. Therefore, the same hierarchy developed in that research will also be adopted in this report and in the following sections all linear models will be studied first followed by nonlinear models.

3.3 Low Order Linear Models

As mentioned in the previous section, linear models are divided into low order and high order models. Low order models comprise a major category of inlet models and will be studied first. Such models may be

Reproduced with permission of the copyright owner. Further reproduction prohibited without permission.

obtained from high order nonlinear or linearized systems using a variety of techniques. The following sections cover the most common techniques for obtaining low order linear inlet models.

3.3.1 Model Reduction Methods

One way of obtaining low order inlet models is by direct model reduction of linearized CFD models. Models of hundreds or perhaps thousands of states may be reduced down to models of just a few dozens of states or less without any sacrifice in accuracy.

An advantage of reduced order models is that they can be analyzed easier and thus provide better understanding of their corresponding higher order models. Also, the computational burden associated with system simulation, control evaluation and design is reduced drastically while the execution time in simulations is shorter. All in all, reduced order models have become almost indispensable to practicing control engineers and inlet models are not an exception.

Reduced order inlet models may be obtained from linearized CFD codes using the following approaches:

The time moment matching method, the matching of the Markov parameters, curve fitting, the aggregation method, the Pade' approximation method, the singular perturbation method, optimal error minimization methods (L_2 and Hankel norm), transformation methods (Davinson's, balancing, component cost analysis), the orthogonal projection method,

Reproduced with permission of the copyright owner. Further reproduction prohibited without permission.

selective modal analysis, robust techniques, methods implemented in MATLAB, and other techniques found in the literature [DS90].

It must be noted that when the full order model is unstable, it is sometimes difficult to develop a reduced order model to model it [DS90]. One way of overcoming this problem might be to follow these steps:

A) Translate the poles of the system on the real frequency axis enough so that the transformed system becomes stable,

B) Reduce the transformed system using any applicable model reduction technique, and finally

C) Apply the inverse transformation to the reduced order model to obtain a model in the original coordinates.

We must caution the reader that this technique may sometimes produce results with varying success or it may not be applicable at all to a model reduction algorithm.

In general, it should be mentioned that not every model reduction technique is applicable equally to every inlet system. While some techniques are more geared towards continuous time systems others are only applicable to discrete-time systems. Also, some techniques are time-domain while others are frequency-domain. Thus, it is the task of the control engineer to identify and analyze the idiosyncracies of a given system and to select the most suitable reduction technique for a particular situation.

Reproduced with permission of the copyright owner. Further reproduction prohibited without permission.

The extensive study of model reduction techniques presented in [DS90] will be very helpful in the selection of the most appropriate reduction technique. Also, a comprehensive analysis of reduction techniques based on the balancing algorithm is given in [FEL89] while balancing with frequency weighting is advocated in [ENN84]. Finally, some additional useful model reduction techniques are found in [AOK68], [CG85], [GCP88], [GLP88], [DH91], and [MHD91] while an expert system for reduced order modeling is presented in [ABU92].

In conclusion, reduced order inlet models are very practical. In many cases, reduced order models produce exactly the same results as do full order models within the specified range of frequencies of interest. Thus, such models should be used as frequently as possible.

3.3.2 Model Reduction of Models Obtained Using the Split Flux Approach

Low order linear inlet models can be obtained indirectly by applying model reduction techniques on the split flux approach which was originally developed by Steger and Warming in [SW81] and has been used frequently in the literature.

According to the split flux technique, the system consists of a collection of many small lumps that are linearized about their steady state conditions. LOL models of internal flow propulsion systems developed using the split flux approach can then be obtained using various model

Reproduced with permission of the copyright owner. Further reproduction prohibited without permission.

reduction techniques. This method of obtaining inlet models was illustrated succesfully in [CHI90].

3.3.3 LOL Inlet Models Obtained Using the Physical Lumping Technique

Another way of obtaining LOL inlet models is by reducing the order of models developed using the physical lumping technique. According to the physical lumping technique, the partial differential equations with the given boundary conditions are not solved explicitly. Instead, the system is discretized with respect to the space variable into N separate interacting lumps. Typically, the standard equations for the conservation of mass, the conservation of linear momentum, and the conservation of energy are manipulated using the equation of state in order to yield three ordinary differential equations for the lump pressure, lump mass flow, and lump temperature, respectively. The resulting set of dynamic equations is then solved for each lump.

System matrices resulting from the physical lumping technique are typically block tridiagonal. This special structure of the system matrix should be taken advantage of when designing a controller for the system or when a simulation of the system is performed. Clearly, as the number of lumps used is increased, better approximations are obtained. However, the order of the resulting system is also increased as is the corresponding execution time in the simulations.

Reproduced with permission of the copyright owner. Further reproduction prohibited without permission.

Hartley in [HAR86] warns that extra care must be exercised in choosing the right discretization method for the physical lumping technique. This is necessary in order to ensure that information about the system propagates in the right direction from one lump to another and hence the correct results are obtained. It must be noted that in a gas dynamics system there are regions of supersonic and subsonic flow [SHA53]. Moreover, in one-dimensional supersonic flow information travels in one direction only while in one-dimensional subsonic flow information may travel in two different directions. Thus, it is more difficult to choose a simulation method for the subsonic case rather than for the supersonic case.

Furthermore, efficient low order models of the NASA Lewis 40-60 inlet were presented in [IHD91]. These inlet models were originally developed using the physical lumping method and were subsequently reduced using the Schur method of balancing that was discussed in [SC89]. Finally, it was reported in [IHD91] that for the NASA Lewis 40-60 inlet, reduced order models derived from the physical lumping technique proved somewhat better than reduced order models obtained using the split flux techique of reference [CHI90].

3.3.4 LOL Inlet Models Obtained Using Input/Output Identification

Optimized low order linear inlet models may also be obtained using input-output identification methods. Under this category fall the recursive

Reproduced with permission of the copyright owner. Further reproduction prohibited without permission.

least squares (RLS), the batch least squares (LS), and the total least squares (TLS) techniques.

The RLS and LS techniques have been two very popular methods in system identification for quite a while. On the other hand, although an analysis of the TLS problem was presented in [GV80], its use in parameter estimation was not advocated until more recently in [HUF87].

Whether using an on-line or off-line identification method, special care must be exercised in order to choose the "right" system order. Namely, the model order must be high enough so that it contains all useful information about the system yet low enough so that the simplest model possible is obtained without underparametrizing the system. Usually, any prior knowledge about the dynamics of the system will help the control engineer make the proper choice. Equally helpful is any knowledge of the initial conditions of the system, especially when nonlinearities may be present.

In [PIE91] an application of the TLS and LS algorithms to a supersonic inlet problem is presented. Frequency, step, and impulse responses of reduced order models of supersonic inlets are computed using the total least squares as well as the least squares algorithms. A useful conclusion of that study is that the TLS algorithm is generally superior to LS for both model reduction and off-line parameter estimation in a low noise environment.

Reproduced with permission of the copyright owner. Further reproduction prohibited without permission.

3.3.5 Reduction of Meromorphic Transfer Functions

The next major category of LOL models encompasses those inlet models which are developed by direct reduction of meromorphic transfer functions.

A function f(z) is said to be meromorphic if it can be expressed as the ratio of two entire functions [MAR66]. Namely,

$$f(z) = \frac{A(z)}{B(z)}$$

where A(z) and B(z) are entire functions. Incidentally, the name *meromorphic* is derived from the Greek words $\mu\acute{\epsilon}\rho o\varsigma$, meaning fraction and $\mu o\rho\phi\acute{\eta}$, meaning form.

Furthermore, an entire function can be defined as a function that is differentiable in the entire complex plane. An equivalent definition states that, an *entire* function f(z) is a function of a complex variable that is analytic in the entire plane of the complex variable z. Alternatively, such a function may be thought of as the limit of an everywhere convergent power series.

As it turns out, the sum, difference, and products of entire funtions is also an entire function. Furthermore, an entire function of an entire function is an entire function. On the other hand, the quotient of two entire functions is an entire function provided the denominator does not vanish anywhere. Finally, every entire function is meromorphic and every

Reproduced with permission of the copyright owner. Further reproduction prohibited without permission.

meromorphic function is transcedental. Consequently, all entire functions are transcedental!

The transfer functions of distributed parameter models of inlets to be discussed later are examples of meromorphic functions, by their own nature. These functions often involve time lags as well as transcedental functions. It is reported in [CHU72] that any meromorphic transfer function can be approximated by sums of exponential functions. Furthermore, exponential functions can be approximated by infinite sums of polynomials using Taylor series expansions. Therefore, meromorphic transfer functions of distributed parameter systems can be simplified by retaining a finite number of terms in their Taylor series expansion. Usually, in a converging algorithm the greater the number of terms, the better the approximation. On the other hand, divergent approximations of system functions, if they exist, are of no practical use to stable systems, although they might be more insightful for unstable systems.

Alternatively, meromorphic transfer functions of inlet models can be simplified using partial fraction expansions. Partial fraction expansions of meromorphic functions are covered extensively in [HEN74]. Many other useful subjects are found in that reference including, expansions of iterated Laplace tranforms, construction of the partial fraction representation of rational functions, and convergence of continued fractions with complex elements.

Finally, other techniques for reducing infinite dimensional systems exist or are expected to appear soon in the literature since model reduction

Reproduced with permission of the copyright owner. Further reproduction prohibited without permission.

of infinite dimensional systems is by no means a solved problem. So far, some techniques are developed in the time-domain and others in the frequency domain. Time-domain techniques are given in [HOF62], [BK79], and [GIB83]. On the other hand, frequency-domain techniques are given in [GLP86], [GP87], [GCP88], [GLP88], [PGZ88], [GKL89], and [HD91].

In particular, [GKL89] presents a reduction technique applicable to time delay systems. The method is based on Fourier transforms and approximate models may be computed using an FFT type algorithm. Also, convergence conditions and frequency response error bounds are computed in terms of the H_∞-norm. Although this technique yields primarily high order approximations of infinite dimensional systems, low order linear models may also be obtained using standard reduction techniques.

In closing, care must be exercised when reducing meromorphic transfer functions of inlets using series expansions or partial fractions. The control engineer must see that an optimum number of terms for the reduced order system is retained while at the same time the performance of the system be satisfactory.

3.3.6 The Cole-Willoh Approach

A widely used inlet modeling method is the Cole-Willoh approach according to which the gas dynamic equations are divided into several lumps and linearized about their operating points. The three flow signals at any lump (k+1) are scaled versions of the flow signals at lump (k) only they have been delayed in time through three distinct time constants

Reproduced with permission of the copyright owner. Further reproduction prohibited without permission.

([WIL68] and [CW75]). The Cole-Willoh approach offers two different approximations for the time delays.

In the first approach, time delays are replaced by discrete-time delays each one corresponding to a lump. In this case, the resulting equations describe three waves, one for each state variable, which travel from lump to lump. Usually, two out of three waves are chosen to travel upstream and the third travels downstream or vice versa. However, in order to assure stability of the algorithm not all three waves are allowed to travel in the same direction unless the flow is supersonic.

On the other hand, in the second Cole-Willoh approach time delays are approximated by Padé approximations. Since three states are needed for each lump of the model the order of the resulting system is calculated using the following formula found in [HAR86],

$$n = 3\,p\,m + 1$$

where,

n = order of resulting system,

p = order of Pade′ approximation,

m = number of lumps.

m must be sufficiently large in order to ensure that the system is accurate yet small enough to ease the computational burden.

Reproduced with permission of the copyright owner. Further reproduction prohibited without permission.

The Cole-Willoh method has been used frequently in the literature. It is a straightforward method, easy to use and be implemented on a personal computer. Additionally, this method can support a shock structure and its many applications have proved that it works very well. However, since the results obtained are dependent on the operating point of each lump, if the operating conditions vary widely, one must recalculate the inlet model each time. This is a disadvantage when large perturbations in the flow field occur.

Overall, the Cole-Willoh approach can give quick insight about an inlet system and is a good method for controller design.

3.3.7 Equivalent Circuit Modeling

Electric circuit analogues have successfully been used in the past for the solution of nonelectrical problems. In particular, in [RG57], Rohman and Grogan exploit the electrical transmission-line theory to where it is possible to derive the driving point impedance and the output frequency response of pneumatic tubing.

The authors use the pneumatic parameters of resistance, inductance, and capacitance which correspond to the analogous electrical quantities of resistance, conductance, and capacitance, respectively. Furthermore, pressure is equivalent to voltage while volumetric flow rate to electric current. Using the above change of variables the authors are then able to derive relations governing frequency response of tubing. The resulting model, which is a distributed parameter model, is first developed on the

Reproduced with permission of the copyright owner. Further reproduction prohibited without permission.

assumption of incompressible flow. However, if modified it can account for compressible flow in the tube, finite-signal amplitude, end effects, fluid inertia as well as heat transfer. Both theoretical and experimental results are plotted for various lengths of tubing and various terminating conditions.

Also, in [HAR86] one may find finite circuit models of inlets using some very simple yet descriptive networks. Again, pressure is made analogous to voltage while mass flow is analogous to current. The resulting capacitive/resistive electical network may then be analyzed using circuit analysis techniques or simulation packages like PSPICE, ECAP, or WATAND.

In reality, the inlet is a distributed parameter system that is modeled with finite-size lumps. The question of how many lumps are enough is clearly important, however the answer depends on the specific application. In practice, however, it is normal precedure to vary the amount of detail in models in order to find the simplest one that seems to answer the questions posed about the system.

Overall, circuit models of inlets can be very useful to electrical engineers, primarily due to the familiarity of electrical engineers with electrical network theory. Circuit models can easily be built or simulated on an analog computer. They can be tested in a laboratory and produce a wealth of information about a system. Finally, such models can provide the engineer with some crude answers about inlets as well as inlet/engine combinations operating in various environments.

Reproduced with permission of the copyright owner. Further reproduction prohibited without permission.

3.3.8 Hydraulic Analogies

Another modeling technique results from the simulation of isentropic gas flows by the use of hydraulic analogies. This method dates back to the second decade of the 20th century.

In reference [MIN74] a method is presented for deducing an isentropic gas flow of a two-dimensional hydraulic analogy. The method is then applied to obtain the flow in a two dimensional internal combustion diffuser during the early phase of the starting flow. The equation of continuity and the balance of momentum equation are transformed into a set of hydraulic analogs and then integration is performed by approximating the spatial derivatives using forward difference schemes.

Finally, in order to gain any meaningful information about the model under consideration, the simulation results obtained are transformed back to the original system coordinates, where they can be analyzed. Although this method yielded satisfactory results in [MIN74] it is believed to be of limited use to the inlet modeling problem.

3.3.9 A Schwarz-Christoffel Transformation Technique

When computing flow past complex body shapes, numerical integration of Schwarz-Christoffel transformations for general curved surfaces may be used. A presentation of this technique is given in [DAV83].

This technique is developed primarily for computing airfoil potentials and stream lines, however, the author suggests that it can also be

Reproduced with permission of the copyright owner. Further reproduction prohibited without permission.

used to describe flows in various channels. The resulting mappings are typically corner mappings, mappings of diverging channels, or multiple corner channel mappings.

In closing, the Schwarz-Christoffel Transformation technique can potentially point towards a new area for further research. Finally, its application to the inlet modeling problem can be greatly increased, due to the ability of the technique to be applied to flow channels of varying cross sectional area.

3.3.10 Supersonic Inlet/Engine Combinations

Another modeling technique is found in [YG88], where an inlet/engine combination is considered. The authors, after first developing an appropriate inlet model, proceed with designing a control system for an inlet/engine combination. Incidentally, some aspects on inlet/engine compatability are presented in [WY73].

The problem is set up such that the overall inlet system has two inputs and two outputs. In particular, the inlet model used is a twelfth order transfer function in the frequency domain. Additional transfer functions are used to represent the dynamics of the bypass door, the bypass actuator, the main fuel pump, and finally the engine. The variables chosen to be controlled are the shock position and the engine speed. As in previous designs, the normal shock must be maintained near the geometrical throat of the inlet to maximize the efficiency of the system.

Reproduced with permission of the copyright owner. Further reproduction prohibited without permission.

On the other hand, the speed of the engine should be insensitive to any disturbance inputs.

In this research, the idea of flow matching of the input and the engine is used and the resulting problem is approached as a stochastic linear quadratic regulator problem. In particular, the performance index which is chosen to be minimized comprises terms proportional to the variance of the shock position increment, the variance of the increment of the engine speed, the variance of the increment of the fuel flow, and finally, the variance of the bypass door control voltage.

In closing, the inlet model used in this research yielded fairly good results and the dynamic performance of the optimal controller was very satisfactory. However, it is not clear from this research paper how the selection of the particular inlet model influences the system performance positively. Nevertheless, the overall results obtained from this reseach effort are very useful to a control engineer particularly since the results are applied to a NASA 48cm/J85 engine combination.

3.3.11 Bond Graphs

The following subsection describes the bond-graph technique, a powerful, although not yet very popular modeling technique that can be used to obtain low order linear inlet models from high order nonlinear or linearized models. The bond-graph technique is discussed in [RK83] and is applicable to various types of systems, i.e., electrical, mechanical, acoustical, thermal, as well as combinations of them.

Reproduced with permission of the copyright owner. Further reproduction prohibited without permission.

Bond graphs are abstract extensions of block diagrams and signal flow graphs and they represent the flow of power between various elements in a system. Each variable in a dynamic system is considered to be either a flow variable or an effort variable. Also, the product of an effort variable with a flow variable equals power. In many cases, in order to describe a system adequately additional types of variables are required. For example, Table 1 below illustrates some analogies that exist between variables found in hydraulic and acoustic circuits and other commonly used generic bond graph variables.

Table 3.1 Equivalence between bond graph variables and flow variables

VARIABLE	FLUID CIRCUIT
Effort	Pressure, P
Flow	Volume flow rate, Q
Momentum or impulse	Integral of pressure, P_p
Displacement	Volume, V
Power	P(t) Q(t)
Energy	$\int Q\, dp_p$, kinetic $\int P\, dV$, potential

Reproduced with permission of the copyright owner. Further reproduction prohibited without permission.

In order to illustrate the use of the bond graph method, a small part of a bond graph of a long fluid line is shown in Figure 3.1. Basically, this graph depicts a second order approximation of a long fluid channel which is modeled as a distributed parameter system. In the figure only two building blocks of the model are shown and the variables I, C, and R describe the properties of the fluid in a given lump. Furthermore, the numbers 0 and 1 are an important part of the bond graph and cannot be omitted or interchanged. The half arrowheads is typical notation used in bond graph applications as is the small bar located normal to the tail or head of the arrow. Clearly, the complete model being a distributed parameter model consists of an infinite number of building blocks connected in series.

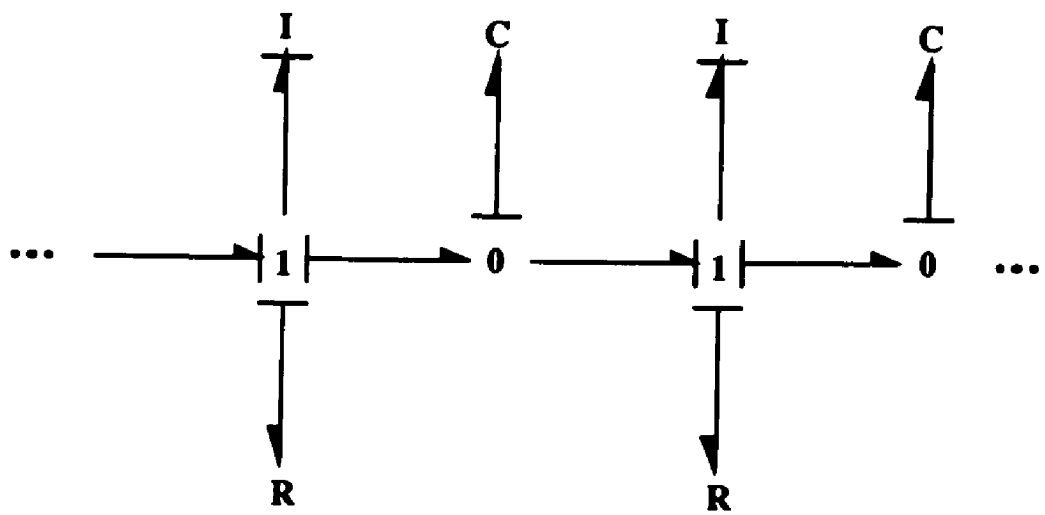


Figure 3.1 A second-order bond graph of a long fluid line

Reproduced with permission of the copyright owner. Further reproduction prohibited without permission.

The questions that arise next are the following: Why should one use bond graphs? Why should one even bother to learn this abstract "bond graph" language? Well, to answer these questions one must recall some of the advantages of the method. As it turns out, in addition to unifying theories from several disciplines, bond graphs possess this important property: Complicated systems represented by bond graphs may be simplified using a set of reduction rules outlined in [RK83]. Therefore, redundacies in a model can be identified and eliminated and hence simpler models can be obtained. This is especially useful in many cases such as when the engineer, in an attempt to include enough details in the model, ends up overmodeling the system.

Overall, the bond-graph technique is a powerful modeling tool that adds a new dimension to the modeling problem. In this author's opinion, this method can be applied to flow propulsion systems, as well. Perhaps, some useful low order inlet models can be generated by applying bond graph minimization techniques. This is especially true today since powerful computer packages to analyze bond graphs and solve design problems have started making their appearance in the market.

3.3.12 The Barry Model

Another modeling technique can be found in [BAR73]. This reference presents some general linear analytical models that are developed to compute changes in inlet throat Mach number and in normal shock

Reproduced with permission of the copyright owner. Further reproduction prohibited without permission.

position due to disturbances in inlet geometry, upstream and downstream (exit) atmospheric flow conditions.

Four analytical models of shock position are developed. The first one is applicable to short inlets and uses the concept of a first-order lag relation for normal shock position.

The second Barry model is applicable to inlets with a long diffuser and unlike the first model, this model has a quadratic lag in the denominator. Furthermore, the shock displacement is proportional to the rate of change of upstream total pressure and temperature.

Next, the third analytical model differs from the first and second models in that it has a first-order plus a quadratic lag in the denominator as well as a lead in the $\Delta(T)$ term and a quadratic lead in the $\Delta(M)$ term, where T stands for temperature and M for Mach Number.

Finally, the fourth analytical model has two quadratic lags, a quadratic lead in the $\Delta(A)$ term and a lead in the $\Delta(P)$ term, where A is the cross sectional area of the inlet and P stands for total pressure. This particular model is derived by linearizing the supersonic inlet model presented in [MAR68].

Overall, all Barry models are relatively easy to use. They can be used for a variety of inlet conditions and due to their simplicity, these models can give the control engineer quick insight about an inlet system. Finally, due to their ability to model many inlet configurations as well as

Reproduced with permission of the copyright owner. Further reproduction prohibited without permission.

inlet/engine combinations and adopt to many different operating environments, the Barry models can be useful for control system design.

3.4 High Order Linear Models

In this section, the techniques used to derive high order linear inlet models will be discussed. It must be remembered that some of the methods discussed in the previous section might also be applied to obtain high order linear inlet models. Thus, in order to avoid duplication, only the techniques that are different from those discussed above will be covered.

High order linear inlet models are very useful to the control engineer. In general, they are more accurate than the low order linear models discussed in the previous section. However, high order linear models require longer execution time in their simulations and their controller structures are more complex. Thus, they are usually used for evaluation and not design!

The major category of high order linear models includes inlet models that are based on Computational Fluid Dynamics (CFD). Basically, computational fluid dynamics is defined as the art of replacing the governing linear or nonlinear partial differential equations with numbers and advancing these numbers in time and/or space in order to obtain a final description of the complete flow field of interest. CFD techniques are based on finite differences or finite elements schemes and they amount to accumulating a lot of useful numbers about the given system. Some useful

Reproduced with permission of the copyright owner. Further reproduction prohibited without permission.

references that can be used for the study of CFD are [RIC57], [AME65], [RM67], [AME69], [ROA76], and [KOL80].

As it turns out, all CFD-based techniques result into some computationally intensive algorithms that must be solved using fast computers. The accuracy of a CFD based model will typically depend on the algorithm chosen as well as the number of nodes that are chosen to represent a particular model. It is not unusual for a CFD code to contain thousands or perhaps tens or hundreds of thousands of nodes that may take up to several hours to be computed even on the fastest parallel computers available. Therefore, in order to optimize the flow of information it is important to choose the most efficient CFD algorithm that is also going to be stable, treat boundary conditions properly, and at the same time capture shocks as well as other interesting phenomena occuring in real inlets. One such algorithm is based on the flux splitting method discussed in an earlier section. As mentioned previously, this technique will yield accurate high order linear inlet models, if applied carefully.

In conclusion, high order linear models are very expensive to use, although they produce accurate results. In order to minimize the computational time in their computer simulations and simplify the respective controller structures, it is strongly suggested that high order linear models be reduced in state dimensions using any applicable model order reduction technique.

Reproduced with permission of the copyright owner. Further reproduction prohibited without permission.

3.5 High Order Nonlinear Inlet Models

High order nonlinear inlet models are typically based on CFD methods. Useful references on commonly used CFD methods were given in the previous section. A review of theoretical and some experimental studies on the unsteady and transient flow of compressible fluid in pipelines was given in [TT87] with special emphasis on implicit and explicit finite difference methods. Furthermore, a numerical investigation of unsteady inlet flowfields is presented in [HWC87] and implicit conservative schemes for the Euler's equations are presented in [WH86].

The main characteristic of CFD based methods is that the resulting models can vary in accuracy. Usually, in any numerical method high degrees of accuracy can be achieved at the expense of increased computational labor. In other words, as the number of state variable increases the corresponding high order nonlinear inlet models become more accurate.

Furthermore, CFD based nonlinear models can be used for control system evaluation but not necessarily for control system design primarily because of the increased complexity associated with designing controllers for nonlinear systems. Since most models in this category are derived from first principles, it is not uncommon for high order nonlinear inlet models to have hundreds of thousands or even millions of states. Thus, in general, the execution time in their simulations is very long while their controllers are expensive to build.

Reproduced with permission of the copyright owner. Further reproduction prohibited without permission.

In addition to physical lumping, high order nonlinear models can be derived using nonlinear flux splitting techniques, flux difference splitting techniques, fundamental laws of physics, as well as implicit, explicit, and explicit-implicit finite difference techniques and finite element analysis techniques. As a word of caution it must be mentioned that, at best, explicit methods can be conditionally stable. In contrast, implicit finite difference methods have the advantage over the explicit methods of being unconditionally stable. Thus, these methods impose no restrictions on the maximum allowable time step.

A commonly used finite difference scheme is the second order MacCormack's method which is a predictor-corrector method ([MAC81] and [ATP84]). As a predictor-corrector algorithm, its main characteristic is that it predicts the flow field in one direction while it corrects its predicted values in the opposite direction. It is reported in [MVA84] that this algorithm is much faster than both the Beam-Warming and split flux algorithms although it is considered to be of medium accuracy [HAR91].

Finally, additional techniques are found in the LAPIN report of [VMP84]. The LAPIN model is a very accurate model, however, its main disadvantage is that it is very slow to use. Thus, when quick insight is needed about an inlet system, it is advisable that other models be used.

In conclusion, high order nonlinear inlet models are best for studying the fundamental laws of physics. In some cases, it may be possible to transform a nonlinear system into a linear system using nonlinear translation techniques. However, this approach is application dependent

Reproduced with permission of the copyright owner. Further reproduction prohibited without permission.

and somewhat of limited use for the majority of nonlinear systems. Finally, until better control techniques for high order nonlinear systems become more readily available, the nonlinear models discussed in this section can only be used to get a better understanding of inlet systems and to evaluate their control needs.

3.6 Low Order Nonlinear Inlet Models

It is reported in [HD91] that there are very few low order nonlinear inlet models. In fact, our independent search in the literature strongly reaffirms this argument.

Naturally, one way to obtain low order nonlinear models is by reducing high order nonlinear models. Model reduction of nonlinear systems is by no means a solved problem. In the past, nonlinear systems have been modeled by expanding the output of a system in a truncated series of polynomials. This approach is studied in [WIE58] and [SNF69].

Alternatively, for a class of nonlinear systems a Volterra series can be used while for others Fourier series, Laguerre or Hermite polynomials. These approaches have been studied in [RS67] and [SM71]. It should also be mentioned that, over the years, other methods have been used to reduce the order of nonlinear systems. However, these techniques have produced results of varying success depending on the system under consideration.

To return to the inlet modeling problem, the low order nonlinear Martin model of [MAR68] should be mentioned. Basically, in this

Reproduced with permission of the copyright owner. Further reproduction prohibited without permission.

reference one can find the theory, governing equations, and assumptions for propulsion system dynamic simulation. Special emphasis is given on the air induction system simulation and air induction control system and engine system simulation. Specifically, the air induction system simulation program is divided into the following phases of operation:

1. Started phase,
2. Unstarting phase,
3. Empty-fill phase,
4. Subcritical phase, and
5. Hammershock phase.

The program code for the Martin model is designed so that phase changes are accomplished automatically through preprogrammed logic. This type of control flow of data was chosen so that smooth simulation results can be obtained.

The Martin report gives a complete account of the geometry of the system, and the initial and boundary conditions that are necessary to drive the system into a specific mode of operation, stable or unstable. However, due to its complexity, it is felt that the Martin model is very impractical to use, especially when the inlet moves through various operating points during the course of flight. Furthermore, it is the opinion of this author that the Martin model is developed from the viewpoint of a computer programmer and not of a control engineer. Therefore, it is felt that

Reproduced with permission of the copyright owner. Further reproduction prohibited without permission.

although this model can be used for control system evaluation, its use in control design seems somewhat limited.

3.7 Concluding Remarks

In this chapter, a review of inlet modeling techniques was presented. Some techniques yielded low order models while others high order models. In general, it can be said that the overall system performance can be understood easier when the system order is small rather than when one deals with hundreds, thousands, or perhaps millions of states.

Also, linearized models tend to be easier to work with, although, they have the disadvantage that they are small perturbation models. This implies that these models are more suited for control system design where the states are regulated around some point inside the operating envelop and large perturbations are not allowed.

As far as numerical methods are concerned, in the past, the greatest difficulty one encountered, while dealing with nonlinear problems, was to verify that the computed results were accurate. Often times, the numerical computation of a boundary value problem became an instability investigation problem! Therefore, it is suggested that to better establish the reliability of the computations, one should compare the computed results with experimental results as frequently as possible.

Finally, in making a choice of the inlet model to be used, one must have a complete knowledge of the intended application. The survey given

Reproduced with permission of the copyright owner. Further reproduction prohibited without permission.

in this chapter is aimed at helping the control engineer to make a good decision. Clearly, the best model should be used, which often results from finding the golden cut of these factors:

A) Ease of computations,

B) Complexity of the resulting controller,

C) Speed of model simulation,

D) Accuracy of model, and

E) Adaptability of the inlet model to perturbations in the operating environment.

The following chapter is the main chapter of this dissertation.

Reproduced with permission of the copyright owner. Further reproduction prohibited without permission.

CHAPTER IV

NEW APPROACHES TO MODELING FLOW PROBLEMS

4.1 Introduction

An important part of an internal propulsion system is a supersonic inlet. An inlet, also called an intake, is an airbreathing device which can be used to convert the kinetic energy of rapidly moving air to potential energy before the air enters the engine. In other words, incoming air enters the upstream end of the inlet and undergoes a compression thus creating a normal shock just aft of the throat of the inlet. The flow then travels through a duct and mixes with injected fuel in the engine to produce an ignition that generates hot gases. Finally, these gases exit the system at high pressure and velocity thus generating a positive thrust that moves the attached vehicle forward.

Inlets may vary in their size, geometry, and special features depending on their intended application. Thus, over the years there have been developed many mathematical models to describe the operation of inlet systems such as supersonic inlets, ramjets, and scramjets. Furthermore, each resulting model is only good for the class of inlet systems it was developed for and, in general, models cannot be freely interchanged. For example, a model of a scramjet cannot be used on a

Reproduced with permission of the copyright owner. Further reproduction prohibited without permission.

ramjet system as the operation of these systems is fundamentally different. Nevertheless, the inlet modeling problem can be thought of as an "air-in-a-pipe" problem, where the flow is governed by Euler's equations, a special form of the Navier-Stokes equations that represent non-viscous compressible flow.

A comprehensive literature search on the inlet modeling problem was presented in Chapter 3. The survey covered a variety of inlet models, linear and nonlinear. Some of the models presented were very accurate while others less accurate. Also, some models were easy to obtain by hand while others require use of powerful computing facilities. The review of inlet modeling techniques of Chapter 4 was intended to serve as a background or starting point for improvement of existing approaches to the understanding and modeling of supersonic inlets.

In general, fluid flow is governed by the nonlinear Navier-Stokes equations. For internal flow applications, however, the flow can often be described adequately by a special form of this set of equations, namely, Euler's equations.

The Euler equations are often given in the quasi-one-dimensional form due to the presence of varying area ducts, along with appropriately chosen initial and boundary conditions. Quasi-one dimensional flow occurs in a channel with a small rate of change of cross section (see Figure 4.1) or between nearly parallel streamlines in which case the velocity components normal to the mean flow direction are small compared to the components parallel to the flow direction.

Reproduced with permission of the copyright owner. Further reproduction prohibited without permission.

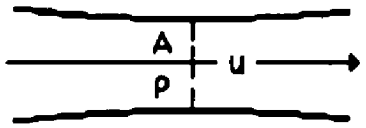


Figure 4.1 A stream tube

The resulting set of equations is nonlinear and includes equations for conservation of mass, conservation of momentum, and conservation of energy. This formulation is more accurate than the one-dimensional set of Euler's equations as it takes into account the cross-sectional area, A(x), of the inlet as the following equations illustrate.

Continuity Equation

$$\frac{\partial(\rho\, A(x))}{\partial t} + \frac{\partial(\rho\, u\, A(x))}{\partial x} = M_s \qquad (4.1)$$

Conservation of Momentum Equation

$$\frac{\partial(\rho\, u\, A(x))}{\partial t} + \frac{\partial[A(x)(p + \rho\, u^2)]}{\partial x} = p\frac{\partial A(x)}{\partial x} + F_s \qquad (4.2)$$

Conservation of Energy Equation

$$\frac{\partial(E_T\, A(x))}{\partial t} + \frac{\partial[A(x)\, u\, (E_T + p)]}{\partial x} = -p\,\frac{\partial A(x)}{\partial t} + Q_s \qquad (4.3)$$

where,

ρ = density,

Reproduced with permission of the copyright owner. Further reproduction prohibited without permission.

A = channel cross section area,

u = velocity vector,

p = pressure,

$E_T = \rho \left(C_v T + \frac{1}{2} u^2 \right)$ = stagnation (total) energy,

M_S = mass bleed term,

F_S = friction term + mass bleed momentum term,

Q_S = heat transfer term + mass bleed energy term.

Over the years, many different approaches have been used for solving the Euler set of equations which result in inlet models of varying degree of accuracy. Also, some of the models developed were better for time domain computations while others were more suitable for frequency-domain calculations. These techniques were presented in some detail in Chapter 4 and generated the following four major classes of inlet models:

A. Low Order Linear Models,

B. High Order Linear Models,

C. Low Order Nonlinear Models, and

D. High Order Nonlinear Models.

Some of the techniques used for the development of inlet models are as follows:

Reproduced with permission of the copyright owner. Further reproduction prohibited without permission.

1. Computational Fluid Dynamics,
2. The Physical Lumping Technique,
3. The Split Flux Approach,
4. Input-Output Identification Techniques,
5. The Meromorphic Transfer Function Approach,
6. The Cole-Willoh Approach,
7. The Equivalent Circuit Modeling Approach,
8. The Hydraulic Analogies Approach,
9. The Schwarz-Christoffel Transformation Technique, and
10. The Bond Graph Technique.

Using model reduction techniques, several models--which belong to the four major classes discussed above--of varying degree of accuracy as well as complexity can be generated. Each model was discussed in some detail in Chapter 4, however, if a more complete description is desired one has to resort to the original references where the inlet models were first developed.

Clearly, in order to select the best model, the control engineer must balance speed with accuracy and userfriendliness with cost. In order to accomplish this, it will be necessary to know what the indented use of the model is; for example, control system assessment, control system design, or

Reproduced with permission of the copyright owner. Further reproduction prohibited without permission.

simply studing the physics of the problem. It must also be made clear that the models mentioned above were developed by ignoring the influence of chemical reactions to the flow as well as boundary layer, viscous and other real gas effects. Usually, these highly nonlinear effects are very important for high speed flows but will be ignored for the relatively low Mach number flows ($M \leq 5$) that we deal with in this project.

If it is assumed that any perturbation in the flow field is small, a linearized set of equations results. Furthermore, if it is also assumed that any energy wave is insignificant, then the conservation of energy equation can be eliminated from the set. This situation is called *isentropic flow*, as the entropy remains constant in the flow field. The resulting system is termed a two-wave system and the describing linearized equations are:

$$\frac{\partial u}{\partial t} + \bar{u}\frac{\partial u}{\partial x} + \frac{c^2}{\bar{\rho}}\frac{\partial \rho}{\partial x} = f_u$$

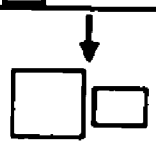
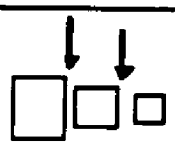
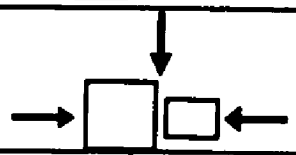
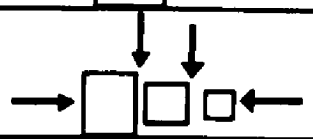
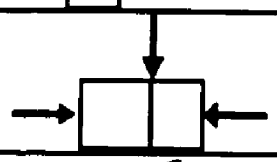
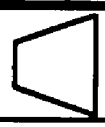
$$\frac{\partial \rho}{\partial t} + \bar{\rho}\frac{\partial u}{\partial x} + \bar{u}\frac{\partial \rho}{\partial x} = f_\rho \qquad (4.4)$$

where, u is the flow velocity, ρ is the density of the medium, the f's are spatially distributed inputs, c is the speed of sound, and the barred variables represent the fixed points around which these equations were linearized.

For the remaining of this chapter, several two- and three-wave theoretical and practical problems based on (4.1)-(4.4) will be studied. The main objective is to develop transfer functions for the flow vector in the Laplace domain as a function of the downstream distance, x. Finally, Table 4.1 outlines the various problems to be studied.

Reproduced with permission of the copyright owner. Further reproduction prohibited without permission.

Table 4.1 Outline of research

Section	Title	Visual Representation
2	The Free-Space Problem	
3	The Bounded Problem	
4	The Two-Channel Free-Space Problem	
5	The N-Channel Free-Space Problem	
6	The Two-Channel Bounded Problem	
7	The N-Channel Bounded Problem	
8	The Two-Channel with Internal Input Free-Space Problem	
9	The N-Channel with Internal Inputs Free-Space Problem	
10	The Two-Channel with Internal Input Bounded Problem	
11	The N-Channel with Internal Inputs Bounded Problem	
12	The Green's Function Problem	
13	The Channel with Exponential Cross-Sectional Area Free-Space Problem	

Reproduced with permission of the copyright owner. Further reproduction prohibited without permission.

4.2 The Free-Space Problem

In this section, one of the basic problems of this research will be addressed, namely *the free-space problem.* This problem is called *free-space* because the linearized set of Euler equations of (4.1)-(4.3) will be solved in free-space, i.e., without imposing any boundary conditions. A brief sketch of this problem is shown in the following figure, which portrays graphically an open flow channel of some finite length L.

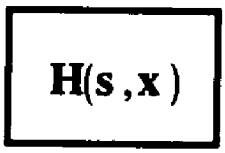


Figure 4.2 The free-space problem

The solution sought is the response of the system at some arbitrary downstream distance x to an arbitrary input at the upstream end of the inlet, namely at x=0. Thus, the resulting open loop or free-space transfer function of the system, H(s,x), must be computed. This section presents a computation of H(s,x) first for the two-wave system and then for the three-wave system.

Knowing the free-space transfer function matrix, H(s,x), will be helpful in computing the responses of more complex systems such as those

Reproduced with permission of the copyright owner. Further reproduction prohibited without permission.

involving multiple lumps or additional external or internal input signals. Also, understanding the dynamics of the open loop system will enable the control engineer to draw useful conclusions about the system behavior and also to tackle more complex problems to be discussed in subsequent sections.

A. The Two-Wave Problem

Using zero initial conditions and Laplace-transforming the system of (4.4) yields:

$$\begin{aligned} s\,u(s,x)+\bar{u}\frac{\partial u(s,x)}{\partial x}+\frac{c^2}{\bar{\rho}}\frac{\partial \rho(s,x)}{\partial x} &= f_u \\ s\,\rho(s,x)+\bar{\rho}\frac{\partial u(s,x)}{\partial x}+\bar{u}\frac{\partial \rho(s,x)}{\partial x} &= f_\rho \end{aligned} \qquad (4.5)$$

where the barred variables are the fixed points around which a small perturbation model of the system is to be obtained. Setting $f_u=f_\rho=0$ in (4.5) and using matrix notation the above system becomes,

$$A\frac{\partial \underline{u}(s,x)}{\partial x}+B\,\underline{u}(s,x)=0 \qquad (4.6)$$

where, the following definitions have been used,

$$A=\begin{bmatrix} \bar{u} & \frac{c^2}{\bar{\rho}} \\ \bar{\rho} & \bar{u} \end{bmatrix},\quad \underline{u}=\begin{bmatrix} u(s,x) \\ \rho(s,x) \end{bmatrix},\quad B=\begin{bmatrix} s & o \\ o & s \end{bmatrix}.$$

Reproduced with permission of the copyright owner. Further reproduction prohibited without permission.

It can be seen that the eigenvalues of A are both real and distinct: $\lambda_1=u+c$ and $\lambda_2=u-c$. Thus, the linearized system is termed strictly hyperbolic. Furthermore, unless u=c, A is always nonsingular and the system of (4.3) can be rewritten as follows,

$$\frac{\partial \underline{u}(s, x)}{\partial x} + A^{-1}B\, \underline{u}(s, x) = 0. \qquad (4.7)$$

A finite difference solution for the propagation of sound in near sonic flows was presented in [HL84]. In this study, it will be assumed that $u \neq c$. Hence, the solution of (4.7) will be given by the following expression:

$$\underline{u}(s, x) = e^{-A^{-1}Bx}\, \underline{u}(s, 0) = H(s, x)\, \underline{u}(s, 0) = H(s, x)\, \underline{u}_{us} \qquad (4.8)$$

where, H(s,x) is called the open loop or *free-space* transfer function matrix of the system and $\underline{u}(s, 0)$ represents an excitation at the upstream section of the flow channel or at x=0. Thus, one must compute $e^{-A^{-1}Bx}$. This is shown in the following subsection.

COMPUTATION OF $e^{-A^{-1}Bx}$

From the previous section recall that,

$$A = \begin{bmatrix} \bar{u} & \frac{c^2}{\bar{\rho}} \\ \bar{\rho} & \bar{u} \end{bmatrix}, \qquad B = \begin{bmatrix} s & 0 \\ 0 & s \end{bmatrix}$$

Reproduced with permission of the copyright owner. Further reproduction prohibited without permission.

and also note that the inverse of A is,

$$A^{-1} = \frac{1}{\bar{u}^2 - c^2}\begin{bmatrix} \bar{u} & -\frac{c^2}{\bar{\rho}} \\ -\bar{\rho} & \bar{u} \end{bmatrix}.$$

Therefore,

$$-A^{-1}B = \frac{-1}{\bar{u}^2 - c^2}\begin{bmatrix} \bar{u} & -\frac{c^2}{\bar{\rho}} \\ -\bar{\rho} & \bar{u} \end{bmatrix}\begin{bmatrix} s & 0 \\ 0 & s \end{bmatrix}$$

$$= \frac{-1}{\bar{u}^2 - c^2}\begin{bmatrix} \bar{u}s & -\frac{c^2}{\bar{\rho}}s \\ -\bar{\rho}s & \bar{u}s \end{bmatrix} = \frac{1}{c^2 - \bar{u}^2}\begin{bmatrix} \bar{u}s & -\frac{c^2}{\bar{\rho}}s \\ -\bar{\rho}s & \bar{u}s \end{bmatrix}.$$

Next let $\tilde{A} = -A^{-1}B$. Then the matrix exponential can be computed by the following formula:

$$e^{-A^{-1}Bx} = e^{\tilde{A}x} = L^{-1}\left\{\left[\tilde{p}\,I - \tilde{A}\right]^{-1}\right\}. \qquad (4.9)$$

However,

$$\left[\tilde{p}\,I - \tilde{A}\right]^{-1} = \left\{\begin{bmatrix} \tilde{p} & 0 \\ 0 & \tilde{p} \end{bmatrix} - \begin{bmatrix} \frac{\bar{u}s}{c^2 - \bar{u}^2} & \frac{-c^2 s}{\bar{\rho}(c^2 - \bar{u}^2)} \\ \frac{-\bar{\rho}s}{c^2 - \bar{u}^2} & \frac{\bar{u}s}{c^2 - \bar{u}^2} \end{bmatrix}\right\}^{-1}$$

Reproduced with permission of the copyright owner. Further reproduction prohibited without permission.

$$= \begin{bmatrix} \tilde{p} - \frac{\bar{u}\,s}{c^2 - \bar{u}^2} & \frac{c^2 s}{\bar{\rho}\,(c^2 - \bar{u}^2)} \\ \frac{\bar{\rho}\,s}{c^2 - \bar{u}^2} & \tilde{p} - \frac{\bar{u}\,s}{c^2 - \bar{u}^2} \end{bmatrix}^{-1}$$

$$= \frac{\begin{bmatrix} \tilde{p} - \frac{\bar{u}\,s}{c^2 - \bar{u}^2} & \frac{-c^2 s}{\bar{\rho}\,(c^2 - \bar{u}^2)} \\ \frac{-\bar{\rho}\,s}{c^2 - \bar{u}^2} & \tilde{p} - \frac{\bar{u}\,s}{c^2 - \bar{u}^2} \end{bmatrix}}{\left(\tilde{p} - \frac{\bar{u}\,s}{c^2 - \bar{u}^2}\right)^2 - \frac{\bar{\rho}\,s}{c^2 - \bar{u}^2}\frac{c^2 s}{\bar{\rho}\,(c^2 - \bar{u}^2)}}$$

$$= \frac{\begin{bmatrix} \tilde{p} - \frac{\bar{u}\,s}{c^2 - \bar{u}^2} & \frac{-c^2 s}{\bar{\rho}\,(c^2 - \bar{u}^2)} \\ \frac{-\bar{\rho}\,s}{c^2 - \bar{u}^2} & \tilde{p} - \frac{\bar{u}\,s}{c^2 - \bar{u}^2} \end{bmatrix}}{\left(\tilde{p} - \frac{\bar{u}\,s}{c^2 - \bar{u}^2}\right)^2 - \left[\frac{c\,s}{(c^2 - \bar{u}^2)}\right]^2}$$

$$= \begin{bmatrix} \frac{\tilde{p} - \frac{\bar{u}\,s}{c^2 - \bar{u}^2}}{\left(\tilde{p} - \frac{\bar{u}\,s}{c^2 - \bar{u}^2}\right)^2 - \left[\frac{c\,s}{(c^2 - \bar{u}^2)}\right]^2} & \frac{\frac{-c^2 s}{\bar{\rho}\,(c^2 - \bar{u}^2)}}{\left(\tilde{p} - \frac{\bar{u}\,s}{c^2 - \bar{u}^2}\right)^2 - \left[\frac{c\,s}{(c^2 - \bar{u}^2)}\right]^2} \\ \frac{\frac{-\bar{\rho}\,s}{c^2 - \bar{u}^2}}{\left(\tilde{p} - \frac{\bar{u}\,s}{c^2 - \bar{u}^2}\right)^2 - \left[\frac{c\,s}{(c^2 - \bar{u}^2)}\right]^2} & \frac{\tilde{p} - \frac{\bar{u}\,s}{c^2 - \bar{u}^2}}{\left(\tilde{p} - \frac{\bar{u}\,s}{c^2 - \bar{u}^2}\right)^2 - \left[\frac{c\,s}{(c^2 - \bar{u}^2)}\right]^2} \end{bmatrix}.$$

Using the following parameters,

$$\alpha = \frac{\bar{u}\,s}{c^2 - \bar{u}^2} \qquad (4.10)$$

Reproduced with permission of the copyright owner. Further reproduction prohibited without permission.

$$\beta^2 = -\left[\frac{c\,s}{(c^2 - \bar{u}^2)}\right]^2 \Rightarrow \beta = j\left[\frac{c\,s}{(c^2 - \bar{u}^2)}\right] \tag{4.11}$$

$$\xi = \frac{-c^2 s}{\bar{\rho}(c^2 - \bar{u}^2)} \tag{4.12}$$

and,

$$\delta = \frac{-\bar{\rho}\,s}{c^2 - \bar{u}^2}\,. \tag{4.13}$$

yields,

$$\frac{\xi}{\beta} = \frac{-c^2 s}{\bar{\rho}(c^2 - \bar{u}^2)} \frac{c^2 - \bar{u}^2}{j\,c\,s} = \frac{j\,c}{\bar{\rho}}$$

and,

$$\frac{\delta}{\beta} = \frac{-\bar{\rho}\,s}{c^2 - \bar{u}^2} \frac{c^2 - \bar{u}^2}{j\,c\,s} = \frac{j\,\bar{\rho}}{c}\,.$$

Thus, the matrix exponential becomes:

$$e^{-A^{-1}Bx} = L^{-1}\left\{\begin{bmatrix} \dfrac{\tilde{p} - \alpha}{(\tilde{p} - \alpha)^2 + \beta^2} & \dfrac{\frac{\xi}{\beta}\beta}{(\tilde{p} - \alpha)^2 + \beta^2} \\ \dfrac{\frac{\delta}{\beta}\beta}{(\tilde{p} - \alpha)^2 + \beta^2} & \dfrac{\tilde{p} - \alpha}{(\tilde{p} - \alpha)^2 + \beta^2} \end{bmatrix}\right\}$$

$$= \begin{bmatrix} e^{\alpha x}\cos(\beta x) & \frac{\xi}{\beta} e^{\alpha x}\sin(\beta x) \\ \frac{\delta}{\beta} e^{\alpha x}\sin(\beta x) & e^{\alpha x}\cos(\beta x) \end{bmatrix} = e^{\alpha x}\begin{bmatrix} \cos(\beta x) & \frac{\xi}{\beta}\sin(\beta x) \\ \frac{\delta}{\beta}\sin(\beta x) & \cos(\beta x) \end{bmatrix}$$

Reproduced with permission of the copyright owner. Further reproduction prohibited without permission.

$$= \exp\left(\frac{\bar{u}\,s}{c^2 - \bar{u}^2}\,x\right)\begin{bmatrix} \cos\left(j\,\frac{c\,s}{c^2 - \bar{u}^2}\,x\right) & \frac{j\,c}{\bar{\rho}}\sin\left(j\,\frac{c\,s}{c^2 - \bar{u}^2}\,x\right) \\ \frac{j\,\bar{\rho}}{c}\sin\left(j\,\frac{c\,s}{c^2 - \bar{u}^2}\,x\right) & \cos\left(j\,\frac{c\,s}{c^2 - \bar{u}^2}\,x\right) \end{bmatrix}$$

$$= \exp\left(\frac{\bar{u}\,s}{c^2 - \bar{u}^2}\,x\right)\begin{bmatrix} \cosh\left(\frac{c\,s}{c^2 - \bar{u}^2}\,x\right) & \frac{-c}{\bar{\rho}}\sinh\left(\frac{c\,s}{c^2 - \bar{u}^2}\,x\right) \\ \frac{-\bar{\rho}}{c}\sinh\left(\frac{c\,s}{c^2 - \bar{u}^2}\,x\right) & \cosh\left(\frac{c\,s}{c^2 - \bar{u}^2}\,x\right) \end{bmatrix}.$$

Thus, H(s,x) is given analytically by the following expression,

$$H(s, x) = \exp\left(\frac{\bar{u}\,s\,x}{c^2 - \bar{u}^2}\right)\begin{bmatrix} \cosh\left(\frac{c\,s\,x}{c^2 - \bar{u}^2}\right) & \frac{-c}{\bar{\rho}}\sinh\left(\frac{c\,s\,x}{c^2 - \bar{u}^2}\right) \\ \frac{-\bar{\rho}}{c}\sinh\left(\frac{c\,s\,x}{c^2 - \bar{u}^2}\right) & \cosh\left(\frac{c\,s\,x}{c^2 - \bar{u}^2}\right) \end{bmatrix}. \qquad (4.14)$$

Note that the existence of hyperbolic functions in H(s,x) is an indication that the resulting transfer function for the system under study is infinite-dimensional since it has an infinite number of poles and zeros.

B. The Three-Wave Problem

In the foregoing section the solution to the two-wave free-space problem was presented. This section deals with the three-wave extension of the problem. The governing equations defined in Section 2.2 can be put in the following equivalent forms:

Reproduced with permission of the copyright owner. Further reproduction prohibited without permission.

$$\frac{\partial}{\partial t}\begin{bmatrix}\rho\\ \rho u\\ \rho E\end{bmatrix}+\frac{\partial}{\partial x}\begin{bmatrix}\rho u\\ \rho u^2+p\\ \rho uH\end{bmatrix}=\begin{bmatrix}0\\ f_{ex}\\ W_f\end{bmatrix} \tag{4.15}$$

or,

$$\frac{\partial}{\partial t}\begin{bmatrix}\rho\\ \rho u\\ \rho E\end{bmatrix}+\frac{\partial}{\partial x}\begin{bmatrix}\rho u\\ \rho u^2+p\\ \rho u\left(E+\frac{p}{\rho}\right)\end{bmatrix}=\begin{bmatrix}0\\ f_{ex}\\ W_f\end{bmatrix} \tag{4.16}$$

or,

$$\frac{\partial}{\partial t}\begin{bmatrix}\rho\\ \rho u\\ \rho E\end{bmatrix}+\frac{\partial}{\partial x}\begin{bmatrix}\rho u\\ \rho u^2+\rho(\gamma-1)\left(E-\frac{1}{2}u^2\right)\\ \rho uE+u\rho(\gamma-1)\left(E-\frac{1}{2}u^2\right)\end{bmatrix}=\begin{bmatrix}0\\ f_{ex}\\ W_f\end{bmatrix} \tag{4.17}$$

or, using vector notation,

$$\frac{\partial Q}{\partial t}+\frac{\partial F}{\partial x}=W \tag{4.18}$$

with,

$$Q=\begin{bmatrix}\rho\\ \rho u\\ \rho E\end{bmatrix}\qquad F=\begin{bmatrix}\rho u\\ \rho u^2+\rho(\gamma-1)\left(E-\frac{1}{2}u^2\right)\\ \rho uE+u\rho(\gamma-1)\left(E-\frac{1}{2}u^2\right)\end{bmatrix}\qquad W=\begin{bmatrix}0\\ f_{ex}\\ W_f\end{bmatrix}.$$

Reproduced with permission of the copyright owner. Further reproduction prohibited without permission.

If one lets,

$$Q = \begin{bmatrix} Q_1 \\ Q_2 \\ Q_3 \end{bmatrix} = \begin{bmatrix} \text{density} \\ \text{momentum} \\ \text{energy} \end{bmatrix}$$

then the dependent variables ρ, u, and E in terms of Q_1, Q_2, and Q_3, are given by the following expressions:

$$\rho = Q_1$$

$$u = \frac{Q_2}{Q_1}$$

$$E = \frac{Q_3}{Q_1} .$$

Linearizing the set of governing equations produces the following expression:

$$\frac{\partial Q}{\partial t} + \frac{\partial F}{\partial Q}\frac{\partial Q}{\partial x} = W \qquad (4.19)$$

where the system Jacobian matrix, J, is given by:

$$J = \frac{\partial F}{\partial Q} = \frac{\partial}{\partial Q}\begin{bmatrix} Q_2 \\ Q_1^{-1}Q_2^2 + (\gamma-1)Q_3 - \frac{1}{2}(\gamma-1)Q_1^{-1}Q_2^2 \\ Q_1^{-1}Q_2Q_3 + Q_1^{-1}Q_2(\gamma-1)Q_3 - \frac{1}{2}(\gamma-1)Q_2^3Q_1^{-2} \end{bmatrix}$$

Reproduced with permission of the copyright owner. Further reproduction prohibited without permission.

$$\Rightarrow J = \frac{\partial F}{\partial Q} = \begin{bmatrix} 0 & 1 & 0 \\ \frac{1}{2}(\gamma - 3)u^2 & -u(\gamma - 3) & \gamma - 1 \\ -\gamma u E + (\gamma - 1)u^3 & \gamma E - \frac{3}{2}(\gamma - 1)u^2 & \gamma u \end{bmatrix}. \qquad (4.20)$$

Clearly, in order to find the eigenvalues of the Jacobian matrix J one must set $|\lambda I - J| = 0$. It is reported in [HOF89] that the three solutions of the resultant cubic characteristic equation are:

$$\lambda_1 = u \qquad (4.21)$$

$$\lambda_2 = u + c \qquad (4.22)$$

$$\lambda_3 = u - c. \qquad (4.23)$$

Furthermore, since all the λ's are real and distinct, the linearized three-wave system is also strictly hyperbolic. Solving the eigenvalue-eigenvector problem the Jacobian matrix can be expressed as follows [HOF89]:

$$J = M\Lambda M^{-1}, \qquad (4.24)$$

where, Λ is the diagonal matrix containing the eigenvalues of the linearized system along its diagonal, i.e.,

$$\Lambda = \begin{bmatrix} \lambda_1 & 0 & 0 \\ 0 & \lambda_2 & 0 \\ 0 & 0 & \lambda_3 \end{bmatrix} = \begin{bmatrix} u & 0 & 0 \\ 0 & u+\lambda & 0 \\ 0 & 0 & u-\lambda \end{bmatrix} \qquad (4.25)$$

and M is the modal matrix containing as its columns the three eigenvectors

Reproduced with permission of the copyright owner. Further reproduction prohibited without permission.

of the linearized system, namely, X_1, X_2, and X_3 as follows:

$$M = [X_1, X_2, X_3].$$

Incidentally, M is given by:

$$M = \begin{bmatrix} 1 & \alpha & \alpha \\ u & (u+c)\alpha & (u-c)\alpha \\ \frac{1}{2}u^2 & \left(\frac{1}{2}u^2+uc+\frac{c^2}{\gamma-1}\right)\alpha & \left(\frac{1}{2}u^2-uc+\frac{c^2}{\gamma-1}\right)\alpha \end{bmatrix} \qquad (4.26)$$

where the parameter α is defined as,

$$\alpha = \frac{\rho}{c\sqrt{2}}. \qquad (4.27)$$

Then M^{-1} is,

$$M^{-1} = \begin{bmatrix} 1-\frac{u^2(\gamma-1)}{2c^2} & \frac{(\gamma-1)u}{c^2} & -\frac{(\gamma-1)}{c^2} \\ \beta\left[(\gamma-1)\frac{u^2}{2} - uc\right] & \beta[c-(\gamma-1)u] & \beta(\gamma-1) \\ \beta\left[(\gamma-1)\frac{u^2}{2} + uc\right] & -\beta[c+(\gamma-1)u] & \beta(\gamma-1) \end{bmatrix} \qquad (4.28)$$

where the parameter β is defined as follows:

$$\beta = \frac{1}{\rho c\sqrt{2}}. \qquad (4.29)$$

Next, let's return our attention to the three-wave homogeneous system. Recall that the governing equation in vector form is:

$$\frac{\partial Q(x,t)}{\partial t} + J\frac{\partial Q(x,t)}{\partial x} = 0 \qquad (4.30)$$

Reproduced with permission of the copyright owner. Further reproduction prohibited without permission.

where J was computed above. Using the following change of variables,

$$Q(x,t) = M\, z(x,t) \tag{4.31}$$

results into the following equation:

$$\frac{\partial z(x,t)}{\partial t} + M^{-1}JM \frac{\partial z(x,t)}{\partial x} = 0$$

which is equivalent to,

$$\frac{\partial z(x,t)}{\partial t} + \Lambda \frac{\partial z(x,t)}{\partial x} = 0 \tag{4.32}$$

since, $\Lambda = M^{-1}JM = Diag[\lambda_1, \lambda_2, \lambda_3]$.

Next Laplace-transforming the above system with respect to the time variable, t, yields:

$$s\, Z(x,s) - z(x,0) = - \Lambda \frac{\partial Z(x,s)}{\partial x}$$

where Z(x,s) is the Laplace transform of z(x,t) and s is the Laplace transform of the time variable t. Assuming zero initial conditions, i.e., z(x,0)=0 simplifies this equation as follows:

$$s\, Z(x,s) = - \Lambda \frac{\partial Z(x,s)}{\partial x}$$

from which the following linear differential equation with constant

Reproduced with permission of the copyright owner. Further reproduction prohibited without permission.

coefficients is derived:

$$\frac{\partial Z(x,s)}{\partial x} + s\,\Lambda^{-1}\,Z(x,s) = 0.$$

Again, Laplace-transforming the above equation with respect to the space variable, x, yields:

$$\tilde{p}\,\tilde{Z}(\tilde{p},s) - Z(0,s) = -\,s\,\Lambda^{-1}\,\tilde{Z}(\tilde{p},s)$$

where, $\tilde{Z}(\tilde{p},s)$ is the Laplace transform of $Z(x,s)$ with respect to the space variable, x, and $\tilde{p}$ is the Laplace transform of the space variable x. Note the deliberate use of (~) to avoid confusion of the Laplace-transform variable with the thermodynamic variable of pressure. Solving the last equation for $\tilde{Z}(\tilde{p},s)$ yields:

$$\tilde{Z}(\tilde{p},s) = \tilde{T}(\tilde{p},s)Z(0,s)$$

where, $\tilde{T}(\tilde{p},s)$ is the transfer function matrix of the system in the new coordinates given by:

$$\tilde{T}(\tilde{p},s) = \left[\tilde{p}I + s\,\Lambda^{-1}\right]^{-1}$$

$$= \begin{bmatrix} \tilde{p}+\frac{s}{u} & 0 & 0 \\ 0 & \tilde{p}+\frac{s}{u+c} & 0 \\ 0 & 0 & \tilde{p}+\frac{s}{u-c} \end{bmatrix}^{-1} = \begin{bmatrix} \frac{1}{\tilde{p}+\frac{s}{u}} & 0 & 0 \\ 0 & \frac{1}{\tilde{p}+\frac{s}{u+c}} & 0 \\ 0 & 0 & \frac{1}{\tilde{p}+\frac{s}{u-c}} \end{bmatrix}.$$

Reproduced with permission of the copyright owner. Further reproduction prohibited without permission.

Finally, returning to the original coordinate system yields,

$$\tilde{Z}(\tilde{p},s) = \tilde{T}(\tilde{p},s)Z(0,s)$$

$$\Rightarrow M^{-1}\tilde{Q}(\tilde{p},s) = \tilde{T}(\tilde{p},s)M^{-1}Q(0,s)$$

$$\Rightarrow \tilde{Q}(\tilde{p},s) = M\tilde{T}(\tilde{p},s)M^{-1}Q(0,s)$$

$$\Rightarrow \tilde{Q}(\tilde{p},s) = \tilde{H}(\tilde{p},s)Q(0,s)$$

where, $\tilde{H}(\tilde{p},s)$ is the transfer function matrix of the three-wave system in the original set of coordinates and is given by:

$$\tilde{H}(\tilde{p},s) = M\tilde{T}(\tilde{p},s)M^{-1}. \qquad (4.33)$$

Computation of H(x,s)

Finally, in order to compute the transfer function of the three-wave system, $\tilde{H}(\tilde{p},s)$ must first be computed. This is shown below.

First recall that, $H(x,s) = L^{-1}\{\tilde{H}(\tilde{p},s)\}$, where the inverse Laplace-transform is taken with respect to the complex space variable $\tilde{p}$. Since M and M^{-1} are independent of $\tilde{p}$, one can safely perform the following computations:

Reproduced with permission of the copyright owner. Further reproduction prohibited without permission.

$$
\begin{aligned}
H(x,s) &= L^{-1}\left\{\tilde{H}(\tilde{p},s)\right\} \\
&= L^{-1}\left\{M\tilde{T}(\tilde{p},s)M^{-1}\right\} \\
&= ML^{-1}\left\{\tilde{T}(\tilde{p},s)\right\}M^{-1} \\
&= MT(x,s)M^{-1}.
\end{aligned}
$$

Since,

$$
T(x,s) = L^{-1}\left\{\tilde{T}(\tilde{p},s)\right\} = L^{-1}\left\{\begin{bmatrix} \frac{1}{\tilde{p}+\frac{s}{u}} & 0 & 0 \\ 0 & \frac{1}{\tilde{p}+\frac{s}{u+c}} & 0 \\ 0 & 0 & \frac{1}{\tilde{p}+\frac{s}{u-c}} \end{bmatrix}\right\} = \begin{bmatrix} e^{-\frac{sx}{u}} & 0 & 0 \\ 0 & e^{-\frac{sx}{u+c}} & 0 \\ 0 & 0 & e^{-\frac{sx}{u-c}} \end{bmatrix},
$$

H(x,s) is given by,

$$
H(x,s) = MT(x,s)M^{-1} = \begin{bmatrix} e^{-\frac{sx}{u}} & \alpha e^{-\frac{sx}{u+c}} & \alpha e^{-\frac{sx}{u-c}} \\ ue^{-\frac{sx}{u}} & (u+c)\alpha e^{-\frac{sx}{u+c}} & (u-c)\alpha e^{-\frac{sx}{u-c}} \\ \frac{u^2 e^{-\frac{sx}{u}}}{2} & \left(\frac{1}{2}u^2+uc+\frac{c^2}{\gamma-1}\right)\alpha e^{-\frac{sx}{u+c}} & \left(\frac{1}{2}u^2-uc+\frac{c^2}{\gamma-1}\right)\alpha e^{-\frac{sx}{u-c}} \end{bmatrix}
$$

Reproduced with permission of the copyright owner. Further reproduction prohibited without permission.

$$\cdot\begin{bmatrix} 1-\frac{u^2(\gamma-1)}{2c^2} & \frac{(\gamma-1)u}{c^2} & -\frac{(\gamma-1)}{c^2} \\ \beta\left[(\gamma-1)\frac{u^2}{2}-uc\right] & \beta[c-(\gamma-1)u] & \beta(\gamma-1) \\ \beta\left[(\gamma-1)\frac{u^2}{2}+uc\right] & -\beta[c+(\gamma-1)u] & \beta(\gamma-1) \end{bmatrix} \qquad (4.34)$$

or, $H(s,x) = [H_{ij}]$, where,

$$H_{11} = \left[1-\frac{u^2(\gamma-1)}{2c^2}\right]e^{-\frac{sx}{u}} + \alpha\beta\left[(\gamma-1)\frac{u^2}{2}-uc\right]e^{-\frac{sx}{u+c}} + \alpha\beta\left[(\gamma-1)\frac{u^2}{2}+uc\right]e^{-\frac{sx}{u-c}},$$

$$H_{12} = \frac{(\gamma-1)u}{c^2}e^{-\frac{sx}{u}} + \alpha\beta[c-(\gamma-1)u]e^{-\frac{sx}{u+c}} - \alpha\beta[c+(\gamma-1)u]e^{-\frac{sx}{u-c}},$$

$$H_{13} = -\frac{(\gamma-1)}{c^2}e^{-\frac{sx}{u}} + \alpha\beta(\gamma-1)e^{-\frac{sx}{u+c}} + \alpha\beta(\gamma-1)e^{-\frac{sx}{u-c}},$$

$$H_{21} = u\left[1-\frac{u^2(\gamma-1)}{2c^2}\right]e^{-\frac{sx}{u}} + (u+c)\alpha\beta\left[(\gamma-1)\frac{u^2}{2}-uc\right]e^{-\frac{sx}{u+c}} + (u-c)\alpha\beta\left[(\gamma-1)\frac{u^2}{2}+uc\right]e^{-\frac{sx}{u-c}},$$

$$H_{22} = \frac{u^2}{c^2}(\gamma-1)e^{-\frac{sx}{u}} + (u+c)\alpha\beta[c-(\gamma-1)u]e^{-\frac{sx}{u+c}} - (u-c)\alpha\beta[c+(\gamma-1)u]e^{-\frac{sx}{u-c}},$$

$$H_{23} = -\frac{(\gamma-1)}{c^2}ue^{-\frac{sx}{u}} + (u+c)\alpha\beta(\gamma-1)e^{-\frac{sx}{u+c}} + (u-c)\alpha\beta(\gamma-1)e^{-\frac{sx}{u-c}},$$

$$H_{31} = \frac{u^2}{2}\left[1-\frac{u^2(\gamma-1)}{2c^2}\right]e^{-\frac{sx}{u}} + \left(\frac{1}{2}u^2+uc+\frac{c^2}{\gamma-1}\right)\alpha\beta\left[(\gamma-1)\frac{u^2}{2}-uc\right]e^{-\frac{sx}{u+c}}$$

$$+\left(\frac{1}{2}u^2-uc+\frac{c^2}{\gamma-1}\right)\alpha\beta\left[(\gamma-1)\frac{u^2}{2}+uc\right]e^{-\frac{sx}{u-c}},$$

Reproduced with permission of the copyright owner. Further reproduction prohibited without permission.

$$H_{32} = \frac{u^2(\gamma-1)u}{2\ c^2}e^{-\frac{sx}{u}} + \left(\frac{1}{2}u^2+uc+\frac{c^2}{\gamma-1}\right)\alpha\beta[c-(\gamma-1)u]e^{-\frac{sx}{u+c}}$$

$$-\left(\frac{1}{2}u^2-uc+\frac{c^2}{\gamma-1}\right)\alpha\beta[c+(\gamma-1)u]e^{-\frac{sx}{u-c}},$$

$$H_{33} = -\frac{u^2(\gamma-1)}{2c^2}e^{-\frac{sx}{u}} + \left(\frac{1}{2}u^2+uc+\frac{c^2}{\gamma-1}\right)\alpha\beta(\gamma-1)e^{-\frac{sx}{u+c}} + \left(\frac{1}{2}u^2-uc+\frac{c^2}{\gamma-1}\right)\alpha\beta(\gamma-1)e^{-\frac{sx}{u-c}}.$$

It can be seen that the transfer function matrix for the three-wave system is made up of functions of the following form,

$$H(x,s) = A\ e^{-ax} + B\ e^{-bx} + C\ e^{-cx}, \qquad (4.35)$$

where, A, B, and C are 3×3 matrices. At a first look, these functions can be thought of as extensions of hyperbolic trigonometric functions. Since little prior work has been done on this subject, the behavior of this type of functions is, in general, unknown at this point. Thus, further research is needed in order to determine the properties of this set of functions, which is very common in engineering applications.

In conclusion, in this section the two- and three-wave free-space was solved using Laplace transform theory. If boundary conditions are applied to the free-space problem, then one arrives at the bounded problem. This problem is discussed in the following section.

Reproduced with permission of the copyright owner. Further reproduction prohibited without permission.

4.3 The Bounded Problem

In the previous section, a solution of the *free-space problem* was presented. In most real systems, however, specific boundary conditions must be imposed to the governing equations in order for a solution to have any physical significance. Hence, we arrive at the *bounded problem,* which is shown in the figure below.

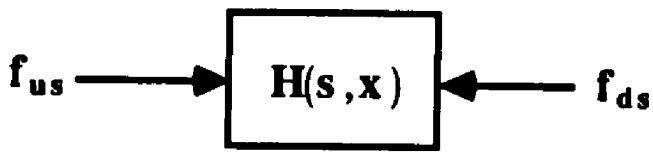


Figure 4.3 The bounded problem

The arrows at both ends of the flow channel indicate that some boundary constraints will be imposed on the describing flow equations of (4.1). In the inlet system, a normal shock will be placed at the upstream boundary in addition to any additional upstream inputs, which can be used to represent perturbations in the free stream atmosphere or control inputs. Also, the boundary condition at the downstream boundary will be simply reflective and perturbation inputs included at that boundary to represent compressor or combustor signals. This situation is depicted in Figure 4.4.

Reproduced with permission of the copyright owner. Further reproduction prohibited without permission.

The sought solution of the bounded problem will be the response of the system at some downstream distance x due to any arbitrary inputs at the upstream and downstream boundaries. Once the transfer function is known, then the response of the system at x=0 can be studied and the effect of changes of the normal shock characteristics as well as the influence of the reflection properties of the downstream boundary to the overall system performance can be examined.

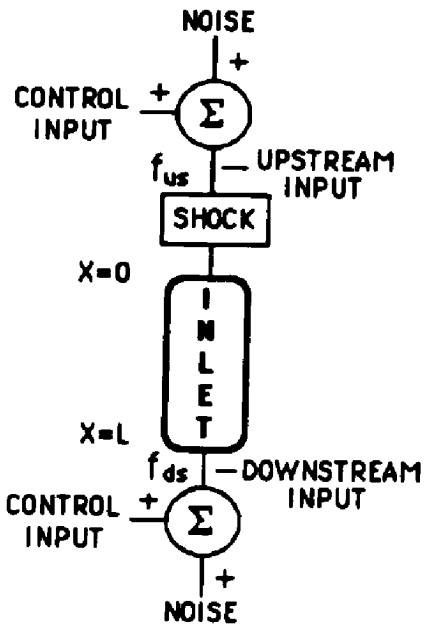


Figure 4.4 A supersonic inlet model

Returning to the system of Figure 4.4, the governing equations with the boundary conditions in a two-wave constant area situation are as follows,

$$\frac{\partial u}{\partial t} + \bar{u}\frac{\partial u}{\partial x} + \frac{\bar{c}^2}{\bar{\rho}}\frac{\partial \rho}{\partial x} = f_u \qquad (4.36)$$

Reproduced with permission of the copyright owner. Further reproduction prohibited without permission.

$$\frac{\partial \rho}{\partial t} + \bar{\rho}\frac{\partial u}{\partial x} + \bar{u}\frac{\partial \rho}{\partial x} = f_\rho \qquad (4.37)$$

$$u_{us} = Z_{us}(s)\,\rho_{us} + f_{us} \qquad (4.38)$$

$$\rho_{ds} = R\,u_{ds} + f_{ds} \qquad (4.39)$$

where, R is a constant representing the reflective boundary and $Z_{us}=Z_{us}(s)$ is a lumped dynamics representing the shock behavior. Furthermore, the boundary conditions given by (4.38) and (4.39) above are illustrated in the following figure.

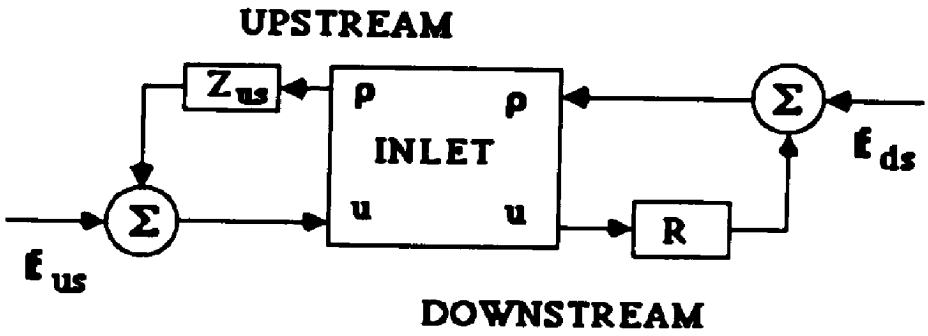


Figure 4.5 A two-wave bounded inlet system

In order to analyze this problem the four system equations and associated boundary conditions described above are Laplace-transformed using zero initial conditions. This process then yields the following set of equations

Reproduced with permission of the copyright owner. Further reproduction prohibited without permission.

$$s\,u(s,x)+\bar{u}\frac{\partial u(s,x)}{\partial x}+\frac{c^2}{\bar{\rho}}\frac{\partial \rho(s,x)}{\partial x}=f_u$$

$$s\,\rho(s,x)+\bar{\rho}\frac{\partial u(s,x)}{\partial x}+\bar{u}\frac{\partial \rho(s,x)}{\partial x}=f_\rho.$$

If $f_u=f_\rho=0$, then using matrix notation the system of (4.36)-(4.37) becomes,

$$A\frac{\partial \underline{u}(s,x)}{\partial x}+B\,\underline{u}(s,x)=0 \qquad (4.40)$$

where,

$$A=\begin{bmatrix}\bar{u} & \frac{c^2}{\bar{\rho}}\\ \bar{\rho} & \bar{u}\end{bmatrix},\quad \underline{u}=\begin{bmatrix}u(s,x)\\ \rho(s,x)\end{bmatrix},\quad B=\begin{bmatrix}s & 0\\ 0 & s\end{bmatrix}.$$

Since the matrix A is nonsingular, the system can be rewritten as,

$$\frac{\partial \underline{u}(s,x)}{\partial x}+A^{-1}B\,\underline{u}(s,x)=0. \qquad (4.41)$$

Next, using the notation of [SF65] the boundary conditions for this system can be expressed as follows,

$$\underbrace{\begin{bmatrix}1 & -Z_{us}\\ 0 & 0\end{bmatrix}}_{M(s)}\underbrace{\begin{bmatrix}u(s,0)\\ \rho(s,0)\end{bmatrix}}_{Q(s,0)}+\underbrace{\begin{bmatrix}0 & 0\\ -R & 1\end{bmatrix}}_{N(s)}\underbrace{\begin{bmatrix}u(s,L)\\ \rho(s,L)\end{bmatrix}}_{Q(s,L)}=\underbrace{\begin{bmatrix}f_{us}\\ f_{ds}\end{bmatrix}}_{Z(s)}$$

or, equivalently,

$$M(s)\,Q(s,0)+N(s)\,Q(s,L)=Z(s). \qquad (4.42)$$

Reproduced with permission of the copyright owner. Further reproduction prohibited without permission.

Finally, using compact notation the last expression becomes,

$$M(s)\, Q_{us} + N(s)\, Q_{ds} = Z(s)$$

where,

$$M(s) = \begin{bmatrix} 1 & -Z_{us} \\ 0 & 0 \end{bmatrix}, \quad N(s) = \begin{bmatrix} 0 & 0 \\ -R & 1 \end{bmatrix}$$

and,

$$Q(s, x) \equiv \underline{u}(s, x) = \begin{bmatrix} u(s, x) \\ \rho(s, x) \end{bmatrix}, \quad Z(s) = \begin{bmatrix} f_{us} \\ f_{ds} \end{bmatrix}.$$

Since $Z(s) \neq 0$, the termination is said to be *nonhomogeneous*. The solution of the free-space system was given in Equations (4.5) and (4.6). Thus, these equations can be used again to derive the transfer function matrix from Z(s) to Q(s,x) with the aid of the following formula, which is derived in reference [SF65],

$$K(s, x) = H(s, x)\left[M(s) + N(s)\, H(s, L)\right]^{-1}. \qquad (4.43)$$

Thus, it can be seen that calculation of K(s,x) requires first computing H(s,L). From (4.14), it follows that,

$$H(s, L) = \exp\left(\frac{\bar{u}\, s\, L}{c^2 - \bar{u}^2}\right) \begin{bmatrix} \cosh\left(\frac{c\, s\, L}{c^2 - \bar{u}^2}\right) & \frac{-c}{\bar{\rho}} \sinh\left(\frac{c\, s\, L}{c^2 - \bar{u}^2}\right) \\ \frac{-\bar{\rho}}{c} \sinh\left(\frac{c\, s\, L}{c^2 - \bar{u}^2}\right) & \cosh\left(\frac{c\, s\, L}{c^2 - \bar{u}^2}\right) \end{bmatrix}. \qquad (4.44)$$

Reproduced with permission of the copyright owner. Further reproduction prohibited without permission.

Also, substituting H(s,x), M(s), N(s), and H(s,L) into (4.43) yields,

$$[M(s) + N(s)\,H(s, L)]^{-1} =$$

$$= \left\{ \begin{bmatrix} 1 & -Z_{us} \\ 0 & 0 \end{bmatrix} + \begin{bmatrix} 0 & 0 \\ -R & 1 \end{bmatrix} \begin{bmatrix} H_{11}(s,L) & H_{12}(s,L) \\ H_{21}(s,L) & H_{22}(s,L) \end{bmatrix} \right\}^{-1}$$

$$= \begin{bmatrix} 1 & -Z_{us} \\ -RH_{11}(s,L)+H_{21}(s,L) & -RH_{12}(s,L)+H_{22}(s,L) \end{bmatrix}^{-1}$$

$$= \frac{\begin{bmatrix} -RH_{12}(s, L)+H_{22}(s,L) & Z_{us} \\ RH_{11}(s, L)-H_{21}(s,L) & 1 \end{bmatrix}}{H_{22}(s,L)-RH_{12}(s,L)-Z_{us}RH_{11}(s,L)+Z_{us}H_{21}(s,L)}.$$

Thus, the transfer function matrix K(s,x) is given by,

$$K(s,x)=H(s,x)[M(s)+N(s)H(s,L)]^{-1} \equiv K_0 \begin{bmatrix} K_1 & K_2 \\ K_3 & K_4 \end{bmatrix} \qquad (4.45)$$

where, the quantities K_0, K_1, K_2, K_3, and K_4 are given below.

$$K_0 = \frac{\exp\left(\frac{\bar{u}\, s\, x}{c^2-\bar{u}^2}\right)}{H_{22}(s,L)-R\,H_{12}(s,L)-Z_{us}\,R\,H_{11}(s,L)+Z_{us}\,H_{21}(s,L)}$$

$$= \frac{\exp\left[\frac{\bar{u}\, s\,(x - L)}{c^2 - \bar{u}^2}\right]}{(1 - Z_{us}\,R)\cosh\left(\frac{c\, s\, L}{c^2-\bar{u}^2}\right) + \left(\frac{R\,c}{\bar{\rho}} - Z_{us}\,\frac{\bar{\rho}}{c}\right)\sinh\left(\frac{c\, s\, L}{c^2-\bar{u}^2}\right)}$$

Reproduced with permission of the copyright owner. Further reproduction prohibited without permission.

$$K_1 = \left\{\cosh\left(\frac{c\,s\,x}{c^2-\bar{u}^2}\right)\left[R\,\frac{c}{\bar{\rho}}\sinh\left(\frac{c\,s\,L}{c^2-\bar{u}^2}\right)+\cosh\left(\frac{c\,s\,L}{c^2-\bar{u}^2}\right)\right]\frac{c}{\bar{\rho}}\cdot\right.$$

$$\left.\sinh\left(\frac{c\,s\,x}{c^2-\bar{u}^2}\right)\left[R\cosh\left(\frac{c\,s\,L}{c^2-\bar{u}^2}\right)+\frac{\bar{\rho}}{c}\sinh\left(\frac{c\,s\,L}{c^2-\bar{u}^2}\right)\right]\right\}\exp\left(\frac{\bar{u}\,s\,L}{c^2-\bar{u}^2}\right)$$

$$= \left\{\cosh\left(\frac{c\,s\,(x-L)}{c^2-\bar{u}^2}\right)+\frac{R\,c}{\bar{\rho}}\sinh\left(\frac{c\,s\,(x-L)}{c^2-\bar{u}^2}\right)\right\}\exp\left(\frac{\bar{u}\,s\,L}{c^2-\bar{u}^2}\right)$$

$$K_2 = Z_{us}\cosh\left(\frac{c\,s\,x}{c^2-\bar{u}^2}\right) - \frac{c}{\bar{\rho}}\sinh\left(\frac{c\,s\,x}{c^2-\bar{u}^2}\right)$$

$$K_3=\left\{\frac{-\bar{\rho}}{c}\sinh\left(\frac{c\,s\,x}{c^2-\bar{u}^2}\right)\left[\frac{R\,c}{\bar{\rho}}\sinh\left(\frac{c\,s\,L}{c^2-\bar{u}^2}\right)+\cosh\left(\frac{c\,s\,L}{c^2-\bar{u}^2}\right)\right]+\right.$$

$$\left.\cosh\left(\frac{c\,s\,x}{c^2-\bar{u}^2}\right)\left[R\cosh\left(\frac{c\,s\,L}{c^2-\bar{u}^2}\right)+\frac{\bar{\rho}}{c}\sinh\left(\frac{c\,s\,L}{c^2-\bar{u}^2}\right)\right]\right\}\exp\left(\frac{\bar{u}\,s\,L}{c^2-\bar{u}^2}\right)$$

$$=\left\{R\cosh\left(\frac{c\,s\,(x-L)}{c^2-\bar{u}^2}\right)+\frac{\bar{\rho}}{c}\sinh\left(\frac{c\,s\,(x-L)}{c^2-\bar{u}^2}\right)\right\}\exp\left(\frac{\bar{u}\,s\,L}{c^2-\bar{u}^2}\right)$$

and,

$$K_4 = \cosh\left(\frac{c\,s\,x}{c^2-\bar{u}^2}\right) - \frac{\bar{\rho}}{c}Z_{us}\sinh\left(\frac{c\,s\,x}{c^2-\bar{u}^2}\right).$$

Finally, the bounded system is as follows:

$$Q(s,x)=\begin{bmatrix} u(s,x) \\ \rho(s,x)\end{bmatrix}=K(s,x)\begin{bmatrix} f_{us} \\ f_{ds}\end{bmatrix}=K(s,x)\,Z(s).$$

Reproduced with permission of the copyright owner. Further reproduction prohibited without permission.

K(s,x) is then referred to as *the transfer function matrix for the given boundary conditions* and is given by,

$$K(s,x)=\begin{bmatrix} K_{11} & K_{12} \\ K_{21} & K_{22} \end{bmatrix} = \frac{\exp\left[\frac{\bar{u}\,s\,(x-L)}{c^2-\bar{u}^2}\right]}{(1-Z_{us}R)\cosh\left(\frac{c\,s\,L}{c^2-\bar{u}^2}\right)+\left(\frac{R\,c}{\bar{\rho}}-Z_{us}\frac{\bar{\rho}}{c}\right)\sinh\left(\frac{c\,s\,L}{c^2-\bar{u}^2}\right)} \cdot$$

$$\begin{bmatrix} \left\{\cosh\left(\frac{c\,s\,(x-L)}{c^2-\bar{u}^2}\right)-\frac{R\,c}{\bar{\rho}}\sinh\left(\frac{c\,s\,(x-L)}{c^2-\bar{u}^2}\right)\right\}\exp\left(\frac{\bar{u}\,s\,L}{c^2-\bar{u}^2}\right) & Z_{us}\cosh\left(\frac{c\,s\,x}{c^2-\bar{u}^2}\right)-\frac{c}{\bar{\rho}}\sinh\left(\frac{c\,s\,x}{c^2-\bar{u}^2}\right) \\ \left\{R\cosh\left(\frac{c\,s\,(x-L)}{c^2-\bar{u}^2}\right)-\frac{\bar{\rho}}{c}\sinh\left(\frac{c\,s\,(x-L)}{c^2-\bar{u}^2}\right)\right\}\exp\left(\frac{\bar{u}\,s\,L}{c^2-\bar{u}^2}\right) & \cosh\left(\frac{c\,s\,x}{c^2-\bar{u}^2}\right)-\frac{\bar{\rho}}{c}Z_{us}\sinh\left(\frac{c\,s\,x}{c^2-\bar{u}^2}\right) \end{bmatrix}. \tag{4.46}$$

It is interesting to note that every term in K(s,x) is a ratio of entire functions. This is true because the quantity M(s)+N(s)H(s,L) as well as its adjoint are a sum of entire functions.

The general procedure for the development of K(s,x) for the three-wave system is basically the same as described above. In fact the transfer function matrix, K(s,x) is given by the same formula as in the two-wave case. However, the matrices M, N as well as the free-space transfer function H(s,x) and the input vector Z(s) are different. As expected, the complexity of the computations is increased significantly since K(s,x) is now a 3×3 transfer function matrix in s and x. Therefore, a general expression for K(s,x) for the three-wave system will not be computed here. However, for the purpose of completeness, the boundary conditions for the three-wave system are given below.

Reproduced with permission of the copyright owner. Further reproduction prohibited without permission.

$$q_1(s,0) = Z_1(s)\, q_3(s,0) \qquad (4.47)$$

$$q_2(s,0) = Z_2(s)\, q_3(s,0) \qquad (4.48)$$

$$q_3(s,L) = R_1\, q_1(s,L) + R_2\, q_2(s,L) + \delta F_{in} \qquad (4.49)$$

or, in matrix form,

$$\begin{bmatrix} 1 & 0 & -Z_1(s) \\ 0 & 1 & -Z_2(s) \\ 0 & 0 & 0 \end{bmatrix} \begin{bmatrix} q_1(s,0) \\ q_2(s,0) \\ q_3(s,0) \end{bmatrix} + \begin{bmatrix} 0 & 0 & 0 \\ 0 & 0 & 0 \\ -R_1 & -R_2 & 1 \end{bmatrix} \begin{bmatrix} q_1(s,L) \\ q_2(s,L) \\ q_3(s,L) \end{bmatrix} = \begin{bmatrix} 0 \\ 0 \\ \delta F_{in} \end{bmatrix}$$

and finally,

$$M(s)\, Q(s,0) + N(s)\, Q(s,L) = Z(s).$$

Graphically, these conditions are shown in the following figure.

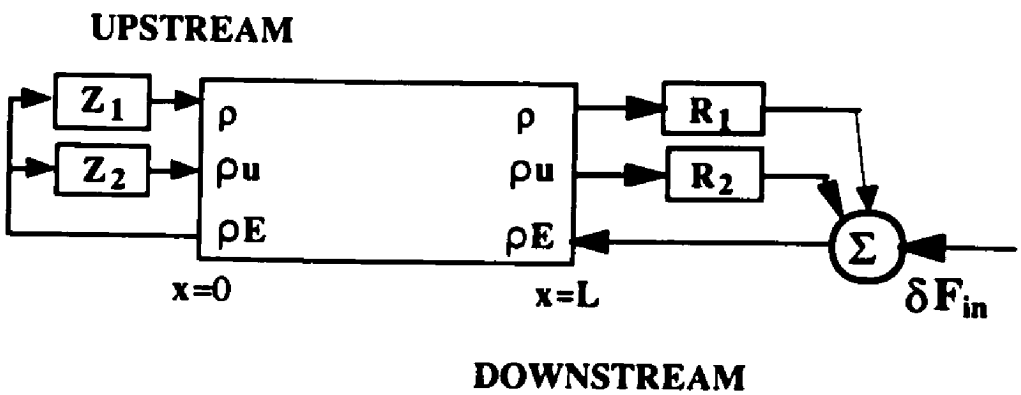


Figure 4.6 Boundary conditions for the three-wave problem

Reproduced with permission of the copyright owner. Further reproduction prohibited without permission.

Also, the three-wave bounded system characteristics are summarized in Table 4.2 below.

Table 4.2 Characteristics of a three-wave bounded system

Quantity	3-Wave
State vector	$Q(s,x)=\begin{bmatrix}\text{density}\\ \text{momentum}\\ \text{energy}\end{bmatrix}=\begin{bmatrix}q_1(s,x)\\ q_2(s,x)\\ q_3(s,x)\end{bmatrix}=\begin{bmatrix}\rho_i(s,x)\\ \rho_i(s,x)u_i(s,x)\\ \rho_i(s,x)E_i(s,x)\end{bmatrix}$
M(s)	$\begin{bmatrix}1 & 0 & -Z_1\\ 0 & 1 & -Z_2\\ 0 & 0 & 0\end{bmatrix}$
N(s)	$\begin{bmatrix}0 & 0 & 0\\ 0 & 0 & 0\\ -R_1 & -R_2 & 1\end{bmatrix}$
Input Vector	$Z(s)=\begin{bmatrix}0\\ 0\\ \delta F_{in}\end{bmatrix}$
Reflection Parameters	R_1, R_2
Shock Dynamics	$Z_1(s), Z_2(s)$

Reproduced with permission of the copyright owner. Further reproduction prohibited without permission.

The Choice of the Shock Transfer Function

It must be clear that the system transfer function K(s,x) can be further complicated by substituting a lumped dynamic system function for $Z_{us}(s)$ to represent the shock behavior. In general, $Z_{us}(s)$ can be a ratio of two polynomials having m zeros and n poles. The corresponding mathematical model for $Z_{us}(s)$ would then be as follows:

$$Z_{us}(s) = \frac{\sum_{i=0}^{m} b_i s^{m-i}}{\sum_{j=0}^{n} a_j s^{n-j}} = \frac{b_0 s^m + b_1 s^{m-1} + \ldots + b_{m-1} s + b_m}{a_0 s^n + a_1 s^{n-1} + \ldots + a_{n-1} s + a_n} \qquad (4.50)$$

where, it is usually assumed that $a_0 \neq 0$, and $b_0 \neq 0$. However, it has been shown experimentally (see references [WIL68] and [CW75]) that $Z_{us}(s)$ can be modeled as a first order system having a fast lag. This suggests that $Z_{us}(s)$ takes the following form:

$$Z_{us}(s) = \frac{Z_0}{s - p} \qquad (4.51)$$

Concluding Remarks

The analytical solution obtained here is an exact solution of the approximate boundary value problem as opposed to the approximate solutions of the approximate boundary value problem considered by Willoh in [WIL68] and Cole and Willoh in [CW75]. The resulting model is very useful to the control engineer. It can provide quick insight about this very complicated system. The solution obtained is in a compact form and one

Reproduced with permission of the copyright owner. Further reproduction prohibited without permission.

can get the answer relatively quickly. In fact, MATLAB programs can be developed to compute frequency responses for various conditions and shock models. Some of the responses will be shown in the next chapter which incidentally is dedicated to applications. Finally, all computed models can be used for control system design using root locus or frequency domain techniques. Since the inputs are assumed to be small, the solution to the problem will be good as long as the conditions for a small perturbation model are met.

In general, the three-wave system should be a better model than the two-wave system when energy losses cannot be neglected. This is true for relatively high Mach numbers.

Finally, it is noted that the two-wave free-space system function matrix for the two-wave system is very similar to that of an electrical transmission line system. In fact, the flow channel is analogous to a transmission line used to drive a general load of impedance $Z_{us}(s)$. Therefore in this analogy, the shock transfer function acts like an impedance, which for maximum power transfer should be matched to the characteristic impedance of the line. At last, both the inlet and the transmission line systems are in a sense identical for $\bar{u} = 0$.

Up to this point two basic problems were discussed: The free-space problem and the bounded problem. The results obtained here will be very useful in the following sections of this chapter, which deal with flows in multiple-channel systems.

Reproduced with permission of the copyright owner. Further reproduction prohibited without permission.

4.4 The Two-Channel Free-Space Problem

In this section, the two-channel problem is discussed. This problem resembles the free-space problem; however, the inlet is now made up of two flow channels or lumps connected together. This configuration is very useful as it can be used to describe some very realistic flow scenarios, particularly those in varying area ducts.

The resulting system structure is illustrated in the following figure and the main objective is to solve for the flow variables in Channels 1 and 2 in terms of the flow at x=0.

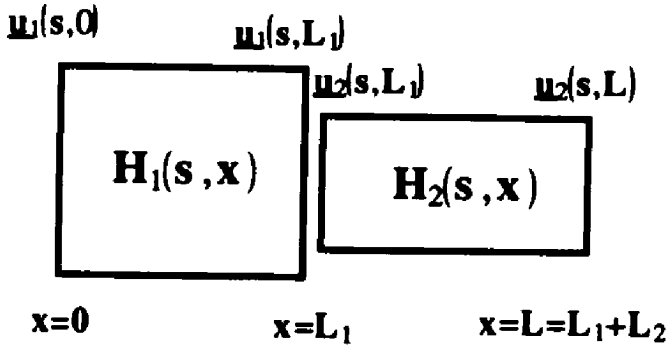


Figure 4.7 The two-channel problem

No external boundary conditions are imposed at this point. However, it is assumed that the flow $\underline{u}(s,x)$ is continuous on the interface of Channels 1 and 2.

Reproduced with permission of the copyright owner. Further reproduction prohibited without permission.

$H_1(s,x)$ denotes the transfer function for Channel 1 and $H_2(s,x)$ is the transfer function for Channel 2 while the flow vectors are $\underline{u}_1(s,x)$ and $\underline{u}_2(s,x)$, respectively. In Channel 1, the governing equation for the flow vector is given by,

$$\underline{u}_1(s,x-x_0)=H_1(s,x-x_0)\,\underline{u}_1(s,x_0) \qquad (4.52)$$

or, since x_0 is simply zero,

$$\underline{u}_1(s,x) = H_1(s,x)\,\underline{u}_1(s,0).$$

This expression is only valid for the interval, $0\le x\le x_1=L_1$. Also, since it is assumed that the transition across the interior boundary is continuous, then the system must obey the following equation exactly at that interior boundary,

$$\underline{u}_1(s,x_1)=H_1(s,x_1-x_0)\,\underline{u}_1(s,x_0)=\underline{u}_2(s,x_1). \qquad (4.53)$$

Next, the flow in Channel 2, that is for $x_1=L_1\le x\le x_2=L_1+L_2$, is computed as follows,

$$\underline{u}_2(s,x-L_1) = H_2(s,x-x_1)\,\underline{u}_2(s,x_1)$$

$$= H_2(s,x-x_1)\,H_1(s,x_1-x_0)\,\underline{u}_1(s,x_0)$$

$$= H_2(s,x-x_1)\,H_1(s,x_1)\,\underline{u}_1(s,0)$$

$$= H_2(s,x-L_1)\,H_1(s,L_1)\,\underline{u}_1(s,0)$$

$$= \tilde{H}(s,x)\,\underline{u}_1(s,0)$$

Reproduced with permission of the copyright owner. Further reproduction prohibited without permission.

where,

$$\tilde{H}(s,x) \equiv H_2(s,x-L_1)\,H_1(s,L_1).$$

Thus, in conclusion the flow for a two-channel system is given by the following general expression:

$$\underline{u}(s,x) = \begin{cases} \underline{u}_1(s,x) = H_1(s,x)\,\underline{u}_1(s,0), & 0 \le x \le x_1 = L_1 \\ \underline{u}_2(s,x) = H_2(s,x-L_1)\,H_1(s,L_1)\,\underline{u}_1(s,0), & L_1 = x_1 \le x \le x_2 = L_1 + L_2. \end{cases} \tag{4.54}$$

Furthermore, the flow in either channel can be deduced if the open loop transfer function H(s,x) is known. In fact, more detailed expressions for $\underline{u}(s,x)$ for a two-channel system could be easily determined using the free-space transfer functions for the two- or three-wave systems that were developed in Section 4.2.

In conclusion, this brief section covered the two-channel free-space problem. An extension of this problem is studied in the following section.

4.5 The N-Channel Free-Space Problem

This section deals with the N-channel problem, which is an extension of the Two-Channel Free-Space Problem, which was discussed in the previous section. This problem is illustrated in the following figure.

Reproduced with permission of the copyright owner. Further reproduction prohibited without permission.

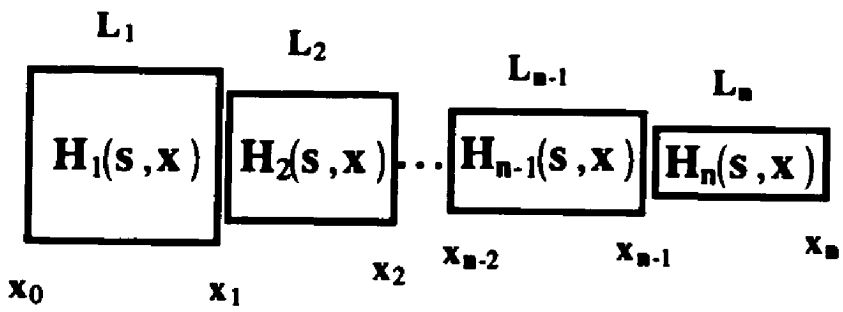


Figure 4.8 The N-channel problem

The objective is to solve for the flow at every interior point under the assumption that the flow variables are continuous on the interfaces of Channels n-1 and n, where the range of n is $2 \le n \le N$ and N represents the total number of lumps.

Let $H_n(s,x)$ denote the transfer function for the n_{th} channel and $u_n(s,x)$ represent the flow in the n_{th} channel. Then, in Channel 1, the governing equation for the flow vector is given by,

$$u_1(s,x-x_0)=H_1(s,x-x_0)\, u_1(s,x_0)$$

where $x_0=0$. Similarly, in Channel 2 one gets,

$$u_2(s,x-x_1)=H_2(s,x-x_1)\, u_2(s,x_1).$$

Likewise, in Channel 3 the flow vector is as follows,

$$u_3(s,x-x_2)=H_3(s,x-x_2)\, u_3(s,x_2).$$

Reproduced with permission of the copyright owner. Further reproduction prohibited without permission.

Finally, generalizing this equation for the n_{th} channel one arrives at the following expression,

$$u_n(s,x-x_{n-1})=H_n(s,x-x_{n-1})\,u_n(s,x_{n-1}). \qquad (4.55)$$

where, $1\le n\le N$.

Next, using the assumption that the flow is continuous on the interface of two consecutive channels one gets,

$$u_n(s,x_{n-1}) = u_{n-1}(s,x_{n-1}) \qquad (4.56)$$

where, $2\le n\le N$, since for a system with N channels there are N-1 interior boundaries. Combining equations (4.50) and (4.51) one obtains,

$$u_n(s,x-x_{n-1})=H_n(s,x-x_{n-1})\,u_n(s,x_{n-1}). \qquad (4.57)$$

However, the flow evaluated at the $(n-1)_{st}$ boundary is as follows,

$$u_{n-1}(s,x_{n-1})=H_{n-1}(s,x_{n-1}-x_{n-2})\,u_{n-1}(s,x_{n-2}).$$

Likewise, at the $(n-2)_{nd}$ boundary one obtains,

$$u_{n-2}(s,x_{n-2})=H_{n-2}(s,x_{n-2}-x_{n-3})\,u_{n-2}(s,x_{n-3})$$

and finally, at the second and first boundary one obtains, respectively,

$$u_2(s,x_2)=H_2(s,x_2-x_1)\,u_2(s,x_1)$$

and

$$u_1(s,x_1)=H_1(s,x_1-x_0)\,u_1(s,x_0).$$

Reproduced with permission of the copyright owner. Further reproduction prohibited without permission.

Linking all of the above equations together (4.52) becomes,

$$\underline{u}_n(s,x-x_{n-1}) = H_n(s,x-x_{n-1})\, H_{n-1}(s,x_{n-1}-x_{n-2})\, \underline{u}_{n-1}(s,x_{n-2})$$

$$= H_n(s,x-x_{n-1})\, H_{n-1}(s,x_{n-1}-x_{n-2})\, H_{n-2}(s,x_{n-2}-x_{n-3})\, \underline{u}_{n-2}(s,x_{n-3})$$

$$= H_n(s,x-x_{n-1})\, H_{n-1}(s,x_{n-1}-x_{n-2})\, H_{n-2}(s,x_{n-2}-x_{n-3})\, H_{n-3}(s,x_{n-3}-x_{n-4})\, \underline{u}_{n-3}(s,x_{n-4})$$

$$\vdots$$

$$= H_n(s,x-x_{n-1})\, H_{n-1}(s,x_{n-1}-x_{n-2}) \cdots H_2(s,x_2-x_1)\, H_1(s,x_1-x_0)\, \underline{u}_1(s,x_0)$$

$$= H_n(s,x-x_{n-1}) \left[\prod_{i=1}^{n-1} H_{n-i}(s,x_{n-i}-x_{n-i-1}) \right] \cdot \underline{u}_1(s,x_0) \,.$$

Thus, the flow in the n_{th} channel is given by the following general expression,

$$\underline{u}_n(s,x) = H_n(s,x-x_{n-1}) \left[\prod_{i=1}^{n-1} H_{n-i}(s,x_{n-i}-x_{n-i-1}) \right] \cdot \underline{u}_1(s,x_0) \,. \qquad (4.58)$$

It must be noted that in the above expression the order of matrix multiplication is important as the matrices do not usually commute.

Moreover, using the results of Section 4.2, more detailed expressions for $\underline{u}_n(s,x)$ can be derived for two- or three-wave systems from the general expression given in (4.53) above. Experience shows that this is a very tedious process for a system containing even as few as three lumps for a two-wave model.

As an alternative to the abstract although straightforward development of the flow in the Nth channel presented above, one might

Reproduced with permission of the copyright owner. Further reproduction prohibited without permission.

want to work with two channels at a time until all channels are linked together (See Figure 4.9 below). Using the theory of Section 4.4, first combine Channel 1 with Channel 2 to get a Superchannel 1/2, Channel 3 with Channel 4 to get a Superchannel 3/4, and so on. Then, combine the superchannels to obtain new superchannels. Repeat this process until all channels are covered and a single Superchannel 1/2/.../N is obtained. This way of computing the system transfer function does not require the multiplication of N subsystem transfer matrices. Instead, the maximum number of subsystem matrices multiplied together at any one step is two!

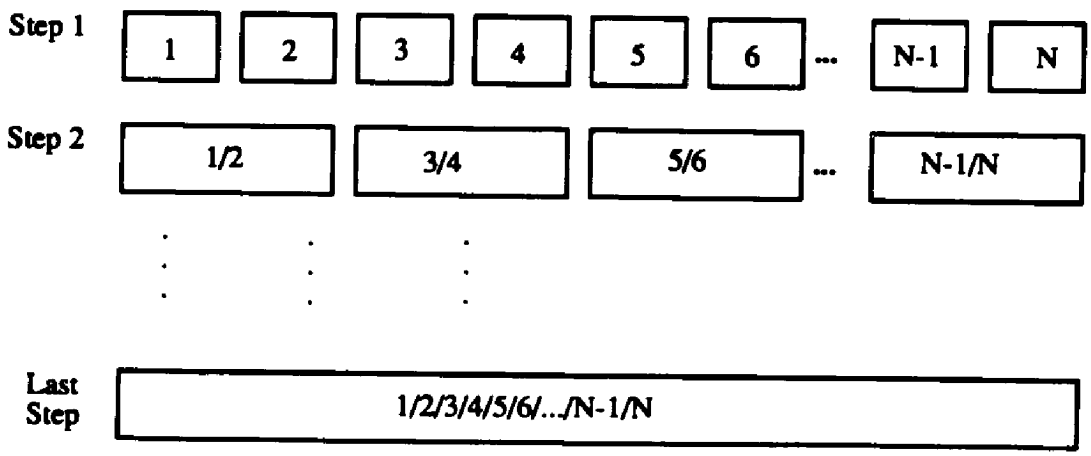


Figure 4.9 An alternative way of computing the system transfer function in combinational flows

In this section, the free-space N-Channel problem was discussed. Moving on, in the following two sections, the bounded versions of the two-

Reproduced with permission of the copyright owner. Further reproduction prohibited without permission.

and N-Channel problems will be presented, namely, the two-Channel bounded problem and the N-Channel bounded problem.

4.6 The Two-Channel Bounded Problem

This section describes the two-channel problem, which is illustrated in Figure 4.10 below. At a first look, this problem is similar to the bounded problem studied in Section 4.3 if the two channels are treated as one channel having an open loop transfer function, H(s,x). In fact, using the theory developed in Section 4.4 one should be able to obtain the composite open loop transfer function matrix, H(s,x), for the two-block system and then develop the transfer function matrix for the bounded two-channel system using the theory of Section 4.3.

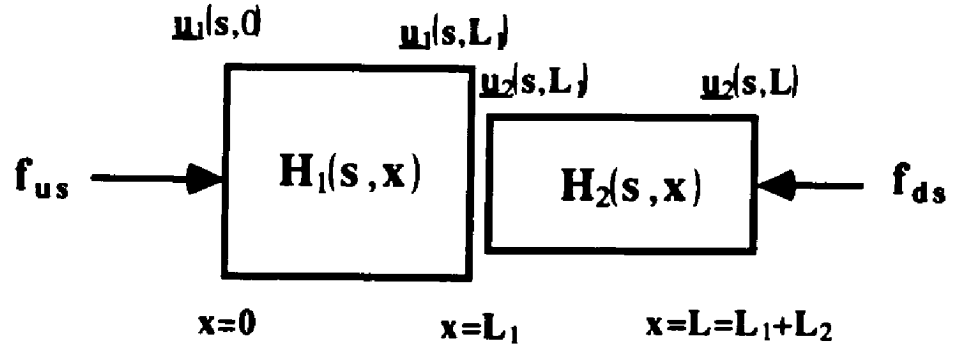


Figure 4.10 The two-channel bounded problem

Reproduced with permission of the copyright owner. Further reproduction prohibited without permission.

As before, it is assumed again that the two flow channels have two distinct transfer functions, namely, $H_1(s,x)$ and $H_2(s,x)$, respectively. Furthermore, the length of Channel 1 is L_1, while the length of Channel 2 is L_2. Finally, the flow vector in Channel 1 is symbolized by $Q_1(s,x)$ or $u_1(s, x)$ and in Channel 2 by $Q_2(s,x)$ or $u_2(s, x)$. Then, in Channel 1, that is at $0 \le x < x_1 = L_1$, one gets,

$$Q_1(s,x) = H_1(s,x)\, Q_1(s,0). \qquad (4.59)$$

In Channel 2, that is for $L_1 = x_1 \le x \le x_2 = L = L_1 + L_2$, one gets

$$Q_2(s,x) = H_2(s,x-L_1)\, Q_1(s,L_1) = H_2(s,x-L_1)\, H_1(s,L_1)\, Q_1(s,0). \qquad (4.60)$$

Next, appropriate boundary conditions--similar to those used in Section 4.3--are applied to the system. For a two-wave system, they are as follows:

$$u_1(s,0) = Z_{us}(s)\, \rho_1(s,0) + f_{us}$$

$$\rho_2(s,L) = R\, \rho_2(s,L) + f_{ds}.$$

Next, the above boundary conditions are put in the following form as in Section 4.3:

$$\begin{bmatrix} 1 & -Z_{us} \\ 0 & 0 \end{bmatrix} \begin{bmatrix} u_1(s,0) \\ \rho_1(s,0) \end{bmatrix} + \begin{bmatrix} 0 & 0 \\ -R(s) & 1 \end{bmatrix} \begin{bmatrix} u_2(s,L) \\ \rho_2(s,L) \end{bmatrix} = \begin{bmatrix} f_{us} \\ f_{ds} \end{bmatrix}$$

or,

$$M(s)\, Q_1(s,0) + N(s)\, Q_2(s,L) = Z(s)$$

where,

Reproduced with permission of the copyright owner. Further reproduction prohibited without permission.

$$M(s) = \begin{bmatrix} 1 & -Z_{us} \\ 0 & 0 \end{bmatrix}, \quad N(s) = \begin{bmatrix} 0 & 0 \\ -R(s) & 1 \end{bmatrix}, \quad Q_i(s, x) = \begin{bmatrix} u_i(s, x) \\ \rho_i(s, x) \end{bmatrix}, \quad Z(s) = \begin{bmatrix} f_{us} \\ f_{ds} \end{bmatrix}.$$

Since,

$$Q_2(s,L) = H_2(s,L-L_1)\, H_1(s,L_1)\, Q_1(s,0),$$

the given boundary conditions can be expressed in terms of $Q_1(s,0)$ only, as follows:

$$\{M(s) + N(s)\, H_2(s,L-L_1)\, H_1(s,L_1)\}\, Q_1(s,0) = Z(s),$$

or, solving for $Q_1(s,0)$ yields:

$$Q_1(s,0) = \{M(s) + N(s)\, H_2(s,L-L_1)\, H_1(s,L_1)\}^{-1}\, Z(s). \qquad (4.61)$$

Finally, the flow along the two-channel system is summarized as follows:

$$Q(s,x) = \begin{cases} H_1(s,x)\, \{M(s)+N(s)H_2(s,L-L_1)H_1(s,L_1)\}^{-1}Z(s), & \text{Channel 1} \\ H_2(s,x-L_1)\, H_1(s,L_1)\{M(s)+N(s)H_2(s,L-L_1)H_1(s,L_1)\}^{-1}Z(s), & \text{Channel 2} \end{cases} \qquad (4.62)$$

It is emphasized again that if a three- or more-wave assumption is made, then the general expression for the flow will be as given above in Equation (4.62). However, in a three-wave situation, the boundary conditions imposed will be as follows:

Reproduced with permission of the copyright owner. Further reproduction prohibited without permission.

$$q_1(s,0) = Z_1(s)\, q_3(s,0)$$

$$q_2(s,0) = Z_2(s)\, q_3(s,0)$$

$$q_3(s,L) = R_1\, q_1(s,L) + R_2\, q_2(s,L) + \delta F_{in}\ ,$$

or, in matrix form,

$$\begin{bmatrix} 1 & -Z_1(s) & 0 \\ 0 & -Z_2(s) & 1 \\ 0 & 0 & 0 \end{bmatrix} \begin{bmatrix} q_1(s,0) \\ q_2(s,0) \\ q_3(s,0) \end{bmatrix} + \begin{bmatrix} 0 & 0 & 0 \\ 0 & 0 & 0 \\ -R_1 & 1 & -R_2 \end{bmatrix} \begin{bmatrix} q_1(s,L) \\ q_2(s,L) \\ q_3(s,L) \end{bmatrix} = \begin{bmatrix} 0 \\ 0 \\ \delta F_{in} \end{bmatrix} \qquad (4.63)$$

and compactly,

$$M(s)\, Q_1(s,0) + N(s)\, Q_2(s,L) = Z(s).$$

More detailed expressions for Q(s,x) will not be presented here.

In this section, the two-channel bounded problem was studied. The next section deals with an extension of this useful problem, namely, the N-Channel bounded problem.

4.7 The N-Channel Bounded Problem

This problem is an extension of the two-channel bounded problem, which was studied in the previous section. It must be noted that in a system containing n blocks there will be n-1 internal boundaries across which the flow will be continuous. Also, the flow Q(s,x) will be assumed to be

Reproduced with permission of the copyright owner. Further reproduction prohibited without permission.

unidirectional, i.e., from left to right or from the upstream end of the system to its downstream end. This arrangement allows us then to apply the flow equations to each individual channel, by starting at the first block and proceeding in a downstream fashion until the nth block is studied, thus analyzing all blocks.

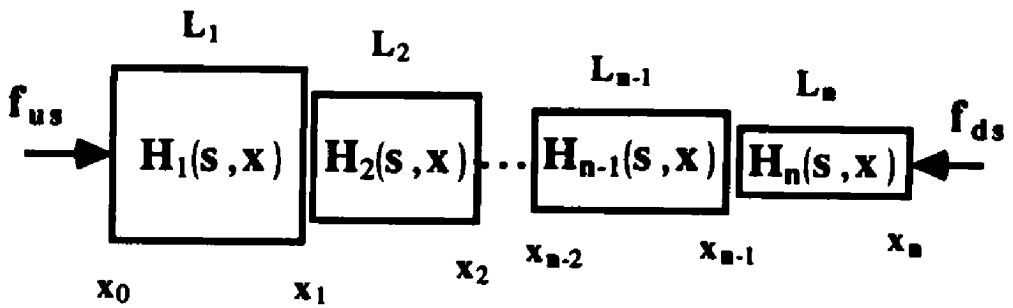


Figure 4.11 The N-channel bounded problem

It should be noted that for this problem, the discussion will focus primarily on two-wave models. For flows involving more that two waves, final answers are not computed explicitly. However, they may readily be developed by substituting all appropriate variables into the general expressions given.

Starting in Channel 1, the describing flow equation is:

$$Q_1(s,x) = u_1(s,x) = H_1(s,x-x_0)u_1(s,x_0) \qquad (4.64)$$

Reproduced with permission of the copyright owner. Further reproduction prohibited without permission.

where, $H_1(s,x)$ is the open loop transfer function corresponding to the first channel. Across the first internal boundary, the following continuity constraint is applied:

$$Q_2(s,x_1) = u_2(s,x_1) = u_1(s,x_1) = Q_1(s,x_1). \tag{4.65}$$

Moving on to Channel 2, one gets:

$$u_2(s,x) = H_2(s,x-x_1)u_1(s,x_1)$$

$$= H_2(s,x-x_1)H_1(s,x_1-x_0)u_0(s,x_0)$$

Since the total length of the flow channel is,

$$L = L_1+L_2+L_3+\cdots+L_n \tag{4.66}$$

then, continuing the above process for the remaining channels and setting $x_0=0$, one obtains the following flow equations, which describe the flow vector $Q_n(s,x)$ in terms of $Q_1(s,0)$:

$$Q_1(s,x) = u_1(s,x) = H_1(s,x-x_0)u_1(s,x_0)$$

$$Q_2(s,x) = H_2(s,x-L_1)H_1(s,L_1)Q_1(s,0)$$

$$Q_3(s,x) = H_3(s,x-L_1-L_2)H_2(s,L_2)H_1(s,L_1)Q_1(s,0).$$

It can be easily observed that a special pattern emerges in the computation of $Q_i(s,x)$, for $i=1,2,\ldots,n$. Therefore, the flow vector in Channel n can be readily found using the following general formula:

$$Q_n(s,x)=H_n(s,x-L_1-\cdots-L_{n-1})\cdot H_{n-1}\left(s,\sum_{i=1}^{n-1}L_i\right)\cdots H_2(s,L_1+L_2)\cdot H_1(s,L_1)\cdot Q_1(s,0)$$

Reproduced with permission of the copyright owner. Further reproduction prohibited without permission.

Next, the following boundary conditions are applied to the open loop system:

$$M(s)\, Q_1(s,0) + N(s)\, Q_n(s,L) = \underline{Z}(s) \qquad (4.67)$$

In a two-wave system the boundary conditions are explicitly written as follows:

$$u_{us}(s,0) = Z(s)\, \rho_{us}(s,0) + f_{us}$$

$$\rho_{ds}(s,L) = R(s)\, u_{ds}(s,L) + f_{ds}$$

or, if rewritten to match Equation (4.67):

$$\begin{bmatrix} 1 & -Z(s) \\ 0 & 0 \end{bmatrix} \begin{bmatrix} u_1(s,0) \\ \rho_1(s,0) \end{bmatrix} + \begin{bmatrix} 0 & 0 \\ -R(s) & 1 \end{bmatrix} \begin{bmatrix} u_n(s,L) \\ \rho_n(s,L) \end{bmatrix} = \begin{bmatrix} f_{us} \\ f_{ds} \end{bmatrix} \equiv \underline{Z}(s).$$

The situation for a two-wave system is depicted graphically in Figure 4.12.

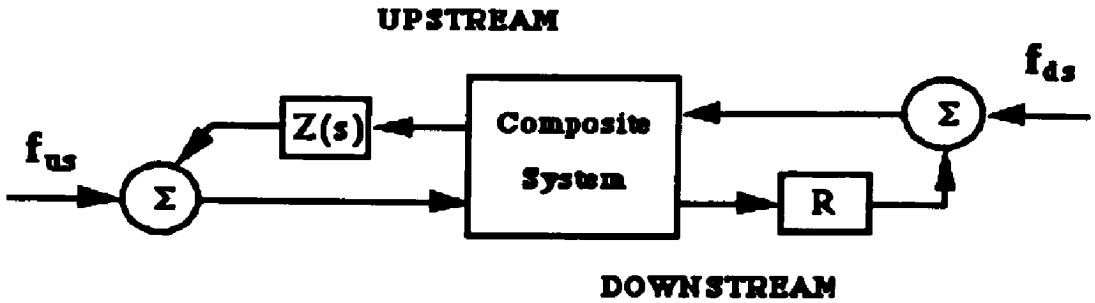


Figure 4.12 A block diagram of a N-channel bounded inlet system

Reproduced with permission of the copyright owner. Further reproduction prohibited without permission.

Next, recall from a Section 4.5 that

$$Q_n(s,x) = \left[H_n(s,x-L_1-\cdots-L_{n-1}) \cdot H_{n-1}(s,L_1+L_2+\cdots+L_{n-1}) \cdots \right.$$

$$\left. \cdots H_2(s,L_1+L_2) \cdot H_1(s,L_1) \right] \cdot Q_1(s,0)$$

$$\Rightarrow Q_n(s,x) = \Theta(s,x,L_i) \cdot Q_1(s,0). \qquad (4.68)$$

where the auxiliary vector $\Theta(s,x,L_i)$ is given by:

$$\Theta(s,x,L_i) = \left[H_n(s,x-L_1-\cdots-L_{n-1}) \cdot H_{n-1}(s,L_1+\cdots+L_{n-1}) \cdots H_2(s,L_1+L_2) \cdot H_1(s,L_1) \right].$$

Thus, equation (4.67) becomes

$$M(s)\, Q_1(s,0) + N(s)\, \Theta(s,L,L_i)\, Q_1(s,0) = Z(s) \qquad (4.69)$$

and for a two-wave system:

$$\begin{bmatrix} 1 & -Z(s) \\ 0 & 0 \end{bmatrix} \begin{bmatrix} u_1(s,0) \\ \rho_1(s,0) \end{bmatrix} + \begin{bmatrix} 0 & 0 \\ -R(s) & 1 \end{bmatrix} \Theta(s,L,L_i) \begin{bmatrix} u_1(s,0) \\ \rho_1(s,0) \end{bmatrix} = \begin{bmatrix} f_{us} \\ f_{ds} \end{bmatrix}.$$

Next, manipulating Equation (4.69) the flow vector $Q_n(s,x)$ can be readily obtained. This procedure requires the following steps.

First one must solve for $Q_1(s,0)$ in terms of the external input vector, namely, $Z(s)$. This is shown below:

$$[M(s) + N(s)\, \Theta(s,L,L_i)]\, Q_1(s,0) = Z(s)$$

$$\Rightarrow Q_1(s,0) = [M(s) + N(s)\, \Theta(s,L,L_i)]^{-1}\, Z(s)$$

Reproduced with permission of the copyright owner. Further reproduction prohibited without permission.

$$\Rightarrow Q_1(s,0) = \Gamma(s,L,L_i)\, Z(s), \qquad (4.70)$$

where the auxilliary variable $\Gamma(s,x,L_i)$ is defined as follows:

$$\Gamma(s,x,L_i) = [M(s) + N(s)\,\Theta(s,x,L_i)]^{-1}.$$

For a two-wave system the following expression holds:

$$\left\{\begin{bmatrix} 1 & -Z(s) \\ 0 & 0 \end{bmatrix} + \begin{bmatrix} 0 & 0 \\ -R(s) & 1 \end{bmatrix}\Theta(s,L,L_i)\right\}\begin{bmatrix} u_1(s,0) \\ \rho_1(s,0) \end{bmatrix} = \begin{bmatrix} f_{us} \\ f_{ds} \end{bmatrix}$$

$$\Rightarrow \begin{bmatrix} u_1(s,0) \\ \rho_1(s,0) \end{bmatrix} = \left\{\begin{bmatrix} 1 & -Z(s) \\ 0 & 0 \end{bmatrix} + \begin{bmatrix} 0 & 0 \\ -R(s) & 1 \end{bmatrix}\Theta(s,L,L_i)\right\}^{-1}\begin{bmatrix} f_{us} \\ f_{ds} \end{bmatrix}$$

$$\Rightarrow Q_1(s,0) = \begin{bmatrix} u_1(s,0) \\ \rho_1(s,0) \end{bmatrix} = \Gamma(s,L,L_i)\begin{bmatrix} f_{us} \\ f_{ds} \end{bmatrix}$$

and the auxiliary variable $\Gamma(s,x,L_i)$ is given by:

$$\Gamma(s,x,L_i) = \left\{\begin{bmatrix} 1 & -Z(s) \\ 0 & 0 \end{bmatrix} + \begin{bmatrix} 0 & 0 \\ -R(s) & 1 \end{bmatrix}\Theta(s,x,L_i)\right\}^{-1}. \qquad (4.71)$$

Next, the expression for $Q_1(s,0)$ of Equation (4.70) above is substituted back into Equation (4.68), thus yielding the flow vector at any point x along the flow line in terms of the external input vector $Z(s)$:

$$Q_n(s,x) = \Phi(s,x,L_i)\, Z(s) \qquad (4.72)$$

Reproduced with permission of the copyright owner. Further reproduction prohibited without permission.

where, the new auxilliary variable $\Phi(s,x,L_i)$ is defined as follows:

$$\Phi(s,x,L_i) \equiv \Theta(s,x,L_i) \cdot \Gamma(s,L,L_i). \qquad (4.73)$$

Finally, given the number of lumps n and the corresponding open loop transfer functions Hi(s,x)'s, for i=1,2,...,n, a more detailed expression for $Q_n(s,x)$ could be derived.

In conclusion, this section dealt with the N-channel bounded problem. The following section examines the Two-Channel with Internal Input Free-Space Problem.

4.8 The Two-Channel with Internal Input Free-Space Problem

This section deals with the flow system of Figure 4.13 below. It is assumed that the two flow channels have two different transfer functions $H_1(s,x)$ and $H_2(s,x)$, respectively. Furthermore, the length of Channel 1 is L_1, while the length of Channel 2 is L_2. An input $\Delta\underline{u}(s)$ is applied to the system at the interior boundary, i.e., at $x=x_1=L_1$, and the objective is now to find the flows in Channels 1 and 2 in terms of $\underline{u}_1(s,0)$ and $\Delta\underline{u}(s)$.

The development begins again at Channel 1, that is at $0\le x<x_1=L_1$, where one gets,

$$\underline{u}_1(s,x)=H_1(s,x)\,\underline{u}_1(s,0). \qquad (4.74)$$

The interior boundary, i.e., the point where $x=x_1=L_1$, is designed such that the system obeys the following equation:

Reproduced with permission of the copyright owner. Further reproduction prohibited without permission.

$$\underline{u}_2(s,x_1) = \underline{u}_1(s,x_1) + \Delta\underline{u}(s)$$
$$= H_1(s,x_1)\,\underline{u}_1(s,0) + \Delta\underline{u}(s).$$

Then, the flow in Channel 2, that is for $L_1=x_1\le x\le x_2=L=L_1+L_2$, is given by,

$$\underline{u}_2(s,x) = H_2(s,x-x_1)\,\underline{u}_2(s,x_1)$$
$$= H_2(s,x-x_1)\,[H_1(s,x_1)\,\underline{u}_1(s,0) + \Delta\underline{u}(s)]$$
$$= H_2(s,x-x_1)\,H_1(s,x_1)\,\underline{u}_1(s,0) + H_2(s,x-x_1)\,\Delta\underline{u}(s).$$

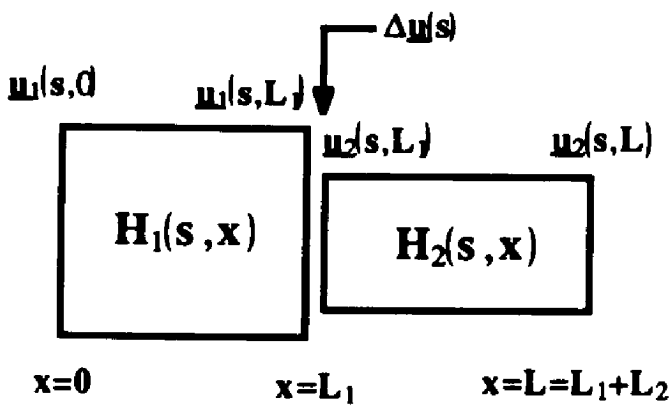


Figure 4.13 A two-channel system with an internal input

Next, the above equation can be put in the following compact form,

$$\underline{u}_2(s,x) = A(s,x)\,\underline{u}_1(s,0) + B(s,x)\,\Delta\underline{u}(s) \qquad (4.75)$$

Reproduced with permission of the copyright owner. Further reproduction prohibited without permission.

where,

$$A(s,x) = H_2(s,x-x_1)\, H_1(s,x_1)$$

$$B(s,x) = H_2(s,x-x_1).$$

This situation is depicted graphically in Figure 4.14 below.

Clearly, the first part of equation (4.75) gives the open-loop response of the system due to the initial conditions at the x=0 point. On the other hand, the second part of equation (4.75) describes the contribution of the internal input to the output of the flow system. Finally, if the interior input $\Delta u(s)$ is zero, then the *Two-channel with internal input free-space* problem simply degenerates to the *Two-channel free-space* problem which was discussed in Section 4.4.

A Special Case (2-Wave system)

To better understand this interesting problem, the exact solution to a two-wave system will be studied. Starting with $H_i(s,x)$, then $H_1(s,x)$ and $H_2(s,x)$ can be computed if the parameters c_1, c_2, $\bar{\rho}_1$, $\bar{\rho}_2$, $\bar{u}_1$, and $\bar{u}_2$ are specified. For a 2-wave system $H_i(s,x)$ is given by,

$$H_i(s,x)=\exp\left(\frac{\bar{u}_i s x}{c_i^2-\bar{u}_i^2}\right)\begin{bmatrix} \cosh\left(\frac{c_i s x}{c_i^2-\bar{u}_i^2}\right) & \frac{-c_i}{\bar{\rho}_i}\sinh\left(\frac{c_i s x}{c_i^2-\bar{u}_i^2}\right) \\ \frac{-\bar{\rho}_i}{c_i}\sinh\left(\frac{c_i s x}{c_i^2-\bar{u}_i^2}\right) & \cosh\left(\frac{c_i s x}{c_i^2-\bar{u}_i^2}\right) \end{bmatrix}, \qquad (4.76)$$

where the subscript i denotes the respective quantity in the i_{th} flow channel.

Reproduced with permission of the copyright owner. Further reproduction prohibited without permission.

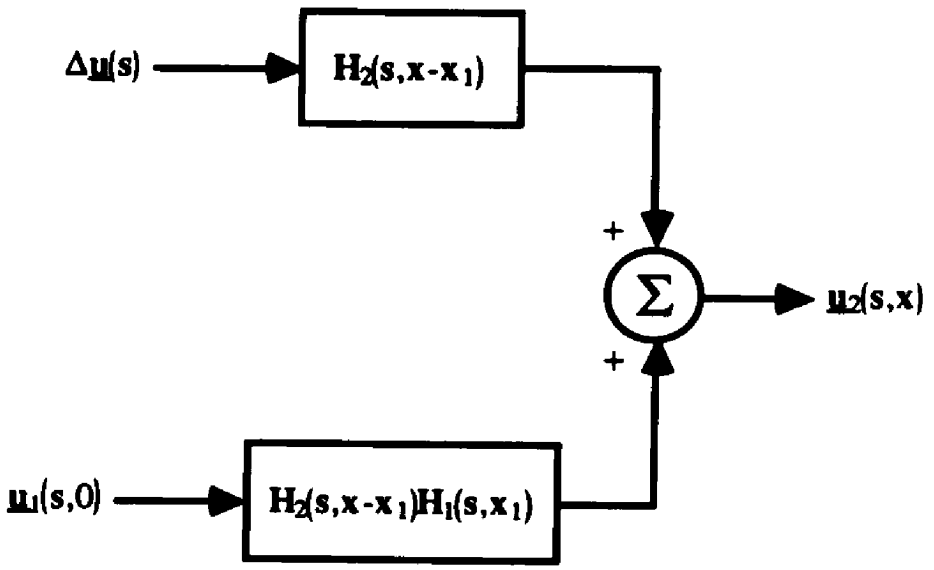


Figure 4.14 Block diagram describing the flow in Channel 2 of a two-channel with internal input flow system

Next, matrices A(s,x) and B(s,x) can be computed using the transfer function matrices $H_1(s,x_1)$, and $H_2(s,x-x_1)$ in the following expressions:

$$A(s,x)=H_2(s,x-x_1)\,H_1(s,x_1)=\exp\left(\frac{\bar{u}_2 s(x-x_1)}{c_2^2-\bar{u}_2^2}\right)\exp\left(\frac{\bar{u}_1 s x_1}{c_1^2-\bar{u}_1^2}\right)\cdot$$

$$\begin{bmatrix} \cosh\left(\frac{c_2 s(x-x_1)}{c_2^2-\bar{u}_2^2}\right) & \frac{-c_2}{\bar{\rho}_2}\sinh\left(\frac{c_2 s(x-x_1)}{c_2^2-\bar{u}_2^2}\right) \\ \frac{-\bar{\rho}_2}{c_2}\sinh\left(\frac{c_2 s(x-x_1)}{c_2^2-\bar{u}_2^2}\right) & \cosh\left(\frac{c_2 s(x-x_1)}{c_2^2-\bar{u}_2^2}\right) \end{bmatrix}\begin{bmatrix} \cosh\left(\frac{c_1 s x_1}{c_1^2-\bar{u}_1^2}\right) & \frac{-c_1}{\bar{\rho}_1}\sinh\left(\frac{c_1 s x_1}{c_1^2-\bar{u}_1^2}\right) \\ \frac{-\bar{\rho}_1}{c_1}\sinh\left(\frac{c_1 s x_1}{c_1^2-\bar{u}_1^2}\right) & \cosh\left(\frac{c_1 s x_1}{c_1^2-\bar{u}_1^2}\right) \end{bmatrix}$$

$$= \exp\left[\left(\frac{\bar{u}_2(x-x_1)}{c_2^2-\bar{u}_2^2}+\frac{\bar{u}_1 x_1}{c_1^2-\bar{u}_1^2}\right)s\right]\begin{bmatrix} A_1 & A_2 \\ A_3 & A_4 \end{bmatrix}$$

Reproduced with permission of the copyright owner. Further reproduction prohibited without permission.

where,

$$A_1 = \cosh\left(\frac{c_2 s(x-x_1)}{c_2^2-\bar{u}_2^2}\right)\cosh\left(\frac{c_1 s x_1}{c_1^2-\bar{u}_1^2}\right) + \frac{\bar{\rho}_1 c_2}{\bar{\rho}_2 c_1}\sinh\left(\frac{c_1 s x_1}{c_1^2-\bar{u}_1^2}\right)\sinh\left(\frac{c_2 s(x-x_1)}{c_2^2-\bar{u}_2^2}\right),$$

$$A_2 = \frac{c_1}{\bar{\rho}_1}\cosh\left(\frac{c_2 s(x-x_1)}{c_2^2-\bar{u}_2^2}\right)\sinh\left(\frac{c_1 s x_1}{c_1^2-\bar{u}_1^2}\right) - \frac{c_2}{\bar{\rho}_2}\sinh\left(\frac{c_2 s(x-x_1)}{c_2^2-\bar{u}_2^2}\right)\cosh\left(\frac{c_1 s x_1}{c_1^2-\bar{u}_1^2}\right),$$

$$A_3 = \frac{\bar{\rho}_2}{c_2}\sinh\left(\frac{c_2 s(x-x_1)}{c_2^2-\bar{u}_2^2}\right)\cosh\left(\frac{c_1 s x_1}{c_1^2-\bar{u}_1^2}\right) - \frac{\bar{\rho}_1}{c_1}\cosh\left(\frac{c_2 s(x-x_1)}{c_2^2-\bar{u}_2^2}\right)\sinh\left(\frac{c_1 s x_1}{c_1^2-\bar{u}_1^2}\right),$$

$$A_4 = \frac{c_1\bar{\rho}_2}{c_2\bar{\rho}_1}\sinh\left(\frac{c_2 s(x-x_1)}{c_2^2-\bar{u}_2^2}\right)\sinh\left(\frac{c_1 s x_1}{c_1^2-\bar{u}_1^2}\right) + \cosh\left(\frac{c_2 s(x-x_1)}{c_2^2-\bar{u}_2^2}\right)\cosh\left(\frac{c_1 s x_1}{c_1^2-\bar{u}_1^2}\right),$$

and,

$$B(s,x) = H_2(s,\, x-x_1)$$

$$= \exp\left(\frac{\bar{u}_2 s(x-x_1)}{c_2^2-\bar{u}_2^2}\right)\begin{bmatrix} \cosh\left(\frac{c_2 s(x-x_1)}{c_2^2-\bar{u}_2^2}\right) & \frac{-c_2}{\bar{\rho}_2}\sinh\left(\frac{c_2 s(x-x_1)}{c_2^2-\bar{u}_2^2}\right) \\ \frac{-\bar{\rho}_2}{c_2}\sinh\left(\frac{c_2 s(x-x_1)}{c_2^2-\bar{u}_2^2}\right) & \cosh\left(\frac{c_2 s(x-x_1)}{c_2^2-\bar{u}_2^2}\right) \end{bmatrix}.$$

In summary, the complete equations for the flow in Channels 1 and 2 are given by:

$$Q(s,x)=\begin{cases} \underline{u}_1(s,x)=H_1(s,x)\underline{u}_1(s,0), & \text{Channel 1} \\ \underline{u}_2(s,x)=H_2(s,x-x_1)H_1(s,x_1)\,\underline{u}_1(s,0)+H_2(s,x-x_1)\Delta\underline{u}(s), & \text{Channel 2.} \end{cases}$$

(4.77)

Reproduced with permission of the copyright owner. Further reproduction prohibited without permission.

It should be noted that the general expression for the flow shown above holds true for a three-wave system, too. In fact, the development of Q(s,x) is a straightforward although somewhat tedious task since, higher order matrix operations must be performed.

In this section, the two-channel with internal input free-space problem was solved. The next section deals with the N-channel with internal inputs free-space problem.

4.9 The N-Channel with Internal Inputs Free-Space Problem

In this section the flow system of Figure 4.15 is studied. This system is an extension of the system studied in the previous section.

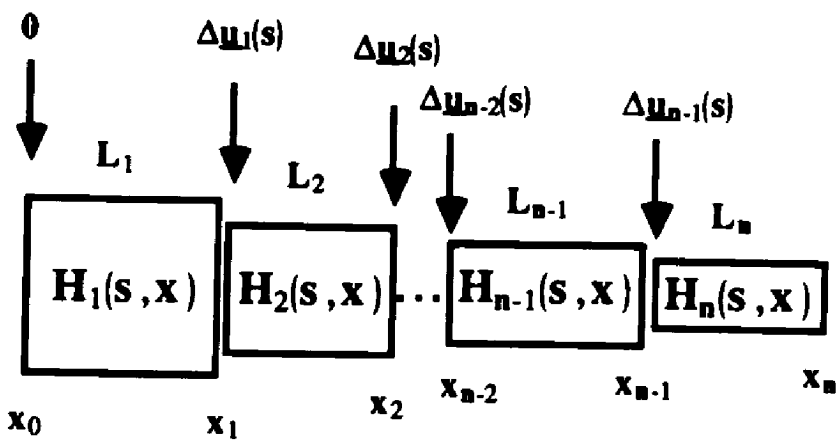


Figure 4.15 The N-channel with internal inputs free-space problem

Reproduced with permission of the copyright owner. Further reproduction prohibited without permission.

The N flow channels are assumed to have N distinct transfer functions $H_1(s,x)$, ... , $H_n(s,x)$, respectively. Also, the lengths of channels 1 through N are L_1, ... , L_N, respectively.

First asssume that the flow at $x=x_0$, i.e., $u_1(s,x_0)$, is given. Then in Channel 1, that is at $0 \le x < x_1 = L_1$, the following equation holds,

$$u_1(s,x-x_0) = H_1(s,x-x_0)\, u_1(s,x_0). \qquad (4.78)$$

Thus just to the left of the first interior boundary the flow is given by,

$$u_1(s,x_1) = H_1(s,x_1-x_0)\, u_1(s,x_0). \qquad (4.79)$$

Just to the right of the interior boundary at $x=x_1=L_1$, the system obeys the following equation:

$$\begin{aligned} u_2(s,x_1) &= u_1(s,x_1) + \Delta u_1(s) \\ &= H_1(s,x_1-x_0)\, u_1(s,x_0) + \Delta u_1(s). \end{aligned}$$

In Channel 2, that is for $x_1 \le x \le x_2 = L_1+L_2$, one then gets the following expression:

$$\begin{aligned} u_2(s,x-x_1) &= H_2(s,x-x_1)\, u_2(s,x_1) \\ &= H_2(s,x-x_1)\left[H_1(s,x_1-x_0)\, u_1(s,x_0) + \Delta u_1(s)\right] \\ &= H_2(s,x-x_1)H_1(s,x_1-x_0)u_1(s,x_0) + H_2(s,x-x_1)\Delta u_1(s). \end{aligned}$$

Thus, just to the left of the second interior boundary the flow is,

$$u_2(s,x_2) = H_2(s,x_2-x_1)H_1(s,x_1-x_0)u_1(s,x_0) + H_2(s,x_2-x_1)\Delta u_1(s). \qquad (4.80)$$

Reproduced with permission of the copyright owner. Further reproduction prohibited without permission.

At the next interior boundary, $x=x_2=L_2$, the system obeys the following equation:

$$u_3(s,x_2) = u_2(s,x_2) + \Delta u_2(s)$$

$$= H_2(s,x_2-x_1)H_1(s,x_1-x_0)\,u_1(s,x_0) + H_2(s,x_2-x_1)\,\Delta u_1(s) + \Delta u_2(s).$$

Then in Channel 3, that is for $x_2 \le x \le x_3 = L_1+L_2+L_3$, one gets the following expression:

$$u_3(s,x-x_2) = H_3(s,x-x_2)\,u_3(s,x_2)$$

$$= H_3(s,x-x_2)\,[H_2(s,x_2-x_1)H_1(s,x_1-x_0)\,u_1(s,x_0) + H_2(s,x_2-x_1)\Delta u_1(s) + \Delta u_2(s)]$$

$$= H_3(s,x-x_2)H_2(s,x_2-x_1)H_1(s,x_1-x_0)\,u_1(s,x_0) + H_3(s,x-x_2)H_2(s,x_2-x_1)\Delta u_1(s) + \Delta u_2(s).$$

Continuing this process for the remaining channels one can get a general expression for the flow in the $(N-1)_{st}$ channel.

$$u_{n-1}(s,x-x_{n-2}) = H_{n-1}(s,x-x_{n-2})\,u_{n-1}(s,x_{n-2})$$

$$= [H_{n-1}(s,x-x_{n-2})H_{n-2}(s,x_{n-2}-x_{n-3}) \cdots H_2(s,x_2-x_1)H_1(s,x_1-x_0)]\,u_1(s,x_0)$$

$$+ [H_{n-1}(s,x-x_{n-2})H_{n-2}(s,x_{n-2}-x_{n-3}) \cdots H_2(s,x_3-x_2)H_1(s,x_2-x_1)]\,\Delta u_1(s)$$

$$+ [H_{n-1}(s,x-x_{n-2})H_{n-2}(s,x_{n-2}-x_{n-3}) \cdots H_2(s,x_4-x_3)H_1(s,x_3-x_2)]\,\Delta u_2(s)$$

$$\vdots \qquad \vdots \qquad \vdots \qquad \vdots$$

$$+ [H_{n-1}(s,x-x_{n-2})H_{n-2}(s,x_{n-2}-x_{n-3})]\,\Delta u_{n-3}(s)$$

$$+ \Delta u_{n-2}(s).$$

Reproduced with permission of the copyright owner. Further reproduction prohibited without permission.

Also,

$$u_{n-1}(s,x_{n-1})=\left[H_{n-1}(s,x_{n-1}-x_{n-2})H_{n-2}(s,x_{n-2}-x_{n-3})\cdots H_2(s,x_2-x_1)H_1(s,x_1-x_0)\right]u_1(s,x_0)$$
$$+\left[H_{n-1}(s,x_{n-1}-x_{n-2})H_{n-2}(s,x_{n-2}-x_{n-3})\cdots H_2(s,x_3-x_2)H_1(s,x_2-x_1)\right]\Delta u_1(s)$$
$$+\left[H_{n-1}(s,x_{n-1}-x_{n-2})H_{n-2}(s,x_{n-2}-x_{n-3})\cdots H_2(s,x_4-x_3)H_1(s,x_3-x_2)\right]\Delta u_2(s)$$
$$\vdots \qquad\qquad \vdots \qquad\qquad \vdots \qquad\qquad \vdots$$
$$+\left[H_{n-1}(s,x_{n-1}-x_{n-2})H_{n-2}(s,x_{n-2}-x_{n-3})\right]\Delta u_{n-3}(s)$$
$$+\Delta u_{n-2}(s).$$

Thus,

$$u_n(s,x_{n-1})=u_{n-1}(s,x_{n-1})+\Delta u_{n-1}(s)$$
$$=\prod_{i=1}^{n-1}\left[H_{n-i}(s,x_{n-i}-x_{n-i-1})\right]u_1(s,x_0)$$
$$+\prod_{i=1}^{n-2}\left[H_{n-i}(s,x_{n-i}-x_{n-i-1})\right]\Delta u_1(s)$$
$$+\prod_{i=1}^{n-3}\left[H_{n-i}(s,x_{n-i}-x_{n-i-1})\right]\Delta u_2(s)$$
$$\vdots \qquad\qquad \vdots \qquad\qquad \vdots$$
$$+\prod_{i=1}^{2}\left[H_{n-i}(s,x_{n-i}-x_{n-i-1})\right]\Delta u_{n-3}(s)$$
$$+\Delta u_{n-2}(s). \qquad (4.81)$$

Also,

$$u_n(s,x-x_{n-1})=H_n(s,x-x_{n-1})u_n(s,x_{n-1})$$
$$=H_n(s,x-x_{n-1})\cdot$$

Reproduced with permission of the copyright owner. Further reproduction prohibited without permission.

$$\left\{\left[\prod_{i=1}^{n-1}\left[H_{n-i}(s,x_{n-i}-x_{n-i-1})\right]\right]u_1(s,x_0)\right.$$

$$+\left[\prod_{i=1}^{n-2}\left[H_{n-i}(s,x_{n-i}-x_{n-i-1})\right]\right]\Delta u_1(s)$$

$$+\left[\prod_{i=1}^{n-3}\left[H_{n-i}(s,x_{n-i}-x_{n-i-1})\right]\right]\Delta u_2(s)$$

$$\vdots \qquad \vdots \qquad \vdots$$

$$\left.+\left[\prod_{i=1}^{2}\left[H_{n-i}(s,x_{n-i}-x_{n-i-1})\right]\right]\Delta u_{n-3}(s)+\Delta u_{n-2}(s)\right\}. \qquad (4.82)$$

Analyzing the above equation, one can see that the flow is made up of a superposition of all contributions of the inflows at each boundary. If all added flows at the interior boundaries are zero, then this problem degenerates to that studied in Section 4.5.

Moreover, the system transfer function can be expressed explicitly if the system order is known. However, even for a two-wave system, this task is very time-consuming.

This brief section dealt with the N-channel bounded with internal inputs free-space problem. The next section examines the two-channel with internal input bounded problem.

Reproduced with permission of the copyright owner. Further reproduction prohibited without permission.

4.10 The Two-Channel with Internal Input Bounded Problem

In this section, the boundary conditions will be applied to the *Two-Channel Free-Space* system, which was studied earlier. Thus, the *Two-Channel with Internal Input Bounded* system, shown in the following figure, results.

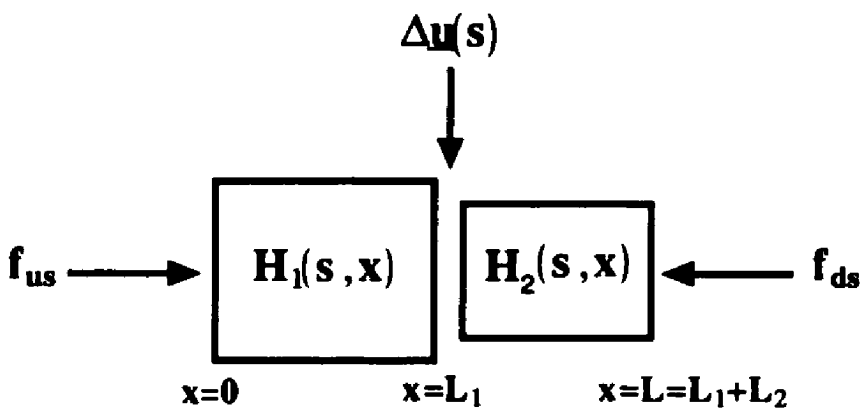


Figure 4.16 The two-channel with internal input bounded problem

The boundary conditions for this problem will depend on the number of state variables used for the modeling of the flow inside the two channels. Thus, the following two- and three-wave problems are to be solved.

A. The Two-Wave Problem

In this important problem, the resulting closed loop system will be such that the downstream input is simply reflective, while the upstream input is a normal shock. Two additional vector inputs f_{us} and f_{ds} will also be present at the upstream and downstream ends of the supersonic inlet,

Reproduced with permission of the copyright owner. Further reproduction prohibited without permission.

respectively. The first input, f_{us}, represents perturbations in the free stream atmosphere while f_{ds} represents compressor or combustor signals. This problem is the simpler of the two to be discussed in this section since the number of state variables used is two.

We shall begin our discussion with the boundary conditions, which are as follows:

$$\boxed{\begin{aligned} u_{us} &= Z_{us}(s)\rho_{us} + f_{us} \\ \rho_{ds} &= Ru_{ds} + f_{ds} \end{aligned}} \quad \text{or} \quad \boxed{\begin{aligned} u(s,0) &= Z_{us}(s)\rho(s,0) + f_{us} \\ \rho(s,L) &= Ru(s,L) + f_{ds} \end{aligned}}$$

These conditions are shown in Figure 4.17 below.

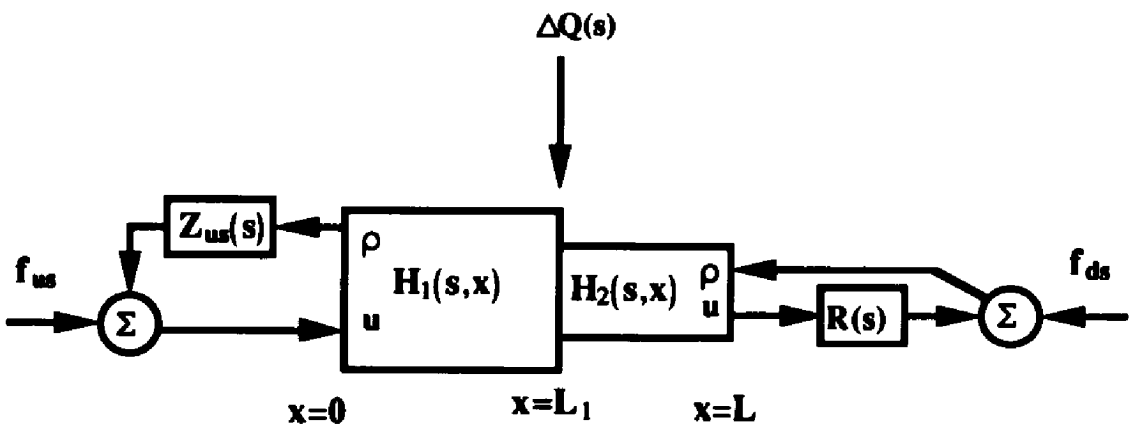


Figure 4.17 Boundary conditions for the two-channel with internal input bounded problem (2-wave)

Using the notation found in [SF65], the above constraints can be put in the following form,

Reproduced with permission of the copyright owner. Further reproduction prohibited without permission.

$$M(s)\,Q_1(s,0) + N(s)\,Q_2(s,L) = Z(s) \qquad (4.83)$$

where,

$$M(s)=\begin{bmatrix} 1 & -Z_{us}(s) \\ 0 & 0 \end{bmatrix}, \quad N(s)=\begin{bmatrix} 0 & 0 \\ -R & 1 \end{bmatrix}, \quad Z(s)=\begin{bmatrix} f_{us} \\ f_{ds} \end{bmatrix}$$

and,

$$Q_1(s,x)=\underline{u}_1(s,x)=\begin{bmatrix} u_1(s,x) \\ \rho_1(s,x) \end{bmatrix}, \qquad Q_2(s,x)=\underline{u}_2(s,x)=\begin{bmatrix} u_2(s,x) \\ \rho_2(s,x) \end{bmatrix}.$$

As before, the flow in Channel 1 is given by:

$$u(s,x) = Q_1(s,x) = H_1(s,x)\,Q_1(s,0). \qquad (4.84)$$

Thus, to the left of the interior boundary of Channels 1 and 2 one gets:

$$u(s,L_1) = Q_1(s,L_1) = H_1(s,L_1)\,Q_1(s,0).$$

On the other hand, just to the right of the interior boundary the following equation holds:

$$u(s,x) = Q_2(s,L_1) = H_1(s,L_1)\,Q_1(s,0) + \Delta\underline{u}(s). \qquad (4.85)$$

Furthermore, in Channel 2 one gets:

$$u(s,x) = Q_2(s,x) = H_2(s,x-L_1)\,Q_2(s,L_1),$$

which is equivalent to the following expression:

Reproduced with permission of the copyright owner. Further reproduction prohibited without permission.

$$u(s,x) = H_2(s,x-L_1)\,[H_1(s,L_1)\,Q_1(s,0) + \Delta u(s)]$$

$$= H_2(s,x-L_1)\,H_1(s,L_1)\,Q_1(s,0) + H_2(s,x-L_1)\,\Delta u(s).$$

Therefore, at x=L, the flow is given by:

$$Q_2(s,L) = Q_2(s,L_1+L_2) = H_2(s,L-L_1)\,H_1(s,L_1)\,Q_1(s,0) + H_2(s,L-L_1)\,\Delta u(s)$$

$$= H_2(s,L_2)\,H_1(s,L_1)\,Q_1(s,0) + H_2(s,L_2)\,\Delta u(s).$$

Substituting $u_2(s,L)$ from above into (4.83) the following expression results:

$$M(s)\,Q_1(s,0) + N(s)\,[H_2(s,L_2)\,H_1(s,L_1)\,Q_1(s,0) + H_2(s,L_2)\Delta u(s)] = Z(s)$$

This expression will next be solved for $Q_1(s,0)$, as this quantity is needed for the computation of the flow vector Q(s,L). The procedure involves first rewriting the above expression as follows:

$$[M(s) + N(s)\,H_2(s,L_2)\,H_1(s,L_1)]\,Q_1(s,0) + N(s)\,H_2(s,L_2)\,\Delta u(s) = Z(s)$$

Next transposing terms yields,

$$[M(s) + N(s)\,H_2(s,L_2)\,H_1(s,L_1)]\,Q_1(s,0) = Z(s) - N(s)\,H_2(s,L_2)\,\Delta u(s)$$

and finally inverting,

$$Q_1(s,0) = [M(s) + N(s)\,H_2(s,L_2)\,H_1(s,L_1)]^{-1}\,[Z(s) - N(s)\,H_2(s,L_2)\,\Delta u(s)]. \qquad (4.86)$$

Reproduced with permission of the copyright owner. Further reproduction prohibited without permission.

Now knowing $Q_1(s,0)$ in terms of $Z(s)$ and $\Delta \underline{u}(s)$ will be useful in determining the flow inside the entire flow line. Namely, in Channel 1 the following equation is readily obtained:

$$u_1(s,x) = Q_1(s,x) = H_1(s,x)\, Q_1(s,0)$$

$$= H_1(s,x)\left\{[M(s) + N(s)\, H_2(s,L_2)\, H_1(s,L_1)]^{-1}\,[Z(s) - N(s)\, H_2(s,L_2)\, \Delta \underline{u}(s)]\right\}$$

$$= H_1(s,x)\,[M(s) + N(s)\, H_2(s,L_2)\, H_1(s,L_1)]^{-1} Z(s)$$

$$- H_1(s,x)\,[M(s) + N(s)\, H_2(s,L_2)\, H_1(s,L_1)]^{-1} N(s)\, H_2(s,L_2)\, \Delta \underline{u}(s)$$

$$\Rightarrow u_1(s,x) \equiv W \cdot Z(s) + Y \cdot \Delta \underline{u}(s). \qquad (4.87)$$

Moreover, the flow in Channel 2 is,

$$u_2(s,x) = Q_2(s,x) = H_2(s,x-L_1)\, H_1(s,L_1)\, Q_1(s,0) + H_2(s,x-L_1)\, \Delta \underline{u}(s)$$

$$= H_2(s,x-L_1)\, H_1(s,L_1)\,[M(s) + N(s)\, H_2(s,L_2)\, H_1(s,L_1)]^{-1}\, Z(s)$$

$$+\left[H_2(s,x-L_1) - H_2(s,x-L_1) H_1(s,L_1)\,[M(s) + N(s) H_2(s,L_2) H_1(s,L_1)]^{-1} N(s) H_2(s,L_2)\right] \Delta \underline{u}(s)$$

$$\Rightarrow u_2(s,x) \equiv P \cdot Z(s) + S \cdot \Delta \underline{u}(s). \qquad (4.88)$$

Finally, from the general solution given above, one can obtain the exact solution for the total flow vector $Q(s,x)$ by substituting $H_1(s,x)$ and $H_2(s,x)$ into $Q_1(s,x)$ and $Q_2(s,x)$. As the following few pages indicates, this will turn out to be a very tedious, yet straightforward, task!

Reproduced with permission of the copyright owner. Further reproduction prohibited without permission.

Recall that the free-space transfer function matrix for a two-wave system is given by:

$$H_i(s,x) = \exp\left(\frac{\bar{u}_i s x}{c_i^2-\bar{u}_i^2}\right)\begin{bmatrix} \cosh\left(\frac{c_i s x}{c_i^2-\bar{u}_i^2}\right) & \frac{-c_i}{\bar{\rho}_i}\sinh\left(\frac{c_i s x}{c_i^2-\bar{u}_i^2}\right) \\ \frac{-\bar{\rho}_i}{c_i}\sinh\left(\frac{c_i s x}{c_i^2-\bar{u}_i^2}\right) & \cosh\left(\frac{c_i s x}{c_i^2-\bar{u}_i^2}\right) \end{bmatrix}$$

where, index i represents the ith channel. Also, let

$$F(s) \equiv H_2(s,L_2)\,H_1(s,L_1) = \begin{bmatrix} F_{11} & F_{12} \\ F_{21} & F_{22} \end{bmatrix} \qquad (4.89)$$

where,

$$F(s) = \exp\left[\left(\frac{\bar{u}_1 L_1}{c_1^2-\bar{u}_1^2} + \frac{\bar{u}_2 L_2}{c_2^2-\bar{u}_2^2}\right)s\right] \cdot$$

$$\begin{bmatrix} \cosh\left(\frac{c_2 s L_2}{c_2^2-\bar{u}_2^2}\right) & \frac{-c_2}{\bar{\rho}_2}\sinh\left(\frac{c_2 s L_2}{c_2^2-\bar{u}_2^2}\right) \\ \frac{-\bar{\rho}_2}{c_2}\sinh\left(\frac{c_2 s L_2}{c_2^2-\bar{u}_2^2}\right) & \cosh\left(\frac{c_2 s L_2}{c_2^2-\bar{u}_2^2}\right) \end{bmatrix}\begin{bmatrix} \cosh\left(\frac{c_1 s L_1}{c_1^2-\bar{u}_1^2}\right) & \frac{-c_1}{\bar{\rho}_1}\sinh\left(\frac{c_1 s L_1}{c_1^2-\bar{u}_1^2}\right) \\ \frac{-\bar{\rho}_1}{c_1}\sinh\left(\frac{c_1 s L_1}{c_1^2-\bar{u}_1^2}\right) & \cosh\left(\frac{c_1 s L_1}{c_1^2-\bar{u}_1^2}\right) \end{bmatrix}$$

or,

$$F_{11}=\exp\left[\left(\frac{\bar{u}_1 L_1}{c_1^2-\bar{u}_1^2} + \frac{\bar{u}_2 L_2}{c_2^2-\bar{u}_2^2}\right)s\right]\left[\frac{\bar{\rho}_1}{\bar{\rho}_2}\frac{c_2}{c_1}\sinh\left(\frac{c_1 s L_1}{c_1^2-\bar{u}_1^2}\right)\sinh\left(\frac{c_2 s L_2}{c_2^2-\bar{u}_2^2}\right)+\cosh\left(\frac{c_1 s L_1}{c_1^2-\bar{u}_1^2}\right)\cosh\left(\frac{c_2 s L_2}{c_2^2-\bar{u}_2^2}\right)\right],$$

$$F_{12}=\exp\left[\left(\frac{\bar{u}_1 L_1}{c_1^2-\bar{u}_1^2} + \frac{\bar{u}_2 L_2}{c_2^2-\bar{u}_2^2}\right)s\right]\left[\frac{-c_1}{\bar{\rho}_1}\sinh\left(\frac{c_1 s L_1}{c_1^2-\bar{u}_1^2}\right)\cosh\left(\frac{c_2 s L_2}{c_2^2-\bar{u}_2^2}\right) - \frac{c_2}{\bar{\rho}_2}\sinh\left(\frac{c_2 s L_2}{c_2^2-\bar{u}_2^2}\right)\cosh\left(\frac{c_1 s L_1}{c_1^2-\bar{u}_1^2}\right)\right],$$

$$F_{21} = \exp\left[\left(\frac{\bar{u}_1 L_1}{c_1^2-\bar{u}_1^2} + \frac{\bar{u}_2 L_2}{c_2^2-\bar{u}_2^2}\right)s\right]\left[\frac{-\bar{\rho}_2}{c_2}\sinh\left(\frac{c_2 s L_2}{c_2^2-\bar{u}_2^2}\right)\cosh\left(\frac{c_1 s L_1}{c_1^2-\bar{u}_1^2}\right) - \frac{\bar{\rho}_1}{c_1}\sinh\left(\frac{c_1 s L_1}{c_1^2-\bar{u}_1^2}\right)\cosh\left(\frac{c_2 s L_2}{c_2^2-\bar{u}_2^2}\right)\right],$$

and,

Reproduced with permission of the copyright owner. Further reproduction prohibited without permission.

$$F_{22}=\exp\left[\left(\frac{\bar{u}_1 L_1}{c_1^2-\bar{u}_1^2}+\frac{\bar{u}_2 L_2}{c_2^2-\bar{u}_2^2}\right)s\right]\left[\frac{\bar{\rho}_2}{\bar{\rho}_1}\frac{c_1}{c_2}\sinh\left(\frac{c_1 s L_1}{c_1^2-\bar{u}_1^2}\right)\sinh\left(\frac{c_2 s L_2}{c_2^2-\bar{u}_2^2}\right)+\cosh\left(\frac{c_1 s L_1}{c_1^2-\bar{u}_1^2}\right)\cosh\left(\frac{c_2 s L_2}{c_2^2-\bar{u}_2^2}\right)\right].$$

Also,

$$[M(s)+N(s)\,H_2(s,L_2)\,H_1(s,L_1)]^{-1}=[M(s)+N(s)\,F(s)]^{-1}=$$

$$=\left\{\begin{bmatrix}1 & -Z_{us}(s)\\ 0 & 0\end{bmatrix}+\begin{bmatrix}0 & 0\\ -R & 1\end{bmatrix}\begin{bmatrix}F_{11} & F_{12}\\ F_{21} & F_{22}\end{bmatrix}\right\}^{-1}=\begin{bmatrix}1 & -Z_{us}(s)\\ F_{21}-RF_{11} & F_{22}-RF_{12}\end{bmatrix}^{-1}$$

$$=\frac{\begin{bmatrix}F_{22}-RF_{12} & Z_{us}(s)\\ RF_{11}-F_{21} & 1\end{bmatrix}}{F_{22}-RF_{12}+Z_{us}(s)\,(F_{21}-RF_{11})}, \qquad (4.90)$$

where,

$$F_{22}-R\,F_{12}=\exp\left[\left(\frac{\bar{u}_1 L_1}{c_1^2-\bar{u}_1^2}+\frac{\bar{u}_2 L_2}{c_2^2-\bar{u}_2^2}\right)s\right]\cdot$$

$$\left\{\frac{\bar{\rho}_2}{\bar{\rho}_1}\frac{c_1}{c_2}\sinh\left(\frac{c_1 s L_1}{c_1^2-\bar{u}_1^2}\right)\sinh\left(\frac{c_2 s L_2}{c_2^2-\bar{u}_2^2}\right)+\cosh\left(\frac{c_1 s L_1}{c_1^2-\bar{u}_1^2}\right)\cosh\left(\frac{c_2 s L_2}{c_2^2-\bar{u}_2^2}\right)\right.$$

$$\left.+R\frac{c_1}{\bar{\rho}_1}\sinh\left(\frac{c_1 s L_1}{c_1^2-\bar{u}_1^2}\right)\cosh\left(\frac{c_2 s L_2}{c_2^2-\bar{u}_2^2}\right)+R\frac{c_2}{\bar{\rho}_2}\sinh\left(\frac{c_2 s L_2}{c_2^2-\bar{u}_2^2}\right)\cosh\left(\frac{c_1 s L_1}{c_1^2-\bar{u}_1^2}\right)\right\},$$

$$R\,F_{11}-F_{21}=\exp\left[\left(\frac{\bar{u}_1 L_1}{c_1^2-\bar{u}_1^2}+\frac{\bar{u}_2 L_2}{c_2^2-\bar{u}_2^2}\right)s\right]\cdot$$

$$\left\{R\frac{\bar{\rho}_1}{\bar{\rho}_2}\frac{c_2}{c_1}\sinh\left(\frac{c_1 s L_1}{c_1^2-\bar{u}_1^2}\right)\sinh\left(\frac{c_2 s L_2}{c_2^2-\bar{u}_2^2}\right)+R\cosh\left(\frac{c_1 s L_1}{c_1^2-\bar{u}_1^2}\right)\cosh\left(\frac{c_2 s L_2}{c_2^2-\bar{u}_2^2}\right)\right.$$

$$\left.+\frac{\bar{\rho}_2}{c_2}\sinh\left(\frac{c_2 s L_2}{c_2^2-\bar{u}_2^2}\right)\cosh\left(\frac{c_1 s L_1}{c_1^2-\bar{u}_1^2}\right)+\frac{\bar{\rho}_1}{c_1}\sinh\left(\frac{c_1 s L_1}{c_1^2-\bar{u}_1^2}\right)\cosh\left(\frac{c_2 s L_2}{c_2^2-\bar{u}_2^2}\right)\right\}.$$

Reproduced with permission of the copyright owner. Further reproduction prohibited without permission.

and,

$$F_{22} - R F_{12} + Z_{us}(s)(F_{21} - R F_{11}) = \exp\left[\left(\frac{\bar{u}_1 L_1}{c_1^2 - \bar{u}_1^2} + \frac{\bar{u}_2 L_2}{c_2^2 - \bar{u}_2^2}\right) s\right] \cdot$$

$$\left\{ \frac{\bar{\rho}_2}{\bar{\rho}_1} \frac{c_1}{c_2} \sinh\left(\frac{c_1 s L_1}{c_1^2 - \bar{u}_1^2}\right) \sinh\left(\frac{c_2 s L_2}{c_2^2 - \bar{u}_2^2}\right) + \cosh\left(\frac{c_1 s L_1}{c_1^2 - \bar{u}_1^2}\right) \cosh\left(\frac{c_2 s L_2}{c_2^2 - \bar{u}_2^2}\right) \right.$$

$$+ R \frac{c_1}{\bar{\rho}_1} \sinh\left(\frac{c_1 s L_1}{c_1^2 - \bar{u}_1^2}\right) \cosh\left(\frac{c_2 s L_2}{c_2^2 - \bar{u}_2^2}\right) + R \frac{c_2}{\bar{\rho}_2} \sinh\left(\frac{c_2 s L_2}{c_2^2 - \bar{u}_2^2}\right) \cosh\left(\frac{c_1 s L_1}{c_1^2 - \bar{u}_1^2}\right)$$

$$- R Z_{us}(s) \frac{\bar{\rho}_1}{\bar{\rho}_2} \frac{c_2}{c_1} \sinh\left(\frac{c_1 s L_1}{c_1^2 - \bar{u}_1^2}\right) \sinh\left(\frac{c_2 s L_2}{c_2^2 - \bar{u}_2^2}\right) - R Z_{us}(s) \cosh\left(\frac{c_1 s L_1}{c_1^2 - \bar{u}_1^2}\right) \cosh\left(\frac{c_2 s L_2}{c_2^2 - \bar{u}_2^2}\right)$$

$$\left. - Z_{us}(s) \frac{\bar{\rho}_2}{c_2} \sinh\left(\frac{c_2 s L_2}{c_2^2 - \bar{u}_2^2}\right) \cosh\left(\frac{c_1 s L_1}{c_1^2 - \bar{u}_1^2}\right) - Z_{us}(s) \frac{\bar{\rho}_1}{c_1} \sinh\left(\frac{c_1 s L_1}{c_1^2 - \bar{u}_1^2}\right) \cosh\left(\frac{c_2 s L_2}{c_2^2 - \bar{u}_2^2}\right) \right\}$$

or,

$$F_{22} - R F_{12} + Z_{us}(s)(F_{21} - R F_{11}) = \exp\left[\left(\frac{\bar{u}_1 L_1}{c_1^2 - \bar{u}_1^2} + \frac{\bar{u}_2 L_2}{c_2^2 - \bar{u}_2^2}\right) s\right] \cdot$$

$$\left\{ \left[\frac{\bar{\rho}_2}{\bar{\rho}_1} \frac{c_1}{c_2} - R Z_{us}(s) \frac{\bar{\rho}_1}{\bar{\rho}_2} \frac{c_2}{c_1} \right] \sinh\left(\frac{c_1 s L_1}{c_1^2 - \bar{u}_1^2}\right) \sinh\left(\frac{c_2 s L_2}{c_2^2 - \bar{u}_2^2}\right) + [1 - R Z_{us}(s)] \cosh\left(\frac{c_1 s L_1}{c_1^2 - \bar{u}_1^2}\right) \cosh\left(\frac{c_2 s L_2}{c_2^2 - \bar{u}_2^2}\right) \right.$$

$$\left. + \left[R \frac{c_1}{\bar{\rho}_1} - Z_{us}(s) \frac{\bar{\rho}_1}{c_1} \right] \sinh\left(\frac{c_1 s L_1}{c_1^2 - \bar{u}_1^2}\right) \cosh\left(\frac{c_2 s L_2}{c_2^2 - \bar{u}_2^2}\right) + \left[R \frac{c_2}{\bar{\rho}_2} - Z_{us}(s) \frac{\bar{\rho}_2}{c_2} \right] \sinh\left(\frac{c_2 s L_2}{c_2^2 - \bar{u}_2^2}\right) \cosh\left(\frac{c_1 s L_1}{c_1^2 - \bar{u}_1^2}\right) \right\} .$$

Finally, the coefficient matrix of $u_1(s,x)$ due to $Z(s)$, i.e., W, is as follows.

$$W = H_1(s,x)\left[M(s) + N(s) H_2(s,L_2) H_1(s,L_1)\right]^{-1} = \begin{bmatrix} W_1 & W_2 \\ W_3 & W_4 \end{bmatrix} =$$

Reproduced with permission of the copyright owner. Further reproduction prohibited without permission.

$$= \frac{\exp\left(\frac{\bar{u}_1 sx}{c_1^2-\bar{u}_1^2}\right)}{F_{22}-RF_{12}+Z_{us}(s)(F_{21}-RF_{11})} \begin{bmatrix} \cosh\left(\frac{c_1 sx}{c_1^2-\bar{u}_1^2}\right) & \frac{-c_1}{\bar{\rho}_1}\sinh\left(\frac{c_1 sx}{c_1^2-\bar{u}_1^2}\right) \\ \frac{-\bar{\rho}_1}{c_1}\sinh\left(\frac{c_1 sx}{c_1^2-\bar{u}_1^2}\right) & \cosh\left(\frac{c_1 sx}{c_1^2-\bar{u}_1^2}\right) \end{bmatrix} \begin{bmatrix} F_{22}-RF_{12} & Z_{us}(s) \\ RF_{11}-F_{21} & 1 \end{bmatrix}$$

$$= \frac{\exp\left(\frac{\bar{u}_1 sx}{c_1^2-\bar{u}_1^2}\right)}{F_{22}-RF_{12}+Z_{us}(s)(F_{21}-RF_{11})}$$

$$\begin{bmatrix} \cosh\left(\frac{c_1 sx}{c_1^2-\bar{u}_1^2}\right)(F_{22}-RF_{12}) - \frac{c_1}{\bar{\rho}_1}\sinh\left(\frac{c_1 sx}{c_1^2-\bar{u}_1^2}\right)(RF_{11}-F_{21}) & \cosh\left(\frac{c_1 sx}{c_1^2-\bar{u}_1^2}\right)Z_{us}(s) - \frac{c_1}{\bar{\rho}_1}\sinh\left(\frac{c_1 sx}{c_1^2-\bar{u}_1^2}\right) \\ \frac{-\bar{\rho}_1}{c_1}\sinh\left(\frac{c_1 sx}{c_1^2-\bar{u}_1^2}\right)(F_{22}-RF_{12}) + \cosh\left(\frac{c_1 sx}{c_1^2-\bar{u}_1^2}\right)(RF_{11}-F_{21}) & \frac{-Z_{us}(s)\bar{\rho}_1}{c_1}\sinh\left(\frac{c_1 sx}{c_1^2-\bar{u}_1^2}\right) + \cosh\left(\frac{c_1 sx}{c_1^2-\bar{u}_1^2}\right) \end{bmatrix}$$

Thus,

$$W_1 = \frac{\exp\left(\frac{\bar{u}_1 sx}{c_1^2-\bar{u}_1^2}\right)\exp\left[\left(\frac{\bar{u}_1 L_1}{c_1^2-\bar{u}_1^2}+\frac{\bar{u}_2 L_2}{c_2^2-\bar{u}_2^2}\right)s\right]}{F_{22}-RF_{12}+Z_{us}(s)(F_{21}-RF_{11})}$$

$$\left\{\cosh\left(\frac{c_1 sx}{c_1^2-\bar{u}_1^2}\right)\left[\frac{\bar{\rho}_2}{\bar{\rho}_1}\frac{c_1}{c_2}\sinh\left(\frac{c_1 sL_1}{c_1^2-\bar{u}_1^2}\right)\sinh\left(\frac{c_2 sL_2}{c_2^2-\bar{u}_2^2}\right)+\cosh\left(\frac{c_1 sL_1}{c_1^2-\bar{u}_1^2}\right)\cosh\left(\frac{c_2 sL_2}{c_2^2-\bar{u}_2^2}\right)\right.\right.$$

$$\left.+R\frac{c_1}{\bar{\rho}_1}\sinh\left(\frac{c_1 sL_1}{c_1^2-\bar{u}_1^2}\right)\cosh\left(\frac{c_2 sL_2}{c_2^2-\bar{u}_2^2}\right)+R\frac{c_2}{\bar{\rho}_2}\sinh\left(\frac{c_2 sL_2}{c_2^2-\bar{u}_2^2}\right)\cosh\left(\frac{c_1 sL_1}{c_1^2-\bar{u}_1^2}\right)\right]$$

$$-\frac{c_1}{\bar{\rho}_1}\sinh\left(\frac{c_1 sx}{c_1^2-\bar{u}_1^2}\right)\left[R\frac{\bar{\rho}_1}{\bar{\rho}_2}\frac{c_2}{c_1}\sinh\left(\frac{c_1 sL_1}{c_1^2-\bar{u}_1^2}\right)\sinh\left(\frac{c_2 sL_2}{c_2^2-\bar{u}_2^2}\right)+R\cosh\left(\frac{c_1 sL_1}{c_1^2-\bar{u}_1^2}\right)\cosh\left(\frac{c_2 sL_2}{c_2^2-\bar{u}_2^2}\right)\right.$$

$$\left.\left.+\frac{\bar{\rho}_2}{c_2}\sinh\left(\frac{c_2 sL_2}{c_2^2-\bar{u}_2^2}\right)\cosh\left(\frac{c_1 sL_1}{c_1^2-\bar{u}_1^2}\right)+\frac{\bar{\rho}_1}{c_1}\sinh\left(\frac{c_1 sL_1}{c_1^2-\bar{u}_1^2}\right)\cosh\left(\frac{c_2 sL_2}{c_2^2-\bar{u}_2^2}\right)\right]\right\},$$

Reproduced with permission of the copyright owner. Further reproduction prohibited without permission.

or,

$$W_1 = \frac{\exp\left[\left(\frac{\bar{u}_1(L_1+x)}{c_1^2-\bar{u}_1^2} + \frac{\bar{u}_2 L_2}{c_2^2-\bar{u}_2^2}\right)s\right]}{F_{22}-RF_{12}+Z_{us}(s)(F_{21}-RF_{11})}$$

$$\left\{\left[\frac{\bar{\rho}_2}{\bar{\rho}_1}\frac{c_1}{c_2}\cosh\left(\frac{c_1 sx}{c_1^2-\bar{u}_1^2}\right) - R\frac{c_2}{\bar{\rho}_2}\sinh\left(\frac{c_1 sx}{c_1^2-\bar{u}_1^2}\right)\right]\sinh\left(\frac{c_1 sL_1}{c_1^2-\bar{u}_1^2}\right)\sinh\left(\frac{c_2 sL_2}{c_2^2-\bar{u}_2^2}\right) +\right.$$

$$+\left[\cosh\left(\frac{c_1 sx}{c_1^2-\bar{u}_1^2}\right) - \frac{c_1}{\bar{\rho}_1}R\sinh\left(\frac{c_1 sx}{c_1^2-\bar{u}_1^2}\right)\right]\cosh\left(\frac{c_1 sL_1}{c_1^2-\bar{u}_1^2}\right)\cosh\left(\frac{c_2 sL_2}{c_2^2-\bar{u}_2^2}\right) +$$

$$+\left[R\frac{c_2}{\bar{\rho}_2}\cosh\left(\frac{c_1 sx}{c_1^2-\bar{u}_1^2}\right) - \frac{\bar{\rho}_2}{\bar{\rho}_1}\frac{c_1}{c_2}\sinh\left(\frac{c_1 sx}{c_1^2-\bar{u}_1^2}\right)\right]\sinh\left(\frac{c_2 sL_2}{c_2^2-\bar{u}_2^2}\right)\cosh\left(\frac{c_1 sL_1}{c_1^2-\bar{u}_1^2}\right) +$$

$$\left.+\left[R\frac{c_1}{\bar{\rho}_1}\cosh\left(\frac{c_1 sx}{c_1^2-\bar{u}_1^2}\right) - \sinh\left(\frac{c_1 sx}{c_1^2-\bar{u}_1^2}\right)\right]\sinh\left(\frac{c_1 sL_1}{c_1^2-\bar{u}_1^2}\right)\cosh\left(\frac{c_2 sL_2}{c_2^2-\bar{u}_2^2}\right)\right\}. \qquad (4.91)$$

$$W_2 = \frac{\exp\left(\frac{\bar{u}_1 sx}{c_1^2-\bar{u}_1^2}\right)\left\{\cosh\left(\frac{c_1 sx}{c_1^2-\bar{u}_1^2}\right)Z_{us}(s) - \frac{c_1}{\bar{\rho}_1}\sinh\left(\frac{c_1 sx}{c_1^2-\bar{u}_1^2}\right)\right\}}{F_{22}-RF_{12}+Z_{us}(s)(F_{21}-RF_{11})}, \qquad (4.92)$$

$$W_3 = \frac{\exp\left(\frac{\bar{u}_1 sx}{c_1^2-\bar{u}_1^2}\right)\exp\left[\left(\frac{\bar{u}_1 L_1}{c_1^2-\bar{u}_1^2} + \frac{\bar{u}_2 L_2}{c_2^2-\bar{u}_2^2}\right)s\right]}{F_{22}-RF_{12}+Z_{us}(s)(F_{21}-RF_{11})}$$

$$\left\{\frac{-\bar{\rho}_1}{c_1}\sinh\left(\frac{c_1 sx}{c_1^2-\bar{u}_1^2}\right)\left[\frac{\bar{\rho}_2}{\bar{\rho}_1}\frac{c_1}{c_2}\sinh\left(\frac{c_1 sL_1}{c_1^2-\bar{u}_1^2}\right)\sinh\left(\frac{c_2 sL_2}{c_2^2-\bar{u}_2^2}\right) + \cosh\left(\frac{c_1 sL_1}{c_1^2-\bar{u}_1^2}\right)\cosh\left(\frac{c_2 sL_2}{c_2^2-\bar{u}_2^2}\right)\right.\right.$$

$$+ R\frac{c_1}{\bar{\rho}_1}\sinh\left(\frac{c_1 sL_1}{c_1^2-\bar{u}_1^2}\right)\cosh\left(\frac{c_2 sL_2}{c_2^2-\bar{u}_2^2}\right) + R\frac{c_2}{\bar{\rho}_2}\sinh\left(\frac{c_2 sL_2}{c_2^2-\bar{u}_2^2}\right)\cosh\left(\frac{c_1 sL_1}{c_1^2-\bar{u}_1^2}\right)$$

$$+ \cosh\left(\frac{c_1 sx}{c_1^2-\bar{u}_1^2}\right)\left[R\frac{\bar{\rho}_1}{\bar{\rho}_2}\frac{c_2}{c_1}\sinh\left(\frac{c_1 sL_1}{c_1^2-\bar{u}_1^2}\right)\sinh\left(\frac{c_2 sL_2}{c_2^2-\bar{u}_2^2}\right) + R\cosh\left(\frac{c_1 sL_1}{c_1^2-\bar{u}_1^2}\right)\cosh\left(\frac{c_2 sL_2}{c_2^2-\bar{u}_2^2}\right)\right.$$

$$\left.\left.+ \frac{\bar{\rho}_2}{c_2}\sinh\left(\frac{c_2 sL_2}{c_2^2-\bar{u}_2^2}\right)\cosh\left(\frac{c_1 sL_1}{c_1^2-\bar{u}_1^2}\right) + \frac{\bar{\rho}_1}{c_1}\sinh\left(\frac{c_1 sL_1}{c_1^2-\bar{u}_1^2}\right)\cosh\left(\frac{c_2 sL_2}{c_2^2-\bar{u}_2^2}\right)\right]\right\}.$$

Reproduced with permission of the copyright owner. Further reproduction prohibited without permission.

or,

$$W_3 = \frac{\exp\left[\left(\frac{\bar{u}_1(L_1+x)}{c_1^2-\bar{u}_1^2} + \frac{\bar{u}_2 L_2}{c_2^2-\bar{u}_2^2}\right)s\right]}{F_{22}-RF_{12} + Z_{us}(s)(F_{21}-RF_{11})}$$

$$\left\{\left[-\frac{\bar{\rho}_2}{c_2}\sinh\left(\frac{c_1 sx}{c_1^2-\bar{u}_1^2}\right) + R\frac{\bar{\rho}_1}{\bar{\rho}_2}\frac{c_2}{c_1}\cosh\left(\frac{c_1 sx}{c_1^2-\bar{u}_1^2}\right)\right]\sinh\left(\frac{c_1 sL_1}{c_1^2-\bar{u}_1^2}\right)\sinh\left(\frac{c_2 sL_2}{c_2^2-\bar{u}_2^2}\right) +\right.$$

$$+\left[-\frac{c_1}{\bar{\rho}_1}\sinh\left(\frac{c_1 sx}{c_1^2-\bar{u}_1^2}\right) + R\cosh\left(\frac{c_1 sx}{c_1^2-\bar{u}_1^2}\right)\right]\cosh\left(\frac{c_1 sL_1}{c_1^2-\bar{u}_1^2}\right)\cosh\left(\frac{c_2 sL_2}{c_2^2-\bar{u}_2^2}\right) +$$

$$+\left[-R\frac{\bar{\rho}_2}{\bar{\rho}_1}\frac{c_1}{c_2}\sinh\left(\frac{c_1 sx}{c_1^2-\bar{u}_1^2}\right) + \frac{\bar{\rho}_2}{c_2}\cosh\left(\frac{c_1 sx}{c_1^2-\bar{u}_1^2}\right)\right]\sinh\left(\frac{c_2 sL_2}{c_2^2-\bar{u}_2^2}\right)\cosh\left(\frac{c_1 sL_1}{c_1^2-\bar{u}_1^2}\right) +$$

$$\left.+\left[-R\sinh\left(\frac{c_1 sx}{c_1^2-\bar{u}_1^2}\right) + \frac{\bar{\rho}_1}{c_1}\cosh\left(\frac{c_1 sx}{c_1^2-\bar{u}_1^2}\right)\right]\sinh\left(\frac{c_1 sL_1}{c_1^2-\bar{u}_1^2}\right)\cosh\left(\frac{c_2 sL_2}{c_2^2-\bar{u}_2^2}\right)\right\}, \qquad (4.93)$$

and finally,

$$W_4 = \frac{\exp\left(\frac{\bar{u}_1 sx}{c_1^2-\bar{u}_1^2}\right)\left\{\frac{-Z_{us}(s)\bar{\rho}_1}{c_1}\sinh\left(\frac{c_1 sx}{c_1^2-\bar{u}_1^2}\right) + \cosh\left(\frac{c_1 sx}{c_1^2-\bar{u}_1^2}\right)\right\}}{F_{22}-RF_{12} + Z_{us}(s)(F_{21}-RF_{11})}. \qquad (4.94)$$

Similarly, the coefficient matrix, Y, of $u_1(s,x)$ due to $\Delta\underline{u}(s)$ is as follows.

$$Y = \begin{bmatrix} Y_1 & Y_2 \\ Y_3 & Y_4 \end{bmatrix} = -W\,N(s)\,H_2(s,L_2) = -\begin{bmatrix} W_1 & W_2 \\ W_3 & W_4 \end{bmatrix}\begin{bmatrix} 0 & 0 \\ -R & 1 \end{bmatrix}H_2(s,L_2) =$$

$$= -\begin{bmatrix} -RW_2 & W_2 \\ -RW_4 & W_4 \end{bmatrix}H_2(s,L_2) = \begin{bmatrix} RW_2 & -W_2 \\ RW_4 & -W_4 \end{bmatrix}H_2(s,L_2) =$$

Reproduced with permission of the copyright owner. Further reproduction prohibited without permission.

$$Y_2 = \frac{\exp\left[\left(\frac{\bar{u}_1 x}{c_1^2-\bar{u}_1^2} + \frac{\bar{u}_2 L_2}{c_2^2-\bar{u}_2^2}\right) s\right]}{F_{22}-RF_{12} + Z_{us}(s)(F_{21}-RF_{11})} \cdot$$

$$\cdot \left\{ \frac{-c_2}{\bar{\rho}_2} \sinh\left(\frac{c_2 s L_2}{c_2^2-\bar{u}_2^2}\right)\left[R \cosh\left(\frac{c_1 s x}{c_1^2-\bar{u}_1^2}\right) Z_{us}(s) - R \frac{c_1}{\bar{\rho}_1} \sinh\left(\frac{c_1 s x}{c_1^2-\bar{u}_1^2}\right)\right] \right.$$

$$\left. + \cosh\left(\frac{c_2 s L_2}{c_2^2-\bar{u}_2^2}\right)\left[- \cosh\left(\frac{c_1 s x}{c_1^2-\bar{u}_1^2}\right) Z_{us}(s) + \frac{c_1}{\bar{\rho}_1} \sinh\left(\frac{c_1 s x}{c_1^2-\bar{u}_1^2}\right)\right] \right\}, \qquad (4.96)$$

$$Y_3 = \frac{\exp\left[\left(\frac{\bar{u}_1 x}{c_1^2-\bar{u}_1^2} + \frac{\bar{u}_2 L_2}{c_2^2-\bar{u}_2^2}\right) s\right]}{F_{22}-RF_{12} + Z_{us}(s)(F_{21}-RF_{11})} \cdot$$

$$\cdot \left\{ \left[\frac{-RZ_{us}(s)\bar{\rho}_1}{c_1} \sinh\left(\frac{c_1 s x}{c_1^2-\bar{u}_1^2}\right) + R \cosh\left(\frac{c_1 s x}{c_1^2-\bar{u}_1^2}\right)\right] \cosh\left(\frac{c_2 s L_2}{c_2^2-\bar{u}_2^2}\right) \right.$$

$$\left. - \frac{\bar{\rho}_2}{c_2} \sinh\left(\frac{c_2 s L_2}{c_2^2-\bar{u}_2^2}\right)\left[\frac{Z_{us}(s)\bar{\rho}_1}{c_1} \sinh\left(\frac{c_1 s x}{c_1^2-\bar{u}_1^2}\right) - \cosh\left(\frac{c_1 s x}{c_1^2-\bar{u}_1^2}\right)\right] \right\}, \qquad (4.97)$$

and finally,

$$Y_4 = \frac{\exp\left[\left(\frac{\bar{u}_1 x}{c_1^2-\bar{u}_1^2} + \frac{\bar{u}_2 L_2}{c_2^2-\bar{u}_2^2}\right) s\right]}{F_{22}-RF_{12} + Z_{us}(s)(F_{21}-RF_{11})} \cdot$$

$$\cdot \left\{ \frac{-c_2}{\bar{\rho}_2} \sinh\left(\frac{c_2 s L_2}{c_2^2-\bar{u}_2^2}\right)\left[\frac{-RZ_{us}(s)\bar{\rho}_1}{c_1} \sinh\left(\frac{c_1 s x}{c_1^2-\bar{u}_1^2}\right) + R \cosh\left(\frac{c_1 s x}{c_1^2-\bar{u}_1^2}\right)\right] \right.$$

$$\left. + \left[\frac{Z_{us}(s)\bar{\rho}_1}{c_1} \sinh\left(\frac{c_1 s x}{c_1^2-\bar{u}_1^2}\right) - \cosh\left(\frac{c_1 s x}{c_1^2-\bar{u}_1^2}\right)\right] \cosh\left(\frac{c_2 s L_2}{c_2^2-\bar{u}_2^2}\right) \right\}. \qquad (4.98)$$

Next, in order to compute the flow vector in Channel 2, the matrices P and S must be first computed using these equations,

Reproduced with permission of the copyright owner. Further reproduction prohibited without permission.

$$P = H_2(s,x-L_1)[W]_{x=L_1} \tag{4.99}$$

and

$$S = H_2(s,x-L_1) - P\,N(s)\,H_2(s,L_2). \tag{4.100}$$

Substituting W into the first expression yields,

$$P = H_2(s,x-L_1)[W]_{x=L_1} \equiv H_2(s,x-L_1)\,W(x=L_1) =$$

$$= \exp\left(\frac{\bar{u}_2 s(x-L_1)}{c_2^2-\bar{u}_2^2}\right)\begin{bmatrix} \cosh\left(\frac{c_2 s(x-L_1)}{c_2^2-\bar{u}_2^2}\right) & -\frac{c_2}{\bar{\rho}_2}\sinh\left(\frac{c_2 s(x-L_1)}{c_2^2-\bar{u}_2^2}\right) \\ -\frac{\bar{\rho}_2}{c_2}\sinh\left(\frac{c_2 s(x-L_1)}{c_2^2-\bar{u}_2^2}\right) & \cosh\left(\frac{c_2 s(x-L_1)}{c_2^2-\bar{u}_2^2}\right) \end{bmatrix}\begin{bmatrix} W_1(x=L_1) & W_2(x=L_1) \\ W_3(x=L_1) & W_4(x=L_1) \end{bmatrix}.$$

Thus,

$$P_1=\exp\left(\frac{\bar{u}_2 s(x-L_1)}{c_2^2-\bar{u}_2^2}\right)\left[\cosh\left(\frac{c_2 s(x-L_1)}{c_2^2-\bar{u}_2^2}\right)W_1(x=L_1) - \frac{c_2}{\bar{\rho}_2}\sinh\left(\frac{c_2 s(x-L_1)}{c_2^2-\bar{u}_2^2}\right)W_3(x=L_1)\right], \tag{4.101}$$

$$P_2=\exp\left(\frac{\bar{u}_2 s(x-L_1)}{c_2^2-\bar{u}_2^2}\right)\left[\cosh\left(\frac{c_2 s(x-L_1)}{c_2^2-\bar{u}_2^2}\right)W_2(x=L_1) - \frac{c_2}{\bar{\rho}_2}\sinh\left(\frac{c_2 s(x-L_1)}{c_2^2-\bar{u}_2^2}\right)W_4(x=L_1)\right], \tag{4.102}$$

$$P_3=\exp\left(\frac{\bar{u}_2 s(x-L_1)}{c_2^2-\bar{u}_2^2}\right)\left[-\frac{\bar{\rho}_2}{c_2}\sinh\left(\frac{c_2 s(x-L_1)}{c_2^2-\bar{u}_2^2}\right)W_1(x=L_1) + \cosh\left(\frac{c_2 s(x-L_1)}{c_2^2-\bar{u}_2^2}\right)W_3(x=L_1)\right], \tag{4.103}$$

and finally,

$$P_4=\exp\left(\frac{\bar{u}_2 s(x-L_1)}{c_2^2-\bar{u}_2^2}\right)\left[-\frac{\bar{\rho}_2}{c_2}\sinh\left(\frac{c_2 s(x-L_1)}{c_2^2-\bar{u}_2^2}\right)W_2(x=L_1) + \cosh\left(\frac{c_2 s(x-L_1)}{c_2^2-\bar{u}_2^2}\right)W_4(x=L_1)\right]. \tag{4.104}$$

Reproduced with permission of the copyright owner. Further reproduction prohibited without permission.

Similarly, S is computed as follows:

$$S = H_2(s,x-L_1) - P\,N(s)\,H_2(s,L_2) = H_2(s,x-L_1) - \begin{bmatrix} P_1 & P_2 \\ P_3 & P_4 \end{bmatrix}\begin{bmatrix} 0 & 0 \\ -R & 1 \end{bmatrix} H_2(s,L_2)$$

$$= H_2(s,x-L_1) - \begin{bmatrix} -RP_2 & P_2 \\ -RP_4 & P_4 \end{bmatrix} H_2(s,L_2)$$

$$= \exp\left(\frac{\bar{u}_2 s(x-L_1)}{c_2^2-\bar{u}_2^2}\right)\begin{bmatrix} \cosh\left(\frac{c_2 s(x-L_1)}{c_2^2-\bar{u}_2^2}\right) & -\frac{c_2}{\bar{\rho}_2}\sinh\left(\frac{c_2 s(x-L_1)}{c_2^2-\bar{u}_2^2}\right) \\ -\frac{\bar{\rho}_2}{c_2}\sinh\left(\frac{c_2 s(x-L_1)}{c_2^2-\bar{u}_2^2}\right) & \cosh\left(\frac{c_2 s(x-L_1)}{c_2^2-\bar{u}_2^2}\right) \end{bmatrix}$$

$$-\exp\left(\frac{\bar{u}_2 s L_2}{c_2^2-\bar{u}_2^2}\right)\begin{bmatrix} -RP_2 & P_2 \\ -RP_4 & P_4 \end{bmatrix}\begin{bmatrix} \cosh\left(\frac{c_2 s L_2}{c_2^2-\bar{u}_2^2}\right) & -\frac{c_2}{\bar{\rho}_2}\sinh\left(\frac{c_2 s L_2}{c_2^2-\bar{u}_2^2}\right) \\ -\frac{\bar{\rho}_2}{c_2}\sinh\left(\frac{c_2 s L_2}{c_2^2-\bar{u}_2^2}\right) & \cosh\left(\frac{c_2 s L_2}{c_2^2-\bar{u}_2^2}\right) \end{bmatrix}.$$

Thus, the coefficient matrix S has the following elements:

$$S_1 = \exp\left(\frac{\bar{u}_2 s(x-L_1)}{c_2^2-\bar{u}_2^2}\right)\cosh\left(\frac{c_2 s(x-L_1)}{c_2^2-\bar{u}_2^2}\right)$$

$$+\exp\left(\frac{\bar{u}_2 s L_2}{c_2^2-\bar{u}_2^2}\right) P_2\left\{R\cosh\left(\frac{c_2 s L_2}{c_2^2-\bar{u}_2^2}\right) + \frac{\bar{\rho}_2}{c_2}\sinh\left(\frac{c_2 s L_2}{c_2^2-\bar{u}_2^2}\right)\right\},$$

$$S_2 = -\frac{c_2}{\bar{\rho}_2}\exp\left(\frac{\bar{u}_2 s(x-L_1)}{c_2^2-\bar{u}_2^2}\right)\sinh\left(\frac{c_2 s(x-L_1)}{c_2^2-\bar{u}_2^2}\right)$$

$$-\exp\left(\frac{\bar{u}_2 s L_2}{c_2^2-\bar{u}_2^2}\right) P_2\left\{R\frac{c_2}{\bar{\rho}_2}\sinh\left(\frac{c_2 s L_2}{c_2^2-\bar{u}_2^2}\right) + \cosh\left(\frac{c_2 s L_2}{c_2^2-\bar{u}_2^2}\right)\right\},$$

Reproduced with permission of the copyright owner. Further reproduction prohibited without permission.

$$S_3 = -\frac{\bar{\rho}_2}{c_2}\exp\left(\frac{\bar{u}_2 s(x-L_1)}{c_2^2-\bar{u}_2^2}\right)\sinh\left(\frac{c_2 s(x-L_1)}{c_2^2-\bar{u}_2^2}\right)$$

$$+\exp\left(\frac{\bar{u}_2 sL_2}{c_2^2-\bar{u}_2^2}\right)P_4\left\{R\cosh\left(\frac{c_2 sL_2}{c_2^2-\bar{u}_2^2}\right)+\frac{\bar{\rho}_2}{c_2}\cosh\left(\frac{c_2 sL_2}{c_2^2-\bar{u}_2^2}\right)\right\},$$

and finally,

$$S_4 = \exp\left(\frac{\bar{u}_2 s(x-L_1)}{c_2^2-\bar{u}_2^2}\right)\cosh\left(\frac{c_2 s(x-L_1)}{c_2^2-\bar{u}_2^2}\right)$$

$$-\exp\left(\frac{\bar{u}_2 sL_2}{c_2^2-\bar{u}_2^2}\right)P_4\left\{R\frac{c_2}{\bar{\rho}_2}\sinh\left(\frac{c_2 sL_2}{c_2^2-\bar{u}_2^2}\right)+\cosh\left(\frac{c_2 sL_2}{c_2^2-\bar{u}_2^2}\right)\right\}.$$

Simplifying the above expressions yields,

$$S_1 = \exp\left(\frac{\bar{u}_2 s(x-L_1)}{c_2^2-\bar{u}_2^2}\right)\left\{\cosh\left(\frac{c_2 s(x-L_1)}{c_2^2-\bar{u}_2^2}\right)+\exp\left(\frac{\bar{u}_2 sL_2}{c_2^2-\bar{u}_2^2}\right)\right.$$

$$\cdot\left[\cosh\left(\frac{c_2 s(x-L_1)}{c_2^2-\bar{u}_2^2}\right)W_2(x=L_1)-\frac{c_2}{\bar{\rho}_2}\sinh\left(\frac{c_2 s(x-L_1)}{c_2^2-\bar{u}_2^2}\right)W_4(x=L_1)\right]$$

$$\left.\cdot\left[R\cosh\left(\frac{c_2 sL_2}{c_2^2-\bar{u}_2^2}\right)+\frac{\bar{\rho}_2}{c_2}\sinh\left(\frac{c_2 sL_2}{c_2^2-\bar{u}_2^2}\right)\right]\right\},$$

or,

$$S_1 = \exp\left(\frac{\bar{u}_2 s(x-L_1)}{c_2^2-\bar{u}_2^2}\right)\left\{\cosh\left(\frac{c_2 s(x-L_1)}{c_2^2-\bar{u}_2^2}\right)+\frac{\exp\left(\frac{\bar{u}_2 s(L_1+L_2)}{c_2^2-\bar{u}_2^2}\right)}{F_{22}-RF_{12}+Z_{us}(s)(F_{21}-RF_{11})}\right.$$

$$\left.\cdot\left[\cosh\left(\frac{c_2 s(x-L_1)}{c_2^2-\bar{u}_2^2}\right)\left[\cosh\left(\frac{c_1 sL_1}{c_1^2-\bar{u}_1^2}\right)Z_{us}(s)-\frac{c_1}{\bar{\rho}_1}\sinh\left(\frac{c_1 sL_1}{c_1^2-\bar{u}_1^2}\right)\right]\right.\right.$$

Reproduced with permission of the copyright owner. Further reproduction prohibited without permission.

$$\cdot\left[\frac{-\bar{c}_2}{\bar{\rho}_2}\sinh\left(\frac{c_2 s(x-L_1)}{c_2^2-\bar{u}_2^2}\right)\left[\frac{-Z_{us}(s)\,\bar{\rho}_1}{c_1}\sinh\left(\frac{c_1 sL_1}{c_1^2-\bar{u}_1^2}\right)+\cosh\left(\frac{c_1 sL_1}{c_1^2-\bar{u}_1^2}\right)\right]\right]$$

$$\cdot\left[R\cosh\left(\frac{c_2 sL_2}{c_2^2-\bar{u}_2^2}\right)+\frac{\bar{\rho}_2}{c_2}\sinh\left(\frac{c_2 sL_2}{c_2^2-\bar{u}_2^2}\right)\right]\Bigg\}, \qquad (4.105)$$

$$S_2=\exp\left(\frac{\bar{u}_2 s(x-L_1)}{c_2^2-\bar{u}_2^2}\right)\Bigg\{-\frac{\bar{c}_2}{\bar{\rho}_2}\sinh\left(\frac{c_2 s(x-L_1)}{c_2^2-\bar{u}_2^2}\right)-\exp\left(\frac{\bar{u}_2 sL_2}{c_2^2-\bar{u}_2^2}\right)$$

$$\cdot\left[\cosh\left(\frac{c_2 s(x-L_1)}{c_2^2-\bar{u}_2^2}\right)W_2(x=L_1)-\frac{\bar{c}_2}{\bar{\rho}_2}\sinh\left(\frac{c_2 s(x-L_1)}{c_2^2-\bar{u}_2^2}\right)W_4(x=L_1)\right]$$

$$\cdot\left[R\frac{\bar{c}_2}{\bar{\rho}_2}\sinh\left(\frac{c_2 sL_2}{c_2^2-\bar{u}_2^2}\right)+\cosh\left(\frac{c_2 sL_2}{c_2^2-\bar{u}_2^2}\right)\right]\Bigg\},$$

or,

$$S_2=\exp\left(\frac{\bar{u}_2 s(x-L_1)}{c_2^2-\bar{u}_2^2}\right)\Bigg\{-\frac{\bar{c}_2}{\bar{\rho}_2}\sinh\left(\frac{c_2 s(x-L_1)}{c_2^2-\bar{u}_2^2}\right)-\frac{\exp\left(\frac{\bar{u}_2 s(L_1+L_2)}{c_2^2-\bar{u}_2^2}\right)}{F_{22}-RF_{12}+Z_{us}(s)(F_{21}-RF_{11})}$$

$$\cdot\left[\cosh\left(\frac{c_2 s(x-L_1)}{c_2^2-\bar{u}_2^2}\right)\left[\cosh\left(\frac{c_1 sL_1}{c_1^2-\bar{u}_1^2}\right)Z_{us}(s)-\frac{\bar{c}_1}{\bar{\rho}_1}\sinh\left(\frac{c_1 sL_1}{c_1^2-\bar{u}_1^2}\right)\right]\right.$$

$$\left.-\frac{\bar{c}_2}{\bar{\rho}_2}\sinh\left(\frac{c_2 s(x-L_1)}{c_2^2-\bar{u}_2^2}\right)\left[\frac{-Z_{us}(s)\,\bar{\rho}_1}{c_1}\sinh\left(\frac{c_1 sL_1}{c_1^2-\bar{u}_1^2}\right)+\cosh\left(\frac{c_1 sL_1}{c_1^2-\bar{u}_1^2}\right)\right]\right]$$

$$\cdot\left[R\frac{\bar{c}_2}{\bar{\rho}_2}\sinh\left(\frac{c_2 sL_2}{c_2^2-\bar{u}_2^2}\right)+\cosh\left(\frac{c_2 sL_2}{c_2^2-\bar{u}_2^2}\right)\right]\Bigg\}, \qquad (4.106)$$

Reproduced with permission of the copyright owner. Further reproduction prohibited without permission.

$$S_3 = \exp\left(\frac{\bar{u}_2 s(x-L_1)}{c_2^2-\bar{u}_2^2}\right)\left\{-\frac{\bar{\rho}_2}{c_2}\sinh\left(\frac{c_2 s(x-L_1)}{c_2^2-\bar{u}_2^2}\right)+\exp\left(\frac{\bar{u}_2 sL_2}{c_2^2-\bar{u}_2^2}\right)\right.$$

$$\cdot\left[-\frac{\bar{\rho}_2}{c_2}\sinh\left(\frac{c_2 s(x-L_1)}{c_2^2-\bar{u}_2^2}\right)W_2(x=L_1)+\cosh\left(\frac{c_2 s(x-L_1)}{c_2^2-\bar{u}_2^2}\right)W_4(x=L_1)\right]$$

$$\left.\cdot\left[R\cosh\left(\frac{c_2 sL_2}{c_2^2-\bar{u}_2^2}\right)+\frac{\bar{\rho}_2}{c_2}\cosh\left(\frac{c_2 sL_2}{c_2^2-\bar{u}_2^2}\right)\right]\right\},$$

or,

$$S_3 = \exp\left(\frac{\bar{u}_2 s(x-L_1)}{c_2^2-\bar{u}_2^2}\right)\left\{-\frac{\bar{\rho}_2}{c_2}\sinh\left(\frac{c_2 s(x-L_1)}{c_2^2-\bar{u}_2^2}\right)+\frac{\exp\left(\frac{\bar{u}_2 s(L_1+L_2)}{c_2^2-\bar{u}_2^2}\right)}{F_{22}-RF_{12}+Z_{us}(s)(F_{21}-RF_{11})}\right.$$

$$\cdot\left[-\frac{\bar{\rho}_2}{c_2}\sinh\left(\frac{c_2 s(x-L_1)}{c_2^2-\bar{u}_2^2}\right)\left[\cosh\left(\frac{c_1 sL_1}{c_1^2-\bar{u}_1^2}\right)Z_{us}(s)-\frac{c_1}{\bar{\rho}_1}\sinh\left(\frac{c_1 sL_1}{c_1^2-\bar{u}_1^2}\right)\right]\right.$$

$$\left.+\cosh\left(\frac{c_2 s(x-L_1)}{c_2^2-\bar{u}_2^2}\right)\left[\frac{-Z_{us}(s)\,\bar{\rho}_1}{c_1}\sinh\left(\frac{c_1 sL_1}{c_1^2-\bar{u}_1^2}\right)+\cosh\left(\frac{c_1 sL_1}{c_1^2-\bar{u}_1^2}\right)\right]\right]$$

$$\left.\cdot\left[R\cosh\left(\frac{c_2 sL_2}{c_2^2-\bar{u}_2^2}\right)+\frac{\bar{\rho}_2}{c_2}\cosh\left(\frac{c_2 sL_2}{c_2^2-\bar{u}_2^2}\right)\right]\right\}, \qquad (4.107)$$

and finally,

$$S_4 = \exp\left(\frac{\bar{u}_2 s(x-L_1)}{c_2^2-\bar{u}_2^2}\right)\left\{\cosh\left(\frac{c_2 s(x-L_1)}{c_2^2-\bar{u}_2^2}\right)-\exp\left(\frac{\bar{u}_2 sL_2}{c_2^2-\bar{u}_2^2}\right)\right.$$

$$\cdot\left[-\frac{\bar{\rho}_2}{c_2}\sinh\left(\frac{c_2 s(x-L_1)}{c_2^2-\bar{u}_2^2}\right)W_2(x=L_1)+\cosh\left(\frac{c_2 s(x-L_1)}{c_2^2-\bar{u}_2^2}\right)W_4(x=L_1)\right]$$

$$\left.\cdot\left[R\frac{c_2}{\bar{\rho}_2}\sinh\left(\frac{c_2 sL_2}{c_2^2-\bar{u}_2^2}\right)+\cosh\left(\frac{c_2 sL_2}{c_2^2-\bar{u}_2^2}\right)\right]\right\},$$

Reproduced with permission of the copyright owner. Further reproduction prohibited without permission.

or,

$$S_4 = \exp\left(\frac{\bar{u}_2 s(x-L_1)}{c_2^2-\bar{u}_2^2}\right)\left\{\cosh\left(\frac{c_2 s(x-L_1)}{c_2^2-\bar{u}_2^2}\right) - \frac{\exp\left(\frac{\bar{u}_2 s(L_1+L_2)}{c_2^2-\bar{u}_2^2}\right)}{F_{22}-RF_{12}+Z_{us}(s)(F_{21}-RF_{11})}\right.$$

$$\cdot\left[-\frac{\bar{\rho}_2}{c_2}\sinh\left(\frac{c_2 s(x-L_1)}{c_2^2-\bar{u}_2^2}\right)\left[\cosh\left(\frac{c_1 sL_1}{c_1^2-\bar{u}_1^2}\right)Z_{us}(s) - \frac{c_1}{\bar{\rho}_1}\sinh\left(\frac{c_1 sL_1}{c_1^2-\bar{u}_1^2}\right)\right]\right.$$

$$\left.+\cosh\left(\frac{c_2 s(x-L_1)}{c_2^2-\bar{u}_2^2}\right)\left[\frac{-Z_{us}(s)\bar{\rho}_1}{c_1}\sinh\left(\frac{c_1 sL_1}{c_1^2-\bar{u}_1^2}\right)+\cosh\left(\frac{c_1 sL_1}{c_1^2-\bar{u}_1^2}\right)\right]\right]$$

$$\left.\cdot\left[R\frac{c_2}{\bar{\rho}_2}\sinh\left(\frac{c_2 sL_2}{c_2^2-\bar{u}_2^2}\right)+\cosh\left(\frac{c_2 sL_2}{c_2^2-\bar{u}_2^2}\right)\right]\right\}. \qquad (4.108)$$

B. The Three-Wave Problem

In the Part A, the analytical solution of the Two-Wave version of the problem under study was presented. In this part, the Three-Wave problem will be set up and its general solution will be outlined.

We begin first with the initial conditions, which are as follows:

$$q_1(s,0) = Z_1(s)\, q_3(s,0)$$

$$q_2(s,0) = Z_2 Z_1(s)\, q_3(s,0)$$

$$q_3(s,L) = R_1\, q_1(s,L) + R_2\, q_2(s,L) + \delta F_{in},$$

Reproduced with permission of the copyright owner. Further reproduction prohibited without permission.

where,

$$Q = \begin{bmatrix} q_1 \\ q_2 \\ q_3 \end{bmatrix} = \begin{bmatrix} \rho \\ \rho u \\ \rho E \end{bmatrix} \qquad (4.109)$$

is the state vector made up of density, momentum, and energy. The boundary conditions for this problem are illustrated in the figure below.

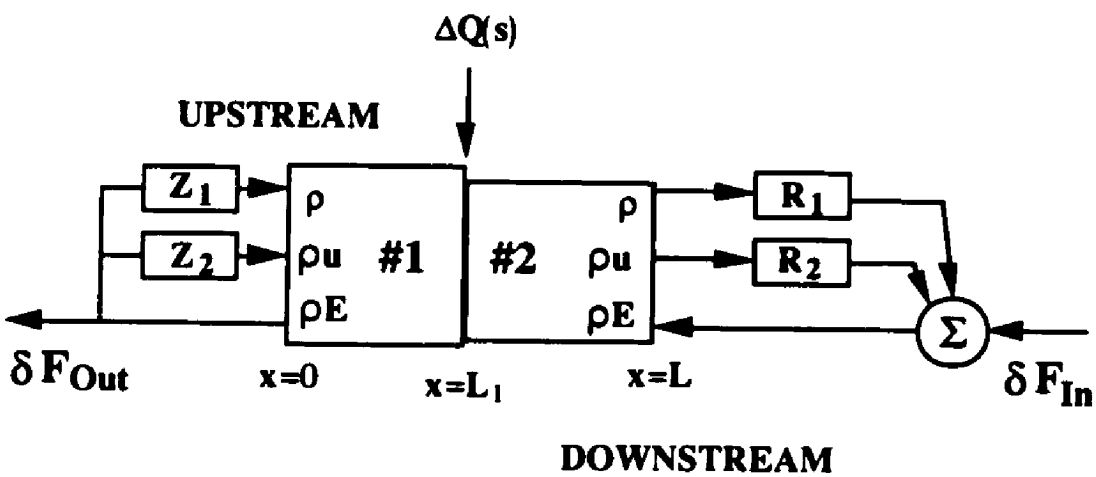


Figure 4.18 Boundary conditions for the three-wave problem

In matrix notation, the above conditions become:

$$\begin{bmatrix} 1 & 0 & -Z_1(s) \\ 0 & 1 & -Z_2(s) \\ 0 & 0 & 0 \end{bmatrix} \begin{bmatrix} q_1(s,0) \\ q_2(s,0) \\ q_3(s,0) \end{bmatrix} + \begin{bmatrix} 0 & 0 & 0 \\ 0 & 0 & 0 \\ -R_1 & -R_2 & 1 \end{bmatrix} \begin{bmatrix} q_1(s,L) \\ q_2(s,L) \\ q_3(s,L) \end{bmatrix} = \begin{bmatrix} 0 \\ 0 \\ \delta F_{in} \end{bmatrix}$$

Reproduced with permission of the copyright owner. Further reproduction prohibited without permission.

which then yields the familiar form,

$$M(s)\,Q_1(s,0) + N(s)\,Q_2(s,L) = Z(s) \qquad (4.110)$$

if,

$$M(s) = \begin{bmatrix} 1 & 0 & -Z_1 \\ 0 & 1 & -Z_2 \\ 0 & 0 & 0 \end{bmatrix}, \quad N(s) = \begin{bmatrix} 0 & 0 & 0 \\ 0 & 0 & 0 \\ -R_1 & -R_2 & 1 \end{bmatrix}$$

and,

$$Q_1(s,0) = \begin{bmatrix} q_1(s,0) \\ q_2(s,0) \\ q_3(s,0) \end{bmatrix}, \quad Q_2(s,L) = \begin{bmatrix} q_1(s,L) \\ q_2(s,L) \\ q_3(s,L) \end{bmatrix}, \quad Z(s) = \begin{bmatrix} 0 \\ 0 \\ \delta F_{in} \end{bmatrix}.$$

Then, the general solution to the Three-Wave problem is as follows:

CHANNEL I:

$$Q_1(s,x) \equiv W \cdot Z(s) + Y \cdot \Delta Q(s)$$

$$= H_1(s,x)\left[M(s) + N(s)\,H_2(s,L_2)\,H_1(s,L_1)\right]^{-1} Z(s)$$

$$- H_1(s,x)\left[M(s) + N(s)\,H_2(s,L_2)\,H_1(s,L_1)\right]^{-1} N(s)\,H_2(s,L_2)\,\Delta Q(s) \qquad (4.111)$$

Reproduced with permission of the copyright owner. Further reproduction prohibited without permission.

CHANNEL II:

$$Q_2(s,x) \equiv P\cdot Z(s) + S\cdot \Delta Q(s)$$

$$= H_2(s,x-L_1)\,H_1(s,L_1)\,[M(s) + N(s)\,H_2(s,L_2)\,H_1(s,L_1)]^{-1}\,Z(s)$$

$$+\left[H_2(s,x-L_1)-H_2(s,x-L_1)H_1(s,L_1)[M(s)+N(s)H_2(s,L_2)H_1(s,L_1)]^{-1}N(s)H_2(s,L_2)\right]\Delta Q(s). \qquad (4.112)$$

Note that, if the following auxilliary variable is used,

$$F(s)=H_2(s,L_2)H_1(s,L_1) \qquad (4.113)$$

then,

$$[M(s)+N(s)H_2(s,L_2)H_1(s,L_1)]^{-1}=[M(s)+N(s)F(s)]^{-1}=$$

$$=\left\{\begin{bmatrix} 1 & 0 & -Z_1 \\ 0 & 1 & -Z_2 \\ 0 & 0 & 0 \end{bmatrix}+\begin{bmatrix} 0 & 0 & 0 \\ 0 & 0 & 0 \\ -R_1 & -R_2 & 1 \end{bmatrix}\begin{bmatrix} F_{11} & F_{12} & F_{13} \\ F_{21} & F_{22} & F_{23} \\ F_{31} & F_{32} & F_{33} \end{bmatrix}\right\}^{-1}$$

$$=\begin{bmatrix} 1 & 0 & -Z_1 \\ 0 & 1 & -Z_2 \\ -R_1F_{11}-R_2F_{21}+F_{31} & -R_1F_{12}-R_2F_{22}+F_{32} & -R_1F_{13}-R_2F_{23}+F_{33} \end{bmatrix}^{-1}$$

Reproduced with permission of the copyright owner. Further reproduction prohibited without permission.

$$= \frac{\begin{bmatrix} Z_2(-R_1F_{12}-R_2F_{22}+F_{32}) & -Z_1(-R_1F_{12}-R_2F_{22}+F_{32}) & Z_1 \\ -R_1F_{13}-R_2F_{23}+F_{33} & & \\ -Z_2(-R_1F_{11}-R_2F_{21}+F_{31}) & -R_1F_{13}-R_2F_{23}+F_{33} & Z_2 \\ & +Z_1(-R_1F_{11}-R_2F_{21}+F_{31}) & \\ -(-R_1F_{11}-R_2F_{21}+F_{31}) & -(-R_1F_{12}-R_2F_{22}+F_{32}) & 1 \end{bmatrix}}{(-R_1F_{11}-R_2F_{21}+F_{31})Z_1+(-R_1F_{12}-R_2F_{22}+F_{32})Z_2-R_1F_{13}-R_2F_{23}+F_{33}}.$$

(4.114)

The last expression can be used in the calculation of $Q_1(s,x)$ and $Q_2(s,x)$. For practical reasons, more detailed expressions for $Q_1(s,x)$ and $Q_2(s,x)$ will not be presented here. However, it is felt that the interested reader has been given enough information and guidance to develop the final analytical expressions for the flow in both channels.

This lengthy section dealt with the two-channel with internal input bounded problem. The N-Channel extention of the problem is discussed in the following section.

4.11 The N-Channel with Internal Inputs Bounded Problem

Consider the flow system illustrated in Figure 4.19. This problem is a generalization of the *N-Channel with Internal Inputs Free-Space* problem, which was studied in Section 4.9.

In this problem, it is assumed that the N flow channels have N distinct transfer functions $H_1(s,x)$, ... , $H_N(s,x)$, respectively. Furthermore,

Reproduced with permission of the copyright owner. Further reproduction prohibited without permission.

the lengths of Channels 1 through N are labeled $L_1, \ldots, L_N$, respectively. The state vector is symbolized by $Q_i(s,x)$ or $\underline{u}_i(s,x)$, where i denotes the i_{th} channel. Also, between two consecutive channels, interior inputs are incorporated into the model. The ith such input is denoted by $\Delta Q_i(s)$ or $\Delta \underline{u}_i(s)$.

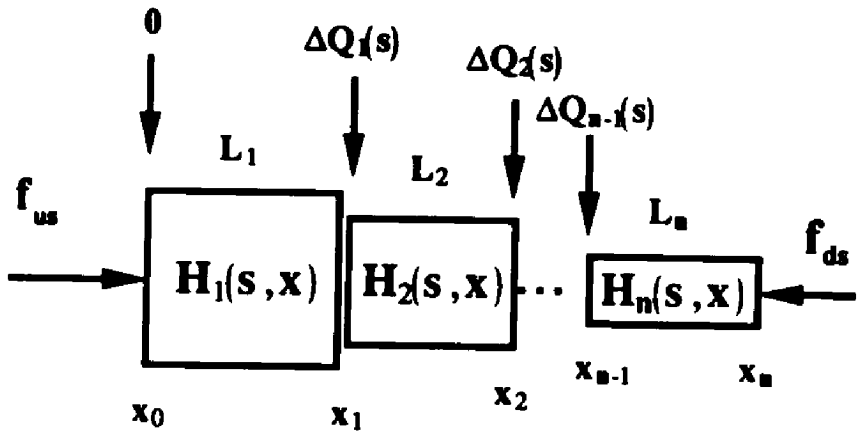


Figure 4.19 The N-channel with internal inputs bounded problem

First, asssume that the flow at $x=x_0$, i.e., $Q_1(s,x_0)$, is given. Then, from Section 4.9, the general expression for the flow inside the Nth channel in terms of $Q_1(s,x_0)$ and the interior inputs is given by:

$$\underline{u}_n(s,x-x_{n-1}) = H_n(s,x-x_{n-1})\, Q_n(s,x_{n-1})$$

$$= H_n(s,x-x_{n-1}) \cdot$$

$$\left\{\left[\prod_{i=1}^{n-1} [H_{n-i}(s,x_{n-i}-x_{n-i-1})]\right] Q_1(s,x_0)\right.$$

Reproduced with permission of the copyright owner. Further reproduction prohibited without permission.

$$+\left[\prod_{i=1}^{n-2}\left[H_{n-i}(s,x_{n-i}-x_{n-i-1})\right]\right]\Delta Q_1(s)$$

$$+\left[\prod_{i=1}^{n-3}\left[H_{n-i}(s,x_{n-i}-x_{n-i-1})\right]\right]\Delta Q_2(s)$$

$$\vdots \qquad \vdots \qquad \vdots$$

$$+\left[\prod_{i=1}^{2}\left[H_{n-i}(s,x_{n-i}-x_{n-i-1})\right]\right]\Delta Q_{n-3}(s)+\Delta Q_{n-2}(s)\Bigg\}. \qquad (4.115)$$

Next, appropriate boundary conditions are applied to the free-space problem. In general, they can be expressed as follows:

$$M(s)\,Q_1(s,0)+N(s)\,Q_n(s,L)=Z(s). \qquad (4.116)$$

Since, $Q_n(s,L)$ is given by:

$$Q_n(s,L-x_{n-1})=H_n(s,L-x_{n-1})\,Q_n(s,x_{n-1})$$

$$=H_n(s,x-x_{n-1})\cdot\left[\prod_{i=1}^{n-1}\left[H_{n-i}(s,x_{n-i}-x_{n-i-1})\right]\right]Q_1(s,x_0)$$

$$+H_n(s,x-x_{n-1})\cdot\left[\prod_{i=1}^{n-2}\left[H_{n-i}(s,x_{n-i}-x_{n-i-1})\right]\right]\Delta Q_1(s)$$

$$+H_n(s,x-x_{n-1})\cdot\left[\prod_{i=1}^{n-3}\left[H_{n-i}(s,x_{n-i}-x_{n-i-1})\right]\right]\Delta Q_2(s)$$

Reproduced with permission of the copyright owner. Further reproduction prohibited without permission.

$$\vdots$$

$$+H_n(s,x-x_{n-1})\cdot\left[\prod_{i=1}^{2}\left[H_{n-i}(s,x_{n-i}-x_{n-i-1})\right]\right]\Delta Q_{n-3}(s)$$

$$+H_n(s,x-x_{n-1})\cdot\Delta Q_{n-2}(s),$$

then, with $x_0=0$, Equation (4.116) becomes:

$$M(s)\,Q_1(s,0)+N(s)H_n(s,x-x_{n-1})\cdot\left[\prod_{i=1}^{n-1}\left[H_{n-i}(s,x_{n-i}-x_{n-i-1})\right]\right]Q_1(s,0)$$

$$+N(s)H_n(s,x-x_{n-1})\cdot\left[\prod_{i=1}^{n-2}\left[H_{n-i}(s,x_{n-i}-x_{n-i-1})\right]\right]\Delta Q_1(s)$$

$$+N(s)H_n(s,x-x_{n-1})\cdot\left[\prod_{i=1}^{n-3}\left[H_{n-i}(s,x_{n-i}-x_{n-i-1})\right]\right]\Delta Q_2(s)$$

$$\vdots$$

$$+N(s)H_n(s,x-x_{n-1})\cdot\left[\prod_{i=1}^{2}\left[H_{n-i}(s,x_{n-i}-x_{n-i-1})\right]\right]\Delta Q_{n-3}(s)$$

$$+N(s)H_n(s,x-x_{n-1})\cdot\Delta Q_{n-2}(s)=Z(s).$$

Solving for $Q_1(s,0)$ yields,

$$Q_1(s,0)=\left[\,M(s)+N(s)H_n(s,x-x_{n-1})\cdot\left[\prod_{i=1}^{n-1}\left[H_{n-i}(s,x_{n-i}-x_{n-i-1})\right]\right]\right]^{-1}\cdot$$

$$\left\{Z(s)-N(s)H_n(s,x-x_{n-1})\cdot\left[\prod_{i=1}^{n-2}\left[H_{n-i}(s,x_{n-i}-x_{n-i-1})\right]\right]\Delta Q_1(s)\right.$$

Reproduced with permission of the copyright owner. Further reproduction prohibited without permission.

$$-N(s)H_n(s,x-x_{n-1})\cdot\left[\prod_{i=1}^{n-3}\left[H_{n-i}(s,x_{n-i}-x_{n-i-1})\right]\right]\Delta Q_2(s)$$

$$\vdots$$

$$-N(s)H_n(s,x-x_{n-1})\cdot\left[\prod_{i=1}^{2}\left[H_{n-i}(s,x_{n-i}-x_{n-i-1})\right]\right]\Delta Q_{n-3}(s)\ -N(s)H_n(s,x-x_{n-1})\cdot\Delta Q_{n-2}(s)\Bigg\rangle$$

(4.117)

and finally,

$$Q_n(s,x-x_{n-1}) = H_n(s,x-x_{n-1})\cdot$$

$$\left\{\left[\prod_{i=1}^{n-1}\left[H_{n-i}(s,x_{n-i}-x_{n-i-1})\right]\right]\cdot\left[M(s)+N(s)H_n(s,x-x_{n-1})\cdot\left[\prod_{i=1}^{n-1}\left[H_{n-i}(s,x_{n-i}-x_{n-i-1})\right]\right]\right]^{-1}\right.$$

$$\Bigg\{Z(s)\ -N(s)H_n(s,x-x_{n-1})\cdot\left[\prod_{i=1}^{n-2}\left[H_{n-i}(s,x_{n-i}-x_{n-i-1})\right]\right]\Delta Q_1(s)$$

$$-N(s)H_n(s,x-x_{n-1})\cdot\left[\prod_{i=1}^{n-3}\left[H_{n-i}(s,x_{n-i}-x_{n-i-1})\right]\right]\Delta Q_2(s)$$

$$\vdots$$

$$-N(s)H_n(s,x-x_{n-1})\cdot\left[\prod_{i=1}^{2}\left[H_{n-i}(s,x_{n-i}-x_{n-i-1})\right]\right]\Delta Q_{n-3}(s)\ -N(s)H_n(s,x-x_{n-1})\cdot\Delta Q_{n-2}(s)\Bigg\}$$

$$+\left[\prod_{i=1}^{n-2}\left[H_{n-i}(s,x_{n-i}-x_{n-i-1})\right]\right]\Delta Q_1(s)+\left[\prod_{i=1}^{n-3}\left[H_{n-i}(s,x_{n-i}-x_{n-i-1})\right]\right]\Delta Q_2(s)$$

$$\vdots$$

$$+\left[\prod_{i=1}^{2}\left[H_{n-i}(s,x_{n-i}-x_{n-i-1})\right]\right]\Delta Q_{n-3}(s)+\Delta Q_{n-2}(s)\Bigg\}\Bigg\}. \qquad \textit{(4.118)}$$

Reproduced with permission of the copyright owner. Further reproduction prohibited without permission.

If one lets,

$$\tilde{\Omega}=H_n(s,x-x_{n-1})\left[\prod_{i=1}^{n-1}\left[H_{n-i}(s,x_{n-i}-x_{n-i-1})\right]\right]\left[M(s)+N(s)H_n(s,x-x_{n-1})\left[\prod_{i=1}^{n-1}\left[H_{n-i}(s,x_{n-i}-x_{n-i-1})\right]\right]\right]^{-1} \tag{4.110}$$

then, collecting like terms yields the following expression for the flow vector:

$$\begin{aligned}
Q_n(s,x-x_{n-1}) &= \tilde{\Omega}Z(s) + \\
&+\left\{\left[\prod_{i=1}^{n-2}\left[H_{n-i}(s,x_{n-i}-x_{n-i-1})\right]\right] - \tilde{\Omega}N(s)H_n(s,x-x_{n-1})\left[\prod_{i=1}^{n-2}\left[H_{n-i}(s,x_{n-i}-x_{n-i-1})\right]\right]\right\}\Delta Q_1(s) \\
&+\left\{\left[\prod_{i=1}^{n-3}\left[H_{n-i}(s,x_{n-i}-x_{n-i-1})\right]\right] - \tilde{\Omega}N(s)H_n(s,x-x_{n-1})\left[\prod_{i=1}^{n-3}\left[H_{n-i}(s,x_{n-i}-x_{n-i-1})\right]\right]\right\}\Delta Q_2(s) \\
&\vdots \\
&+\left\{\left[\prod_{i=1}^{2}\left[H_{n-i}(s,x_{n-i}-x_{n-i-1})\right]\right] - \tilde{\Omega}N(s)H_n(s,x-x_{n-1})\left[\prod_{i=1}^{2}\left[H_{n-i}(s,x_{n-i}-x_{n-i-1})\right]\right]\right\}\Delta Q_{n-3}(s) \\
&+\left\{1-\tilde{\Omega}N(s)H_n(s,x-x_{n-1})\right\}\Delta Q_{n-2}(s).
\end{aligned} \tag{4.120}$$

Finally, knowing the order of the model, an explicit expression for the flow vector Q(s,x) may be computed. The next section discusses the Green's function problem.

Reproduced with permission of the copyright owner. Further reproduction prohibited without permission.

4.12 The Green's Function Problem

In this section, the Green's function problem will be studied. A pictorial representration of this important problem is shown in the following figure.

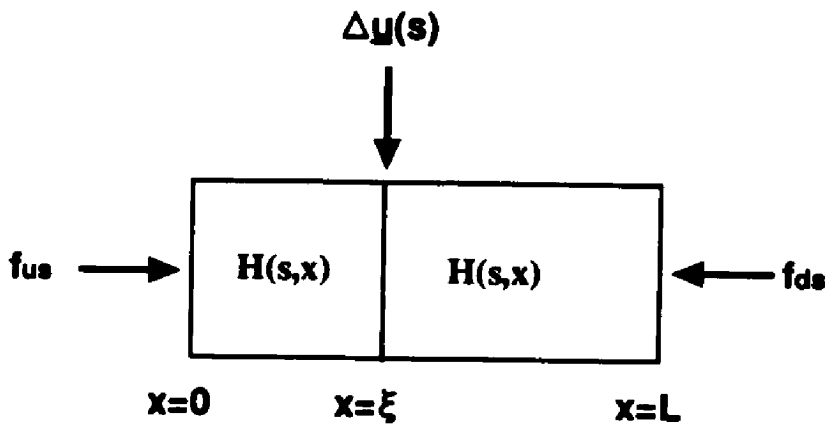


Figure 4.20 The Green's function problem

The point where the interior input is applied, namely at $x=\xi$, divides the inlet in two sections or channels. Since both channels of the given system have the same properties, then it follows that their transfer functions would be of the same form. That is,

$$H_1(s,x)=H_2(s,x)=H(s,x), \qquad (4.121)$$

where, in a two-wave system H(s,x) is

Reproduced with permission of the copyright owner. Further reproduction prohibited without permission.

$$H(s,x)=\exp\left(\frac{\bar{u}sx}{c^2-\bar{u}^2}\right)\begin{bmatrix} \cosh\left(\frac{csx}{c^2-\bar{u}^2}\right) & \frac{-c}{\bar{\rho}}\sinh\left(\frac{csx}{c^2-\bar{u}^2}\right) \\ \frac{-\bar{\rho}}{c}\sinh\left(\frac{csx}{c^2-\bar{u}^2}\right) & \cosh\left(\frac{csx}{c^2-\bar{u}^2}\right) \end{bmatrix} \qquad (4.122)$$

and in a three-wave system, the nine elements of H(s,x) are given by:

$$H_{11} = \left[1-\frac{u^2(\gamma-1)}{2c^2}\right]e^{-\frac{sx}{u}} + \frac{1}{2c^2}\left[(\gamma-1)\frac{u^2}{2} - uc\right]e^{-\frac{sx}{u+c}} + \frac{1}{2c^2}\left[(\gamma-1)\frac{u^2}{2} + uc\right]e^{-\frac{sx}{u-c}},$$

$$H_{12} = \frac{(\gamma-1)u}{c^2}e^{-\frac{sx}{u}} + \frac{1}{2c^2}[c-(\gamma-1)u]e^{-\frac{sx}{u+c}} - \frac{1}{2c^2}[c+(\gamma-1)u]e^{-\frac{sx}{u-c}},$$

$$H_{13} = -\frac{(\gamma-1)}{c^2}e^{-\frac{sx}{u}} + \frac{1}{2c^2}(\gamma-1)e^{-\frac{sx}{u+c}} + \frac{1}{2c^2}(\gamma-1)e^{-\frac{sx}{u-c}},$$

$$H_{21} = u\left[1-\frac{u^2(\gamma-1)}{2c^2}\right]e^{-\frac{sx}{u}} + (u+c)\frac{1}{2c^2}\left[(\gamma-1)\frac{u^2}{2} - uc\right]e^{-\frac{sx}{u+c}} + (u-c)\frac{1}{2c^2}\left[(\gamma-1)\frac{u^2}{2} + uc\right]e^{-\frac{sx}{u-c}},$$

$$H_{22} = \frac{u^2}{c^2}(\gamma-1)e^{-\frac{sx}{u}} + (u+c)\frac{1}{2c^2}[c-(\gamma-1)u]e^{-\frac{sx}{u+c}} - (u-c)\frac{1}{2c^2}[c+(\gamma-1)u]e^{-\frac{sx}{u-c}},$$

$$H_{23} = -\frac{(\gamma-1)}{c^2}ue^{-\frac{sx}{u}} + (u+c)\frac{1}{2c^2}(\gamma-1)e^{-\frac{sx}{u+c}} + (u-c)\frac{1}{2c^2}(\gamma-1)e^{-\frac{sx}{u-c}},$$

$$H_{31} = \frac{u^2}{2}\left[1-\frac{u^2(\gamma-1)}{2c^2}\right]e^{-\frac{sx}{u}} + \left(\frac{1}{2}u^2+uc+\frac{c^2}{\gamma-1}\right)\frac{1}{2c^2}\left[(\gamma-1)\frac{u^2}{2} - uc\right]e^{-\frac{sx}{u+c}}$$

$$+ \left(\frac{1}{2}u^2-uc+\frac{c^2}{\gamma-1}\right)\frac{1}{2c^2}\left[(\gamma-1)\frac{u^2}{2} + uc\right]e^{-\frac{sx}{u-c}},$$

Reproduced with permission of the copyright owner. Further reproduction prohibited without permission.

$$H_{32} = \frac{u^2(\gamma-1)}{2c^2}\frac{u}{}e^{-\frac{sx}{u}} + \left(\frac{1}{2}u^2+uc+\frac{c^2}{\gamma-1}\right)\frac{1}{2c^2}[c-(\gamma-1)u]e^{-\frac{sx}{u+c}}$$

$$-\left(\frac{1}{2}u^2-uc+\frac{c^2}{\gamma-1}\right)\frac{1}{2c^2}[c+(\gamma-1)u]e^{-\frac{sx}{u-c}},$$

$$H_{33} = -\frac{u^2(\gamma-1)}{2c^2}e^{-\frac{sx}{u}} + \left(\frac{1}{2}u^2+uc+\frac{c^2}{\gamma-1}\right)\frac{1}{2c^2}(\gamma-1)e^{-\frac{sx}{u+c}} + \left(\frac{1}{2}u^2-uc+\frac{c^2}{\gamma-1}\right)\frac{1}{2c^2}(\gamma-1)e^{-\frac{sx}{u-c}}.$$

Note that the state vectors in the two- and three-wave models are defined respectively as follows:

$$\underline{u} = \begin{bmatrix} u(s,x) \\ \rho(s,x) \end{bmatrix} = \begin{bmatrix} \text{velocity} \\ \text{density} \end{bmatrix}, \text{ and } Q = \begin{bmatrix} q_1(s,x) \\ q_2(s,x) \\ q_3(s,x) \end{bmatrix} = \begin{bmatrix} \rho \\ \rho u \\ \rho E \end{bmatrix} = \begin{bmatrix} \text{density} \\ \text{momentum} \\ \text{energy} \end{bmatrix}.$$

In Channel 1, that is when $0 \le x < \xi$, one gets,

$$\underline{u}_1(s,x) = H(s,x)\,\underline{u}_1(s,0). \qquad (4.123)$$

At the interior boundary $x=\xi$, the governing equation is

$$\underline{u}_2(s,\xi) = \underline{u}_1(s,\xi) + \Delta\underline{u}(s)$$
$$= H(s,\xi)\,\underline{u}_1(s,0) + \Delta\underline{u}(s).$$

Also, in the second channel, that is for $\xi \le x \le L$, one gets

$$\underline{u}_2(s,x) = H(s,x-\xi)\,\underline{u}_2(s,x_1)$$
$$= H(s,x-\xi)\,[H(s,\xi)\,\underline{u}_1(s,0) + \Delta\underline{u}(s)]$$
$$= H(s,x-\xi)\,H(s,\xi)\,\underline{u}_1(s,0) + H(s,x-\xi)\,\Delta\underline{u}(s).$$

Reproduced with permission of the copyright owner. Further reproduction prohibited without permission.

The above equation can be put in the compact form

$$\underline{u}_2(s,x) = A(s,x)\,\underline{u}_1(s,0) + B(s,x)\,\Delta\underline{u}(s) \qquad (4.124)$$

where,

$$A(s,x) = H(s,x-\xi)\,H(s,\xi) \qquad (4.125)$$

$$B(s,x) = H(s,x-\xi). \qquad (4.126)$$

Using the following trigonometric identities,

$$\sinh(A \pm B) = \sinh A \cosh B \pm \cosh A \sinh B$$

$$\cosh(A \pm B) = \cosh A \cosh B \pm \sinh A \sinh B,$$

the transmittivity property of the state transition matrix can be verified. Incidentally, this property of the state transition matrix states that for any value of x, the following expression holds true:

$$H(s,x-\xi)\,H(s,\xi) = H(s,x). \qquad (4.127)$$

For example, in a two-wave system,

$$H(s,x-\xi)\,H(s,\xi) = \exp\left[\left(\frac{\bar{u}(x-\xi)}{c^2-\bar{u}^2} + \frac{\bar{u}\xi}{c^2-\bar{u}^2}\right)s\right] \cdot$$

$$\begin{bmatrix} \cosh\left(\frac{cs(x-\xi)}{c^2-\bar{u}^2}\right) & \frac{-c}{\bar{\rho}}\sinh\left(\frac{cs(x-\xi)}{c^2-\bar{u}^2}\right) \\ \frac{-\bar{\rho}}{c}\sinh\left(\frac{cs(x-\xi)}{c^2-\bar{u}^2}\right) & \cosh\left(\frac{cs(x-\xi)}{c^2-\bar{u}^2}\right) \end{bmatrix} \begin{bmatrix} \cosh\left(\frac{csx}{c^2-\bar{u}^2}\right) & \frac{-c}{\bar{\rho}}\sinh\left(\frac{csx}{c^2-\bar{u}^2}\right) \\ \frac{-\bar{\rho}}{c}\sinh\left(\frac{csx}{c^2-\bar{u}^2}\right) & \cosh\left(\frac{csx}{c^2-\bar{u}^2}\right) \end{bmatrix}$$

Reproduced with permission of the copyright owner. Further reproduction prohibited without permission.

$$= \exp\left(\frac{\bar{u}sx}{c^2-\bar{u}^2}\right)\begin{bmatrix} \cosh\left(\frac{cs(x-\xi)}{c^2-\bar{u}^2}+\frac{cs\xi}{c^2-\bar{u}^2}\right) & \frac{-c}{\bar{\rho}}\sinh\left(\frac{cs(x-\xi)}{c^2-\bar{u}^2}+\frac{cs\xi}{c^2-\bar{u}^2}\right) \\ \frac{-\bar{\rho}}{c}\sinh\left(\frac{cs(x-\xi)}{c^2-\bar{u}^2}+\frac{cs\xi}{c^2-\bar{u}^2}\right) & \cosh\left(\frac{cs(x-\xi)}{c^2-\bar{u}^2}+\frac{cs\xi}{c^2-\bar{u}^2}\right) \end{bmatrix}$$

$$= \exp\left(\frac{\bar{u}sx}{c^2-\bar{u}^2}\right)\begin{bmatrix} \cosh\left(\frac{csx}{c^2-\bar{u}^2}\right) & \frac{-c}{\bar{\rho}}\sinh\left(\frac{csx}{c^2-\bar{u}^2}\right) \\ \frac{-\bar{\rho}}{c}\sinh\left(\frac{csx}{c^2-\bar{u}^2}\right) & \cosh\left(\frac{csx}{c^2-\bar{u}^2}\right) \end{bmatrix} \equiv H(s,x).$$

Also, for the same system, the auxiliary matrices A(s,x) and B(s,x) become:

$$A(s,x)\equiv H(s,x)=\exp\left(\frac{\bar{u}sx}{c^2-\bar{u}^2}\right)\begin{bmatrix} \cosh\left(\frac{csx}{c^2-\bar{u}^2}\right) & \frac{-c}{\bar{\rho}}\sinh\left(\frac{csx}{c^2-\bar{u}^2}\right) \\ \frac{-\bar{\rho}}{c}\sinh\left(\frac{csx}{c^2-\bar{u}^2}\right) & \cosh\left(\frac{csx}{c^2-\bar{u}^2}\right) \end{bmatrix} \qquad (4.128)$$

$$B(s,x)\equiv H(s,x-\xi)=\exp\left(\frac{\bar{u}s(x-\xi)}{c^2-\bar{u}^2}\right)\begin{bmatrix} \cosh\left(\frac{cs(x-\xi)}{c^2-\bar{u}^2}\right) & \frac{-c}{\bar{\rho}}\sinh\left(\frac{cs(x-\xi)}{c^2-\bar{u}^2}\right) \\ \frac{-\bar{\rho}}{c}\sinh\left(\frac{cs(x-\xi)}{c^2-\bar{u}^2}\right) & \cosh\left(\frac{cs(x-\xi)}{c^2-\bar{u}^2}\right) \end{bmatrix}. \qquad (4.129)$$

Thus, in Channel 2 one obtains the following equation for the flow,

$$\underline{u}_2(s,x) = H(s,x)\,\underline{u}_1(s,0) + H(s,x-\xi)\,\Delta\underline{u}(s). \qquad (4.130)$$

Next, the given boundary conditions are applied to the two-wave system.

$$\boxed{\begin{aligned} u_{1us} &= Z_{us}(s)\rho_{1us}+f_{us} \\ \rho_{2ds} &= Ru_{2ds}+f_{ds} \end{aligned}} \quad \text{or} \quad \boxed{\begin{aligned} u_1(s,0) - Z_{us}(s)\rho_1(s,0) &= f_{us} \\ \rho_2(s,L) - Ru_2(s,L) &= f_{ds} \end{aligned}}$$

Reproduced with permission of the copyright owner. Further reproduction prohibited without permission.

Using the notation of reference [SF65], the boundary conditions are then put in the following form,

$$\begin{bmatrix} 1 & -Z_{us}(s) \\ 0 & 0 \end{bmatrix}\begin{bmatrix} u_1(s,0) \\ \rho_1(s,0) \end{bmatrix}+\begin{bmatrix} 0 & 0 \\ -R & 1 \end{bmatrix}\begin{bmatrix} u_2(s,L) \\ \rho_2(s,L) \end{bmatrix}=\begin{bmatrix} f_{us} \\ f_{ds} \end{bmatrix} \qquad (4.131)$$

or, more compactly

$$M(s)\underline{u}_1(s,0)+N(s)\underline{u}_2(s,L)=Z(s) \qquad (4.132)$$

where,

$$M(s)=\begin{bmatrix} 1 & -Z_{us}(s) \\ 0 & 0 \end{bmatrix},\ N(s)=\begin{bmatrix} 0 & 0 \\ -R & 1 \end{bmatrix},\ Z(s)=\begin{bmatrix} f_{us} \\ f_{ds} \end{bmatrix}.$$

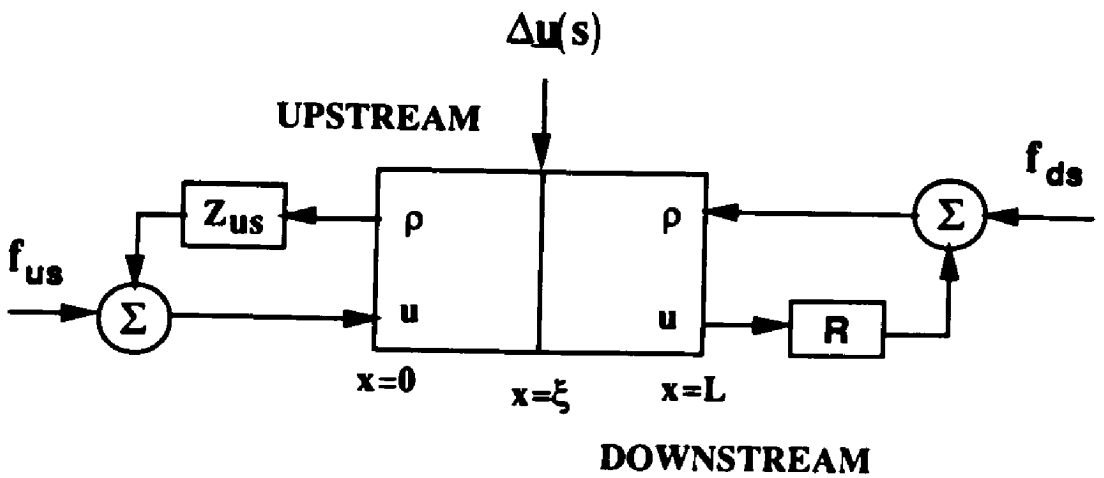


Figure 4.21 Boundary conditions for the two-wave problem

On the other hand, if a three-wave model is used, then the following boundary constraints should be used:

Reproduced with permission of the copyright owner. Further reproduction prohibited without permission.

$$q_1(s,0) = Z_1(s)\, q_3(s,0)$$

$$q_2(s,0) = Z_2(s)\, q_3(s,0)$$

$$q_3(s,L) = R_1\, q_1(s,L) + R_2\, q_2(s,L) + \delta F_{in}\ ,$$

or, in matrix form,

$$\begin{bmatrix} 1 & 0 & -Z_1(s) \\ 0 & 1 & -Z_2(s) \\ 0 & 0 & 0 \end{bmatrix} \begin{bmatrix} q_1(s,0) \\ q_2(s,0) \\ q_3(s,0) \end{bmatrix} + \begin{bmatrix} 0 & 0 & 0 \\ 0 & 0 & 0 \\ -R_1 & -R_2 & 1 \end{bmatrix} \begin{bmatrix} q_1(s,L) \\ q_2(s,L) \\ q_3(s,L) \end{bmatrix} = \begin{bmatrix} 0 \\ 0 \\ \delta F_{in} \end{bmatrix} \qquad (4.133)$$

and finally,

$$M(s)\, Q_1(s,0) + N(s)\, Q_2(s,L) = Z(s).$$

This set of constraints is illustrated in Figure 4.22.

Before we go on, it seems appropriate to draw some analogies between the two-wave and three-wave systems. These are illustrated in the following table. From the general expressions for the flow that will be developed below, one can go from the two-wave solution to the three-wave solution by doing some appropriate substitution. The development of the general expressions are carried out using the two-wave notation. It should be noted parenthetically that a double notation is needed in order to distinguish the two- from the three-wave model. Nevertheless, the general expressions for the flow are valid for both models.

Reproduced with permission of the copyright owner. Further reproduction prohibited without permission.

Table 4.3 Notation list for 2- & 3-wave systems

Quantity	2-Wave	3-Wave
State vector	$\underline{u}_i(s,x) = \begin{bmatrix} u_i(s,x) \\ \rho_i(s,x) \end{bmatrix}$	$Q_i(s,x) = \begin{bmatrix} q_1(s,x) \\ q_2(s,x) \\ q_3(s,x) \end{bmatrix} = \begin{bmatrix} \rho_i(s,x) \\ \rho_i(s,x)u_i(s,x) \\ \rho_i(s,x)E_i(s,x) \end{bmatrix}$
M(s)	$\begin{bmatrix} 1 & -Z_{us}(s) \\ 0 & 0 \end{bmatrix}$	$\begin{bmatrix} 1 & 0 & -Z_1 \\ 0 & 1 & -Z_2 \\ 0 & 0 & 0 \end{bmatrix}$
N(s)	$\begin{bmatrix} 0 & 0 \\ -R & 1 \end{bmatrix}$	$\begin{bmatrix} 0 & 0 & 0 \\ 0 & 0 & 0 \\ -R_1 & -R_2 & 1 \end{bmatrix}$
External Input Vector	$Z(s) = \begin{bmatrix} f_{us} \\ f_{ds} \end{bmatrix}$	$Z(s) = \begin{bmatrix} 0 \\ 0 \\ \delta F_{in} \end{bmatrix}$
Interior Input Vector	$\Delta\underline{u}(s)$	$\Delta Q(s)$
Reflection Coefficients	R	R_1, R_2
Shock Dynamics	Z_{us}	Z_1, Z_2

Now, the next step in the development of the system transfer function is to solve for the unknown flow vector $\underline{u}_1(s,0)$ in terms of the inputs $Z(s)$ and $\Delta\underline{u}(s)$. This is shown below:

Reproduced with permission of the copyright owner. Further reproduction prohibited without permission.

$$M(s)\,\underline{u}_1(s,0) = \underline{Z}(s) - N(s)\,\underline{u}_2(s,L)$$

$$\Rightarrow M(s)\,\underline{u}_1(s,0) = \underline{Z}(s) - N(s)\,[\,H(s,L)\,\underline{u}_1(s,0) + H(s,L-\xi)\,]\,\Delta\underline{u}(s)$$

$$\Rightarrow M(s)\,\underline{u}_1(s,0) + N(s)\,H(s,L)\,\underline{u}_1(s,0) = \underline{Z}(s) - N(s)\,H(s,L-\xi)\,\Delta\underline{u}(s)$$

$$\Rightarrow [M(s) + N(s)\,H(s,L)]\,\underline{u}_1(s,0) = \underline{Z}(s) - N(s)\,H(s,L-\xi)\,\Delta\underline{u}(s)$$

Thus,

$$\underline{u}_1(s,0) = [M(s) + N(s)\,H(s,L)]^{-1}\,[\underline{Z}(s) - N(s)\,H(s,L-\xi)\,\Delta\underline{u}(s)]. \qquad (4.134)$$

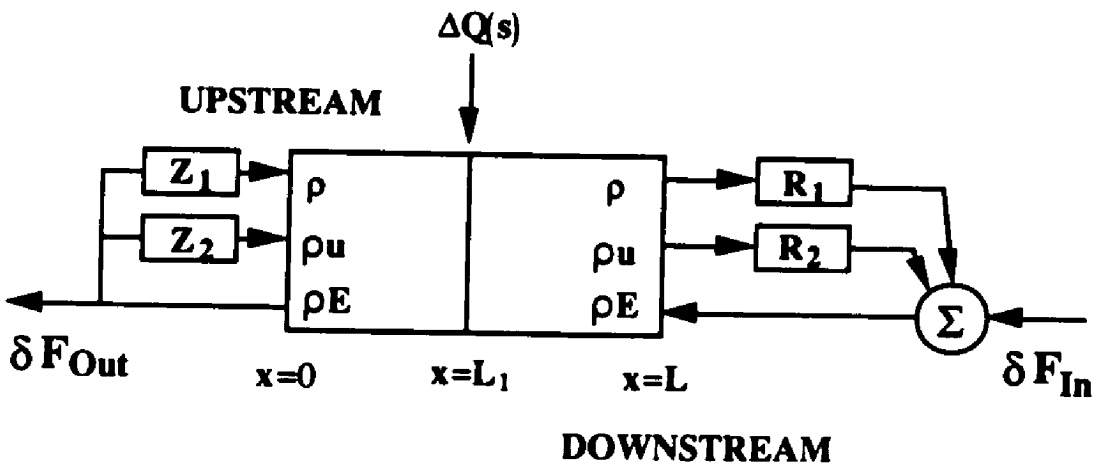


Figure 4.22 Boundary conditions for the three-wave problem

Applying the distributive law to the above expression yields the following expression for $\underline{u}_1(s,0)$:

Reproduced with permission of the copyright owner. Further reproduction prohibited without permission.

$$\underline{u}_1(s,0)=[M(s)+N(s)H(s,L)]^{-1}\underline{Z}(s)-[M(s)+N(s)H(s,L)]^{-1}N(s)H(s,L-\xi)\Delta\underline{u}(s)$$

and substituting $\underline{u}_1(s,0)$ into $\underline{u}_2(s,x)$ yields,

$$\underline{u}_2(s,x)=\{H(s,x)[M(s)+N(s)H(s,L)]^{-1}\}\underline{Z}(s)$$
$$-[M(s)+N(s)H(s,L)]^{-1}N(s)H(s,L-\xi)\Delta\underline{u}(s)+H(s,x-\xi)\Delta\underline{u}(s)$$

Furthermore, substituting the system transfer function for the given boundary conditions, i.e., $K(s,x)=H(s,x)[M(s)+N(s)H(s,L)]^{-1}$, into $\underline{u}_2(s,x)$ yields the following expression:

$$\underline{u}_2(s,x)=K(s,x)\underline{Z}(s)+\{H(s,x-\xi)-[M(s)+N(s)H(s,L)]^{-1}N(s)H(s,L-\xi)\}\Delta\underline{u}(s). \quad (4.135)$$

It should be noted that the last expression is valid in the region where $\xi\le x\le L$, namely, in Channel 2.

Finally, the flow in Channel 1, $\underline{u}_1(s,x)$, in terms of the input vectors is derived from $\underline{u}_1(s,0)$ in a similar fashion:

$$\underline{u}_1(s,x)=H(s,x)\ \underline{u}_1(s,0)=H(s,x)[M(s)+N(s)H(s,L)]^{-1}\{\underline{Z}(s)-N(s)H(s,L-\xi)\Delta\underline{u}(s)\}$$

$$\Rightarrow\underline{u}_1(s,x)=K(s,x)\ \{\underline{Z}(s)-N(s)H(s,L-\xi)\Delta\underline{u}(s)\}.$$

Therefore for $0\le x\le\xi$, the general solution to the problem is given by

$$\underline{u}_1(s,x)=K(s,x)\underline{Z}(s)-K(s,x)N(s)H(s,L-\xi)\Delta\underline{u}(s). \quad (4.136)$$

In conclusion, $\underline{u}(s,x)$ can be computed from the following formula:

$$\underline{u}(s,x)=K(s,x)\underline{Z}(s)+G(s,x;\xi)\Delta\underline{u}(s) \quad (4.137)$$

Reproduced with permission of the copyright owner. Further reproduction prohibited without permission.

where,

$$G(s,x;\xi)=\begin{cases} G_1(s,x;\xi), & 0\le x<\xi, \quad \text{(Channel 1)} \\ G_2(s,x;\xi), & \xi\le x\le L, \quad \text{(Channel 2)}. \end{cases} \tag{4.138}$$

$G(s,x;\xi)$ is referred to as the Green's Transfer Matrix for the given system. If the two-wave model is used, then the following 2×2 matrix is obtained:

$$G_1(s,x;\xi)=-K(s,x)N(s)H(s,L-\xi)\equiv\begin{bmatrix} \tilde{g}_{11} & \tilde{g}_{12} \\ \tilde{g}_{21} & \tilde{g}_{22} \end{bmatrix} \tag{4.139}$$

and, if the three-wave model is used, then the following 3×3 matrix results,

$$G_1(s,x;\xi)=-K(s,x)N(s)H(s,L-\xi)\equiv\begin{bmatrix} \tilde{g}_{11} & \tilde{g}_{12} & \tilde{g}_{13} \\ \tilde{g}_{21} & \tilde{g}_{22} & \tilde{g}_{23} \\ \tilde{g}_{31} & \tilde{g}_{32} & \tilde{g}_{33} \end{bmatrix}. \tag{4.140}$$

Similarly, the following expressions, valid in Channel 2, are obtained:

$$G_2(s,x;\xi)=\left\{H(s,x-\xi)-\left[M(s)+N(s)H(s,L)\right]^{-1}N(s)H(s,L-\xi)\right\}\equiv\begin{bmatrix} \hat{g}_{11} & \hat{g}_{12} \\ \hat{g}_{21} & \hat{g}_{22} \end{bmatrix}, \tag{4.141}$$

for a two-wave model and

$$G_2(s,x;\xi)=\left\{H(s,x-\xi)-\left[M(s)+N(s)H(s,L)\right]^{-1}N(s)H(s,L-\xi)\right\}\equiv\begin{bmatrix} \hat{g}_{11} & \hat{g}_{12} & \hat{g}_{13} \\ \hat{g}_{21} & \hat{g}_{22} & \hat{g}_{23} \\ \hat{g}_{31} & \hat{g}_{32} & \hat{g}_{33} \end{bmatrix}, \tag{4.142}$$

Reproduced with permission of the copyright owner. Further reproduction prohibited without permission.

for a three-wave model. Next, exact solutions for $G_1(s,x;\xi)$ and $G_2(s,x;\xi)$ can be readily obtained by substituting the proper matrices in the above expressions and then performing the required computations. Even for a 2×2 model, writing out the analytical solutions for $G(s,x;\xi)$, is a rather laborious task as the discussion in the following sections indicates. On the other hand, for practical considerations, the computation of $G(s,x;\xi)$ for a three-wave model will not be carried out in this dissertation. However, it is strongly felt that the reader has been given enough information and guidance to work out the three-wave solution for $G(s,x;\xi)$. Thus, this Herculean task is reserved for future work.

A. Computation of $G_1(s,x;\xi)$

Recall that the general expression for $G_1(s,x;\xi)$ is given by

Two-Wave:

$$G_1(s,x;\xi)=-K(s,x)N(s)H(s,L-\xi)\equiv\begin{bmatrix} \tilde{g}_{11} & \tilde{g}_{12} \\ \tilde{g}_{21} & \tilde{g}_{22} \end{bmatrix}, \qquad (4.143)$$

Three-Wave:

$$G_1(s,x;\xi)=-K(s,x)N(s)H(s,L-\xi)\equiv\begin{bmatrix} \tilde{g}_{11} & \tilde{g}_{12} & \tilde{g}_{13} \\ \tilde{g}_{21} & \tilde{g}_{22} & \tilde{g}_{23} \\ \tilde{g}_{31} & \tilde{g}_{32} & \tilde{g}_{33} \end{bmatrix}. \qquad (4.144)$$

Using the two-wave model, substitution of $K(\cdot)$, $N(\cdot)$, and $H(\cdot)$ into the first expression yields the following elements for $G_1(s,x;\xi)$:

Reproduced with permission of the copyright owner. Further reproduction prohibited without permission.

$$\tilde{g}_{11}=\frac{\exp\left[\frac{\bar{u}s(x-L)}{c^2-\bar{u}^2}\right]\left[Z_{us}\cosh\left(\frac{csx}{c^2-\bar{u}^2}\right)-\frac{c}{\bar{\rho}}\sinh\left(\frac{csx}{c^2-\bar{u}^2}\right)\right]}{(1-Z_{us}R)\cosh\left(\frac{csL}{c^2-\bar{u}^2}\right)+\left(\frac{Rc}{\bar{\rho}}-Z_{us}\frac{\bar{\rho}}{c}\right)\sinh\left(\frac{csL}{c^2-\bar{u}^2}\right)}\cdot$$

$$\cdot\exp\left[\frac{\bar{u}s(L-\xi)}{c^2-\bar{u}^2}\right]\left\{R\cosh\left(\frac{cs(L-\xi)}{c^2-\bar{u}^2}\right)+\frac{\bar{\rho}}{c}\sinh\left(\frac{cs(L-\xi)}{c^2-\bar{u}^2}\right)\right\}$$

or,

$$\tilde{g}_{11}=\frac{\exp\left[\frac{\bar{u}s(x-\xi)}{c^2-\bar{u}^2}\right]\left[Z_{us}\cosh\left(\frac{csx}{c^2-\bar{u}^2}\right)-\frac{c}{\bar{\rho}}\sinh\left(\frac{csx}{c^2-\bar{u}^2}\right)\right]\left\{R\cosh\left(\frac{cs(L-\xi)}{c^2-\bar{u}^2}\right)+\frac{\bar{\rho}}{c}\sinh\left(\frac{cs(L-\xi)}{c^2-\bar{u}^2}\right)\right\}}{(1-Z_{us}R)\cosh\left(\frac{csL}{c^2-\bar{u}^2}\right)+\left(\frac{Rc}{\bar{\rho}}-Z_{us}\frac{\bar{\rho}}{c}\right)\sinh\left(\frac{csL}{c^2-\bar{u}^2}\right)};$$

(4.145)

$$\tilde{g}_{12}=\frac{\exp\left[\frac{\bar{u}s(x-L)}{c^2-\bar{u}^2}\right]\left[Z_{us}\cosh\left(\frac{csx}{c^2-\bar{u}^2}\right)-\frac{c}{\bar{\rho}}\sinh\left(\frac{csx}{c^2-\bar{u}^2}\right)\right]}{(1-Z_{us}R)\cosh\left(\frac{csL}{c^2-\bar{u}^2}\right)+\left(\frac{Rc}{\bar{\rho}}-Z_{us}\frac{\bar{\rho}}{c}\right)\sinh\left(\frac{csL}{c^2-\bar{u}^2}\right)}\cdot$$

$$\cdot\exp\left[\frac{\bar{u}s(L-\xi)}{c^2-\bar{u}^2}\right]\left\{\cosh\left(\frac{cs(L-\xi)}{c^2-\bar{u}^2}\right)+\frac{Rc}{\bar{\rho}}\sinh\left(\frac{cs(L-\xi)}{c^2-\bar{u}^2}\right)\right\}$$

or, after simplifying,

$$\tilde{g}_{12}=\frac{\exp\left[\frac{\bar{u}s(x-\xi)}{c^2-\bar{u}^2}\right]\left[Z_{us}\cosh\left(\frac{csx}{c^2-\bar{u}^2}\right)-\frac{c}{\bar{\rho}}\sinh\left(\frac{csx}{c^2-\bar{u}^2}\right)\right]\left\{\cosh\left(\frac{cs(L-\xi)}{c^2-\bar{u}^2}\right)+\frac{Rc}{\bar{\rho}}\sinh\left(\frac{cs(L-\xi)}{c^2-\bar{u}^2}\right)\right\}}{(1-Z_{us}R)\cosh\left(\frac{csL}{c^2-\bar{u}^2}\right)+\left(\frac{Rc}{\bar{\rho}}-Z_{us}\frac{\bar{\rho}}{c}\right)\sinh\left(\frac{csL}{c^2-\bar{u}^2}\right)};$$

(4.146)

Reproduced with permission of the copyright owner. Further reproduction prohibited without permission.

$$\tilde{g}_{21}=\frac{\exp\left[\frac{\bar{u}s(x-L)}{c^2-\bar{u}^2}\right]\left[\cosh\left(\frac{csx}{c^2-\bar{u}^2}\right)-Z_{us}\frac{\bar{\rho}}{c}\sinh\left(\frac{csx}{c^2-\bar{u}^2}\right)\right]}{(1-Z_{us}R)\cosh\left(\frac{csL}{c^2-\bar{u}^2}\right)+\left(\frac{Rc}{\bar{\rho}}-Z_{us}\frac{\bar{\rho}}{c}\right)\sinh\left(\frac{csL}{c^2-\bar{u}^2}\right)}\cdot$$

$$\cdot\exp\left[\frac{\bar{u}s(L-\xi)}{c^2-\bar{u}^2}\right]\left\{R\cosh\left(\frac{cs(L-\xi)}{c^2-\bar{u}^2}\right)+\frac{\bar{\rho}}{c}\sinh\left(\frac{cs(L-\xi)}{c^2-\bar{u}^2}\right)\right\}$$

or,

$$\tilde{g}_{21}=\frac{\exp\left[\frac{\bar{u}s(x-\xi)}{c^2-\bar{u}^2}\right]\left[\cosh\left(\frac{csx}{c^2-\bar{u}^2}\right)-Z_{us}\frac{\bar{\rho}}{c}\sinh\left(\frac{csx}{c^2-\bar{u}^2}\right)\right]\left\{R\cosh\left(\frac{cs(L-\xi)}{c^2-\bar{u}^2}\right)+\frac{\bar{\rho}}{c}\sinh\left(\frac{cs(L-\xi)}{c^2-\bar{u}^2}\right)\right\}}{(1-Z_{us}R)\cosh\left(\frac{csL}{c^2-\bar{u}^2}\right)+\left(\frac{Rc}{\bar{\rho}}-Z_{us}\frac{\bar{\rho}}{c}\right)\sinh\left(\frac{csL}{c^2-\bar{u}^2}\right)};$$

(4.147)

and finally,

$$\tilde{g}_{22}=\frac{\exp\left[\frac{\bar{u}s(x-L)}{c^2-\bar{u}^2}\right]\left[\cosh\left(\frac{csx}{c^2-\bar{u}^2}\right)-Z_{us}\frac{c}{\bar{\rho}}\sinh\left(\frac{csx}{c^2-\bar{u}^2}\right)\right]}{(1-Z_{us}R)\cosh\left(\frac{csL}{c^2-\bar{u}^2}\right)+\left(\frac{Rc}{\bar{\rho}}-Z_{us}\frac{\bar{\rho}}{c}\right)\sinh\left(\frac{csL}{c^2-\bar{u}^2}\right)}\cdot$$

$$\cdot\exp\left[\frac{\bar{u}s(L-\xi)}{c^2-\bar{u}^2}\right]\left\{\cosh\left(\frac{cs(L-\xi)}{c^2-\bar{u}^2}\right)+\frac{Rc}{\bar{\rho}}\sinh\left(\frac{cs(L-\xi)}{c^2-\bar{u}^2}\right)\right\}$$

or,

$$\tilde{g}_{22}=\frac{-\exp\left[\frac{\bar{u}s(x-\xi)}{c^2-\bar{u}^2}\right]\left[\cosh\left(\frac{csx}{c^2-\bar{u}^2}\right)-Z_{us}\frac{c}{\bar{\rho}}\sinh\left(\frac{csx}{c^2-\bar{u}^2}\right)\right]\left\{\cosh\left(\frac{cs(L-\xi)}{c^2-\bar{u}^2}\right)+\frac{Rc}{\bar{\rho}}\sinh\left(\frac{cs(L-\xi)}{c^2-\bar{u}^2}\right)\right\}}{(1-Z_{us}R)\cosh\left(\frac{csL}{c^2-\bar{u}^2}\right)+\left(\frac{Rc}{\bar{\rho}}-Z_{us}\frac{\bar{\rho}}{c}\right)\sinh\left(\frac{csL}{c^2-\bar{u}^2}\right)}.$$

(4.148)

Reproduced with permission of the copyright owner. Further reproduction prohibited without permission.

B. Computation of $G_2(s,x;\xi)$.

Next, $G_2(s,x;\xi)$ will be computed from the following general expression which was derived above:

Two-Wave:

$$G_2(s,x;\xi)=\left\{H(s,x-\xi)-\left[M(s)+N(s)H(s,L)\right]^{-1}N(s)H(s,L-\xi)\right\}\equiv\begin{bmatrix}\hat{g}_{11} & \hat{g}_{12}\\ \hat{g}_{21} & \hat{g}_{22}\end{bmatrix}, \tag{4.149}$$

Three-Wave:

$$G_2(s,x;\xi)=\left\{H(s,x-\xi)-\left[M(s)+N(s)H(s,L)\right]^{-1}N(s)H(s,L-\xi)\right\}\equiv\begin{bmatrix}\hat{g}_{11} & \hat{g}_{12} & \hat{g}_{13}\\ \hat{g}_{21} & \hat{g}_{22} & \hat{g}_{23}\\ \hat{g}_{31} & \hat{g}_{32} & \hat{g}_{33}\end{bmatrix}. \tag{4.150}$$

Again, for the two-wave case, since,

$$\left[M(s)+N(s)H(s,L)\right]^{-1}=\frac{\begin{bmatrix}-RH_{12}(s,L)+H_{22}(s,L) & Z_{us}\\ RH_{11}(s,L)-H_{21}(s,L) & 1\end{bmatrix}}{H_{22}(s,L)-RH_{12}(s,L)-Z_{us}RH_{11}(s,L)+Z_{us}H_{21}(s,L)} \tag{4.151}$$

and

$$\left[M(s)+N(s)H(s,L)\right]^{-1}N(s)=\frac{\begin{bmatrix}-RZ_{us} & Z_{us}\\ -R & 1\end{bmatrix}}{\exp\left(\frac{\bar{u}sL}{c^2-\bar{u}^2}\right)\left[\left(1-Z_{us}R\right)\cosh\left(\frac{csL}{c^2-\bar{u}^2}\right)+\left(R\frac{c}{\rho}-Z_{us}\frac{\bar{\rho}}{c}\right)\sinh\left(\frac{csL}{c^2-\bar{u}^2}\right)\right]}$$

there follows that $G_2(s,x;\xi)$ can be written explicity as follows:

Reproduced with permission of the copyright owner. Further reproduction prohibited without permission.

$$G_2(s,x;\xi) = \exp\left(\frac{\bar{u}s(x-\xi)}{c^2-\bar{u}^2}\right)\begin{bmatrix} \cosh\left(\frac{cs(x-\xi)}{c^2-\bar{u}^2}\right) & \frac{-c}{\rho}\sinh\left(\frac{cs(x-\xi)}{c^2-\bar{u}^2}\right) \\ \frac{-\rho}{c}\sinh\left(\frac{cs(x-\xi)}{c^2-\bar{u}^2}\right) & \cosh\left(\frac{cs(x-\xi)}{c^2-\bar{u}^2}\right) \end{bmatrix} -$$

$$\frac{\begin{bmatrix} -RZ_{us} & Z_{us} \\ -R & 1 \end{bmatrix}\begin{bmatrix} \cosh\left(\frac{cs(L-\xi)}{c^2-\bar{u}^2}\right) & \frac{-c}{\rho}\sinh\left(\frac{cs(L-\xi)}{c^2-\bar{u}^2}\right) \\ \frac{-\rho}{c}\sinh\left(\frac{cs(L-\xi)}{c^2-\bar{u}^2}\right) & \cosh\left(\frac{cs(L-\xi)}{c^2-\bar{u}^2}\right) \end{bmatrix}}{\exp\left(\frac{\bar{u}s\xi}{c^2-\bar{u}^2}\right)\left[(1-Z_{us}R)\cosh\left(\frac{csL}{c^2-\bar{u}^2}\right)+\left(R\frac{c}{\rho}-Z_{us}\frac{\rho}{c}\right)\sinh\left(\frac{csL}{c^2-\bar{u}^2}\right)\right]}$$

or,

$$G_2(s,x;\xi) = \exp\left(\frac{\bar{u}s(x-\xi)}{c^2-\bar{u}^2}\right)\begin{bmatrix} \cosh\left(\frac{cs(x-\xi)}{c^2-\bar{u}^2}\right) & \frac{-c}{\rho}\sinh\left(\frac{cs(x-\xi)}{c^2-\bar{u}^2}\right) \\ \frac{-\rho}{c}\sinh\left(\frac{cs(x-\xi)}{c^2-\bar{u}^2}\right) & \cosh\left(\frac{cs(x-\xi)}{c^2-\bar{u}^2}\right) \end{bmatrix} -$$

$$\frac{\begin{bmatrix} -Z_{us}\left(R\cosh\left(\frac{cs(L-\xi)}{c^2-\bar{u}^2}\right)+\frac{\rho}{c}\sinh\left(\frac{cs(L-\xi)}{c^2-\bar{u}^2}\right)\right) & Z_{us}\left(\frac{Rc}{\rho}\sinh\left(\frac{cs(L-\xi)}{c^2-\bar{u}^2}\right)+\cosh\left(\frac{cs(L-\xi)}{c^2-\bar{u}^2}\right)\right) \\ -\left(R\cosh\left(\frac{cs(L-\xi)}{c^2-\bar{u}^2}\right)+\frac{\rho}{c}\sinh\left(\frac{cs(L-\xi)}{c^2-\bar{u}^2}\right)\right) & \left(\frac{Rc}{\rho}\sinh\left(\frac{cs(L-\xi)}{c^2-\bar{u}^2}\right)+\cosh\left(\frac{cs(L-\xi)}{c^2-\bar{u}^2}\right)\right) \end{bmatrix}}{\exp\left(\frac{\bar{u}s\xi}{c^2-\bar{u}^2}\right)\left[(1-Z_{us}R)\cosh\left(\frac{csL}{c^2-\bar{u}^2}\right)+\left(R\frac{c}{\rho}-Z_{us}\frac{\rho}{c}\right)\sinh\left(\frac{csL}{c^2-\bar{u}^2}\right)\right]} \quad (4.152)$$

Reproduced with permission of the copyright owner. Further reproduction prohibited without permission.

Therefore, the elements of $G_2(s,x;\xi)$ in the two-wave model are as follows:

$$\hat{g}_{11} = \frac{\exp\left(\frac{\bar{u}s(x-\xi)}{c^2-\bar{u}^2}\right)\cosh\left(\frac{cs(x-\xi)}{c^2-\bar{u}^2}\right) + Z_{us}\left\{R\cosh\left(\frac{cs(L-\xi)}{c^2-\bar{u}^2}\right)+\frac{\bar{\rho}}{c}\sinh\left(\frac{cs(L-\xi)}{c^2-\bar{u}^2}\right)\right\}}{\exp\left(\frac{\bar{u}s\xi}{c^2-\bar{u}^2}\right)\left[(1-Z_{us}R)\cosh\left(\frac{csL}{c^2-\bar{u}^2}\right)+\left(R\frac{c}{\bar{\rho}}-Z_{us}\frac{\bar{\rho}}{c}\right)\sinh\left(\frac{csL}{c^2-\bar{u}^2}\right)\right]} \quad (4.153)$$

$$\hat{g}_{12} = \frac{\frac{-c}{\bar{\rho}}\exp\left(\frac{\bar{u}s(x-\xi)}{c^2-\bar{u}^2}\right)\sinh\left(\frac{cs(x-\xi)}{c^2-\bar{u}^2}\right) - Z_{us}\left\{\frac{Rc}{\bar{\rho}}\sinh\left(\frac{cs(L-\xi)}{c^2-\bar{u}^2}\right)+\cosh\left(\frac{cs(L-\xi)}{c^2-\bar{u}^2}\right)\right\}}{\exp\left(\frac{\bar{u}s\xi}{c^2-\bar{u}^2}\right)\left[(1-Z_{us}R)\cosh\left(\frac{csL}{c^2-\bar{u}^2}\right)+\left(R\frac{c}{\bar{\rho}}-Z_{us}\frac{\bar{\rho}}{c}\right)\sinh\left(\frac{csL}{c^2-\bar{u}^2}\right)\right]}, \quad (4.154)$$

$$\hat{g}_{21} = \frac{\frac{-\bar{\rho}}{c}\exp\left(\frac{\bar{u}s(x-\xi)}{c^2-\bar{u}^2}\right)\sinh\left(\frac{cs(x-\xi)}{c^2-\bar{u}^2}\right) + \left\{R\cosh\left(\frac{cs(L-\xi)}{c^2-\bar{u}^2}\right)+\frac{\bar{\rho}}{c}\sinh\left(\frac{cs(L-\xi)}{c^2-\bar{u}^2}\right)\right\}}{\exp\left(\frac{\bar{u}s\xi}{c^2-\bar{u}^2}\right)\left[(1-Z_{us}R)\cosh\left(\frac{csL}{c^2-\bar{u}^2}\right)+\left(\frac{Rc}{\bar{\rho}}-Z_{us}\frac{\bar{\rho}}{c}\right)\sinh\left(\frac{csL}{c^2-\bar{u}^2}\right)\right]}, \quad (4.155)$$

and finally,

$$\hat{g}_{22} = \frac{\exp\left(\frac{\bar{u}s(x-\xi)}{c^2-\bar{u}^2}\right)\cosh\left(\frac{cs(x-\xi)}{c^2-\bar{u}^2}\right) - \left\{\frac{Rc}{\bar{\rho}}\sinh\left(\frac{cs(L-\xi)}{c^2-\bar{u}^2}\right)+\cosh\left(\frac{cs(L-\xi)}{c^2-\bar{u}^2}\right)\right\}}{\exp\left(\frac{\bar{u}s\xi}{c^2-\bar{u}^2}\right)\left[(1-Z_{us}R)\cosh\left(\frac{csL}{c^2-\bar{u}^2}\right)+\left(\frac{Rc}{\bar{\rho}}-Z_{us}\frac{\bar{\rho}}{c}\right)\sinh\left(\frac{csL}{c^2-\bar{u}^2}\right)\right]}. \quad (4.156)$$

In conclusion then, the Green's function problem is a tedious although a very straightforward problem to solve. It closely resembles the *Two-Channel with Internal Input Bounded* problem of Section 4.10. The only significant difference between the two problems is that, in this section a single open loop transfer function matrix H(s,x) is used at either side of the interior boundary, while in Section 4.10 two distinct transfer function

Reproduced with permission of the copyright owner. Further reproduction prohibited without permission.

matrices $H_1(s,x)$ and $H_2(s,x)$ are needed. Thus, the Green's function method provides a much more compact solution than the method of Section 4.10 since only one free space transfer function matrix is needed. If the two transfer functions $H_1(s,x)$ and $H_2(s,x)$ are made the same then the resulting models derived from applying the theories of Sections 4.10 and 4.12 become identical. Finally, references [BUT69], and [BUT83] give a comprehensive study of Green's function theory and [BUT82] catalogues the Green's functions for many distributed parameter systems but, not the system covered in this section.

4.13 A Channel with Exponential Cross-Sectional Area

Up to this point, only problems having channels of constant cross-sectional area have been considered. In this section, a special case of a channel with varying cross-sectional area will be studied (see Figure 4.23 below).

First, a two-wave assumption will be made for the flow model and the cross sectional area of the flow channel will be varied exponentially with the downstream distance x. Thus, the following system of equations will be studied,

$$\frac{\partial u(t,x)}{\partial t} + \bar{u}\frac{\partial u(t,x)}{\partial x} + \frac{c^2}{\bar{\rho}}\frac{\partial \rho(t,x)}{\partial x} = 0 \qquad (4.157)$$

Reproduced with permission of the copyright owner. Further reproduction prohibited without permission.

$$\frac{\partial \rho(t,x)}{\partial t} + \bar{\rho}\frac{\partial u(t,x)}{\partial x} + \bar{u}\frac{\partial \rho(t,x)}{\partial x} + \frac{1}{A(x)}\frac{dA(x)}{dx}[\bar{\rho}\, u(t,x) + \bar{u}\,\rho(t,x)] = 0 \qquad (4.158)$$

where, the cross sectional area A is given by,

$$A(x) = e^{ax}. \qquad (4.159)$$

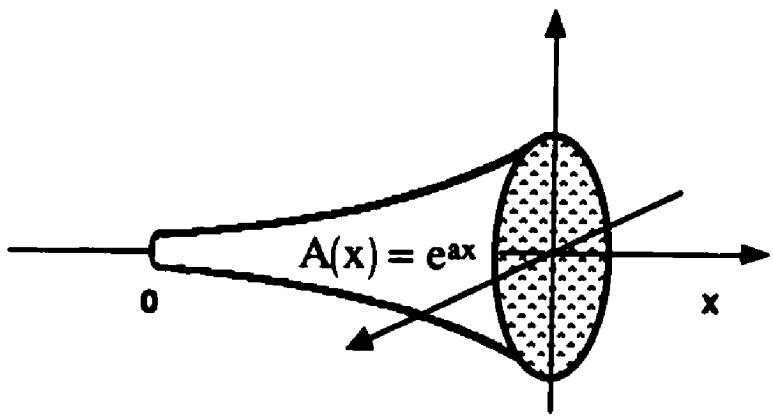


Figure 4.23 A channel with exponentially varying cross-sectional area

Differentiating A(x) with respect to x yields,

$$\frac{\partial A(x)}{\partial x} = \frac{dA(x)}{dx} = a\, e^{ax}$$

Reproduced with permission of the copyright owner. Further reproduction prohibited without permission.

and thus,

$$\frac{1}{A}\frac{dA(x)}{dx} = \frac{a\,e^{ax}}{e^{ax}} = a.$$

Therefore the given system becomes,

$$\frac{\partial u(t,x)}{\partial t} + \bar{u}\frac{\partial u(t,x)}{\partial x} + \frac{c^2}{\bar{\rho}}\frac{\partial \rho(t,x)}{\partial x} = 0 \qquad (4.160)$$

$$\frac{\partial \rho(t,x)}{\partial t} + \bar{\rho}\frac{\partial u(t,x)}{\partial x} + \bar{u}\frac{\partial \rho(t,x)}{\partial x} + a\left[\bar{\rho}\,u(t,x) + \bar{u}\,\rho(t,x)\right] = 0. \qquad (4.161)$$

Laplace transforming both equations with respect to the time variable and using zero initial conditions yields,

$$s\,u(s,x) + \bar{u}\frac{\partial u(s,x)}{\partial x} + \frac{c^2}{\bar{\rho}}\frac{\partial \rho(s,x)}{\partial x} = 0$$

$$s\,\rho(s,x) + \bar{\rho}\frac{\partial u(s,x)}{\partial x} + \bar{u}\frac{\partial \rho(s,x)}{\partial x} + a\left[\bar{\rho}\,u(s,x) + \bar{u}\,\rho(s,x)\right] = 0.$$

In matrix form the above system becomes,

$$\begin{bmatrix} \bar{u} & \frac{c^2}{\bar{\rho}} \\ \bar{\rho} & \bar{u} \end{bmatrix}\begin{bmatrix} \frac{\partial u(s,x)}{\partial x} \\ \frac{\partial \rho(s,x)}{\partial x} \end{bmatrix} + \begin{bmatrix} s & 0 \\ a\bar{\rho} & s+a\bar{u} \end{bmatrix}\begin{bmatrix} u(s,x) \\ \rho(s,x) \end{bmatrix} = \begin{bmatrix} 0 \\ 0 \end{bmatrix}.$$

$$\Rightarrow \begin{bmatrix} \frac{\partial u(s,x)}{\partial x} \\ \frac{\partial \rho(s,x)}{\partial x} \end{bmatrix} = \frac{1}{c^2 - \bar{u}^2}\begin{bmatrix} \bar{u} & -\frac{c^2}{\bar{\rho}} \\ -\bar{\rho} & \bar{u} \end{bmatrix}\begin{bmatrix} s & 0 \\ a\bar{\rho} & s+a\bar{u} \end{bmatrix}\begin{bmatrix} u(s,x) \\ \rho(s,x) \end{bmatrix}$$

Reproduced with permission of the copyright owner. Further reproduction prohibited without permission.

$$\Rightarrow \begin{bmatrix} \frac{\partial u(s,x)}{\partial x} \\ \frac{\partial \rho(s,x)}{\partial x} \end{bmatrix} = \frac{1}{c^2 - \bar{u}^2} \begin{bmatrix} \bar{u}s - ac^2 & -\frac{c^2}{\bar{\rho}}(s+a\bar{u}) \\ -\bar{\rho}s + a\bar{\rho}\,\bar{u} & \bar{u}(s+a\bar{u}) \end{bmatrix} \begin{bmatrix} u(s,x) \\ \rho(s,x) \end{bmatrix}$$

$$\Rightarrow \begin{bmatrix} \frac{\partial u(s,x)}{\partial x} \\ \frac{\partial \rho(s,x)}{\partial x} \end{bmatrix} = \begin{bmatrix} \frac{\bar{u}s - ac^2}{c^2 - \bar{u}^2} & -\frac{c^2}{\bar{\rho}} \frac{s+a\bar{u}}{c^2 - \bar{u}^2} \\ \frac{(a\bar{u}-s)\bar{\rho}}{c^2 - \bar{u}^2} & \frac{\bar{u}(s+a\bar{u})}{c^2 - \bar{u}^2} \end{bmatrix} \begin{bmatrix} u(s,x) \\ \rho(s,x) \end{bmatrix}$$

$$\Rightarrow \frac{\partial Q(s,x)}{\partial x} = E\,Q(s,x). \qquad (4.162)$$

Where E is defined as follows,

$$E = \begin{bmatrix} \frac{\bar{u}s - ac^2}{c^2 - \bar{u}^2} & -\frac{c^2}{\bar{\rho}} \frac{s+a\bar{u}}{c^2 - \bar{u}^2} \\ \frac{(a\bar{u}-s)\bar{\rho}}{c^2 - \bar{u}^2} & \frac{\bar{u}(s+a\bar{u})}{c^2 - \bar{u}^2} \end{bmatrix} \qquad (4.163)$$

and Q(s,x) is given by,

$$Q(s,x) = \begin{bmatrix} u(s,x) \\ \rho(s,x) \end{bmatrix}.$$

The solution to this problem is given by,

$$Q(s,x) = e^{E(x-x_0)}\,Q(s,x_0). \qquad (4.164)$$

Letting $x_0=0$, yields

$$Q(s,x) = e^{Ex}\,Q(s,0) \equiv H(s,x)\,Q(s,0). \qquad (4.165)$$

Reproduced with permission of the copyright owner. Further reproduction prohibited without permission.

Thus, in order to calculate Q(s,x), the system transfer function matrix, H(s,x), must first be computed. By definition,

$$e^{Ex}=L^{-1}\left\{[p\,I - E]^{-1}\right\} \qquad (4.166)$$

where, I is the identity matrix, L is the Laplace operator, and p is the Laplace transform variable. Thus,

$$e^{Ex}=L^{-1}\left\{\begin{bmatrix} p\frac{\bar{u}s-ac^2}{c^2-\bar{u}^2} & \frac{c^2}{\bar{\rho}}\frac{s+a\bar{u}}{c^2-\bar{u}^2} \\ \frac{(s-a\bar{u})\bar{\rho}}{c^2-\bar{u}^2} & p\frac{\bar{u}(s+a\bar{u})}{c^2-\bar{u}^2} \end{bmatrix}^{-1}\right\}$$

$$=L^{-1}\left\{\frac{\begin{bmatrix} p\frac{\bar{u}(s+a\bar{u})}{c^2-\bar{u}^2} & -\frac{c^2}{\bar{\rho}}\frac{s+a\bar{u}}{c^2-\bar{u}^2} \\ \frac{-(s-a\bar{u})\bar{\rho}}{c^2-\bar{u}^2} & p\frac{\bar{u}s-ac^2}{c^2-\bar{u}^2} \end{bmatrix}}{\left[p^2+\frac{\bar{u}(s+a\bar{u})(\bar{u}s-ac^2)}{(c^2-\bar{u}^2)^2}\right]-\left[\frac{\bar{u}(s+a\bar{u})+(\bar{u}s-ac^2)}{c^2-\bar{u}^2}\right]p-\frac{c^2(s^2-a^2\bar{u}^2)}{c^2-\bar{u}^2}}\right\}$$

$$=L^{-1}\left\{\frac{\begin{bmatrix} p\frac{\bar{u}(s+a\bar{u})}{c^2-\bar{u}^2} & -\frac{c^2}{\bar{\rho}}\frac{s+a\bar{u}}{c^2-\bar{u}^2} \\ \frac{(a\bar{u}-s)\bar{\rho}}{c^2-\bar{u}^2} & p\frac{\bar{u}s-ac^2}{c^2-\bar{u}^2} \end{bmatrix}}{\left[p^2+\left[\frac{-2\bar{u}s+a(c^2-\bar{u}^2)}{c^2-\bar{u}^2}\right]p+\frac{\bar{u}(s+a\bar{u})(\bar{u}s-ac^2)-c^2(s+a\bar{u})(s-a\bar{u})}{(c^2-\bar{u}^2)^2}\right]}\right\}.$$

Reproduced with permission of the copyright owner. Further reproduction prohibited without permission.

However,

$$p^2+\left[a-\frac{2\bar{u}s}{c^2-\bar{u}^2}\right]p+(s+a\bar{u})\frac{\left[\bar{u}\left(\bar{u}s-ac^2\right)-c^2\left(s-a\bar{u}\right)\right]}{\left(c^2-\bar{u}^2\right)^2}$$

$$=p^2+\left(a-\frac{2\bar{u}s}{c^2-\bar{u}^2}\right)p+(s+a\bar{u})\frac{\left[\bar{u}^2s-a\bar{u}c^2-c^2s+a\bar{u}c^2\right]}{\left(c^2-\bar{u}^2\right)^2}$$

$$=p^2+\left(a-\frac{2\bar{u}s}{c^2-\bar{u}^2}\right)p-\frac{s(s+a\bar{u})}{\left(c^2-\bar{u}^2\right)}.$$

Furthermore, it is interesting to note that the quantity

$$\Delta=p^2+\left(a-\frac{2\bar{u}s}{c^2-\bar{u}^2}\right)p-\frac{s(s+a\bar{u})}{\left(c^2-\bar{u}^2\right)} \qquad (4.167)$$

can be factored out as follows,

$$\Delta=p^2+\left(a-\frac{2\bar{u}s}{c^2-\bar{u}^2}\right)p-\frac{s(s+a\bar{u})}{\left(c^2-\bar{u}^2\right)}$$

$$=p^2-2\left(-\frac{a}{2}+\frac{\bar{u}s}{c^2-\bar{u}^2}\right)p-\frac{s(s+a\bar{u})}{\left(c^2-\bar{u}^2\right)}+\left(-\frac{a}{2}+\frac{\bar{u}s}{c^2-\bar{u}^2}\right)^2+\left(-\frac{a}{2}+\frac{\bar{u}s}{c^2-\bar{u}^2}\right)^2$$

$$=\left[p-\left(\frac{\bar{u}s}{c^2-\bar{u}^2}-\frac{a}{2}\right)\right]^2+\left[-\left(\frac{\bar{u}s}{c^2-\bar{u}^2}-\frac{a}{2}\right)^2-\frac{s(s+a\bar{u})}{\left(c^2-\bar{u}^2\right)}\right]$$

$$=\left[p-\tilde{A}\right]^2+\tilde{B}^2. \qquad (4.168)$$

where,

$$\tilde{A}=\frac{\bar{u}s}{c^2-\bar{u}^2}-\frac{a}{2} \qquad (4.169)$$

$$\tilde{B}^2=-\left[\left(\frac{\bar{u}s}{c^2-\bar{u}^2}-\frac{a}{2}\right)^2+\frac{s(s+a\bar{u})}{\left(c^2-\bar{u}^2\right)}\right]$$

Reproduced with permission of the copyright owner. Further reproduction prohibited without permission.

and,

$$\tilde{B} = j\left[\left(\frac{\bar{u}s}{c^2 - \bar{u}^2} - \frac{a}{2}\right)^2 + \frac{s(s+a\bar{u})}{(c^2 - \bar{u}^2)}\right]^{\frac{1}{2}}. \qquad (4.170)$$

Thus, e^{Ex} becomes

$$e^{Ex} = L^{-1}\left\{\frac{1}{(p-\tilde{A})^2+\tilde{B}^2}\begin{bmatrix} p\frac{\bar{u}(s+a\bar{u})}{c^2-\bar{u}^2} & -\frac{c^2}{\bar{\rho}}\frac{s+a\bar{u}}{c^2-\bar{u}^2} \\ \frac{(a\bar{u}-s)\bar{\rho}}{c^2-\bar{u}^2} & p\frac{\bar{u}s-ac^2}{c^2-\bar{u}^2} \end{bmatrix}\right\}$$

$$= L^{-1}\left\{\begin{bmatrix} \frac{p\frac{\bar{u}(s+a\bar{u})}{c^2-\bar{u}^2}}{(p-\tilde{A})^2+\tilde{B}^2} & \frac{\frac{c^2}{\bar{\rho}}\frac{s+a\bar{u}}{c^2-\bar{u}^2}}{(p-\tilde{A})^2+\tilde{B}^2} \\ \frac{\frac{(a\bar{u}-s)\bar{\rho}}{c^2-\bar{u}^2}}{(p-\tilde{A})^2+\tilde{B}^2} & \frac{p\frac{\bar{u}s-ac^2}{c^2-\bar{u}^2}}{(p-\tilde{A})^2+\tilde{B}^2} \end{bmatrix}\right\}$$

$$= L^{-1}\left\{\begin{bmatrix} \frac{p-\tilde{C}}{(p-\tilde{A})^2+\tilde{B}^2} & \frac{\tilde{D}}{(p-\tilde{A})^2+\tilde{B}^2} \\ \frac{\tilde{E}}{(p-\tilde{A})^2+\tilde{B}^2} & \frac{p-\tilde{F}}{(p-\tilde{A})^2+\tilde{B}^2} \end{bmatrix}\right\}$$

$$= L^{-1}\left\{\begin{bmatrix} \frac{p-\tilde{A}}{(p-\tilde{A})^2+\tilde{B}^2} + \frac{\tilde{A}-\tilde{C}}{\tilde{B}}\frac{\tilde{B}}{(p-\tilde{A})^2+\tilde{B}^2} & \frac{\tilde{D}}{\tilde{B}}\frac{\tilde{B}}{(p-\tilde{A})^2+\tilde{B}^2} \\ \frac{\tilde{E}}{\tilde{B}}\frac{\tilde{B}}{(p-\tilde{A})^2+\tilde{B}^2} & \frac{p-\tilde{A}}{(p-\tilde{A})^2+\tilde{B}^2} + \frac{\tilde{A}-\tilde{F}}{\tilde{B}}\frac{\tilde{B}}{(p-\tilde{A})^2+\tilde{B}^2} \end{bmatrix}\right\}$$

$$= e^{\tilde{A}x}\begin{bmatrix} \cos(\tilde{B}x) + \frac{\tilde{A}-\tilde{C}}{\tilde{B}}\sin(\tilde{B}x) & \frac{\tilde{D}}{\tilde{B}}\sin(\tilde{B}x) \\ \frac{\tilde{E}}{\tilde{B}}\sin(\tilde{B}x) & \cos(\tilde{B}x) + \frac{\tilde{A}-\tilde{F}}{\tilde{B}}\sin(\tilde{B}x) \end{bmatrix}$$

Reproduced with permission of the copyright owner. Further reproduction prohibited without permission.

$$= e^{\tilde{A}x}\begin{bmatrix} \cos(j\tilde{G}x) + \frac{\tilde{A}-\tilde{C}}{j\tilde{G}}\sin(j\tilde{G}x) & \frac{\tilde{D}}{j\tilde{G}}\sin(j\tilde{G}x) \\ \frac{\tilde{E}}{j\tilde{G}}\sin(j\tilde{G}x) & \cos(j\tilde{G}x) + \frac{\tilde{A}-\tilde{F}}{j\tilde{G}}\sin(j\tilde{G}x) \end{bmatrix}$$

$$= e^{\tilde{A}x}\begin{bmatrix} \cosh(\tilde{G}x) + \frac{\tilde{A}-\tilde{C}}{\tilde{G}}\sinh(\tilde{G}x) & \frac{\tilde{D}}{\tilde{G}}\sinh(\tilde{G}x) \\ \frac{\tilde{E}}{\tilde{G}}\sinh(\tilde{G}x) & \cosh(\tilde{G}x) + \frac{\tilde{A}-\tilde{F}}{\tilde{G}}\sinh(\tilde{G}x) \end{bmatrix},$$

where the parameters $\tilde{C}$, $\tilde{D}$, $\tilde{E}$, $\tilde{F}$, and $\tilde{G}$ are defined as follows:

$$\tilde{C}=\frac{\bar{u}(s+a\bar{u})}{c^2-\bar{u}^2}, \quad \tilde{D}=-\frac{c^2}{\bar{\rho}}\frac{s+a\bar{u}}{c^2-\bar{u}^2}, \quad \tilde{E}=\frac{(a\bar{u}-s)\bar{\rho}}{c^2-\bar{u}^2}, \tag{4.171}$$

$$\tilde{F}=\frac{\bar{u}s-ac^2}{c^2-\bar{u}^2}, \quad \tilde{G}=\left[\left(\frac{\bar{u}s}{c^2-\bar{u}^2}-\frac{a}{2}\right)^2+\frac{s(s+a\bar{u})}{(c^2-\bar{u}^2)}\right]^{\frac{1}{2}}\equiv\frac{\tilde{B}}{j}. \tag{4.172}$$

Therefore, the transfer function matrix H(s,x) is given by:

$$H(s,x) = e^{\tilde{A}x}\begin{bmatrix} \cosh(\tilde{G}x) + \frac{\tilde{A}-\tilde{C}}{\tilde{G}}\sinh(\tilde{G}x) & \frac{\tilde{D}}{\tilde{G}}\sinh(\tilde{G}x) \\ \frac{\tilde{E}}{\tilde{G}}\sinh(\tilde{G}x) & \cosh(\tilde{G}x) + \frac{\tilde{A}-\tilde{F}}{\tilde{G}}\sinh(\tilde{G}x) \end{bmatrix}. \tag{4.173}$$

This free-space transfer function can now be used as in earlier sections of Chapter 5 to solve problems involving ducts with exponentially varying cross-sectional areas.

4.14 Concluding Remarks

In this Chapter, several two-and three-wave theoretical flow problems were studied. Transfer functions for the flow vector in the

Reproduced with permission of the copyright owner. Further reproduction prohibited without permission.

Laplace domain as functions of the downstream distance x were developed for each channel configuration.

The following chapter focuses on some applications of the flow models that were developed in this chapter.

Reproduced with permission of the copyright owner. Further reproduction prohibited without permission.

CHAPTER V

MODELING INTERNAL FLOWS

5.1 Introduction

In the previous chapter, several theoretical as well as practical flow problems were solved. Collectively these problems are classified as "air-in-a-pipe" problems.

This chapter provides the reader with some supplementary pieces of information that would be needed to apply the theory developed in Chapter 4 to any practical flow scenario. It must be made clear that the quantitative dimensions of many facets of these problems are configuration-specific. Thus, one must be careful not to generalize results obtained here to arbitrary systems even though they might look alike.

The following section gives an overview of some of the key technologies for air-breathing propulsion that are in use today. Next, Section 5.3 covers the modes of operation of linearized compressible flow and Section 5.4 shows how input and output variables other than the chosen state variables may be incorporated into an existing model. In Section 5.5, a specific inlet system is analyzed using the theory presented in Chapter 4, and Section 5.6 guides the reader through the software code which was developed for simulating several flow scenarios.

Reproduced with permission of the copyright owner. Further reproduction prohibited without permission.

5.2 Key Technologies for Air-Breathing Propulsion

Some of the key technologies for air-breathing propulsion are the supersonic inlets, ramjets, and scramjets. These components are designed such that various levels of performance (expressed in Mach numbers) can be achieved as flow passes through them. Figure 5.1 below summarizes the speed regime definitions used to quantify fluid flow.

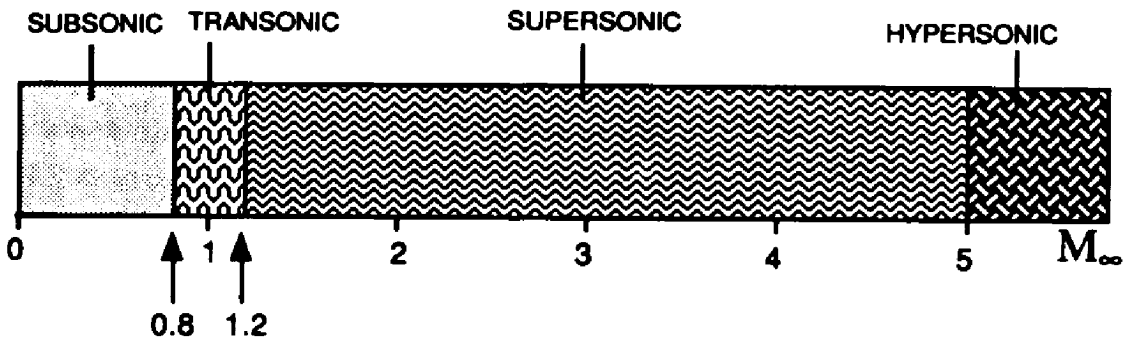


Figure 5.1 How to describe the speed

A description of an inlet of an air-breathing engine was given in Chapter 2. Typically, an inlet is made up primarily of a converging-diverging channel (See Figure 5.2). The inlet operates at supersonic speeds and its main function is to decelerate the incoming flow to subsonic velocities. This can be achieved either by shaping the geometry of the inlet carefully or by positioning the normal shock near the throat of the inlet.

Reproduced with permission of the copyright owner. Further reproduction prohibited without permission.

In fact, to the left of the shock the flow is supersonic while to its right the flow is subsonic. Also, the closer the shock is to the throat, the more efficient the inlet is.

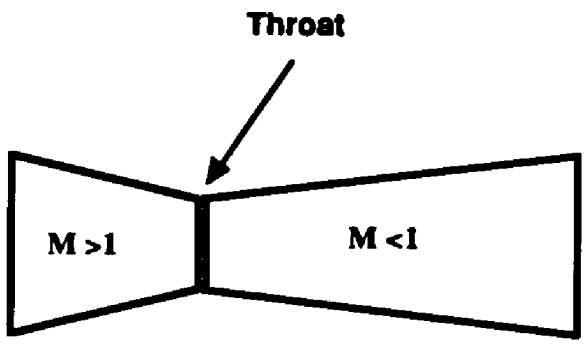


Figure 5.2 Cross section of a typical inlet

Ramjets, on the other hand, have more complicated components than inlets (see Figure 5.3). The flow goes from supersonic at Station 1 to subsonic at Station 2. Past the main flame the flow remains subsonic at Station 5 and becomes supersonic past Station 6, the exhaust nozzle throat.

Finally, a scramjet is a supersonic combustion ramjet. Here, a detonation wave is formed and the flow through the combustor itself remains supersonic (see Figure 5.4).

Reproduced with permission of the copyright owner. Further reproduction prohibited without permission.

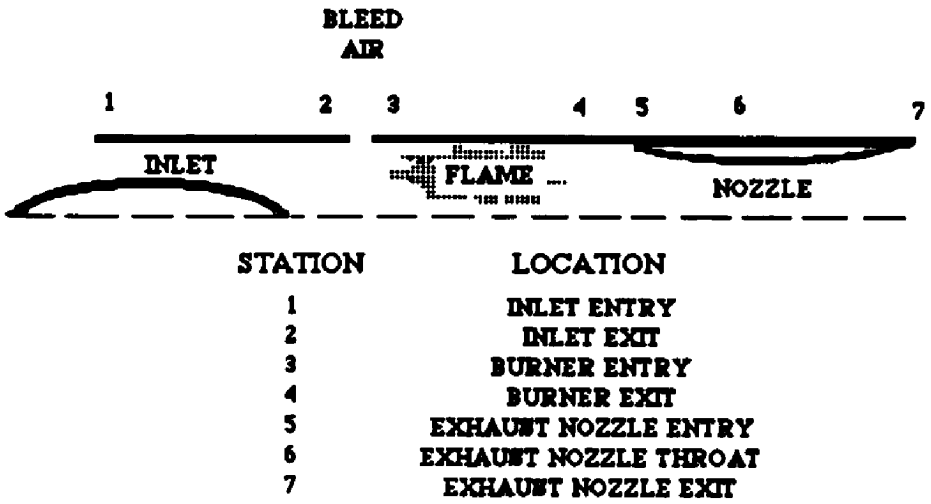


Figure 5.3 Cross section of a ramjet

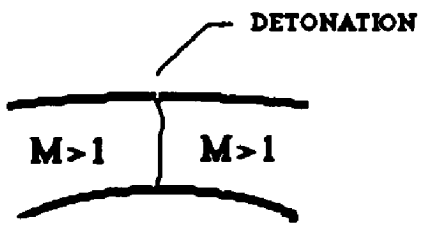


Figure 5.4 Cross section of a simplified supersonic combustion ramjet

This section provided the reader with an overview of the principal technologies for air-breathing technologies. The following section presents the modes of operation of a system which undergoes compressible flow.

Reproduced with permission of the copyright owner. Further reproduction prohibited without permission.

5.3 Modes of Operation in Compressible Flow

This parenthetic section describes the modes of operation in linearized compressible flow. Thus, the link between a particular system behavior and its corresponding mathematical model is made. The ensuing discussion will be very helpful to the controls engineer in deciding the right way of connecting blocks of different flow characteristics..

It was mentioned in Chapter 2 that compressible flow may be sufficiently represented by three equations derived from the law of conservation of mass, the balance of linear momentum, and the conservation of energy. In a linearized three-wave flow model one may recall that the open loop eigenvalues are given by:

$\lambda_1=u+c$, $\lambda_2=u$, and $\lambda_3=u-c$.

Depending on the algebraic sign of the λ_i's one can distinguish three modes of operation in a flow channel. These are illustrated in Table 5.1 below.

In Case I, all system eigenvalues are positive and there are three waves traveling downstream. The flow system is said to operate in the supersonic regime. Any boundary conditions imposed at the upstream end of the inlet will determine the flow across the entire flow channel uniquely. In other words, all inflow boundary variables must be specified as such variables are not constrained by the interior flow solution and no

Reproduced with permission of the copyright owner. Further reproduction prohibited without permission.

information can pass upstream from the flow to the inflow boundary. On the other hand, the flow variables at the outflow boundary are determined by the interior flow only. Consequently, no additional constraints can be applied at the downstream end of the inlet system.

Table 5.1 Modes of operation in a three-wave system

CASE I	CASE II	CASE III
$\lambda_1=u+c>0$ $\lambda_2=u>0$ $\lambda_3=u-c>0$	$\lambda_1=u+c>0$ $\lambda_2=u>0$ $\lambda_3=u-c<0$	$\lambda_1=u+c>0$ $\lambda_2=u<0$ $\lambda_3=u-c<0$
ALL λ's POSITIVE	2 λ's POSITIVE 1 λ NEGATIVE	1 λ POSITIVE 2 λ's NEGATIVE
→ → →	→ → ←	→ ← ←
SUPERSONIC REGIME	SUBSONIC REGIME	SUBSONIC REGIME WITH FLOW REVERSAL

In Case II, two waves travel downstream while the third travels upstream and thus information travels both ways. Carefully chosen boundary conditions may be applied at both ends of the flow system. The inlet system is said to operate in the subsonic regime.

Reproduced with permission of the copyright owner. Further reproduction prohibited without permission.

Finally, in Case III, two waves travel upstream while the third travels downstream. In this case the inlet system is said to operate in the subsonic regime, however, flow reversal occurs and this mode of operation is unsafe and thus should be avoided. Hot gases can exit from the inlet opening and spill over to the inlet housing with unpredictable and often catastrophic results. This case will not be considered any further.

When there is a transition across regimes I and II a normal shock wave is formed. Across a normal shock a rise in static pressure and a drop in flow velocity occur. On the other hand, when there is a transition from regime III to regime II a hammershock is formed.

If the traveling waves are examined qualitatively, one can see that those corresponding to λ_1 or λ_3 are acoustic waves. These waves can travel with sound and can be "heard". On the other hand, waves corresponding to λ_2 are inertial or entropy or kinetic energy waves. Such waves can be "felt".

It must be made clear that a two-wave model retains only two eigenvalues, namely λ_1 and λ_3. In this case, only the two acoustic waves are kept while the inertial wave is lost. Experience shows that when the Mach number is above .3 the three wave model should be used. Energy losses become too significant to be ignored.

This section described the modes of operation in three wave linearized compressible flow. The next section describes how supplemental

Reproduced with permission of the copyright owner. Further reproduction prohibited without permission.

input and/or output variables to the state variables chosen are incorporated into an existing model.

5.4 Inputs and Outputs

It is often useful to derive expressions for input/output variables other than the variables chosen in a particular state vector. In the ensuing discussion, practical expressions for several input and/or output variables with respect to the chosen state variables are developed.

If ρ, ρu, and ρE are the primary state variables used in a three-wave model, then pressure can be found using the following expression,

$$P = (\gamma-1)\left[\rho E-\frac{1}{2}\rho u^2\right] = \rho\,(\gamma-1)\left[E-\frac{1}{2}u^2\right].$$

Then, if one lets,

$$Q_1=\rho, \quad Q_2=\rho u, \text{ and } \quad Q_3=\rho E,$$

to denote the primary state variables used, the expression for pressure becomes,

$$P = (\gamma-1)\left[Q_3-\frac{1}{2}Q_2^2Q_1^{-1}\right].$$

Next, perturbations of pressure due to small changes in the primary state variables can be derived using partial differentiation as follows,

Reproduced with permission of the copyright owner. Further reproduction prohibited without permission.

$$\partial P = (\gamma-1)\left[\left(\frac{dQ_3}{dQ_3}\right)\partial Q_3 - \frac{1}{2Q_1}\left(\frac{d(Q_2^2)}{dQ_2}\right)\partial Q_2 - \frac{1}{2}Q_2^2\left(\frac{d\left(\frac{1}{Q_1}\right)}{dQ_1}\right)\partial Q_1\right]$$

$$= (\gamma-1)\left[\partial Q_3 - \frac{1}{2Q_1}(2Q_2)\,\partial Q_2 - \frac{1}{2}Q_2^2\,(-Q_1^{-2})\,\partial Q_1\right]$$

$$= (\gamma-1)\left[\partial(\rho E) - u\,\partial(\rho u) + \frac{1}{2}u^2\,\partial(\rho)\right]$$

$$= (\gamma-1)\begin{bmatrix} \frac{u^2}{2} & -u & 1 \end{bmatrix}\begin{bmatrix} \partial(\rho) \\ \partial(\rho u) \\ \partial(\rho E) \end{bmatrix}.$$

If only two state variables are used, ρ and u, then the following expression for pressure holds:

$$P = (\gamma-1)\left[\overline{E}_T - \frac{1}{2}\rho u^2\right].$$

Linearizing yields,

$$\partial P = (\gamma-1)\,\partial\left[\overline{E}_T - \frac{1}{2}\rho u^2\right] = \frac{1-\gamma}{2}\,\partial(\rho u^2).$$

Thus,

$$\partial P = (1-\gamma)\rho u\,\partial(u) + (1-\gamma)\frac{u^2}{2}\,\partial(\rho).$$

To make a change of pressure an input to the system under study, one proceeds as follows. Starting with

$$P = (\gamma-1)\left[\rho E - \frac{1}{2}\rho u^2\right],$$

Reproduced with permission of the copyright owner. Further reproduction prohibited without permission.

one can rearrange terms to get,

$$\text{Energy} = \rho E = \frac{P}{(\gamma-1)} + \frac{1}{2}\rho u^2.$$

Rewriting the above equation in terms of the primary state variables and linearizing yields,

$$(\rho E) = \frac{1}{(\gamma-1)} P + \frac{1}{2} \frac{(\rho u)^2}{\rho}$$

$$\Rightarrow \partial(\rho E) = \frac{1}{(\gamma-1)} \partial P - \frac{1}{2} u^2 \partial\rho + u\, \partial(\rho u)\,.$$

The above equation can be used at the boundary of a system to determine the energy in a three-wave model (see Figure 5.5 below). The coefficients of $\partial\rho$ and $\partial(\rho u)$ are the so-called reflection coefficients or parameters that were discussed in Chapter 2. As an added bonus, the above discussion also shows how the reflection coefficients can be picked; namely, in such a way as to match the coefficients of the perturbed variables.

Relations for additional inputs or outputs of temperature, Mach number, internal energy, stagnation enthalpy, entropy, etc. may be derived in a similar fashion as above by using partial differentiation. Due to the many possibilities that exist, only a few more examples will be presented below: temperature, specific entropy, and Mach number inputs and/or outputs. It is strongly felt that the interested reader has been given enough information to derive any additional input or output variables needed in his specific application.

Reproduced with permission of the copyright owner. Further reproduction prohibited without permission.

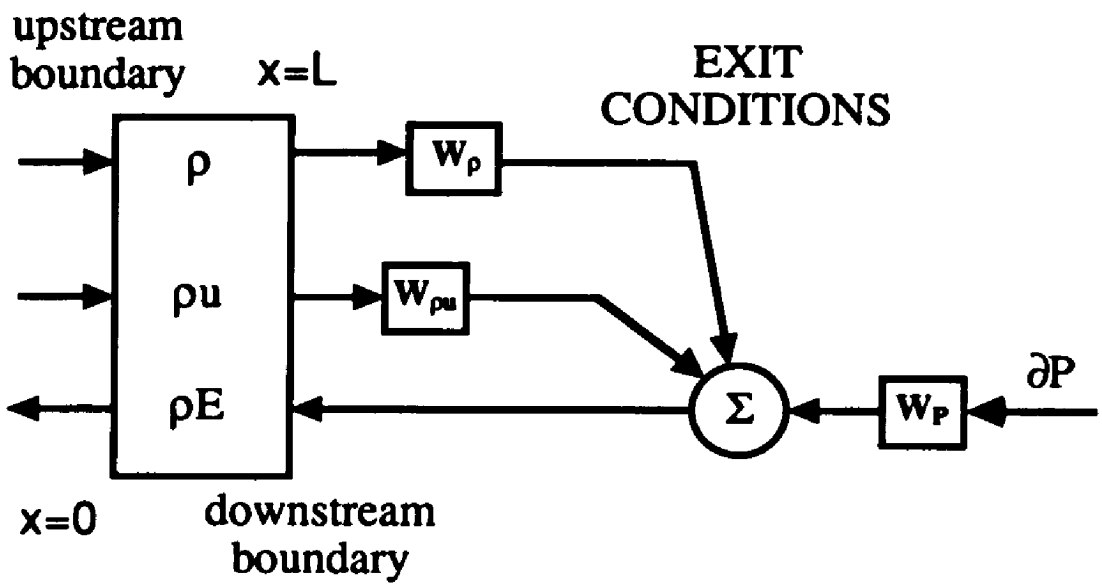


Figure 5.5 Exit boundary with a pressure input

Recall that temperature is given by $T=P/(\rho R)$, where, R is the gas constant of the particular gas. Substituting the expression for pressure into the temperature equation and linearizing yields an expression for an output of temperature in terms of the primary variables used:

$$T = \frac{1}{\rho R}(\gamma-1)\rho\left(E - \frac{1}{2}u^2\right)$$

$$= \frac{(\gamma-1)}{R}\left(\frac{1}{\rho}(\rho E) - \frac{1}{2}\frac{(\rho u)^2}{\rho^2}\right)$$

$$\Rightarrow \partial T = \frac{(\gamma-1)}{\rho R}\left[(u^2 - E)\,\partial\rho - u\,\partial(\rho u) + \partial(\rho E)\right].$$

Reproduced with permission of the copyright owner. Further reproduction prohibited without permission.

This equation is useful in monitoring the temperature in a system around the linearization point. In order to express a change of temperature as an input to the system, the last equation should be rearranged as follows:

$$\partial(\rho E) = (E - u^2)\,\partial\rho + u\,\partial(\rho u) + \frac{\rho R}{(\gamma-1)}\,\partial T.$$

From [AND82], a change in entropy is defined as

$$\partial s = c_p \frac{\partial T}{T} - R \frac{\partial P}{P},$$

where, R is the specific gas constant. Substituting ∂T and ∂P into the above equation yields,

$$\partial s = \begin{bmatrix} \frac{C_p(\gamma-1)(u^2 - E)}{T\rho R} - \frac{R(\gamma-1)u^2}{2P} \\ \left(\frac{-C_p(\gamma-1)u}{T\rho R} + \frac{R(\gamma-1)u}{P}\right) \\ \frac{C_p(\gamma-1)}{T\rho R} - \frac{R(\gamma-1)}{P} \end{bmatrix}^T \begin{bmatrix} \partial\rho \\ \partial(\rho u) \\ \partial(\rho E) \end{bmatrix}.$$

Since

$$C_p = \frac{\gamma R}{\gamma-1}$$

and

$$T = \frac{P}{\rho R},$$

then ∂s becomes,

Reproduced with permission of the copyright owner. Further reproduction prohibited without permission.

$$\partial s = \begin{bmatrix} \frac{\gamma R(u^2 - E)}{P} - \frac{R(\gamma-1)u^2}{2P} \\ \frac{-\gamma R u}{P} + \frac{R(\gamma-1)u}{P} \\ \frac{\gamma R}{P} - \frac{R(\gamma-1)}{P} \end{bmatrix}^T \begin{bmatrix} \partial\rho \\ \partial(\rho u) \\ \partial(\rho E) \end{bmatrix}$$

and finally,

$$\partial s = \frac{R}{P}\left[(\gamma+1)\frac{u^2}{2} - \gamma E, \; -u, \; 1\right]\begin{bmatrix} \partial\rho \\ \partial(\rho u) \\ \partial(\rho E) \end{bmatrix}.$$

Finally, the Mach number is defined as M=u/c, where the speed of sound, c, is given by,

$$c = \sqrt{\gamma(\gamma-1)\left(E - \frac{1}{2}u^2\right)}.$$

Thus, the Mach number equation can be rewritten as follows:

$$M = \frac{u}{c} = \frac{u}{\sqrt{\gamma(\gamma-1)\left(E - \frac{1}{2}u^2\right)}} = \frac{1}{\sqrt{\gamma(\gamma-1)}}\frac{1}{\sqrt{\left(\frac{E}{u^2} - \frac{1}{2}\right)}}$$

$$= \frac{1}{\sqrt{\gamma(\gamma-1)}}\left(\frac{\rho(\rho E)}{(\rho u)^2} - \frac{1}{2}\right)^{-\frac{1}{2}} = \frac{1}{\sqrt{\gamma(\gamma-1)}}\left[\rho(\rho u)^{-2}(\rho E) - \frac{1}{2}\right]^{-\frac{1}{2}}.$$

Reproduced with permission of the copyright owner. Further reproduction prohibited without permission.

Linearizing the above equation yields the following equation:

$$\partial M = \frac{1}{\sqrt{\gamma(\gamma-1)}}\,\partial\left(\left[\rho\,(\rho u)^{-2}(\rho E) - \frac{1}{2}\right]^{-\frac{1}{2}}\right)$$

$$= \frac{-1}{2\sqrt{\gamma(\gamma-1)}}\left(\frac{E}{u^2} - \frac{1}{2}\right)^{-\frac{3}{2}}\partial\left(\rho\,(\rho u)^{-2}(\rho E) - \frac{1}{2}\right)$$

$$= \frac{-1}{2\rho u^2\sqrt{\gamma(\gamma-1)\left(\frac{E}{u^2} - \frac{1}{2}\right)^3}}\left(E\,\partial\rho - \frac{2E}{u}\,\partial(\rho u) + \partial(\rho E)\right)$$

$$= -\sqrt{\frac{2}{\gamma(\gamma-1)(2E-u^2)^3}}\left[\frac{uE}{\rho}\,\partial\rho - \frac{2E}{\rho}\,\partial(\rho u) + \frac{u}{\rho}\,\partial(\rho E)\right]$$

$$= \frac{1}{\rho\, c\,(2E - u^2)}\left(-u\,E\,\partial\rho + 2\,E\,\partial(\rho u) - u\,\partial(\rho E)\right).$$

Rearranging the terms of the above equation produces the following expression for an input of Mach number to the system:

$$\partial(\rho E) = -\frac{\rho\, c}{u}(2E - u^2)\,\partial M - E\,\partial\rho + 2\frac{E}{u}\,\partial(\rho u).$$

It is often convenient to make use of stagnation variables when applicable. A stagnation property will be designated by adding a subscript T to its symbol. For example, the variation of the total or stagnation pressure, P_T is found by linearizing the following formula:

$$P_T = P\left(1 + \frac{\gamma-1}{2}M^2\right)^{\frac{\gamma}{\gamma-1}} = (\gamma-1)\left(\rho E - \frac{1}{2}\rho u^2\right)\left(1 + \frac{\gamma-1}{2}M^2\right)^{\frac{\gamma}{\gamma-1}}.$$

Reproduced with permission of the copyright owner. Further reproduction prohibited without permission.

Thus,

$$\ln(P_T) = \ln(\gamma-1) + \ln\left(\rho E - \frac{1}{2}\rho u^2\right) + \frac{\gamma}{\gamma-1}\ln\left(1+\frac{\gamma-1}{2}M^2\right)$$

and,

$$\frac{\partial P_T}{P_T} = \frac{\partial\left(\rho E - \frac{1}{2}\rho u^2\right)}{\rho E - \frac{1}{2}\rho u^2} + \frac{\gamma}{2}\frac{\partial(M^2)}{1+\frac{\gamma-1}{2}M^2}$$

$$= \frac{1}{\rho E - \frac{1}{2}\rho u^2}\partial(\rho E) - \frac{1}{2\left(\rho E - \frac{1}{2}\rho u^2\right)}\partial(\rho u^2) + \frac{\gamma M\,\partial(M)}{1+\frac{\gamma-1}{2}M^2}$$

$$= \frac{1}{\rho E - \frac{1}{2}\rho u^2}\partial(\rho E) - \frac{1}{2\left(\rho E - \frac{1}{2}\rho u^2\right)}\partial(\rho u^2) + \frac{\gamma M\left[-u\,E\,\partial\rho + 2\,E\,\partial(\rho u) - u\,\partial(\rho E)\right]}{\rho\, c\,(2\,E - u^2)\left(1+\frac{\gamma-1}{2}M^2\right)}$$

$$= \frac{1}{\rho E - \frac{1}{2}\rho u^2}\partial(\rho E) - \frac{1}{2\left(\rho E - \frac{1}{2}\rho u^2\right)}\partial(\rho u^2) - \frac{\gamma M u E}{\rho\, c\,(2\,E - u^2)\left(1+\frac{\gamma-1}{2}M^2\right)}\partial\rho$$

$$+ \frac{2\gamma M E}{\rho\, c\,(2\,E - u^2)\left(1+\frac{\gamma-1}{2}M^2\right)}\partial(\rho u) - \frac{\gamma M u}{\rho\, c\,(2\,E - u^2)\left(1+\frac{\gamma-1}{2}M^2\right)}\partial(\rho E)$$

$$= -\frac{\gamma M u E}{\rho\, c\,(2\,E - u^2)\left(1+\frac{\gamma-1}{2}M^2\right)}\partial\rho + \frac{2\gamma M E}{\rho\, c\,(2\,E - u^2)\left(1+\frac{\gamma-1}{2}M^2\right)}\partial(\rho u)$$

$$+ \left(\frac{1}{\rho E - \frac{1}{2}\rho u^2} - \frac{\gamma M u}{\rho\, c\,(2\,E - u^2)\left(1+\frac{\gamma-1}{2}M^2\right)}\right)\partial(\rho E) - \frac{1}{2\left(\rho E - \frac{1}{2}\rho u^2\right)}\partial(\rho u^2).$$

Reproduced with permission of the copyright owner. Further reproduction prohibited without permission.

Since

$$\partial(\rho u^2) = \partial((\rho u)^2 \rho^{-1}) = -u^2\,\partial(\rho) + 2u\,\partial(\rho u)\,,$$

then,

$$\frac{\partial P_T}{P_T} = \left(- \frac{\gamma M u E}{2\rho c \left(E - \frac{u^2}{2}\right)\left(1 + \frac{\gamma-1}{2} M^2\right)} + \frac{u^2}{2\rho\left(E - \frac{1}{2}u^2\right)} \right) \partial\rho$$

$$+ \left(\frac{\gamma M E}{\rho c \left(E - \frac{u^2}{2}\right)\left(1 + \frac{\gamma-1}{2} M^2\right)} - \frac{u}{\rho\left(E - \frac{1}{2}u^2\right)} \right) \partial(\rho u)$$

$$+ \left(\frac{1}{\rho\left(E - \frac{1}{2}u^2\right)} - \frac{\gamma M u}{2\rho c \left(E - \frac{u^2}{2}\right)\left(1 + \frac{\gamma-1}{2} M^2\right)} \right) \partial(\rho E)\,.$$

Finally, an input of total pressure to the system is given by the following expression:

$$\partial(\rho E) = \frac{1}{\frac{1}{\rho\left(E - \frac{1}{2}u^2\right)} - \frac{\gamma M^2}{2\rho \left(E - \frac{u^2}{2}\right)\left(1 + \frac{\gamma-1}{2} M^2\right)}} \frac{\partial P_T}{P_T}$$

$$+ \frac{\frac{\gamma M^2 E}{2\rho\left(E - \frac{u^2}{2}\right)\left(1 + \frac{\gamma-1}{2} M^2\right)} - \frac{u^2}{2\rho\left(E - \frac{1}{2}u^2\right)}}{\frac{1}{\rho\left(E - \frac{1}{2}u^2\right)} - \frac{\gamma M^2}{2\rho \left(E - \frac{u^2}{2}\right)\left(1 + \frac{\gamma-1}{2} M^2\right)}} \partial\rho$$

Reproduced with permission of the copyright owner. Further reproduction prohibited without permission.

$$+\frac{\dfrac{u}{\rho\left(E-\frac{1}{2}u^2\right)}-\dfrac{\gamma M^2 E}{\rho u\left(E-\frac{u^2}{2}\right)\left(1+\frac{\gamma-1}{2}M^2\right)}}{\dfrac{1}{\rho\left(E-\frac{1}{2}u^2\right)}-\dfrac{\gamma M^2}{2\rho\left(E-\frac{u^2}{2}\right)\left(1+\frac{\gamma-1}{2}M^2\right)}}\partial(\rho u).$$

Similarly, a perturbation in the total or stagnation temperature is found by linearizing the following formula:

$$T_T=\frac{P_T}{R\rho_T}=\frac{(\gamma-1)\left(\rho E-\frac{1}{2}\rho u^2\right)\left(1+\frac{\gamma-1}{2}M^2\right)^{\frac{\gamma}{\gamma-1}}}{R\left(1+\frac{\gamma-1}{2}M^2\right)^{\frac{1}{\gamma-1}}}=\frac{1}{C_v}\left(\rho E-\frac{1}{2}\rho u^2\right)\left(1+\frac{\gamma-1}{2}M^2\right).$$

Thus,

$$\partial T_T=\frac{1}{C_v}\left[\left(1+\frac{\gamma-1}{2}M^2\right)\left[\partial(\rho E)-\frac{1}{2}\partial(\rho u^2)\right]+M(\gamma-1)\left(\rho E-\frac{1}{2}\rho u^2\right)\partial(M)\right]$$

$$=\frac{1}{C_v}\left(1+\frac{\gamma-1}{2}M^2\right)\partial(\rho E)-\frac{1}{2C_v}\left(1+\frac{\gamma-1}{2}M^2\right)\partial(\rho u^2)$$

$$+\frac{M}{C_v}(\gamma-1)\left(\rho E-\frac{1}{2}\rho u^2\right)\partial(M)$$

$$=\frac{1}{C_v}\left(1+\frac{\gamma-1}{2}M^2\right)\partial(\rho E)-\frac{1}{2C_v}\left(1+\frac{\gamma-1}{2}M^2\right)(-u^2\,\partial\rho+2u\,\partial(\rho u))$$

$$+\frac{M(\gamma-1)}{2c\,C_v}(-u\,E\,\partial\rho+2\,E\,\partial(\rho u)-u\,\partial(\rho E))$$

and, after some simplification,

Reproduced with permission of the copyright owner. Further reproduction prohibited without permission.

$$\partial T_T = \left[\frac{u^2}{2C_v}\left(1+\frac{\gamma-1}{2}M^2\right) - \frac{M^2E(\gamma-1)}{2C_v}\right]\partial\rho$$

$$+\left[\frac{ME(\gamma-1)}{c\,C_v} - \frac{u}{C_v}\left(1+\frac{\gamma-1}{2}M^2\right)\right]\partial(\rho u)$$

$$+\left[\frac{1}{C_v}\left(1+\frac{\gamma-1}{2}M^2\right) - \frac{M^2(\gamma-1)}{2C_v}\right]\partial(\rho E)\,.$$

Finally, one can compute a perturbation in the specific entropy using the following formula:

$$\partial S = \frac{C_p}{T_T}\partial T_T - R\frac{\partial P_T}{P_T} =$$

$$= \left(\frac{\gamma u^2}{2T_T}\left(1+\frac{\gamma-1}{2}M^2\right) - \frac{M^2E\gamma(\gamma-1)}{2T_T} + \frac{R\gamma MuE}{2\rho c\left(E-\frac{u^2}{2}\right)\left(1+\frac{\gamma-1}{2}M^2\right)} - \frac{Ru^2}{2\rho\left(E-\frac{1}{2}u^2\right)}\right)\partial\rho$$

$$+\left(\frac{EM\gamma(\gamma-1)}{cT_T} - \frac{\gamma u}{T_T}\left(1+\frac{\gamma-1}{2}M^2\right) - \frac{R\gamma ME}{\rho c\left(E-\frac{u^2}{2}\right)\left(1+\frac{\gamma-1}{2}M^2\right)} + \frac{Ru}{\rho\left(E-\frac{1}{2}u^2\right)}\right)\partial(\rho u)$$

$$+\left(\frac{\gamma}{T_T}\left(1+\frac{\gamma-1}{2}M^2\right) - \frac{M^2\gamma(\gamma-1)}{2T_T} - \frac{R}{\rho\left(E-\frac{1}{2}u^2\right)} + \frac{R\gamma Mu}{2\rho c\left(E-\frac{u^2}{2}\right)\left(1+\frac{\gamma-1}{2}M^2\right)}\right)\partial(\rho E)\,.$$

In this section, useful expressions for several input and/or output variables with respect to the chosen state variables were developed. In the following section of this chapter, a specific practical inlet system will be analyzed using the theory presented in Chapter 4 and the results of this section.

Reproduced with permission of the copyright owner. Further reproduction prohibited without permission.

5.5 An Illustrative Example

In Chapter 4, many practical and theoretical problems were set up and solved. The sought solution for a particular configuration was the resulting transfer function matrix in the complex frequency-space domain.

In this section, a specific inlet system will be analyzed using the theory presented so far in this dissertation. The flow system under study is made up of two channels. In the first channel, the flow is supersonic while in the second channel the flow is subsonic. The two channels are related internally through the Cole-Willoh conditions while at the downstream end of the inlet system appropriate terminating conditions are applied. Finally, a three-wave model assumption is made for the flow. The objective is to determine the transfer function matrix relating the applied inputs to the flow vector at some downstream distance x from the throat of the inlet. A block diagram of the resulting system is shown in the figure below.

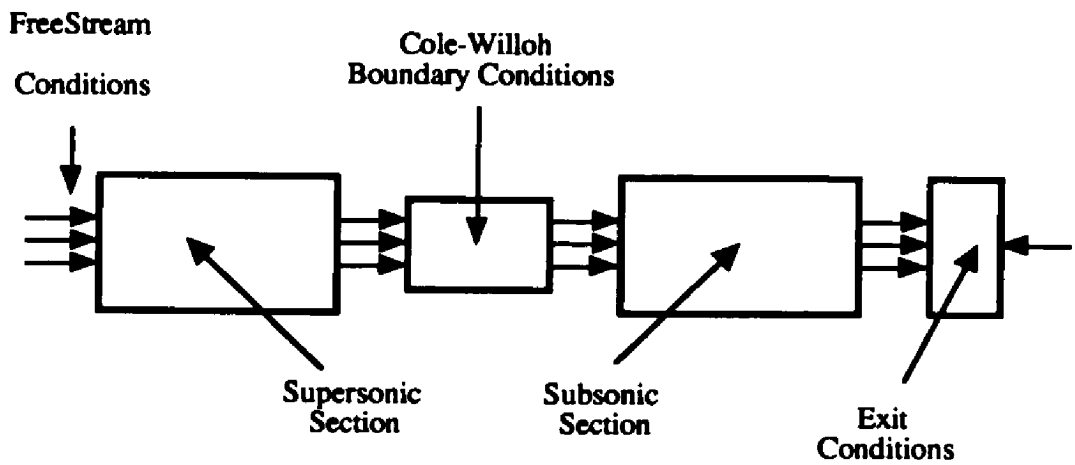


Figure 5.6 An inlet system

Reproduced with permission of the copyright owner. Further reproduction prohibited without permission.

Since, the flow in the first channel is supersonic, all information will travel downstream, and thus the flow in this channel will depend solely on the inputs applied at the inflow boundary of Channel 1.

On the other hand, in the subsonic section of the system, information will flow in both directions. The Cole-Willoh conditions are put in between the supersonic and subsonic sections of the flow system and in a sense act as a regulator of the flow of information between the two channels. Finally, at the downstream end of the system, a reflective boundary is assumed with an additional downstream pressure input. First, recall that the Cole-Willoh boundary conditions are written in the Laplace domain as follows,

$$\begin{bmatrix} \frac{\partial P_T(s)}{P_T} \\ \frac{\partial \dot{W}(s)}{\dot{W}} \\ \frac{\partial S(s)}{R} \end{bmatrix}_2 = \begin{bmatrix} C_4 & \frac{C_1}{C_r} & \frac{C_1}{7} \\ 0 & 1 & 0 \\ \frac{6}{7}C_1 & -\frac{C_1}{C_r} & C_5 \end{bmatrix} \begin{bmatrix} \frac{\partial P_T(s)}{P_T} \\ \frac{\partial \dot{W}(s)}{\dot{W}} \\ \frac{\partial S(s)}{R} \end{bmatrix}_1 + \begin{bmatrix} -C_1\left(R_c \frac{A'}{A} + C_2 s\right) \\ C_B + C_r C_3 s \\ C_1\left(R_c \frac{A'}{A} - C_3 s\right) \end{bmatrix} X_s.$$

where, subscript 1 denotes the station at the outflow boundary of the supersonic channel and subscript 2 refers to the station just aft of the normal shock, i.e., at the inflow boundary of the subsonic channel. For consistency, it is necessary to rewrite the above set of boundary conditions in terms of the state vector used in Chapter 4, namely, $[\rho, \rho u, \rho E]^T$. For a constant-cross-sectional-area channel, the airflow rate is, $\dot{W} = \tilde{A}\rho u$ and thus differentiating and linearizing yields,

Reproduced with permission of the copyright owner. Further reproduction prohibited without permission.

$$\ln\dot{W} = \ln(\rho u) + \ln(\tilde{A})$$

$$\frac{\partial\dot{W}(s)}{\dot{W}} = \frac{1}{\rho u}\partial(\rho u) = \begin{bmatrix} 0 & \frac{1}{\rho u} & 0 \end{bmatrix}\begin{bmatrix} \partial(\rho) \\ \partial(\rho u) \\ \partial(\rho E) \end{bmatrix}.$$

Furthermore,

$$\mu = \begin{bmatrix} \frac{\partial P_T(s)}{P_T} \\ \frac{\partial\dot{W}(s)}{\dot{W}} \\ \frac{\partial S(s)}{R} \end{bmatrix} = \begin{bmatrix} \Theta_{11} & \Theta_{12} & \Theta_{13} \\ \Theta_{21} & \Theta_{22} & \Theta_{23} \\ \Theta_{31} & \Theta_{32} & \Theta_{33} \end{bmatrix}\begin{bmatrix} \partial(\rho) \\ \partial(\rho u) \\ \partial(\rho E) \end{bmatrix} = \Theta\,\sigma$$

or, $\mu=\Theta\sigma$, where,

$$\mu = \begin{bmatrix} \frac{\partial P_T(s)}{P_T} \\ \frac{\partial\dot{W}(s)}{\dot{W}} \\ \frac{\partial S(s)}{R} \end{bmatrix}, \Theta = \begin{bmatrix} \Theta_{11} & \Theta_{12} & \Theta_{13} \\ \Theta_{21} & \Theta_{22} & \Theta_{23} \\ \Theta_{31} & \Theta_{32} & \Theta_{33} \end{bmatrix}, \sigma = \begin{bmatrix} \partial(\rho) \\ \partial(\rho u) \\ \partial(\rho E) \end{bmatrix}.$$

From the previous section, the elements of Θ are as follows:

$$\Theta_{11} = -\frac{\gamma M u E}{2\rho c\left(E - \frac{u^2}{2}\right)\left(1 + \frac{\gamma-1}{2}M^2\right)} + \frac{u^2}{2\rho\left(E - \frac{1}{2}u^2\right)},$$

$$\Theta_{12} = \frac{\gamma M E}{\rho c\left(E - \frac{u^2}{2}\right)\left(1 + \frac{\gamma-1}{2}M^2\right)} - \frac{u}{\rho\left(E - \frac{1}{2}u^2\right)},$$

Reproduced with permission of the copyright owner. Further reproduction prohibited without permission.

$$\Theta_{13} = \frac{1}{\rho\left(E-\frac{1}{2}u^2\right)} - \frac{\gamma M u}{2\rho c\left(E-\frac{u^2}{2}\right)\left(1+\frac{\gamma-1}{2}M^2\right)},$$

$$\Theta_{21} = 0,$$

$$\Theta_{22} = \frac{1}{\rho u},$$

$$\Theta_{23} = 0,$$

$$\Theta_{31} = \frac{\gamma u^2}{2T_T}\left(1+\frac{\gamma-1}{2}M^2\right) - \frac{M^2 E\gamma(\gamma-1)}{2T_T} + \frac{R\gamma M^2 E}{2\rho\left(E-\frac{u^2}{2}\right)\left(1+\frac{\gamma-1}{2}M^2\right)} - \frac{Ru^2}{2\rho\left(E-\frac{1}{2}u^2\right)},$$

$$\Theta_{32} = \frac{EM\gamma(\gamma-1)}{cT_T} - \frac{\gamma u}{T_T}\left(1+\frac{\gamma-1}{2}M^2\right) - \frac{R\gamma ME}{\rho c\left(E-\frac{u^2}{2}\right)\left(1+\frac{\gamma-1}{2}M^2\right)} + \frac{Ru}{\rho\left(E-\frac{1}{2}u^2\right)},$$

and,

$$\Theta_{33} = \frac{\gamma}{T_T}\left(1+\frac{\gamma-1}{2}M^2\right) - \frac{M^2\gamma(\gamma-1)}{2T_T} - \frac{R}{\rho\left(E-\frac{1}{2}u^2\right)} + \frac{R\gamma M^2}{2\rho\left(E-\frac{u^2}{2}\right)\left(1+\frac{\gamma-1}{2}M^2\right)}.$$

Also, in general,

$$\sigma = \Theta^{-1}\mu,$$

and

$$\mu_2 = \Phi\,\mu_1 + \Gamma\,X_s$$

$$\Rightarrow\ \sigma_2 = \Theta_R^{-1}\,\Phi\,\Theta_L\,\sigma_1 + \Theta_R^{-1}\Gamma\ X_s \equiv \varphi\,\sigma_1 + \hat{\Gamma}\,X_s,$$

where, Θ_L and Θ_R are the transformation matrices to the left and the right

Reproduced with permission of the copyright owner. Further reproduction prohibited without permission.

of the shock respectively,

$$\Phi = \begin{bmatrix} C_4 & \frac{C_1}{C_r} & \frac{C_1}{7} \\ 0 & 1 & 0 \\ \frac{6}{7}C_1 & -\frac{C_1}{C_r} & C_5 \end{bmatrix}, \qquad \Gamma = \begin{bmatrix} -C_1\left(R_c \frac{A'}{A} + C_2\, s\right) \\ C_B + C_r C_3\, s \\ C_1\left(R_c \frac{A'}{A} - C_3\, s\right) \end{bmatrix},$$

and,

$$\varphi \equiv \Theta_R^{-1}\, \Phi\, \Theta_L = \begin{bmatrix} \varphi_{11} & \varphi_{12} & \varphi_{13} \\ \varphi_{21} & \varphi_{22} & \varphi_{23} \\ \varphi_{31} & \varphi_{32} & \varphi_{33} \end{bmatrix}, \qquad \hat{\Gamma} = \Theta_R^{-1}\, \Gamma = \begin{bmatrix} \hat{\Gamma}_1 \\ \hat{\Gamma}_2 \\ \hat{\Gamma}_3 \end{bmatrix}.$$

If the three components of the flow vector at the downstream end of the supersonic channel are designated as $Q_1(s,L_1)$, $Q_2(s,L_1)$, and $Q_3(s,L_1)$, with L_1 being the length of Channel 1, and the flow vector in the subsonic channel has components $q_1(s,x)$, $q_2(s,x)$, and $q_3(s,x)$, where x is measured from the exit boundary of Channel 1, then

$$[\sigma]_1 = Q_{L_1} = \begin{bmatrix} Q_1(s,L_1) \\ Q_2(s,L_1) \\ Q_3(s,L_1) \end{bmatrix}, \qquad [\sigma]_2 = q_0 = \begin{bmatrix} q_1(s,0) \\ q_2(s,0) \\ q_3(s,0) \end{bmatrix}.$$

Also, at the exit of the system the following condition holds:

$$q_3(s,L) = w_P \frac{\partial P_T}{P_{T_E}} + w_\rho\, q_1(s,L) + w_{\rho u}\, q_2(s,L),$$

where the weights w_P, w_ρ, and $w_{\rho u}$, computed in the previous section and repeated here, are

Reproduced with permission of the copyright owner. Further reproduction prohibited without permission.

$$w_P = \frac{1}{\frac{1}{\rho\left(E-\frac{1}{2}u^2\right)} - \frac{\gamma M^2}{2\rho\left(E-\frac{u^2}{2}\right)\left(1+\frac{\gamma-1}{2}M^2\right)}},$$

$$w_\rho = \frac{\frac{\gamma M^2 E}{2\rho\left(E-\frac{u^2}{2}\right)\left(1+\frac{\gamma-1}{2}M^2\right)} - \frac{u^2}{2\rho\left(E-\frac{1}{2}u^2\right)}}{\frac{1}{\rho\left(E-\frac{1}{2}u^2\right)} - \frac{\gamma M^2}{2\rho\left(E-\frac{u^2}{2}\right)\left(1+\frac{\gamma-1}{2}M^2\right)}},$$

and

$$w_{\rho u} = \frac{\frac{u}{\rho\left(E-\frac{1}{2}u^2\right)} - \frac{\gamma M^2 E}{\rho u\left(E-\frac{u^2}{2}\right)\left(1+\frac{\gamma-1}{2}M^2\right)}}{\frac{1}{\rho\left(E-\frac{1}{2}u^2\right)} - \frac{\gamma M^2}{2\rho\left(E-\frac{u^2}{2}\right)\left(1+\frac{\gamma-1}{2}M^2\right)}}.$$

Using matrix notation the exit condition becomes

$$\begin{bmatrix} -w_\rho & -w_{\rho u} & 1 \end{bmatrix} \begin{bmatrix} q_1(s,L) \\ q_2(s,L) \\ q_3(s,L) \end{bmatrix} = w_p \frac{\partial P_T}{P_{T_E}}.$$

This expression can be rewritten compactly as follows:

$$F^T q_L = F^T q_E = w_p \frac{\partial P_T}{P_{T_E}} = w_p \, \delta D_{IN}$$

where, subscript E denotes exit conditions,

Reproduced with permission of the copyright owner. Further reproduction prohibited without permission.

$$F^T = \begin{bmatrix} -w_\rho & -w_{\rho u} & 1 \end{bmatrix}, \quad q_L = \begin{bmatrix} q_1(s,L) \\ q_2(s,L) \\ q_3(s,L) \end{bmatrix},$$

and δD_{IN} is a downstream perturbation input of total pressure. Since,

$$q_E = q(s,L) = H(s,L)\, q(s,0) = H_L\, q_0,$$

and

$$\sigma_2 = q_0 = \varphi\, \sigma_1 + \hat{\Gamma}\, X_s = \varphi\, Q_{L_1} + \hat{\Gamma}\, X_s$$

then the exit condition becomes:

$$F^T q_E = F^T H_L\, q_0 = w_P\, \delta D_{IN}$$

$$\Rightarrow F^T H_L\left(\varphi Q_{L_1} + \hat{\Gamma}\, X_s\right) = w_P\, \delta D_{IN} \Rightarrow F^T H_L \hat{\Gamma}\, X_s = -\, F^T H_L \varphi Q_{L_1} + w_P\, \delta D_{IN}$$

$$\Rightarrow F^T H_L \varphi Q_{L_1} + F^T H_L \hat{\Gamma}\, X_s = w_P\, \delta D_{IN} \Rightarrow F^T H_L \hat{\Gamma}\, X_s = -F^T H_L \varphi Q_{L_1} + w_P\, \delta D_{IN}$$

$$\Rightarrow X_s = -\left(F^T H_L \hat{\Gamma}\right)^{-1} F^T H_L \varphi\, Q_{L_1} + \left(F^T H_L \hat{\Gamma}\right)^{-1} w_P\, \delta D_{IN}$$

$$\Rightarrow X_s = -\frac{F^T H_L \varphi}{F^T H_L \hat{\Gamma}}\, Q_{L_1} + \frac{w_P}{F^T H_L \hat{\Gamma}}\, \delta D_{IN}\,.$$

This last equation is very important as it expresses the shock position as a function of a downstream perturbation of total pressure, δD_{IN}, and the exit flow of Channel 1, Q_{L_1}. Since,

$$Q_{L_1} = Q(s,L_1) = H(s,L_1)\, Q(s,0) = H_{L_1}\, Q_0$$

then, the shock position in terms of upstream (δU_{IN}) and downstream

Reproduced with permission of the copyright owner. Further reproduction prohibited without permission.

(δD_{IN}) perturbation inputs of total pressure is given by the following formula:

$$X_s = -\frac{F^T H_L \varphi}{F^T H_L \hat{\Gamma}} H_{L_1} \Theta_L^{-1} \begin{bmatrix} 1 \\ 0 \\ 0 \end{bmatrix} \delta U_{IN} + \frac{w_P}{F^T H_L \hat{\Gamma}} \delta D_{IN}.$$

Finally, for a general upstream perturbation, the above equation becomes

$$X_s = -\frac{F^T H_L \varphi}{F^T H_L \hat{\Gamma}} H_{L_1} \Theta_L^{-1} \Delta U_{IN} + \frac{w_P}{F^T H_L \hat{\Gamma}} \delta D_{IN},$$

where, ΔU_{IN} is the following input vector:

$$\Delta U_{IN} = \begin{bmatrix} \Delta(\text{Pressure}) \\ \Delta(\text{Flow rate}) \\ \Delta(\text{Entropy}) \end{bmatrix}.$$

Also, if the exit boundary conditions are given in terms of the Cole-Willoh variables, then the shock position is given by:

$$X_s = -\frac{F^T \Theta_R H_L \varphi}{F^T \Theta_R H_L \hat{\Gamma}} H_{L_1} \Theta_L^{-1} \Delta U_{IN} + \frac{w_P}{F^T \Theta_R H_L \hat{\Gamma}} \delta D_{IN}.$$

In this example, the methodology of incorporating the Cole-Willoh boundary conditions in a cascaded system, representative of a typical inlet, was presented. The Cole-Willoh conditions that describe the normal shock dynamics in the inlet system were interfaced between the downstream end of the supersonic section and the upstream end of the subsonic section. Additional constraint equations were also imposed at the downstream end of the subsonic section of the system to represent appropriate exit

Reproduced with permission of the copyright owner. Further reproduction prohibited without permission.

conditions. The resulting problem was solved and the general solution was expressed as a transfer function in the complex frequency domain. Finally, to draw an analogy, it is mentioned that the Cole-Willoh conditions in a sense slow down the flow and act as a step down "matching" transformer, thereby matching the outflow of the supersonic channel to the inflow of the subsonic channel.

5.6 Simulations

There are many flow scenarios that could be duplicated artificially using computer simulation. Several programs are written to simulate some of the key models that were studied in the previous sections. The complete program listings can be found at Appendix C. At the outset, it should be mentioned that the developed models are very flexible and can be readily reconfigured or interconnected to match various flow situations.

By studying the theory of Chapter 4 and the aforementioned programs, the interested reader can get a good insight about a particular flow scenario. Thus, experimentation is highly recommended.

The programs are basically separated in two major categories, namely those that cover two-wave models and those that simulate three-wave systems. They correspond to the following important problems of Chapter 4: a) The Bounded Problem, b) the Two-Channel with internal Input Bounded Problem, and c) The Green's Function Problem. Some additional programs are also included for the inlet problem of the

Reproduced with permission of the copyright owner. Further reproduction prohibited without permission.

preceding section. The given programs are capable of producing Bode Magnitude and Phase plots, 3-D Log-Magnitude plots and contour plots of 3-D meshplots. The 3-D Log-Magnitude plots can be thought of as originally flat rubber sheets that have been stretched by the poles pushing up and the zeros pushing down at the critical frequencies. In contrast, in a plain 3-D Magnitude plot the imaginary flat rubber sheet has been pushed up at the pole locations and fastened down at each zero. On the other hand, the contour plots of the 3-D Log-Magnitude plots are useful in locating the pole locations of a flow system in the s-plane thus determining the system stability. By looking at the contour magnitude plots, one can identify the location of a pole or zero of a flow system at the center of concentric simply connected closed curves. In stable systems no poles can occur in the right of the $j\omega$-axis.

Steady-state data for the NASA Lewis Mach 2.5 40-60 inlet can be found at Appendix B. The information presented there is an expanded version of what can be found in [CHI90]. The data provided is very useful to the control engineer in obtaining small perturbation models of flow systems, for simulation purposes, using the techniques of Chapter 4. The tabulated values are simply the linearization points at a downstream distance x of the flow channel. From the given quantities, average values for a supersonic or subsonic section of the inlet system can be computed. These values can be used to determine time delays involved as well as define suitable upstream and downstream inflow and outflow boundary

Reproduced with permission of the copyright owner. Further reproduction prohibited without permission.

conditions in small perturbation models of "air-in-a-pipe" type flow systems.

All responses corresponding to a given program along with a list of the conditions used are grouped together and presented in Appendix D. In the responses, the normalization approach of [CW75] was followed. For practical considerations, in a given model only a limited number of outputs for a limited number of inputs is presented at Appendix D. The interested reader will be able to generate additional outputs for any choice of inputs with the aid of the theory presented in this chapter and the mathematical relations among the various thermodynamic properties given in an earlier chapter. The responses computed were validated using the frequency responses found in the NASP report of [HMB89] and shown in Figures 5.7 and 5.8 below. These responses correspond to changes of shock position due to downstream pressure perturbations. As a general rule frequency responses of "air-in-a-pipe" models start out flat, then resonate and roll-off then resonate some more and roll-off again and so on [HAR94]. Also, for stability, the phases should roll off to $-\infty$ as frequency is increased.

A case by case discussion of the frequency responses of Appendix D follows. Some intuitive guessing was done to determine system parameters not completely specified in available literature sources at this time. The dynamic performance of the models studied will be analyzed qualitatively.

Case A-1 covers the two-wave bounded problem. For convenience, a separate set of responses is repeated in Figures 5.9 and 5.10. This was done in order to emphasize the importance of the reflection parameter R.

Reproduced with permission of the copyright owner. Further reproduction prohibited without permission.

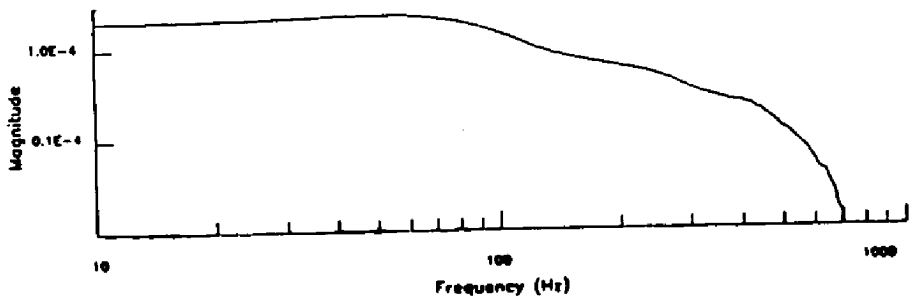


Fig. 5.7 Normalized magnitude response of shock position due to downstream pressure perturbations (NASP Report)

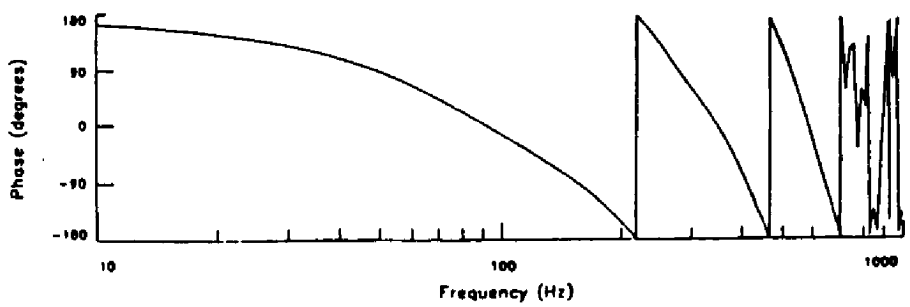


Fig. 5.8 Normalized phase response of shock position due to downstream pressure perturbations (NASP Report)

Reproduced with permission of the copyright owner. Further reproduction prohibited without permission.

A slight change in R can cause a drastic improvement in the response of the shock position. Furthermore, different models may be fine-tuned by appropriately choosing the shock transfer function $Z_{us}(s)$. Thus, one can see that the frequency-based models developed in this study offer a lot of flexibility, which is a very desirable attribute of any model since important structural properties of a system may be analysed systematically. In order to speed up the fine-tuning process of the derived models some heuristics on choosing the inflow and outflow parameters of a model are given in Section 5.7 below. These guidelines apply to all models covered in this dissertation.

Next, returning to the shock position response of Case A-1, one can see that this follows closely the resonate and roll off pattern described above, although it should be noted that for the set of conditions chosen the first resonance occurs at a higher frequency than that of the NASP report. Again, this problem can be corrected by appropriately choosing R and $Z_{us}(s)$. In the case of Figures 5.9 and 5.10, R had to be reduced to 1e-6. The unwrapped phase in both responses were in very good agreement and by examining the meshplots and contour plots of Case A-2 it is clearly that for the chosen set of parameters the open loop system is stable. The contour plots showed that all pole locations were on the left-half s-plane while for the complex frequency range selected, no zeros existed.

Cases B-1 yielded results comparable to Case A-1 and the NASP report. The parameters to be chosen were the two upstream shock transfer functions $Z_1(s)$ and $Z_2(s)$ as well as downstream boundary parameters.

Reproduced with permission of the copyright owner. Further reproduction prohibited without permission.

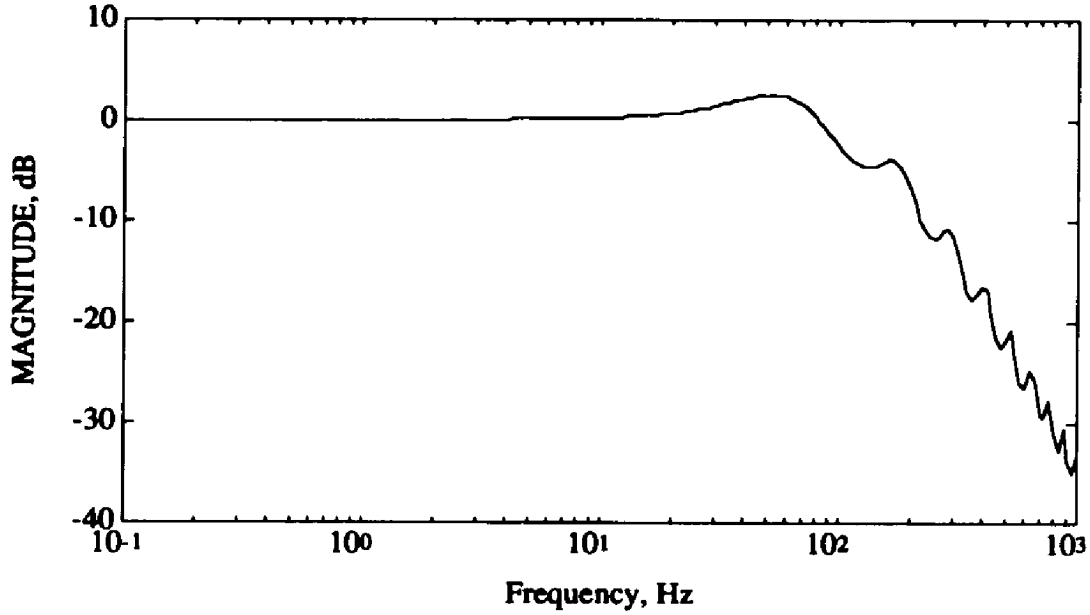


Fig. 5.9 Normalized magnitude response of X_S (CASE A)

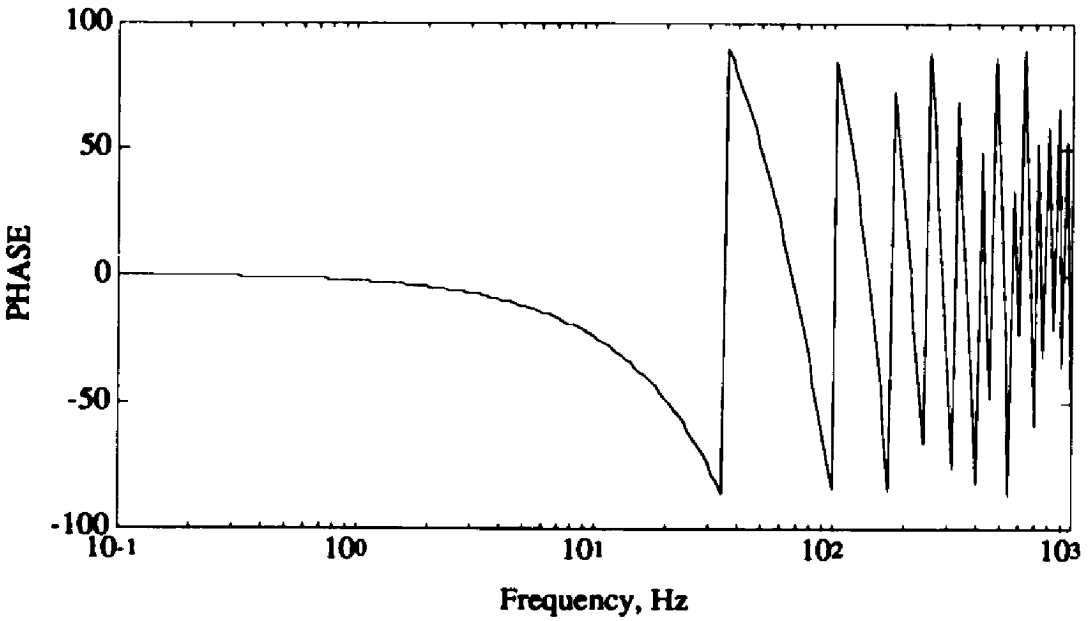


Fig. 5.10 Normalized phase response of X_S (CASE A)

Reproduced with permission of the copyright owner. Further reproduction prohibited without permission.

Case C covered the Two-Channel with Internal Input Problem and Case D the Green's Function Problem. These cases could not be validated directly from experimental data but their respective responses were checked against each other. Namely, the conditions applied to Case D-1 were applied to Case C-1 and the resulting responses are shown in Figures 5.11 and 5.12 below. Cases C and D yielding identical responses for the same conditions validated models obtained from both approaches.

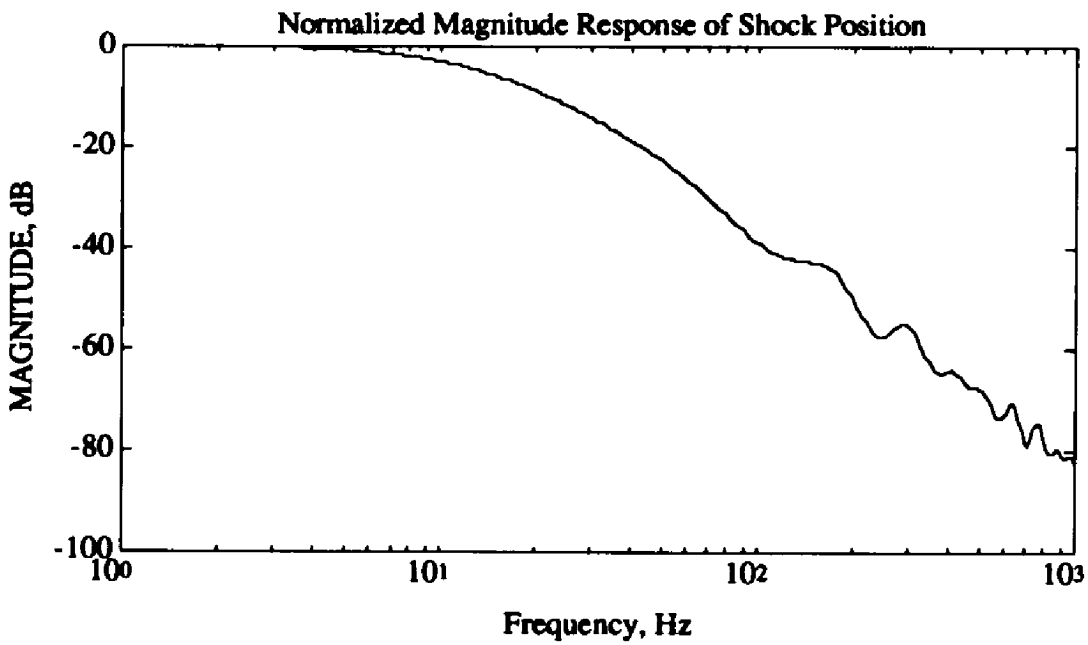


Fig. 5.11 Normalized magnitude response of shock position due to downstream pressure perturbations (Cases C and D)

Reproduced with permission of the copyright owner. Further reproduction prohibited without permission.

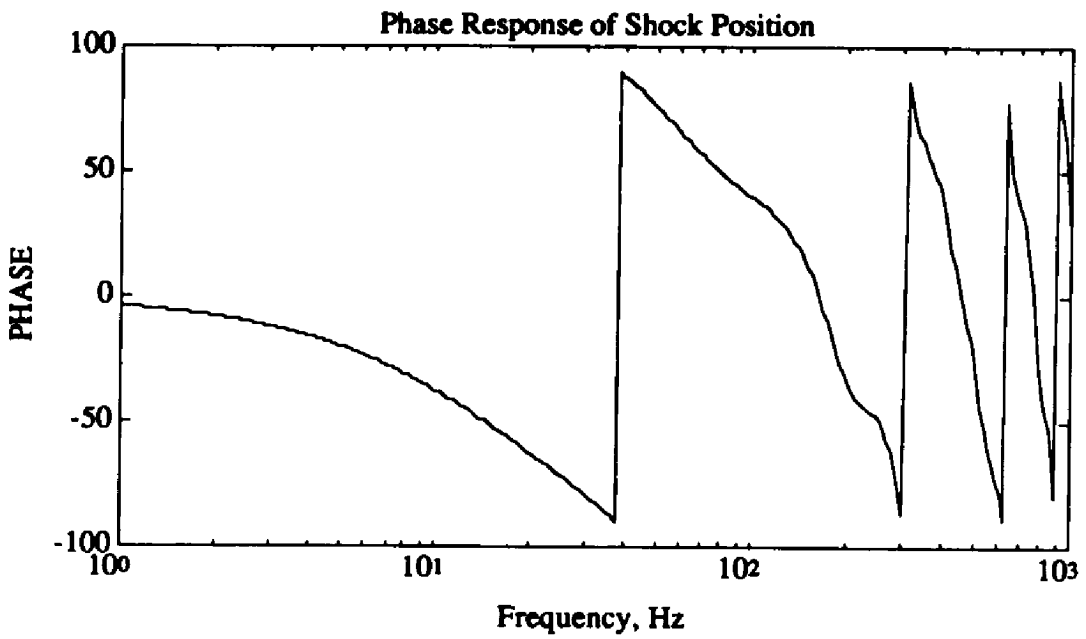


Fig. 5.12 Normalized phase response of shock position due to downstream pressure perturbations (Cases C and D)

Finally, Case E has the best assumptions about the real inlet and some useful data was obtained from [CW75] which expedited the simulation process. The resulting models are repeated in Figures 5.13 and 5.14 and one can see that they are in excellent agreement with what was expected. This result epitomizes the research performed and validates the inlet models derived using the new approaches proposed in this study.

Reproduced with permission of the copyright owner. Further reproduction prohibited without permission.

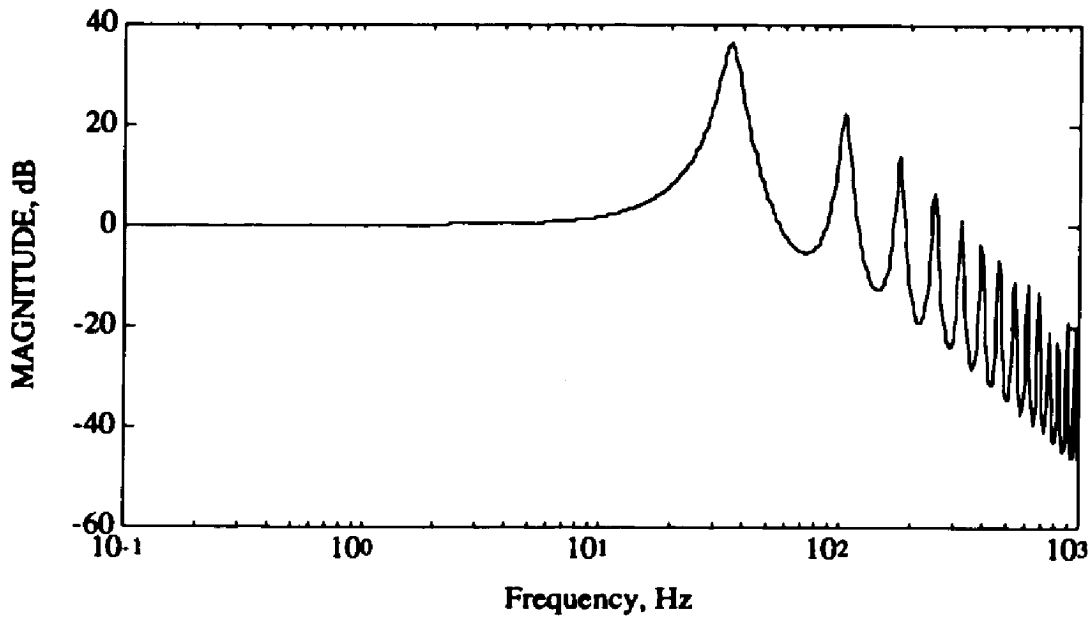


Fig. 5.13 Normalized magnitude response of X_S (Case E)

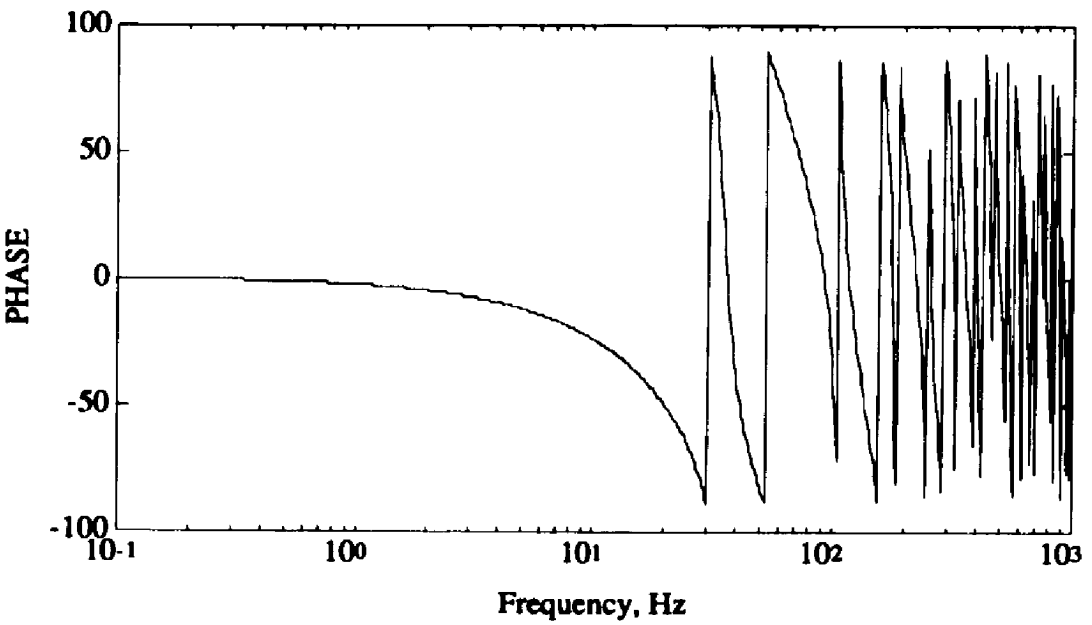


Fig. 5.14 Normalized phase response of X_S (Case E)

Reproduced with permission of the copyright owner. Further reproduction prohibited without permission.

5.7 Qualitative Guidelines for Choosing Model Parameters

In order to aid the reader in resolving some of the difficulties that might be encountered during the simulation process, the following set of guidelines was established:

1) Choose the reflection parameters at the output boundaries carefully. Their algebraic sign as well as magnitude must be selected such that the system loop-gain is not relatively large thereby causing a model to become unstable. Usually, in a system with time delays closed-loop stability is increased by decreasing the loop-gain. Also, when a model is scaled so must be the reflection parameters in order to maintain overall system stability.

3) The frequency range selected must be such that all important dynamics about a system under study are captured. This is especially true when 3-D Magnitude plots are generated. Sometimes poles or zeros can "hide" behind a three-dimensional plot. Thus, meshplots should always be accompanied by their respective contour plots and a sufficient number of contour levels should be chosen.

4) In many cases, the significance of a model parameter Π can be studied by producing three-dimensional magnitude plots of the given system configuration in the $j\omega$-Π plain.

5) When certain knowledge about a system is known, it should be incorporated into its respective model.

Reproduced with permission of the copyright owner. Further reproduction prohibited without permission.

6) In reviewing the literature, it was noted that many sets of notation were used to represent similar flow properties. When two different systems must be lumped together, care must be exercised to ensure that the added system does not act as a load to the original system and vice-versa. Also, all necessary transformations must be made in the describing partial differential equations as well as the applied boundary conditions in order to ensure that both systems are expressed in the same set of state variables.

7) Results obtained from a given simulation are good only in the context of a specific flow scenario and, in general, should not be generalized.

5.8 Concluding Remarks

This chapter provided the reader with some supplementary pieces of information that would be needed to apply the theory developed in Chapter 4 to any practical flow scenario.

A specific inlet configuration was analyzed, which was made up of a supersonic channel, a subsonic channel and the associated internal and external set of boundary conditions. The internal input was part of what could be a separate system represented by the Cole-Willoh shock equations. Thus, the problem solved was a modification of the Two-Channel with Internal Input Bounded problem. Simulations results for this and other benchmark problems were compared to previously published results for model validation purposes. The simulations proved that the resulting

Reproduced with permission of the copyright owner. Further reproduction prohibited without permission.

models are versatile, readily adaptable to different upstream and downstream boundary conditions and very insightful. The derived models retain the important structural properties of a given system and are useful for control system studies.

The following chapter summarizes the contributions of this dissertation and presents some ideas for additional research in this area.

Reproduced with permission of the copyright owner. Further reproduction prohibited without permission.

CHAPTER VI

SUMMARY AND FUTURE RESEARCH

6.1 Summary

This dissertation dealt with modeling of flow propulsion systems. The main objective of the research was to develop exact analytical solutions of linearized versions of partial differential equation systems describing internal flows using Laplace-transform methods. In contrast to models developed using CFD techniques, the models obtained in this dissertation are frequency-based and thus offer the control engineer essential intuition about the structural properties of a flow system.

Application of Laplace-transform theory yielded transfer function models that are in closed-form. As such, these solutions offer quick insight about a system. The resulting models retain the important dynamical characteristics of a system and can be very useful for control system analysis and design using root locus, frequency domain and robust control techniques.

The dissertation was organized as follows: First, the flow modeling problem was introduced in Chapter 1 and relevant background information was presented in Chapter 2. Next, a review of existing inlet modeling

Reproduced with permission of the copyright owner. Further reproduction prohibited without permission.

techniques was presented in Chapter 3. Following that, a description of the analytical and software tools used was given in Chapter 4. In Chapter 4, systematic solutions of several original practical and theoretical problems posed were presented using the newly developed technique. The remainder of this section enlists the main contributions of this research effort while the next and final section presents some ideas for future work in the subject.

First of all, in antithesis to previous approaches taken in the past, in this research, time delays--so often encountered in flow problems--are not replaced by their Padé approximants. Instead, the describing partial differential equations are solved analytically in the complex frequency-space domain. This approach fits in the hierarchy in the meromorphic transfer function modeling approach alluded to in Chapter 3 and provides exact solutions to approximate [i.e., linearized] flow problems. Philosophically speaking obtaining an exact solution of an approximate problem is, in general, far more accurate than obtaining an approximate solution of an approximate problem. Furthermore, the resulting models being transfer functions in the frequency-space domain facilitate control system analysis and design using known frequency domain techniques. The new technique enables the control engineer to examine the dynamical aspects of flow instead of just look at static flow problems. Finally, if desired, time responses can be readily obtained using numerical inverse Laplace transform techniques.

Reproduced with permission of the copyright owner. Further reproduction prohibited without permission.

Another significant contribution of this work was the development of a new approach for modeling compressible flow inside an inlet using Green's functions. The Green's function model is useful in simulating flows with internally applied inputs. An example is an inlet system containing an internal disturbance generator, which may be used to regulate the pressure and thus the shock position. As expected the solutions obtained using the Green's function approach were exactly the same as those obtained by solving the Two-Channel with internal input bounded problem with both flow channels made identical.

In this dissertation, the two-wave flow in a channel with an exponentially varying cross-sectional area was studied. This is a nice extension of the Free-space problem. It is made possible thanks to the special structure of the transfer function matrix of the Free-space problem and the properies of the hyperbolic functions. Again, in this problem, if the cross-sectional area is assumed constant the results obtained match those of the Free-Space problem.

In Chapter 5 an extension of the Cole-Willoh approach was presented. The Cole-Willoh conditions were incorporated into a Two-channel with internal input three-wave bounded problem. The shock position output of the system was expressed not only as a function of the perturbations of upstream variables but also of any downstream variables as well! Resulting models were then validated using available data for the NASA Lewis Mach 2.5 40-60 inlet.

Reproduced with permission of the copyright owner. Further reproduction prohibited without permission.

This chapter is followed by a list of references used throught this dissertation and also four appendices. The first one contains a glossary of terms, the second one actual data for the NASA Lewis Mach 2.5 40-60 inlet, the third all software code used to implement the models of Chapters 4 and 5, and the last one frequency responses corresponding to key problems of Chapters 4 and 5.

6.2 Directions for Future Research

When one delves into the vast world of gas dynamics it is unlikely that he or she may find all answers to all problems. In fact, she or he will soon discover that it is impossible to ever run out of problems to solve.

Working in this fascinating field for some time now this author cannot help but recall the words of Hippocrates, *"Life is short, the craft is so long."* So many are the potential applications and/or extensions of this work that in this author's opinions many fruitful years of research may be dedicated in further researching this fascinating subject. Many problems lead naturally to others. For example, two-channel solutions can be repeated for three- or more-channel systems.

Alternatively, solutions in several different sets of state variables may be obtained using system coordinate transformations. Also, many flow problems may be re-defined as initial valued problems [HAR92]. For that matter, the responses of systems to various initial conditions can be studied.

Reproduced with permission of the copyright owner. Further reproduction prohibited without permission.

Using the proposed methodology various types of combinational flows may be studied. These might include inlet/engine combinations, branching flows, choked flows, and flows in channels of varying cross-sectional areas. Furthermore, responses to specific compressor or combustor input/output signals and/or perturbations in the free stream atmosphere may be studied and other shock models can be tried out for a given flow configuration.

A new set of combination flow models may be developed using Cole-Willoh type conditions at the interior boundaries of multiple-channel models.

In another front, the theory presented herein could be extended to cover flows with multiple species. Many real flows contain several species of fluids each one being considered independent of the others. This approach would require solutions to N-dimensional systems of partial differential equations.

Ultimately, static flow problems can be re-examined as special cases of the non-static problems solved in this dissertation. More insight to existing solutions may thus be obtained

Electrical analogues of the presented problems may be developed. This will be not only an extension of this work but also of previous work done by Rohman and Grogan in [RG57]. Further testing and experimentation in this area is expected to yield interesting results.

Reproduced with permission of the copyright owner. Further reproduction prohibited without permission.

In this dissertation a ground-up approach was taken in developing the flow models. Knowing what we now know from this research, it would be interesting to take a top-down approach in the modeling problem. Namely, develop the most general model first, then study each subproblem simply as a special case of the general model. For example, two-wave systems would be special cases of N-wave systems and models for systems with constant cross-sectional areas would be special cases of models of systems of varying cross-sectional area channels. For increased efficiency, this approach should be totally computer-based.

In yet another front, the stability of interconnected blocks of distributed-parameter systems can be studied. Starting with series or parallel combinations of systems, more complicated configurations could be analyzed and rules be drawn guarantying total system stability.

Finally, an expert fuzzy system for the flow modeling problem can be developed using the theory presented in this dissertation and accumulated experience of test engineers working with inlet models. Such a system should have an excellent knowledge base and an appropriately-chosen set of linguistic variables and fuzzy sets in order to operate efficiently. It could help in the development of fine practical inlet models.

Reproduced with permission of the copyright owner. Further reproduction prohibited without permission.

REFERENCES

[ABU92] Naser Abu Khamseh, *An Improved Expert System for Reduced Order Modeling*, Masters Thesis, Electrical Engineering Department, University of Akron, May 1992.

[AME65] W. F. Ames, *Nonlinear Partial Differential Equations in Engineering*, Academic Press, New York, NY, 1965.

[AME69] W. F. Ames, *Numerical Methods for Partial Differential Equations*, Barnes and Noble, Inc., New York, NY, 1969.

[AND82] J. D. Anderson, Jr., *Modern Compressible Flow, with Historical Perspective*, McGraw-Hill, New York, 1982.

[AOK68] M. Aoki, "Control of large scale systems by aggregation," in *IEEE Transactions on Automatic Control*, Vol. AC-13, No. 3, pp. 246-253, 1968.

[ATP84] D. A. Anderson, J. C. Tannehill, and R. H. Pletcher, *Computational Fluid Mechanics and Heat Transfer*, Hemishpere, New York, 1984.

[BAR73] F. B. Barry, *Frequency of Supersonic Inlet Unstarts Due to Atmospheric Turbulence*, of Hamilton Standard, HSER-5838 & NAS2-4515, October 1973.

[BK79] H. T. Banks and F. Kappel, "Spline approximations for functional differential equations," in *Journal of Differential Equations*, Vol. 34, pp. 496-522, 1979.

[BUT69] A. G. Butkovskiy, *Distibuted Control Systems*, American Elsevier Publishing Company, New York, 1969.

Reproduced with permission of the copyright owner. Further reproduction prohibited without permission.

[BUT82] A. G. Butkovskiy, *Green's Functions and Transfer Function Handbook*, Ellis Horwood Ltd., Chichester, England, 1982.

[BUT83] A. G. Butkovskiy, *Structural Theory of Distributed Systems*, Ellis Horwood Ltd., Chichester, England, 1983.

[CG85] R. F. Curtain and K. Glover, "Balanced realizations of infinite dimensional systems," in *Proceedings of the Workshop on Operator Theory and its Applications*, Amsterdam, 1985.

[CH90] Amy Chicatelli and Tom T. Hartley, "Methods for developing linear reduced models for internal flow propulsion systems," submitted to *AIAA Journal of Propulsion and Power*, 1990 (under review).

[CHA79] M. Hanif Chaudhry, *Applied Hydraulic Transients*, Van Nostrand Reinhold, New York, 1979.

[CHI90] Amy Chicatelli, *Methods for Developing Linear Reduced Models of Internal Flow Propulsion Systems*, Masters Thesis, The University of Akron, 1990.

[CHU72] R. V. Churchill, *Operational Mathematics*, McGraw-Hill, New York, 1972.

[COL77] Gary L. Cole, *Atmospheric Effects on Inlets for Supersonic Cruise Aircraft*, NASA TM X-73647, July 1977.

[CW75] G. L. Cole and R. G. Willoh, *Analysis of the Dynamic Response of A Supersonic Inlet to Flow Field Perturbations Upstream of the Normal Shock*, NASA TN D-7839, January 1975.

[DAV83] R. T. Davis, "Numerical methods for coordinate generation based on a mapping technique," in *Computational Methods for Turbulent, Transonic, and Viscous Flows*, edited by J. A. Essers, Hemishpere Publishing Corporation, Washington, DC, 1983.

Reproduced with permission of the copyright owner. Further reproduction prohibited without permission.

[DH91] Benzad Dariush and Tom T. Hartley, *Reduced Order Modeling of Distributed Parameter Systems*, Electrical Engineering Department, The University of Akron, 1991.

[DS90] J. A. De Abreu-Garcia and A. D. Sarantopoulos, *Model Reduction Techniques*, Electrical Engineering Department, The University of Akron, revised September 1990.

[ENN84] Dale Enns, *Model Reduction for Control System Design*, PhD Dissertation, Stanford University, 1984.

[FEL89] Georges C. Felfli, *Critical Analysis of Balancing Techniques*, Masters Thesis, The University of Akron, 1989.

[GCP88] K. Glover, R. F. Curtain, and J. R. Partington, "Realization and approximation of linear infinite dimensional systems with error bounds," in *SIAM Journal on Control and Optimization*, Vol. 26, pp. 863-898, 1988.

[GIB83] J. S. Gibson, "Linear-quadratic optimal control of hereditary systems: Infinite dimensional Riccati equations and numerical approximation," in *SIAM Journal on Control and Optimization*, Vol. 21, pp. 95-139, 1983.

[GKL89] G. Gu, P. P. Khargonekhar, and E. B. Lee, "Approximation of infinite dimensional systems," in *IEEE Transactions on Automatic Control*, Vol. AC-34, No. 6, pp. 610-619, 1989.

[GLP86] K. Glover, J. Lam, and J. R. Partington, "Balanced realization and Hankel-norm approximation of systems involving delays," in *Proceedings of the IEEE Conference on Decision and Control*, Athens, Greece, pp. 1810-1815, December 1986.

[GLP88] K. Glover, J. Lam, and J. R. Partington, *Rational Approximation of A Class of Infinite Dimensional Systems*, Cambridge University Report CUED/F-INFENG/TR.20, 1988.

[GP87] K. Glover, and J. R. Partington, "Bounds on the achievable accuracy in model reduction," in *Modelling, Robustness, and*

Reproduced with permission of the copyright owner. Further reproduction prohibited without permission.

Sensitivity Reduction in Control Systems, edited by R. F. Curtain, Springer-Verlag, New York, pp. 95-118, 1987.

[GV80] G. H. Golub and C. F. Van Loan, "An analysis of the TLS problem," in *SIAM Journal on Numerical Analysis*, Vol. 17, No. 6, pp. 883-893, December 1980.

[HAR86] Tom T. Hartley, "A review of inlet modeling techniques for control applications," Summer Faculty Fellow Report, NASA Lewis Research Center, Cleveland, Ohio, August 1986.

[HAR87] S. I. Hariharan, "Nonlinear acoustic wave propagation in atmosphere," in *Quarterly of Applied Mathematics*, Vol. XLV, No. 4, pp. 735-748, December 1987.

[HAR89] S. I. Hariharan, *Time Domain Numerical Calculations of Unsteady Vortical Flows about A Flat Plate Airfoil*, NASA TM-102318, September 1989.

[HAR91] Tom T. Hartley, "A hierarchy for modeling high speed propulsion systems," in *The Ohio Academy of Science Journal*, vol.91, no. 2, p. 67, 1991.

[HAR92] S. I. Hariharan, *Private consultation.*

[HAR94] Tom T. Hartley, *Private communication.*

[HD91] T. T. Hartley and J. A. De Abreu-Garcia, *A Hierarchy for Modeling High Speed Propulsion Systems*, Final Report, NASA Grant NAG 3-904, NASA Lewis Research Center, December 1991.

[HEN74] P. Henrici, *Applied and Computational Complex Analysis*, 3 Vols., John Wiley and Sons, New York, 1974.

[HIL76] F. B. Hilderbrand, *Advanced Calculus for Applications*, Prentice-Hall, Englewood Cliffs, New Jersey, 1976.

[HIR90] Ch. Hirsch, *Numerical Computation of Internal and External Flows*, 2 vols., Wiley & Sons, Chichester, 1990.

Reproduced with permission of the copyright owner. Further reproduction prohibited without permission.

[HL84] S. I. Hariharan and Harold C. Lester, "A finite difference solution for the propagation of sound in near sonic flows," in *Journal of the Acoustical Society of America*, 75 (4), pp.1052-1061, April 1984.

[HMB89] T.T. Hartley, K. Melcher, and W. M. Btuton, "Near Real-Time, Large Perturbation Simulation of Internal Flows," (u), NASP Technical Memorandum 1062, June 1989.

[HOF62] K. Hoffman, *Banach Spaces of Analytic Functions*, Prentice-Hall, Englewood Cliffs, NJ, 1962.

[HOF89] Klaus A. Hoffman, *Computational Fluid Dynamics for Engineers*, Engineering Education System, Austin, Texas, 1989.

[HP89] S. I. Hariharan and Yu Ping, "Linear and nonlinear acoustic wave propagation in the atmosphere," in *SIAM Journal on Scientific and Statistical Computing*, Vol. 10, No. 3, pp. 488-514, May 1989.

[HUF87] S. Van Huffel, *Analysis of the TLS problem and its use in Parameter Estimation*, Ph.D. Dissertation, Electrical Engineering Department, K. V. Leuven, Heverlee, Belgium, 1987.

[HUR57] Herbert G. Hurrell, *Analysis of Shock Motion in Ducts during Disturbances in Downstream Pressure*, NACA TN 4090, September 1957.

[HWC87] T. Hsieh, A. B. Wardlaw Jr., and P. Collins, "Numerical investigation of unsteady inlet flowfields," in *AIAA Journal*, Vol. 25. No. 1, pp. 75-81, January 1987.

[IHD91] S. M. Immel, T. T. Hartley, and J. A. De Abreu Garcia, *Physical Lumping Methods for Developing Linear Reduced Models for High Speed Propulsion Systems*, Electrical Engineering Department, The University of Akron, December 1991.

Reproduced with permission of the copyright owner. Further reproduction prohibited without permission.

[KOL80] Wolfgang Kollmann, *Computational Fluid Dynamics*, 2 vols., Hemishpere Publishing Corporation, Washington, 1980.

[LZ72] Bruce Lehtinen and John R. Zeller, "Application of Quadratic Optimization to Supersonic Inlet Control," in *Automatica*, Vol. 8, pp. 563-574, 1972.

[MAC81] R. W. MacCormack, "A numerical method for solving the equations of compressible viscous flow," *AIAA paper 81-0110*, presented at the 19th Aerospace Sciences Meeting, St. Louis, Missouri, January 12-15, 1981.

[MAR66] A. I. Markushevich, *Entire Functions*, American Elsevier Publishing Company, Inc., New York, 1966.

[MAR68] Arnold W. Martin, *Propulsion System Dynamic Simulation, Theory and Equations*, NASA CR-928, March 1968.

[MHD92] F. Mossayebi, T. T. Hartley, and J. A. De Abreu Garcia, "A fundamental theorem for the model reduction of nonlinear systems," in *The Journal of The Franklin Institute*, Vol. 329, No. 1, pp. 145-153, 1992.

[MIN74] F. U. Minhas, "Boundary value problems of two-dimensional isentropic gas flow," in *Numerical Methods in Fluid Dynamics*, edited by C. A. Brebbia and J. J. Connor, Pentech Press, London, 1974.

[MOR39] P. M. Morse, "The transmission of sound inside pipes," *Journal of the Acoustical Society of America*, Vol. 11, pp. 205-210, October 1939.

[MVA84] W. R. Martindale, M. O. Varner, and J. C. Adams, Jr., *Large Perturbation Flow Field Analysis and Simulation for supersonic inlets, Program User's Manual*, Sverdrup report prepared for NASA under Contract No. NAS3-23682, 1984.

Reproduced with permission of the copyright owner. Further reproduction prohibited without permission.

[PGZ88] J. R. Partington, K. Glover, H. J. Zwart, and R. F. Curtain, "L^∞ approximation and nuclearity of delay systems," in *Systems and Control Letters*, Vol. 10, pp. 59-65, 1988.

[PIE91] Liane Piercy, *Robust Model Reduction and Control of Internal Propulsion Systems*, Masters Thesis, The University of Akron, 1991.

[RG57] C. P. Rohmann and E. C. Grogan, "On the dynamics of pneumatic transmission lines," in *Transactions of the ASME*, pp. 853-874, May 1957.

[RIC57] R. D. Richtmyer, *Difference Methods for Initial-Value Problems*, Interscience Publishers, Inc., New York, 1957.

[RIC86] W. B. Richards, *Propagation of Sound Waves in Tubes of Noncircular Cross Section*, NASA TP-2601, 1986.

[RK83] R. C. Rosenberg and D. C. Karnopp, *Introduction to Physical System Dynamics*, Mc Graw-Hill, New York, 1983.

[RM67] R. D. Richtmyer and K. W. Morton, *Difference Methods for Initial-Value Problems*, 2nd ed., Interscience Publishers, Wiley, New York, 1967.

[ROA76] Patrick J. Roache, *Computational Fluid Dynamics*, Hermosa Publishers, Albuquerque, NM, 1976.

[RS67] D. J. Roy and J. Sherman, "A learning technique for Volterra series modeling" in *IEEE Transactions on Automatic Control*, AC-12, pp. 761-764, 1967.

[SC89] M. G. Safonov and R. Y. Chiang, "A Schur method for balanced truncation model reduction", in *IEEE Transactions on Automatic Control*, Vol. 34, No. 7, pp. 729-733, July 1989.

[SF65] R. J. Schwarz and B. Friedland, *Linear Systems*, McGraw-Hill, New York, 1965.

Reproduced with permission of the copyright owner. Further reproduction prohibited without permission.

[SH91] A. D. Sarantopoulos and Tom T. Hartley, "Modeling of linear isentropic flow systems," in *Proceedings of IEEE International Conference on Systems Engineering*, pp. 442-445, August 1991.

[SHA53] A. H. Shapiro, *The Dynamics and Thermodynamics of Compressible Fluid Flow*, 2 vols., The Roland Press Company, New York, 1953.

[SM71] A. P. Sage and J. L. Melsa, *System Identification*, Academic Press, New York, 1971.

[SNF69] G. N. Saridis, Z. J. Nicolic, and K. S. Fu, "Stochastic approximation algorithm for system identification, estimation, and decomposition of mixtures" in *IEEE Transactions on Systems Science and Cybernetics*, SSC-5, pp. 8-15, 1969.

[SW81] J. L. Steger and R. F. Warming, "Flux vector splitting of the inviscid gas dynamics equations with application to finite-difference methods," in *Journal of Computational Physics*, Vol. 40, pp. 263-293, 1981.

[TT87] A. R. D. Thorley and C. H. Tiley, "Unsteady and transient flow of compressible fluids in pipelines-a review of theoretical and some experimental studies," in *The International Journal of Heat and Fluid Flow*, Vol. 8, No. 1, pp. 3-15, March 1987.

[VMP84] M. O. Varner, W. R. Martindale, W. J. Phares, K. R. Kneile, and J. C. Adams, Jr., *Large Perturbation Flow Field Analysis and Simulation for Supersonic Inlets*, NASA CR-174676, June 1984.

[WH86] Stephen F. Wornom and Mahamed M. Hafez,"Implicit conservative schemes for the Euler equations," in *AIAA Journal*, Vol. 24, No. 2, pp. 215-223, February 1986.

[WIE58] N. Wiener, *Nonlinear Problems in Random Theory*, MIT Press, Cambridge, MA, 1958.

Reproduced with permission of the copyright owner. Further reproduction prohibited without permission.

[WIL68] R. G. Willoh, *A Mathematical Analysis of Supersonic Inlet Dynamics*, NASA TN D-4969, December 1968.

[WY73] D. D. Williams and J. O. Yost, "Some aspects of inlet/engine flow compatibility," in *Aeronautical Journal*, vol. 77, pp. 483-492, September 1973.

[YG88] Jiahn-Bo Yarng and Yan-Shen Guan, "Optimal control of supersonic inlet/engine combination," in *Journal of Guidance and Control*, Vol. 11, No. 2, pp. 137-145, March/April 1988.

Reproduced with permission of the copyright owner. Further reproduction prohibited without permission.

APPENDICES

Reproduced with permission of the copyright owner. Further reproduction prohibited without permission.

APPENDIX A

GLOSSARY OF TERMS

The purpose of this appendix is to introduce the reader to the essential fluid and gas dynamics terminology that will appear throughout this report. For more information on any of the terms given below, the interested reader is advised to turn his attention to the many references found at the end of the report.

Acoustics is a field of fluid motion in which the fluid velocities are very small compared to the speed of sound, although the fractional variations in pressure, density, and temperature are of significant magnitude.

An **Adiabatic process** is a process in which no heat enters or leaves a system. In fluid flow this is equivalent to say that the rate of heat transfer across the control surface is zero.

The **Boundary layer** is the layer next to a body within which the major effects of viscosity are concentrated. It is a region in the flow where the velocity rises gradually from zero to the full value found in the main stream. The boundary layer effect is not detectable beyond a certain distance outside which the flow of a viscous fluid resembles closely that of an inviscid fluid.

Reproduced with permission of the copyright owner. Further reproduction prohibited without permission.

Buzz is termed the rapid oscillatory movement of a normal shock inside a supersonic inlet. Simulating a buzz is a difficult problem as large perturbation models must be developed.

A Bypass door is an opening on the side of an inlet that can be used as a control input to dump excess air out of the duct so that pressure waves do not push the normal shock forward ahead of the throat of the inlet.

At any Mach number, there exists a critical amount of heat that will drive the stream Mach number to unity. This is the condition for **choked flow** or **thermal choking.** Heat added in excess of the critical amount will cause a decrease in mass flux through the duct.

Compressible flow is flow in which the flow density is changing with respect to time.

Computational fluid dynamics is the art of replacing the governing nonlinear partial differential equations with numbers and advancing these numbers in space and/or time to obtain a final description of the complete flow field of interest. The end result of this technique is to obtain a collection of useful numbers about the system.

The **Critical area** is the throat area corresponding to sonic speed for the given mass flow.

Critical flow represents the onset of hypersonic flow.

Density is defined as the mass per unit volume of a substance.

Reproduced with permission of the copyright owner. Further reproduction prohibited without permission.

A Diffuser or **recuperator** is a gradual, tapered, enlargement used to reduce the velocity of the fluid gradually, and thus eliminate, as far as possible, the eddies responsible for the dissipation of energy.

Dynamic pressure is that part of the stagnation pressure due to the motion.

Energy is the property of a system that is a measure of its capacity for doing work.

Enthalpy, also synonymous with total heat and heat content, is a thermodynamic function of a system equal to the sum of its internal energy and the product of its pressure and volume.

The **Entropy** of a system is a measure of its degree of disorder. It is not a conserved property since it can be produced.

The **equation of continuity** is a statement of the conservation of mass principle in terms of field properties at a point. It states that the mass-flow rate across a system boundary is equal to the rate of storage of mass within that system.

The **equations of state** show the relationship between the pressure, volume, temperature, and density of a substance.

The **first law of thermodynamics** states that for any mass system the net heat supplied to the system equals the increase in energy of the system plus all the energy that leaves the system as work is done. This law,

Reproduced with permission of the copyright owner. Further reproduction prohibited without permission.

as applied to the flow of fluids, keeps account of the various interchanges of energy that occur.

A **Fluid** is any substance that deforms continuously under the action of shearing forces and takes the shape of the vessel containing it.

Friction forces are tangential or shearing forces developed across the common boundary of two fluid particles moving at different velocities. Such forces do not exist in an inviscid fluid.

Hypersonic flow is any flow having a speed in excess of Mach 5. Usually, dissociation of molecules occurs.

An **inlet** of an airbreathing engine such as a ramjet and a turbojet is a diffuser that operates at supersonic speeds and is required to decelerate the flow to subsonic velocities. Subsonic engines also have inlets.

Internal energy is a thermodynamic function of a system that changes by an amount equal to the algebraic sum of the heat received by the system and the work done on it. The internal energy of a system is equal to the sum of all the kinetic and the potential energies of the molecules and is never absolutely determined. However, only changes in its values are important.

Irrotational flow is called a flow for which the circulation around every curve is and remains zero.

An **Isentropic process** is any reversible adiabadic process. During such a process the change of entropy is zero.

Reproduced with permission of the copyright owner. Further reproduction prohibited without permission.

The **law of conservation of mass** is an empirical law which states that mass may neither be created nor destroyed. In other words, the mass of a system of fixed identity is constant. This law forms the basis for "Newtonian Mechanics."

The **Mach number,** named after the Austrian physicist Ernst Mach (1838-1916), is a dimensionless quantity that signifies the effect of compressibility. It is defined as the ratio of the speed of a fluid or body to the local speed of sound. Heat added subsonically will raise the Mach number, while heat added supersonically will lower the Mach number.

The **Navier-Stokes equations** are the exact equations of motion for a viscous fluid. They were derived by Navier in France in 1827 and independently by Stokes in England in 1845.

A shock is called a **normal shock** when the plane of the shock is normal to the direction of the flow. In a normal shock, there is no change in the direction of fluid flow before and after the shock. The flow upstream of the shock is supersonic, while that downstream is subsonic and at a higher pressure.

A shock is called an **oblique shock,** when the plane of the shock is inclined to the direction of flow of gas. The fluid passing through an oblique shock changes its direction. An oblique shock, for example, may arise when supersonic flow is caused to change direction by a boundary surface converging towards the flow.

Reproduced with permission of the copyright owner. Further reproduction prohibited without permission.

One-dimensional flow is termed the flow in which all the flow parameters may be expressed as functions of time and one space coordinate only. In many practical problems, the conditions for one-dimensional flow are very nearly fulfilled.

A flow is said to take place in an **open channel** if the liquid is bounded only by side walls.

The **Prandtl-Meyer angle** is the angle through which a stream, initially at sonic velocity, must be turned to reach the given Mach number M.

The **Rankine-Hugoniot** conditions are used to determine the flow variables immediately upstream of a shock and also to determine the shock position.

A Reversible process is a process in which dissipative phenomena are absent. Therefore, such a process can be run backwards.

The **Reynolds number,** Re, is the ratio of the magnitude of inertia forces to that of viscous forces. It is a dimensionless constant which can be used to compare one flow with another. For any particle, a high value of Re indicates that inertia forces dominate the flow while viscous forces play only a small part. On the other hand, a small value of Re indicates that the viscous forces are more significant than inertia forces.

Rotational flow is called the flow in a region where the vorticity is other than zero.

Reproduced with permission of the copyright owner. Further reproduction prohibited without permission.

Quasi-one dimensional flow is termed the flow which occurs in a channel with small rate of change of cross section or between nearly parallel streamlines. The velocity components normal to the mean flow direction are small compared to the flow direction (the flow velocity is everywhere axial).

A **shock** is a discontinuity in supersonic flow. It is accompanied with a rise in static pressure and a fall in velocity (from supersonic to subsonic). The Euler equations do not hold right at a shock. Across the shock, there is an increase in entropy since the process is irreversible and adiabatic. Shocks can be observed in wind tunnel experiments or by Schlieren photography.

A steady flow is called **sonic** if the flow speed is equal to the local speed of sound. Such a flow is not possible in a converging or diverging channel but it can occur only at a constriction (throat).

A **Sonic boom** is the loud noise originating from the backward projected shock waves set up by an aircraft or missile traveling at supersonic speeds.

Sound is a physiological sensation received by the ear which is caused by a vibrating source and transmitted as a longitudinal pressure wave motion through a material medium.

Specific. When used before the name of an extensive physical quantity, it implies "divided by mass." For example, specific enthalpy is enthalpy per unit mass.

Reproduced with permission of the copyright owner. Further reproduction prohibited without permission.

Speed of sound, also called **acoustic velocity** or **sonic velocity** is the velocity of propagation of sound waves. It is a function of temperature and the nature of the propagating medium and it therefore can vary from point to point.

Stagnation pressure is defined as the pressure which would be reached if the fluid were brought to rest by an isentropic process. The stagnation pressure is reduced across a normal shock.

A **Stagnation point** is a point in a fluid stream where the velocity is zero.

A **Stationary shock** is a shock wave which occurs in steady flow.

Steady flow is flow in which the various flow parameters, such as velocity, pressure, and density, at any point do not change with time.

A steady flow is called **subsonic** if the flow speed is less that the local speed of sound. If such a flow occurs then information is able to propagate upstream. A subsonic flow decelerates in an diverging channel and accelerates in a converging channel.

A steady flow is called **supersonic** if the flow speed is greater than the local speed of sound. In a supersonic flow all information propagates downstream and changes of density in the flow can no longer be neglected. Supersonic flow usually adjusts to downstream obstacles by undergoing discontinuous changes referred to as shocks. Furthermore, a supersonic

Reproduced with permission of the copyright owner. Further reproduction prohibited without permission.

flow accelerates in an expanding or divergent channel and decelerates in a converging channel.

Two dimensional flow is flow in which the flow parameters are functions of time and two space coordinates only.

Unsteady flow is called the flow in which the flow parameters change with time.

Variable geometry inlets are inlets which are used to optimize the performance of an aircraft flying at supersonic speeds. They typically consist of a translating centerbody which if moved forward causes the throat area to increase. By varying the throat area, the throat Mach number can be kept above one, even if the free stream Mach number decreases. Due to their importance in maintaining an overall optimum system performance, there is a need for control systems to control variable geometry inlets.

Viscosity is the stickiness of a fluid and its tendency to resist relative motion within itself. More rigorously, viscosity is the rate of change of shear strain.

Reproduced with permission of the copyright owner. Further reproduction prohibited without permission.

APPENDIX B

NASA LEWIS MACH 2.5 40-60 INLET DATA

This appendix contains computed data for the NASA Lewis Mach 2.5 40-60 mixed compression inlet. The tabulated values can be used to develop small perturbation inlet models and determine the inflow and outflow boundary conditions.

Reproduced with permission of the copyright owner. Further reproduction prohibited without permission.

40-60 INLET DATA			$\gamma = 1.4$			
N	LENGHT	DENSITY	MASSFLOW	ENERGY	VELOCITY	SPECIFIC ENERGY
1	0.1427	3.3261e-4	0.6187	978.86	1860.14	2.9430e+6
2	0.2854	3.4841e-4	0.6422	1022.18	1843.23	2.9338e+6
3	0.4281	3.6703e-4	0.6692	1073.01	1823.28	2.9235e+6
4	0.5708	3.8920e-4	0.7006	1133.21	1800.10	2.9116e+6
5	0.7135	4.1833e-4	0.7407	1211.74	1770.61	2.8966e+6
6	0.8562	4.5941e-4	0.7948	1321.41	1730.05	2.8763e+6
7	0.9989	5.1552e-4	0.8643	1469.42	1676.56	2.8504e+6
8	1.1416	5.9170e-4	0.9506	1667.06	1606.56	2.8174e+6
9	1.2843	6.8451e-4	1.0436	1903.51	1524.59	2.7808e+6
10	1.4270	8.0715e-4	1.1458	2209.09	1419.56	2.7369e+6
11	1.5697	9.1045e-4	1.2133	2460.65	1332.64	2.7027e+6
12	1.7124	9.4969e-4	1.2344	2555.09	1299.79	2.6904e+6
13	1.8551	9.4600e-4	1.2324	2546.03	1302.75	2.6914e+6
14	1.9978	9.3331e-4	1.2259	2515.90	1313.50	2.6957e+6
15	2.1405	9.0439e-4	1.2098	2446.01	1337.70	2.7046e+6
16	2.2832	8.6285e-4	1.1842	2345.17	1372.43	2.7179e+6
17	2.4259	8.1293e-4	1.1499	2223.24	1414.51	2.7348e+6
18	2.5686	7.5621e-4	1.1061	2083.06	1462.69	2.7546e+6
19	2.7113	6.9773e-4	1.0556	1936.75	1512.91	2.7758e+6
20	2.8540	6.4524e-4	1.0057	1804.08	1558.64	2.7960e+6
21	2.9967	5.9902e-4	0.9582	1682.80	1599.61	2.8093e+6
22	3.1394	5.5888e-4	0.9143	1582.19	1635.95	2.8310e+6
23	3.2821	1.1533e-3	0.9292	2890.29	805.69	2.5061e+6
24	3.4248	1.3227e-3	0.8396	3315.79	634.76	2.5068e+6
25	3.5675	1.3217e-3	0.8408	3313.64	636.15	2.5071e+6
26	3.7102	1.3278e-3	0.8322	3326.71	626.75	2.5054e+6
27	3.8529	1.3401e-3	0.8141	3353.03	607.49	2.5021e+6
28	3.9956	1.3530e-3	0.7937	3380.58	586.62	2.4986e+6
29	4.1383	1.3678e-3	0.7685	3411.96	561.85	2.4945e+6
30	4.2810	1.3781e-3	0.7498	3433.77	544.08	2.4917e+6
31	4.4237	1.3807e-3	0.7450	3439.31	539.58	2.4910e+6
32	4.5664	1.3763e-3	0.7534	3430.00	547.41	2.4922e+6
33	4.7091	1.3733e-3	0.7587	3423.00	552.46	2.4925e+6
34	4.8518	1.3687e-3	0.7671	3413.82	560.46	2.4942e+6
35	4.9945	1.3633e-3	0.7763	3402.40	569.43	2.4957e+6
36	5.1372	1.3619e-3	0.7789	3399.30	571.92	2.4960e+6
37	5.2799	1.3552e-3	0.7900	3385.14	582.94	2.4979e+6
38	5.4226	1.3561e-3	0.7886	3387.13	581.52	2.4977e+6
39	5.5653	1.3646e-3	0.7744	3405.10	567.49	2.4953e+6
40	5.7080	1.3790e-3	0.7481	3435.67	542.49	2.4914e+6
41	5.8507	1.3920e-3	0.7229	3463.18	519.32	2.4879e+6

STEADY-STATE VALUES

LUMPS		DENSITY	MASSFLOW	ENERGY	VELOCITY	SPECIFIC ENERGY
1-22		6.5866e-4	0.9846	1825.93	1554.45	2.7988e+6
23-41		1.3492e-3	0.7880	3368.94	586.23	2.4971e+6

Reproduced with permission of the copyright owner. Further reproduction prohibited without permission.

Continued

SPECIFIC INT. ENERGY	INTERNAL ENERGY	PRESSURE	SPEED OF SOUND	MACH #	TEMPERATURE
1.2129e+6	403.43	161.37	824.15	2.2570	282.73
1.2351e+6	430.32	172.13	831.66	2.2163	287.90
1.2613e+6	462.94	185.18	840.44	2.1694	294.01
1.2915e+6	502.63	201.05	850.42	2.1167	301.04
1.3291e+6	555.99	222.40	862.72	2.0524	309.81
1.3798e+6	633.89	253.56	879.02	1.9681	321.63
1.4449e+6	744.89	297.96	899.54	1.8638	336.82
1.5269e+6	903.46	361.39	924.69	1.7374	355.92
1.6186e+6	1107.98	443.19	952.07	1.6013	377.31
1.7293e+6	1395.82	558.33	984.08	1.4425	403.11
1.8147e+6	1652.21	660.88	1008.09	1.3219	423.01
1.8457e+6	1752.86	701.14	1016.66	1.2785	430.24
1.8428e+6	1743.28	697.31	1015.85	1.2824	429.55
1.8330e+6	1710.79	684.32	1013.16	1.2964	427.28
1.8099e+6	1636.84	654.73	1006.74	1.3287	421.88
1.7762e+6	1532.56	613.02	997.32	1.3761	414.02
1.7344e+6	1409.97	563.99	985.53	1.4353	404.29
1.6849e+6	1274.12	509.65	971.35	1.5058	392.74
1.6313e+6	1138.24	455.30	955.80	1.5829	380.27
1.5813e+6	1020.32	408.13	941.02	1.6563	368.60
1.5299e+6	916.43	366.57	925.60	1.7282	356.61
1.4928e+6	834.32	333.73	914.32	1.7892	347.98
2.1815e+6	2515.97	1006.39	1105.29	0.7289	508.52
2.3054e+6	3049.32	1219.73	1136.23	0.5587	537.38
2.3048e+6	3046.20	1218.48	1136.07	0.5600	537.24
2.3090e+6	3065.92	1226.37	1137.12	0.5512	538.23
2.3176e+6	3105.75	1242.30	1139.22	0.5333	540.22
2.3265e+6	3147.78	1259.11	1141.42	0.5139	542.31
2.3366e+6	3196.07	1278.43	1143.91	0.4912	544.67
2.3437e+6	3229.79	1291.92	1145.62	0.4749	546.31
2.3454e+6	3238.32	1295.33	1146.05	0.4708	546.72
2.3424e+6	3223.79	1289.52	1145.30	0.4780	546.00
2.3399e+6	3213.42	1285.37	1144.71	0.4826	545.44
2.3371e+6	3198.86	1279.54	1144.03	0.4899	544.79
2.3336e+6	3181.38	1272.55	1143.16	0.4981	543.96
2.3325e+6	3176.57	1270.63	1142.88	0.5004	543.69
2.3280e+6	3154.88	1261.95	1141.78	0.5106	542.65
2.3286e+6	3157.84	1263.13	1141.94	0.5092	542.80
2.3343e+6	3185.37	1274.15	1143.33	0.4964	544.12
2.3443e+6	3232.75	1293.10	1145.77	0.4735	546.45
2.3531e+6	3275.47	1310.19	1147.92	0.4524	548.50

SPECIFIC INT. ENERGY	INTERNAL ENERGY	PRESSURE	SPEED OF SOUND	MACH #	TEMPERATURE
1.5730e+6	1080.15	432.06	936.38	1.6821	366.67
2.3234e+6	3136.60	1254.64	1140.62	0.5144	541.58

Reproduced with permission of the copyright owner. Further reproduction prohibited without permission.

Continued			
TOTAL TEMPERATURE	TOTAL PRESSURE	TOTAL DENSITY	TOTAL SPEED OF SOUND
570.78	3305.39	1.9261e-3	1171.00
570.74	3158.17	1.9279e-3	1170.96
570.77	2997.02	1.9272e-3	1170.99
570.80	2825.78	1.9268e-3	1171.02
570.80	2630.08	1.9275e-3	1171.02
570.80	2395.02	1.9276e-3	1171.02
570.82	2134.35	1.9276e-3	1171.04
570.79	1859.04	1.9271e-3	1171.01
570.81	1606.90	1.9270e-3	1171.03
570.87	1362.47	1.9264e-3	1171.09
570.86	1207.72	1.9262e-3	1171.08
570.88	1157.84	1.9261e-3	1171.11
570.84	1162.15	1.9259e-3	1171.06
570.91	1178.16	1.9260e-3	1171.13
570.85	1215.78	1.9261e-3	1171.08
570.83	1274.12	1.9259e-3	1171.05
570.87	1352.45	1.9259e-3	1171.09
570.86	1454.00	1.9261e-3	1171.08
570.82	1575.86	1.9262e-3	1171.04
570.85	1703.83	1.9259e-3	1171.07
569.63	1836.88	1.9317e-3	1169.82
570.79	1966.84	1.9258e-3	1171.01
562.56	724.14	1.4846e-3	1162.54
570.93	664.23	1.5389e-3	1171.15
570.93	664.69	1.5388e-3	1171.15
570.94	661.65	1.5388e-3	1171.16
570.94	655.62	1.5388e-3	1171.17
570.96	649.38	1.5388e-3	1171.19
570.95	642.34	1.5388e-3	1171.18
570.95	637.54	1.5388e-3	1171.18
570.96	636.36	1.5389e-3	1171.18
570.95	638.42	1.5389e-3	1171.18
570.85	639.67	1.5389e-3	1171.07
570.94	641.94	1.5389e-3	1171.16
570.95	644.44	1.5388e-3	1171.18
570.93	645.12	1.5389e-3	1171.15
570.94	648.29	1.5388e-3	1171.17
570.95	647.89	1.5388e-3	1171.18
570.93	643.88	1.5390e-3	1171.16
570.95	637.12	1.5388e-3	1171.18
570.95	631.19	1.5389e-3	1171.18
TOTAL TEMPERATURE	TOTAL PRESSURE	TOTAL DENSITY	TOTAL SPEED OF SOUND
570.77	1879.99	1.9268e-3	1170.99
570.50	650.20	1.5360e-3	1170.71

Reproduced with permission of the copyright owner. Further reproduction prohibited without permission.

APPENDIX C

PROGRAM LISTINGS

This appendix contains the MATLAB program listings used in this dissertation. They correspond to the following problems:

PROGRAM NAME	PROBLEM SOLVED
A_two_wave	Two-wave bounded
A_two_wave_mesh	Two-wave bounded (Mesh plots)
B_three_wave	Three-wave bounded
B_three_wave_mesh	Three-wave bounded (Mesh plots)
C_two_wave_blocks	Two-wave bounded with internal input
C_three_wave_blocks	Three-wave bounded with internal input
D_two_wave_Green	Two-wave Green's function
D_three_wave_Green	Three-wave Green's function
E_CW	Inlet with Cole-Willoh Conditions
E_CW_Mesh	Inlet with Cole-Willoh Conditions (Mesh plots)

Reproduced with permission of the copyright owner. Further reproduction prohibited without permission.

```
%   Program:        A_two_wave
%   Last update:    July 4, 1994
%   Source Code:    Edu-Matlab

clear;echo off;hold off;clc
g=1.4; L=3.61; x=0; p=-1010; m=.78; R=1e-6;
r=0.00136; Z0=1010; Ebar=3350;
N=200; d1=-1; d2=3;
w=2*pi*logspace(d1,d2,N); j=sqrt(-1); s=j*w; f=w/2/pi;
u=m/r;
c=(g*(g-1)*(Ebar-m*m/2/r)/r)^.5;
M=u/c;
Z=(s-p).\(Z0*ones(s));
xL=x-L;
cu=c*c-u*u;
csx=c.*s*x/cu;
csL=c.*s*L/cu;
csxL=c.*s*xL/cu;
usL=u.*s*L/cu;
K_0n=exp(u*s*xL/cu);
K_0d=(1-Z*R).*cosh(csL)+((R*c/r)-(Z*r/c)).*sinh(csL);
K_0=K_0n./K_0d;
K11=K_0.*((cosh(csxL)-(R*c/r).*sinh(csxL)).*exp(usL));
K12=K_0.*(Z.*cosh(csx)-(c/r)*sinh(csx));
K21=K_0.*((R*cosh(csxL)-(r/c)*sinh(csxL)).*exp(usL));
K22=K_0.*(cosh(csx)-(r*Z/c).*sinh(csx));
PRESSURE=(g-1)*(-.5*u*u*K22-r*u*K12);
MAG=abs(PRESSURE)/max(abs(PRESSURE));
PHA=atan(imag(PRESSURE)./real(PRESSURE))*180/pi;
semilogx(f,20*log(MAG))
title('Normalized Magnitude Response of Pressure')
xlabel('Frequency, Hz'), ylabel('MAGNITUDE, dB')
pause
```

Reproduced with permission of the copyright owner. Further reproduction prohibited without permission.

```
semilogx(f,PHA)
title('Phase Response of Pressure')
xlabel('Frequency, Hz'), ylabel('PHASE')
pause
position=Z.*PRESSURE;
MAG=abs(position)/max(abs(position));
PHA=atan(imag(position)./real(position))*180/pi;
semilogx(f,20*log(MAG))
title('Normalized Magnitude Response of Shock Position')
xlabel('Frequency, Hz'), ylabel('MAGNITUDE, dB')
pause
semilogx(f,PHA)
title('Phase Response of Shock Position')
xlabel('Frequency, Hz'), ylabel('PHASE')
end      % of program
```

Reproduced with permission of the copyright owner. Further reproduction prohibited without permission.

```
%   Program:        A_two_wave_mesh
%   Last update:    July 4, 1994
%   Source Code:    Edu-Matlab

clear;
j=sqrt(-1);
g=1.4; L=2.57; x=0; p=-1010; m=.78; R=6e-6;
r=0.00136; Z0=1010;   Ebar=3350;
u=m/r;
c=(g*(g-1)*(Ebar-m*m/2/r)/r)^.5;
M=u/c;
%   Generate complex frequency grid
% sc=-936:36:936;     % >> 53 pts.
sc=-936:60:936;     % >> 32 pts.
ci=3*sc';
sigma=ones(length(ci),1)*sc;
w=ci*ones(length(sc),1)';
s=sigma+(j*w);
%   Compute closed-loop system parameters
xL=x-L;
cu=c*c-u*u;
csx=c.*s*x/cu;
csL=c.*s*L/cu;
csxL=c.*s*xL/cu;
usL=u.*s*L/cu;
Z=(s-p).\(Z0*ones(s));
K_0n=exp(u*s*xL/cu);
K_0d=(1-Z*R).*cosh(csL)+((R*c/r)-(Z*r/c)).*sinh(csL);
K_0=K_0n./K_0d;
K_11=(cosh(csxL)-(R*c/r).*sinh(csxL)).*exp(usL);
K_12=Z.*cosh(csx)-(c/r)*sinh(csx);
K_21=(R*cosh(csxL)-(r/c)*sinh(csxL)).*exp(usL);
K_22=cosh(csx)-(r*Z/c).*sinh(csx);
```

Reproduced with permission of the copyright owner. Further reproduction prohibited without permission.

```
K11=K_0.*K_11;
K12=K_0.*K_12;
K21=K_0.*K_21;
K22=K_0.*K_22;
f=w/2/pi;
levels=30;
PRESSURE=(1-g)*(.5*u*u*K22+r*u*K12);
MAG=abs(PRESSURE);
mesh(log(MAG)),pause, contour(log(MAG),levels, sc,3*sc)
xlabel('Real(s)'), ylabel('Imag(s)')
title('Contours of Equal Magnitude of Pressure')
pause
position=Z.*PRESSURE;
MAG=abs(position);
mesh(log(MAG)),pause, contour(log(MAG),levels, sc,3*sc)
xlabel('Real(s)'), ylabel('Imag(s)')
title('Contours of Equal Magnitude of Shock Position')
end;        % of PROGRAM
```

Reproduced with permission of the copyright owner. Further reproduction prohibited without permission.

```
%   Program:        B_three_wave
%   Last update:    July 4, 1994
%   Source Code:    Edu-Matlab

clear; echo off; clc ; subplot; hold off
r=0.00136;      g=1.4;
x=0;      L=2.57;   m=.78;  Ebar=3350;
N=200;   d1=-1;  d2=3;
w=2*pi*logspace(d1,d2,N);
j=sqrt(-1);    s=j*w;    f=w/2/pi;
u=586.23;
c=1140.62;
p1=-300;   Z01=1010;
R1=-u^2/2;
p2=-1010;  Z02=1010;
R2=u;
M=0.5144;
Z1=(s-p1).\(Z01*ones(s));
Z2=(s-p2).\(Z02*ones(s));
AB=1/2/c/c;
E1=exp(-s*x/u);
E2=exp(-s*x/(u+c));
E3=exp(-s*x/(u-c));
E1L=exp(-s*L/u);
E2L=exp(-s*L/(u+c));
E3L=exp(-s*L/(u-c));
A11=(1-u*u*(g-1)/2/c/c);
A12=(g-1)*u/c/c;
A13=-(g-1)/c/c;
A21=u*(1-u*u*(g-1)/2/c/c);
A22=u*u*(g-1)/c/c;
A23=-(g-1)*u/c/c;
A31=u*u*(1-u*u*(g-1)/2/c/c)/2;
```

Reproduced with permission of the copyright owner. Further reproduction prohibited without permission.

```
A32=u*u*u*(g-1)/2/c/c;
A33=-u*u*(g-1)/2/c/c;
B11=AB*((g-1)*u*u/2-u*c);
B12=AB*(c-(g-1)*u);
B13=AB*(g-1);
B21=(u+c)*AB*((g-1)*u*u/2-u*c);
B22=(u+c)*AB*(c-(g-1)*u);
B23=(u+c)*AB*(g-1);
B31=(.5*u*u+u*c+c*c/(g-1))*AB*((g-1)*u*u/2-u*c);
B32=(.5*u*u+u*c+c*c/(g-1))*AB*(c-(g-1)*u);
B33=(.5*u*u+u*c+c*c/(g-1))*AB*(g-1);
C11=AB*((g-1)*u*u/2+u*c);
C12=-AB*(c+(g-1)*u);
C13=AB*(g-1);
C21=(u-c)*AB*((g-1)*u*u/2+u*c);
C22=-(u-c)*AB*(c+(g-1)*u);
C23=(u-c)*AB*(g-1);
C31=(.5*u*u-u*c+c*c/(g-1))*AB*((g-1)*u*u/2+u*c);
C32=-(.5*u*u-u*c+c*c/(g-1))*AB*(c+(g-1)*u);
C33=(.5*u*u-u*c+c*c/(g-1))*AB*(g-1);
H11=A11*E1+B11*E2+C11*E3;
H12=A12*E1+B12*E2+C12*E3;
H13=A13*E1+B13*E2+C13*E3;
H21=A21*E1+B21*E2+C21*E3;
H22=A22*E1+B22*E2+C22*E3;
H23=A23*E1+B23*E2+C23*E3;
H31=A31*E1+B31*E2+C31*E3;
H32=A32*E1+B32*E2+C32*E3;
H33=A33*E1+B33*E2+C33*E3;
F11=A11*E1L+B11*E2L+C11*E3L;
F12=A12*E1L+B12*E2L+C12*E3L;
F13=A13*E1L+B13*E2L+C13*E3L;
F21=A21*E1L+B21*E2L+C21*E3L;
```

Reproduced with permission of the copyright owner. Further reproduction prohibited without permission.

```
F22=A22*E1L+B22*E2L+C22*E3L;
F23=A23*E1L+B23*E2L+C23*E3L;
F31=A31*E1L+B31*E2L+C31*E3L;
F32=A32*E1L+B32*E2L+C32*E3L;
F33=A33*E1L+B33*E2L+C33*E3L;
[MM,NN]=size(s);
Y11=ones(MM,NN);
Y12=zeros(MM,NN);
Y13=-Z1;
Y21=zeros(MM,NN);
Y22=ones(MM,NN);
Y23=-Z2;
Y31=-R1*F11-R2*F21+F31;
Y32=-R1*F12-R2*F22+F32;
Y33=-R1*F13-R2*F23+F33;
DELTA=Y33-Y23.*Y32-Y13.*Y31;
W11=(Y33-Y32.*Y23)./DELTA;
W12=Y32.*Y13./DELTA;
W13=-Y13./DELTA;
W21=Y31.*Y23./DELTA;
W22=(Y33-Y31.*Y13)./DELTA;
W23=-Y23./DELTA;
W31=-Y31./DELTA;
W32=-Y32./DELTA;
W33=-ones(MM,NN)./DELTA;
K11=(H11.*W11+H12.*W21+H13.*W31);
K21=(H21.*W11+H22.*W21+H23.*W31);
K31=(H31.*W11+H32.*W21+H33.*W31);
K12=(H11.*W12+H12.*W22+H13.*W32);
K22=(H21.*W12+H22.*W22+H23.*W32);
K32=(H31.*W12+H32.*W22+H33.*W32);
K13=(H11.*W13+H12.*W23+H13.*W33);
K23=(H21.*W13+H22.*W23+H23.*W33);
```

Reproduced with permission of the copyright owner. Further reproduction prohibited without permission.

```
K33=(H31.*W13+H32.*W23+H33.*W33);
pressure=(g-1)*(.5*u*u*K13-u*K23+K33);
MAG=abs(pressure);
PHA=atan(imag(pressure)./real(pressure))*180/pi;
semilogx(f,20*log(MAG/MAG(1)))
title('Normalized Magnitude Response of Pressure')
xlabel('Frequency, Hz'), ylabel('MAGNITUDE, dB')
pause
semilogx(f,PHA)
title('Phase Response of Pressure')
xlabel('Frequency, Hz'), ylabel('PHASE')
pause
position=Z1.*pressure;
MAG=abs(position);
PHA=atan(imag(position)./real(position))*180/pi;
semilogx(f,20*log(MAG/MAG(1)))
title('Normalized Magnitude Response of Shock Position')
xlabel('Frequency, Hz'), ylabel('MAGNITUDE, dB')
pause
semilogx(f,PHA)
title('Phase Response of Shock Position')
xlabel('Frequency, Hz'), ylabel('PHASE')
end     % of program
```

Reproduced with permission of the copyright owner. Further reproduction prohibited without permission.

```
%   Program:        B_three_wave_mesh
%   Last update:    July 4, 1994
%   Source Code:    Edu-Matlab

echo on; clc ; subplot; hold off; clear
r=0.00136;      g=1.4;
x=0;        L=110/30.48;    m=.78;  Ebar=3350;
N=200;
j=sqrt(-1);
sc=-936:60:936;      % >> 32 pts.
ci=3*sc';
sigma=ones(length(ci),1)*sc;      w=ci*ones(length(sc),1)';
s=sigma+(j*w);
u=m/r;
c=(g*(g-1)*(Ebar-m*m/2/r)/r)^.5;
M=u/c;
p1=-1010; Z01=1010;      R1=-u^2/2;
p2=-1010; Z02=1010;      R2=u;
Z1=(s-p1).\(Z01*ones(s));
Z2=(s-p2).\(Z02*ones(s));
AB=1/2/c/c;
E1=exp(-s*x/u);
E2=exp(-s*x/(u+c));
E3=exp(-s*x/(u-c));
E1L=exp(-s*L/u);
E2L=exp(-s*L/(u+c));
E3L=exp(-s*L/(u-c));
A11=(1-u*u*(g-1)/2/c/c);
A12=(g-1)*u/c/c;
A13=-(g-1)/c/c;
A21=u*(1-u*u*(g-1)/2/c/c);
A22=u*u*(g-1)/c/c;
A23=-(g-1)*u/c/c;
```

Reproduced with permission of the copyright owner. Further reproduction prohibited without permission.

```
A31=u*u*(1-u*u*(g-1)/2/c/c)/2;
A32=u*u*u*(g-1)/2/c/c;
A33=-u*u*(g-1)/2/c/c;
B11=AB*((g-1)*u*u/2-u*c);
B12=AB*(c-(g-1)*u);
B13=AB*(g-1);
B21=(u+c)*AB*((g-1)*u*u/2-u*c);
B22=(u+c)*AB*(c-(g-1)*u);
B23=(u+c)*AB*(g-1);
B31=(.5*u*u+u*c+c*c/(g-1))*AB*((g-1)*u*u/2-u*c);
B32=(.5*u*u+u*c+c*c/(g-1))*AB*(c-(g-1)*u);
B33=(.5*u*u+u*c+c*c/(g-1))*AB*(g-1);
C11=AB*((g-1)*u*u/2+u*c);
C12=-AB*(c+(g-1)*u);
C13=AB*(g-1);
C21=(u-c)*AB*((g-1)*u*u/2+u*c);
C22=-(u-c)*AB*(c+(g-1)*u);
C23=(u-c)*AB*(g-1);
C31=(.5*u*u-u*c+c*c/(g-1))*AB*((g-1)*u*u/2+u*c);
C32=-(.5*u*u-u*c+c*c/(g-1))*AB*(c+(g-1)*u);
C33=(.5*u*u-u*c+c*c/(g-1))*AB*(g-1);
H11=A11*E1+B11*E2+C11*E3;
H12=A12*E1+B12*E2+C12*E3;
H13=A13*E1+B13*E2+C13*E3;
H21=A21*E1+B21*E2+C21*E3;
H22=A22*E1+B22*E2+C22*E3;
H23=A23*E1+B23*E2+C23*E3;
H31=A31*E1+B31*E2+C31*E3;
H32=A32*E1+B32*E2+C32*E3;
H33=A33*E1+B33*E2+C33*E3;
clear E1 E2 E3
F11=A11*E1L+B11*E2L+C11*E3L;
F12=A12*E1L+B12*E2L+C12*E3L;
```

Reproduced with permission of the copyright owner. Further reproduction prohibited without permission.

```
F13=A13*E1L+B13*E2L+C13*E3L;
F21=A21*E1L+B21*E2L+C21*E3L;
F22=A22*E1L+B22*E2L+C22*E3L;
F23=A23*E1L+B23*E2L+C23*E3L;
F31=A31*E1L+B31*E2L+C31*E3L;
F32=A32*E1L+B32*E2L+C32*E3L;
F33=A33*E1L+B33*E2L+C33*E3L;
clear E1L E2L E3L
[MM,NN]=size(s);
Y11=ones(MM,NN);
Y12=zeros(MM,NN);
Y13=-Z1;
Y21=zeros(MM,NN);
Y22=ones(MM,NN);
Y23=-Z2;
Y31=-R1*F11-R2*F21+F31;
Y32=-R1*F12-R2*F22+F32;
Y33=-R1*F13-R2*F23+F33;
DELTA=Y33-Y23.*Y32-Y13.*Y31;
W11=(Y33-Y32.*Y23)./DELTA;
W12=Y32.*Y13./DELTA;
W13=-Y13./DELTA;
W21=Y31.*Y23./DELTA;
W22=(Y33-Y31.*Y13)./DELTA;
W23=-Y23./DELTA;
W31=-Y31./DELTA;
W32=-Y32./DELTA;
W33=-ones(MM,NN)./DELTA;
K11=(H11.*W11+H12.*W21+H13.*W31);
K21=(H21.*W11+H22.*W21+H23.*W31);
K31=(H31.*W11+H32.*W21+H33.*W31);
K12=(H11.*W12+H12.*W22+H13.*W32);
K22=(H21.*W12+H22.*W22+H23.*W32);
```

Reproduced with permission of the copyright owner. Further reproduction prohibited without permission.

```
K32=(H31.*W12+H32.*W22+H33.*W32);
K13=(H11.*W13+H12.*W23+H13.*W33);
K23=(H21.*W13+H22.*W23+H23.*W33);
K33=(H31.*W13+H32.*W23+H33.*W33);
PRESSURE=(g-1)*(.5*u*u*K13-u*K23+K33);
MAG=abs(PRESSURE);
levels=30;
mesh(20*log(MAG)),pause, contour(20*log(MAG),levels, sc,3*sc)
xlabel('Real(s)'), ylabel('Imag(s)')
title('Contours of Equal Magnitude of Pressure')
pause
position=Z1.*PRESSURE;
MAG=abs(position);
levels=30;
mesh(20*log(MAG)),pause, contour(20*log(MAG),levels, sc,3*sc)
xlabel('Real(s)'), ylabel('Imag(s)')
title('Contours of Equal Magnitude of Shock Position')
end % of loop
end     % of program
```

Reproduced with permission of the copyright owner. Further reproduction prohibited without permission.

```
%   Program:        C_two_wave_Blocks
%   Last update:    July 4, 1994
%   Source code:    Edu-Matlab

clear
echo off
clc
subplot
hold off
u1=1554.45;
r1=0.00065866;
c1=936.38;
g1=1.4;
u2=586.23;
r2=0.0013492;
c2=1140.62;
g2=1.4;
L1=28/30.48;
L=110/30.48;
L2=L-L1;
x=0;    % Location of shock
d1=0;
d2=3;
N=200;
p=-1010;
R=6*1e-6;  Z0=1e6;
w=2*pi*logspace(d1,d2,N);
j=sqrt(-1);
f=w/2/pi;
s=j*w;
cu1=c1*c1-u1*u1;
cu2=c2*c2-u2*u2;
usL1=u1.*s*L1/cu1;
```

Reproduced with permission of the copyright owner. Further reproduction prohibited without permission.

```
usL2=u2.*s*L2/cu2;
usL=usL1+usL2;
usx1=u1.*s*x/cu1;
usx2=u2.*s*x/cu2;
u2sL1=u2.*s*L1/cu2;
csL1=c1.*s*L1/cu1;
csL2=c2.*s*L2/cu2;
csx1=c1.*s*x/cu1;
csx2=c2.*s*x/cu2;
c2sL1=c2.*s*L1/cu2;
F11=exp(usL).*(r1*c2/r2/c1*sinh(csL1).*sinh(csL2)+
cosh(csL1).*cosh(csL2));
F12=exp(usL).*(-c1/r1*sinh(csL1).*cosh(csL2)-
c2/r2*sinh(csL2).*cosh(csL1));
F21=exp(usL).*(-r2/c2*sinh(csL2).*cosh(csL1)-
r1/c1*sinh(csL1).*cosh(csL2));
F22=exp(usL).*(r2*c1/r1/c2*sinh(csL1).*sinh(csL2)+
cosh(csL1).*cosh(csL2));
Z=(s-p).\(Z0*ones(s));
den=F22-R*F12+Z.*(F21-R*F11);
clear F11 F12 F21 F22
if x>=0 & x<L1,
E1=(r2*c1/r1/c2*cosh(csx1)-
R*c2/r2*sinh(csx1)).*sinh(csL1).*sinh(csL2);
E2=(cosh(csx1)-c1*R/r1*sinh(csx1)).*cosh(csL1).*cosh(csL2);
E3=(R*c2/r2*cosh(csx1)-
r2*c1/r1/c2*sinh(csx1)).*sinh(csL2).*cosh(csL1);
E4=(R*c1/r1*cosh(csx1)-sinh(csx1)).*sinh(csL1).*cosh(csL2);
W1=exp(usL+usx1)./den.*(E1+E2+E3+E4);
W2=exp(usx1)./den.*(Z.*cosh(csx1)-c1/r1.*sinh(csx1));
E1=(-r2/c2*sinh(csx1)+
R*r1*c2/r2/c1*cosh(csx1)).*sinh(csL1).*sinh(csL2);
E2=(-c1/r1*sinh(csx1)+R*cosh(csx1)).*cosh(csL1).*cosh(csL2);
```

Reproduced with permission of the copyright owner. Further reproduction prohibited without permission.

```
E3=(-R*r2*c1/r1/c2*sinh(csx1)+
r2/c2.*cosh(csx1)).*sinh(csL2).*cosh(csL1);
E4=(-R*sinh(csx1)+r1/c1*cosh(csx1)).*sinh(csL1).*cosh(csL2);
W3=exp(usL+usx1)./den.*(E1+E2+E3+E4);
W4=exp(usx1)./den.*(-Z*r1/c1.*sinh(csx1)+cosh(csx1));
clear E3 E4
E1=(R*cosh(csx1).*Z-R*c1/r1*sinh(csx1)).*cosh(csL2);
E2=-r2/c2*sinh(csL2).*(-cosh(csx1).*Z+c1/r1*sinh(csx1));
Y1=exp(usx1+usL2)./den.*(E1+E2);
E1=-c2/r2*sinh(csL2).*(R*cosh(csx1).*Z-R*c1/r1*sinh(csx1));
E2=cosh(csL2).*(-cosh(csx1).*Z+c1/r1*sinh(csx1));
Y2=exp(usx1+usL2)./den.*(E1+E2);
E1=(-R*Z*r1/c1.*sinh(csx1)+R*cosh(csx1)).*cosh(csL2);
E2=-r2/c2*sinh(csL2).*(Z*r1/c1.*sinh(csx1)-cosh(csx1));
Y3=exp(usx1+usL2)./den.*(E1+E2);
E1=-c2/r2*sinh(csL2).*(-R*Z*r1/c1.*sinh(csx1)+R*cosh(csx1));
E2=(Z*r1/c1.*sinh(csx1)-cosh(csx1)).*cosh(csL2);
Y4=exp(usx1+usL2)./den.*(E1+E2);
pressure=(1-g1)*(.5*u1*u1*W2+r1*u1*W4);
MAG=abs(pressure);
PHA=atan(imag(pressure)./real(pressure))*180/pi;
semilogx(f,20*log(MAG/MAG(1)))
title('Normalized Magnitude Response of Pressure')
xlabel('Frequency, Hz'), ylabel('MAGNITUDE, dB')
pause
semilogx(f,PHA)
title('Phase Response of Pressure')
xlabel('Frequency, Hz'), ylabel('PHASE')
pause
position=Z.*pressure;
MAG=abs(position);
PHA=atan(imag(position)./real(position))*180/pi;
semilogx(f,20*log(MAG/MAG(1)))
```

Reproduced with permission of the copyright owner. Further reproduction prohibited without permission.

```
title('Normalized Magnitude Response of Shock Position')
xlabel('Frequency, Hz'), ylabel('MAGNITUDE, dB')
pause
semilogx(f,PHA)
title('Phase Response of Shock Position')
xlabel('Frequency, Hz'), ylabel('PHASE')
elseif x>=L1 & x<=L,
E1=(r2*c1/r1/c2*cosh(csL1)-
R*c2/r2*sinh(csL1)).*sinh(csL1).*sinh(csL2);
E2=(cosh(csL1)-c1*R/r1*sinh(csL1)).*cosh(csL1).*cosh(csL2);
E3=(R*c2/r2*cosh(csL1)-
r2*c1/r1/c2*sinh(csL1)).*sinh(csL2).*cosh(csL1);
E4=(R*c1/r1*cosh(csL1)-sinh(csL1)).*sinh(csL1).*cosh(csL2);
W1L=exp(usL+usL1)./den.*(E1+E2+E3+E4);
W2L=exp(usL1)./den.*(Z.*cosh(csL1)-c1/r1.*sinh(csL1));
E1=(-r2/c2*sinh(csL1)+
R*r1*c2/r2/c1*cosh(csL1)).*sinh(csL1).*sinh(csL2);
E2=(-c1/r1*sinh(csL1)+R*cosh(csL1)).*cosh(csL1).*cosh(csL2);
E3=(-R*r2*c1/r1/c2*sinh(csL1)+
r2/c2*cosh(csL1)).*sinh(csL2).*cosh(csL1);
E4=(-R*sinh(csL1)+r1/c1*cosh(csL1)).*sinh(csL1).*cosh(csL2);
W3L=exp(usL+usL1)./den.*(E1+E2+E3+E4);
W4L=exp(usL1)./den.*(-Z*r1/c1.*sinh(csL1)+cosh(csL1));
P1=exp(usx2-u2sL1).*(cosh(csx2-c2sL1).*W1L-
c2/r2*sinh(csx2-c2sL1).*W3L);
P2=exp(usx2-u2sL1).*(cosh(csx2-c2sL1).*W2L-
c2/r2*sinh(csx2-c2sL1).*W4L);
P3=exp(usx2-u2sL1).*(-r2/c2*sinh(csx2-c2sL1).*W1L+
cosh(csx2-c2sL1).*W3L);
P4=exp(usx2-u2sL1).*(-r2/c2*sinh(csx2-c2sL1).*W2L+
cosh(csx2-c2sL1).*W4L);
S1=exp(usx2-u2sL1).*cosh(csx2-
c2sL1)+exp(usL2).*P2.*(R*cosh(csL2)+r2/c2*sinh(csL2));
```

Reproduced with permission of the copyright owner. Further reproduction prohibited without permission.

```
S2=-c2/r2*exp(usx2-u2sL1).*sinh(csx2-c2sL1)-
exp(usL2).*P2.*(R*c2/r2*sinh(csL2)+cosh(csL2));
S3=-r2/c2*exp(usx2-u2sL1).*sinh(csx2-
c2sL1)+exp(usL2).*P4.*(R*cosh(csL2)+r2/c2*cosh(csL2));
S4=exp(usx2-u2sL1).*cosh(csx2-c2sL1)-
exp(usL2).*P4.*(R*c2/r2*sinh(csL2)+cosh(csL2));
pressure=(1-g2)*(.5*u2*u2*P2+r2*u2*P4);
MAG=abs(pressure);
PHA=atan(imag(pressure)./real(pressure))*180/pi;
semilogx(f,20*log(MAG/MAG(1)))
title('Normalized Magnitude Response of Pressure')
xlabel('Frequency, Hz'), ylabel('MAGNITUDE, dB')
pause
semilogx(f,PHA)
title('Phase Response of Pressure')
xlabel('Frequency, Hz'), ylabel('PHASE')
pause
position=Z.*pressure;
MAG=abs(position);
PHA=atan(imag(position)./real(position))*180/pi;
semilogx(f,20*log(MAG/MAG(1)))
title('Normalized Magnitude Response for Shock Position')
xlabel('Frequency, Hz'), ylabel('MAGNITUDE, dB')
pause
semilogx(f,PHA)
title('Phase Response for Shock Position')
xlabel('Frequency, Hz'), ylabel('PHASE')
end   % of if loop
end     % of program
```

Reproduced with permission of the copyright owner. Further reproduction prohibited without permission.

```
%   Program:        C_three_wave_Blocks
%   Last update:    July 4, 1994
%   Source code:    Edu-Matlab

clear
echo off
casesen on
clc
subplot
hold off
u1=800;     r1=0.002;     c1=1000;     g1=1.4;
u2=586.23;  r2=0.0013492; c2=1140.62;  g2=1.4;
% u1=u2; r1=r2; c1=c2; g1=1.4; % Check results with Green's Function
x=0;        L=110/30.48;  L1=28/30.48;  L2=L-L1;
N=300;   d1=-3;  d2=3;
w=2*pi*logspace(d1,d2,N);
j=sqrt(-1);    s=j*w;    f=w/2/pi;
p1=-300;  Z01=1;  R1=-1e4;
p2=-1000; Z02=1;  R2=500;
Z1=(s-p1).\(Z01*ones(s));       Z2=(s-p2).\(Z02*ones(s));
AB1=1/2/c1/c1;
AB2=1/2/c2/c2;
A11=(1-u1*u1*(g1-1)/2/c1/c1);
A12=(g1-1)*u1/c1/c1;
A13=-(g1-1)/c1/c1;
A21=u1*(1-u1*u1*(g1-1)/2/c1/c1);
A22=u1*u1*(g1-1)/c1/c1;
A23=-(g1-1)*u1/c1/c1;
A31=u1*u1*(1-u1*u1*(g1-1)/2/c1/c1)/2;
A32=u1*u1*u1*(g1-1)/2/c1/c1;
A33=-u1*u1*(g1-1)/2/c1/c1;
At11=(1-u2*u2*(g2-1)/2/c2/c2);
At12=(g2-1)*u2/c2/c2;
```

Reproduced with permission of the copyright owner. Further reproduction prohibited without permission.

```
At13=-(g2-1)/c2/c2;
At21=u2*(1-u2*u2*(g2-1)/2/c2/c2);
At22=u2*u2*(g2-1)/c2/c2;
At23=-(g2-1)*u2/c2/c2;
At31=u2*u2*(1-u2*u2*(g2-1)/2/c2/c2)/2;
At32=u2*u2*u2*(g2-1)/2/c2/c2;
At33=-u2*u2*(g2-1)/2/c2/c2;
B11=AB1*((g1-1)*u1*u1/2-u1*c1);
B12=AB1*(c1-(g1-1)*u1);
B13=AB1*(g1-1);
B21=(u1+c1)*AB1*((g1-1)*u1*u1/2-u1*c1);
B22=(u1+c1)*AB1*(c1-(g1-1)*u1);
B23=(u1+c1)*AB1*(g1-1);
B31=(.5*u1*u1+u1*c1+c1*c1/(g1-1))*AB1*((g1-1)*u1*u1/2-u1*c1);
B32=(.5*u1*u1+u1*c1+c1*c1/(g1-1))*AB1*(c1-(g1-1)*u1);
B33=(.5*u1*u1+u1*c1+c1*c1/(g1-1))*AB1*(g1-1);
Bt11=AB2*((g2-1)*u2*u2/2-u2*c2);
Bt12=AB2*(c2-(g2-1)*u2);
Bt13=AB2*(g2-1);
Bt21=(u2+c2)*AB2*((g2-1)*u2*u2/2-u2*c2);
Bt22=(u2+c2)*AB2*(c2-(g2-1)*u2);
Bt23=(u2+c2)*AB2*(g2-1);
Bt31=(.5*u2*u2+u2*c2+c2*c2/(g2-1))*AB2*((g2-1)*u2*u2/2-u2*c2);
Bt32=(.5*u2*u2+u2*c2+c2*c2/(g2-1))*AB2*(c2-(g2-1)*u2);
Bt33=(.5*u2*u2+u2*c2+c2*c2/(g2-1))*AB2*(g2-1);
C11=AB1*((g1-1)*u1*u1/2+u1*c1);
C12=-AB1*(c1+(g1-1)*u1);
C13=AB1*(g1-1);
C21=(u1-c1)*AB1*((g1-1)*u1*u1/2+u1*c1);
C22=-(u1-c1)*AB1*(c1+(g1-1)*u1);
C23=(u1-c1)*AB1*(g1-1);
C31=(.5*u1*u1-u1*c1+c1*c1/(g1-1))*AB1*((g1-1)*u1*u1/2+u1*c1);
C32=-(.5*u1*u1-u1*c1+c1*c1/(g1-1))*AB1*(c1+(g1-1)*u1);
```

Reproduced with permission of the copyright owner. Further reproduction prohibited without permission.

```
C33=(.5*u1*u1-u1*c1+c1*c1/(g1-1))*AB1*(g1-1);
Ct11=AB2*((g2-1)*u2*u2/2+u2*c2);
Ct12=-AB2*(c2+(g2-1)*u2);
Ct13=AB2*(g2-1);
Ct21=(u2-c2)*AB2*((g2-1)*u2*u2/2+u2*c2);
Ct22=-(u2-c2)*AB2*(c2+(g2-1)*u2);
Ct23=(u2-c2)*AB2*(g2-1);
Ct31=(.5*u2*u2-u2*c2+c2*c2/(g2-1))*AB2*((g2-1)*u2*u2/2+u2*c2);
Ct32=-(.5*u2*u2-u2*c2+c2*c2/(g2-1))*AB2*(c2+(g2-1)*u2);
Ct33=(.5*u2*u2-u2*c2+c2*c2/(g2-1))*AB2*(g2-1);
%  Compute H1(s,x)=[h]
E1x=exp(-s*x/u1);
E2x=exp(-s*x/(u1+c1));
E3x=exp(-s*x/(u1-c1));
h11=A11*E1x+B11*E2x+C11*E3x;
h12=A12*E1x+B12*E2x+C12*E3x;
h13=A13*E1x+B13*E2x+C13*E3x;
h21=A21*E1x+B21*E2x+C21*E3x;
h22=A22*E1x+B22*E2x+C22*E3x;
h23=A23*E1x+B23*E2x+C23*E3x;
h31=A31*E1x+B31*E2x+C31*E3x;
h32=A32*E1x+B32*E2x+C32*E3x;
h33=A33*E1x+B33*E2x+C33*E3x;
%  Compute H1(s,L1)=[c]
E1L1=exp(-s*L1/u1);
E2L1=exp(-s*L1/(u1+c1));
E3L1=exp(-s*L1/(u1-c1));
c11=A11*E1L1+B11*E2L1+C11*E3L1;
c12=A12*E1L1+B12*E2L1+C12*E3L1;
c13=A13*E1L1+B13*E2L1+C13*E3L1;
c21=A21*E1L1+B21*E2L1+C21*E3L1;
c22=A22*E1L1+B22*E2L1+C22*E3L1;
c23=A23*E1L1+B23*E2L1+C23*E3L1;
```

Reproduced with permission of the copyright owner. Further reproduction prohibited without permission.

```
c31=A31*E1L1+B31*E2L1+C31*E3L1;
c32=A32*E1L1+B32*E2L1+C32*E3L1;
c33=A33*E1L1+B33*E2L1+C33*E3L1;
%  Compute H2(s,L2)=[d]
Et1L2=exp(-s*L2/u2);
Et2L2=exp(-s*L2/(u2+c2));
Et3L2=exp(-s*L2/(u2-c2));
d11=At11*Et1L2+Bt11*Et2L2+Ct11*Et3L2;
d12=At12*Et1L2+Bt12*Et2L2+Ct12*Et3L2;
d13=At13*Et1L2+Bt13*Et2L2+Ct13*Et3L2;
d21=At21*Et1L2+Bt21*Et2L2+Ct21*Et3L2;
d22=At22*Et1L2+Bt22*Et2L2+Ct22*Et3L2;
d23=At23*Et1L2+Bt23*Et2L2+Ct23*Et3L2;
d31=At31*Et1L2+Bt31*Et2L2+Ct31*Et3L2;
d32=At32*Et1L2+Bt32*Et2L2+Ct32*Et3L2;
d33=At33*Et1L2+Bt33*Et2L2+Ct33*Et3L2;
F11=d11.*c11+d12.*c21+d13.*c31;
F21=d21.*c11+d22.*c21+d23.*c31;
F31=d31.*c11+d32.*c21+d33.*c31;
F12=d11.*c12+d12.*c22+d13.*c32;
F22=d21.*c12+d22.*c22+d23.*c32;
F32=d31.*c12+d32.*c22+d33.*c32;
F13=d11.*c13+d12.*c23+d13.*c33;
F23=d21.*c13+d22.*c23+d23.*c33;
F33=d31.*c13+d32.*c23+d33.*c33;
[MM,NN]=size(s);
y11=ones(MM,NN);
y12=zeros(MM,NN);
y13=-Z1;
y21=zeros(MM,NN);
y22=ones(MM,NN);
y23=-Z2;
y31=-R1*F11-R2*F21+F31;
```

Reproduced with permission of the copyright owner. Further reproduction prohibited without permission.

```
y32=-R1*F12-R2*F22+F32;
y33=-R1*F13-R2*F23+F33;
DELTA=y33-y23.*y32-y13.*y31;
I11=(y33-y32.*y23)./DELTA;
I12=y32.*y13./DELTA;
I13=-y13./DELTA;
I21=y31.*y23./DELTA;
I22=(y33-y31.*y13)./DELTA;
I23=-y23./DELTA;
I31=-y31./DELTA;
I32=-y32./DELTA;
I33=-ones(MM,NN)./DELTA;
if x>=0 & x<L1,
% compute Q1(s,x) = [W] Z(s) + [Y] dQ(s)
W11=h11.*I11+h12.*I21+h13.*I31;
W21=h21.*I11+h22.*I21+h23.*I31;
W31=h31.*I11+h32.*I21+h33.*I31;
W12=h11.*I12+h12.*I22+h13.*I32;
W22=h21.*I12+h22.*I22+h23.*I32;
W32=h31.*I12+h32.*I22+h33.*I32;
W13=h11.*I13+h12.*I23+h13.*I33;
W23=h21.*I13+h22.*I23+h23.*I33;
W33=h31.*I13+h32.*I23+h33.*I33;
%  Non-zero elements of G
G31=-R1*d11-R2*d21+d31;
G32=-R1*d12-R2*d22+d32;
G33=-R1*d13-R2*d23+d33;
%  Compute [Y]
Y11=-W13.*G31;
Y12=-W13.*G32;
Y13=-W13.*G33;
Y21=-W23.*G31;
Y22=-W23.*G32;
```

Reproduced with permission of the copyright owner. Further reproduction prohibited without permission.

```
Y23=-W23.*G33;
Y31=-W33.*G31;
Y32=-W33.*G32;
Y33=-W33.*G33;
pressure_F=(g1-1)*(.5*u1*u1*Y13-u1*Y23+Y33);
pressure_Q=(g1-1)*(.5*u1*u1*W13-u1*W23+W33);
elseif x>=L1 & x<=L,
% next compute Q2(s,x)
%  Compute H2(s,x-L1)=[e]
Et1xL1=exp(-s*(x-L1)/u2);
Et2xL1=exp(-s*(x-L1)/(u2+c2));
Et3xL1=exp(-s*(x-L1)/(u2-c2));
e11=At11*Et1xL1+Bt11*Et2xL1+Ct11*Et3xL1;
e12=At12*Et1xL1+Bt12*Et2xL1+Ct12*Et3xL1;
e13=At13*Et1xL1+Bt13*Et2xL1+Ct13*Et3xL1;
e21=At21*Et1xL1+Bt21*Et2xL1+Ct21*Et3xL1;
e22=At22*Et1xL1+Bt22*Et2xL1+Ct22*Et3xL1;
e23=At23*Et1xL1+Bt23*Et2xL1+Ct23*Et3xL1;
e31=At31*Et1xL1+Bt31*Et2xL1+Ct31*Et3xL1;
e32=At32*Et1xL1+Bt32*Et2xL1+Ct32*Et3xL1;
e33=At33*Et1xL1+Bt33*Et2xL1+Ct33*Et3xL1;
%  Compute [p]=[c]*[I]
p11=c11.*I11+c12.*I21+c13.*I31;
p21=c21.*I11+c22.*I21+c23.*I31;
p31=c31.*I11+c32.*I21+c33.*I31;
p12=c11.*I12+c12.*I22+c13.*I32;
p22=c21.*I12+c22.*I22+c23.*I32;
p32=c31.*I12+c32.*I22+c33.*I32;
p13=c11.*I13+c12.*I23+c13.*I33;
p23=c21.*I13+c22.*I23+c23.*I33;
p33=c31.*I13+c32.*I23+c33.*I33;
%  Compute [P]
P11=e11.*p11+e12.*p21+e13.*p31;
```

Reproduced with permission of the copyright owner. Further reproduction prohibited without permission.

```
P21=e21.*p11+e22.*p21+e23.*p31;
P31=e31.*p11+e32.*p21+e33.*p31;
P12=e11.*p12+e12.*p22+e13.*p32;
P22=e21.*p12+e22.*p22+e23.*p32;
P32=e31.*p12+e32.*p22+e33.*p32;
P13=e11.*p13+e12.*p23+e13.*p33;
P23=e21.*p13+e22.*p23+e23.*p33;
P33=e31.*p13+e32.*p23+e33.*p33;
%  Non-zero elements of Q
q31=-R1*d11-R2*d31+d31;
q32=-R1*d12-R2*d32+d32;
q33=-R1*d13-R2*d33+d33;
%  Compute [S]
S11=e11-P13.*q31;
S12=e12-P13.*q32;
S13=e13-P13.*q33;
S21=e21-P23.*q31;
S22=e22-P23.*q32;
S23=e23-P23.*q33;
S31=e31-P33.*q31;
S32=e32-P33.*q32;
S33=e33-P33.*q33;
pressure_F=(g2-1)*(.5*u2*u2*P13-u2*P23+P33);
pressure_Q=(g2-1)*(.5*u2*u2*S13-u2*S23+S33);
end   % of if loop
MAG=abs(pressure_F);
PHA=atan(imag(pressure_F)./real(pressure_F))*180/pi;
% To check Green's Function:
% MAG=abs(pressure_Q);
%  PHA=atan(imag(pressure_Q)./real(pressure_Q))*180/pi;
semilogx(f,20*log(MAG/MAG(1)))
title('Normalized Magnitude Response of Pressure')
xlabel('Frequency, Hz'), ylabel('MAGNITUDE, dB')
```

Reproduced with permission of the copyright owner. Further reproduction prohibited without permission.

```
pause
semilogx(f,PHA)
title('Phase Response of Pressure')
xlabel('Frequency, Hz'), ylabel('PHASE')
pause
position_F=Z1.*pressure_F;
position_Q=Z1.*pressure_Q;
MAG=abs(position_F);
PHA=atan(imag(position_F)./real(position_F))*180/pi;
% To check Green's Function:
% MAG=abs(position_Q);
%  PHA=atan(imag(position_Q)./real(position_Q))*180/pi;
semilogx(f,20*log(MAG/MAG(1)))
title('Normalized Magnitude Response of Shock Position')
xlabel('Frequency, Hz'), ylabel('MAGNITUDE, dB')
pause
semilogx(f,PHA)
title('Phase Response of Shock Position')
xlabel('Frequency, Hz'), ylabel('PHASE')
end     % of program
```

Reproduced with permission of the copyright owner. Further reproduction prohibited without permission.

```
%   Program:        D_two_wave_Green
%   Last update:    July 4, 1994
%   Source Code:    Edu-Matlab

clear
echo off
clc
subplot
hold off
u=586.23;
r=0.0013492;
c=1140.62;
g=1.4;
x=0;
ksi=28/30.48;
L=110/30.48;
d1=0;
d2=4;
N=300;
w=2*pi*logspace(d1,d2,N);
f=w/2/pi;
j=sqrt(-1);
s=j*w;
Z0=1010;
R=-2*r*u;
p=-300;
Z=(s-p).\(Z0*ones(s));
xL=x-L;
xksi=x-ksi;
Lksi=L-ksi;
cu=c*c-u*u;
csx=c.*s*x/cu;
csL=c.*s*L/cu;
```

Reproduced with permission of the copyright owner. Further reproduction prohibited without permission.

```
csxL=c.*s*xL/cu;
usL=u.*s*L/cu;
csLksi=c.*s*Lksi/cu;
csxksi=c.*s*xksi/cu;
Kn=exp(u*s*xksi/cu);
Kd=exp(u*s*ksi/cu);
if x>=0 & x<ksi,
den=(1-Z.*R).*cosh(csL)+(R*c/r-Z.*r/c).*sinh(csL);
E=(Z.*cosh(csx)-c/r*sinh(csx)).*(R*cosh(csLksi)+r/c.*sinh(csLksi));
g11t=Kn.*E./den;
E=(Z.*cosh(csx)-c/r*sinh(csx)).*(cosh(csLksi)+R*c/r.*sinh(csLksi));
g12t=Kn.*E./den;
E=(cosh(csx)-Z*r/c.*sinh(csx)).*(R*cosh(csLksi)+r/c*sinh(csLksi));
g21t=Kn.*E./den;
E=(cosh(csx)-Z*c/r.*sinh(csx)).*(cosh(csLksi)+R*c/r*sinh(csLksi));
g22t=-Kn.*E./den;
g11=g11t;g12=g12t;g21=g21t;g22=g22t;
clear E g11h g12h g21h g22h
elseif x>=ksi & x<=L,
g11h=(Kn.*cosh(csxksi)+Z.*(R*cosh(csLksi)+
r/c*sinh(csLksi))))./Kd./den;
g12h=(-c/r*Kn.*sinh(csxksi)-
Z.*(R*c/r*sinh(csLksi)+cosh(csLksi))))./Kd./den;
g21h=(-r/c*Kn.*sinh(csxksi)+
(R*cosh(csLksi)+r/c*sinh(csLksi))))./Kd./den;
g22h=(Kn.*cosh(csxksi)-
(R*c/r*sinh(csLksi)+cosh(csLksi))))./Kd./den;
g11=g11h;g12=g12h;g21=g21h;g22=g22h;
clear g11h g12h g21h g22h
end   % of if loop
pressure=(g-1)*(-.5*u*u*g22-r*u*g12);
MAG=abs(pressure);
PHA=atan(imag(pressure)./real(pressure))*180/pi;
```

Reproduced with permission of the copyright owner. Further reproduction prohibited without permission.

```
semilogx(f,20*log(MAG/MAG(1)))
title('Normalized Magnitude Response of Pressure')
xlabel('Frequency, Hz'), ylabel('MAGNITUDE, dB')
pause
semilogx(f,PHA)
title('Phase Response of Pressure')
xlabel('Frequency, Hz'), ylabel('PHASE')
pause
position=Z.*pressure;
MAG=abs(position);
PHA=atan(imag(position)./real(position))*180/pi;
semilogx(f,20*log(MAG/MAG(1)))
title('Normalized Magnitude Response of Shock Position')
xlabel('Frequency, Hz'), ylabel('MAGNITUDE, dB')
pause
semilogx(f,PHA)
title('Phase Response of Shock Position')
xlabel('Frequency, Hz'), ylabel('PHASE')
end     % of program
```

Reproduced with permission of the copyright owner. Further reproduction prohibited without permission.

```
%   Program:        D_three_wave_Green
%   Last update:    July 4, 1994
%   Source code:    Edu-Matlab

clear; echo off; casesen on; clc; subplot; hold off
u=586.23; c=1140.62; g=1.4; x=0; L=110/30.48; ksi=28/30.48;
Lksi=L-ksi;
N=500;   d1=-1;  d2=3;  w=2*pi*logspace(d1,d2,N);
j=sqrt(-1);   s=j*w;   f=w/2/pi;
p1=-300;   Z01=1010;  R1=-u^2/2;
p2=-1000;  Z02=1010;  R2=u;
Z1=(s-p1).\(Z01*ones(s));     Z2=(s-p2).\(Z02*ones(s));
%   Define system matrices A, B, C
AB=1/2/c/c;
A11=(1-u*u*(g-1)/2/c/c);
A12=(g-1)*u/c/c;
A13=-(g-1)/c/c;
A21=u*(1-u*u*(g-1)/2/c/c);
A22=u*u*(g-1)/c/c;
A23=-(g-1)*u/c/c;
A31=u*u*(1-u*u*(g-1)/2/c/c)/2;
A32=u*u*u*(g-1)/2/c/c;
A33=-u*u*(g-1)/2/c/c;
B11=AB*((g-1)*u*u/2-u*c);
B12=AB*(c-(g-1)*u);
B13=AB*(g-1);
B21=(u+c)*AB*((g-1)*u*u/2-u*c);
B22=(u+c)*AB*(c-(g-1)*u);
B23=(u+c)*AB*(g-1);
B31=(.5*u*u+u*c+c*c/(g-1))*AB*((g-1)*u*u/2-u*c);
B32=(.5*u*u+u*c+c*c/(g-1))*AB*(c-(g-1)*u);
B33=(.5*u*u+u*c+c*c/(g-1))*AB*(g-1);
C11=AB*((g-1)*u*u/2+u*c);
```

Reproduced with permission of the copyright owner. Further reproduction prohibited without permission.

```
C12=-AB*(c+(g-1)*u);
C13=AB*(g-1);
C21=(u-c)*AB*((g-1)*u*u/2+u*c);
C22=-(u-c)*AB*(c+(g-1)*u);
C23=(u-c)*AB*(g-1);
C31=(.5*u*u-u*c+c*c/(g-1))*AB*((g-1)*u*u/2+u*c);
C32=-(.5*u*u-u*c+c*c/(g-1))*AB*(c+(g-1)*u);
C33=(.5*u*u-u*c+c*c/(g-1))*AB*(g-1);
%   Compute H(s,x)=[h]
E1x=exp(-s*x/u);
E2x=exp(-s*x/(u+c));
E3x=exp(-s*x/(u-c));
h11=A11*E1x+B11*E2x+C11*E3x;
h12=A12*E1x+B12*E2x+C12*E3x;
h13=A13*E1x+B13*E2x+C13*E3x;
h21=A21*E1x+B21*E2x+C21*E3x;
h22=A22*E1x+B22*E2x+C22*E3x;
h23=A23*E1x+B23*E2x+C23*E3x;
h31=A31*E1x+B31*E2x+C31*E3x;
h32=A32*E1x+B32*E2x+C32*E3x;
h33=A33*E1x+B33*E2x+C33*E3x;
%   Compute H(s,L)=[F]
E1L=exp(-s*L/u);
E2L=exp(-s*L/(u+c));
E3L=exp(-s*L/(u-c));
F11=A11*E1L+B11*E2L+C11*E3L;
F12=A12*E1L+B12*E2L+C12*E3L;
F13=A13*E1L+B13*E2L+C13*E3L;
F21=A21*E1L+B21*E2L+C21*E3L;
F22=A22*E1L+B22*E2L+C22*E3L;
F23=A23*E1L+B23*E2L+C23*E3L;
F31=A31*E1L+B31*E2L+C31*E3L;
F32=A32*E1L+B32*E2L+C32*E3L;
```

Reproduced with permission of the copyright owner. Further reproduction prohibited without permission.

```
F33=A33*E1L+B33*E2L+C33*E3L;
[MM,NN]=size(s);
y11=ones(MM,NN);
y12=zeros(MM,NN);
y13=-Z1;
y21=zeros(MM,NN);
y22=ones(MM,NN);
y23=-Z2;
y31=-R1*F11-R2*F21+F31;
y32=-R1*F12-R2*F22+F32;
y33=-R1*F13-R2*F23+F33;
%   Compute inv[M(s)+N(s)H(s,L)]=[I]
DELTA=y33-y23.*y32-y13.*y31;
I11=(y33-y32.*y23)./DELTA;
I12=y32.*y13./DELTA;
I13=-y13./DELTA;
I21=y31.*y23./DELTA;
I22=(y33-y31.*y13)./DELTA;
I23=-y23./DELTA;
I31=-y31./DELTA;
I32=-y32./DELTA;
I33=-ones(MM,NN)./DELTA;
%   Compute K(s,x)
K11=h11.*I11+h12.*I21+h13.*I31;
K21=h21.*I11+h22.*I21+h23.*I31;
K31=h31.*I11+h32.*I21+h33.*I31;
K12=h11.*I12+h12.*I22+h13.*I32;
K22=h21.*I12+h22.*I22+h23.*I32;
K32=h31.*I12+h32.*I22+h33.*I32;
K13=h11.*I13+h12.*I23+h13.*I33;
K23=h21.*I13+h22.*I23+h23.*I33;
K33=h31.*I13+h32.*I23+h33.*I33;
%   Compute H(s,L-ksi)=[d]
```

Reproduced with permission of the copyright owner. Further reproduction prohibited without permission.

```
E1Lksi=exp(-s*Lksi/u);
E2Lksi=exp(-s*Lksi/(u+c));
E3Lksi=exp(-s*Lksi/(u-c));
d11=A11*E1Lksi+B11*E2Lksi+C11*E3Lksi;
d12=A12*E1Lksi+B12*E2Lksi+C12*E3Lksi;
d13=A13*E1Lksi+B13*E2Lksi+C13*E3Lksi;
d21=A21*E1Lksi+B21*E2Lksi+C21*E3Lksi;
d22=A22*E1Lksi+B22*E2Lksi+C22*E3Lksi;
d23=A23*E1Lksi+B23*E2Lksi+C23*E3Lksi;
d31=A31*E1Lksi+B31*E2Lksi+C31*E3Lksi;
d32=A32*E1Lksi+B32*E2Lksi+C32*E3Lksi;
d33=A33*E1Lksi+B33*E2Lksi+C33*E3Lksi;
% Non-zero elements of [W]
W31=-R1*d11-R2*d21+d31;
W32=-R1*d12-R2*d22+d32;
W33=-R1*d13-R2*d23+d33;
if x>=0 & x<ksi,
% Compute [G]
G11=-K13.*W31;
G12=-K13.*W32;
G13=-K13.*W33;
G21=-K23.*W31;
G22=-K23.*W32;
G23=-K23.*W33;
G31=-K33.*W31;
G32=-K33.*W32;
G33=-K33.*W33;
pressure=(g-1)*(.5*u*u*G13-u*G23+G33);
elseif x>=ksi & x<=L,
% Compute H(s,x-ksi)=[e]
E1xksi=exp(-s*(x-ksi)/u);
E2xksi=exp(-s*(x-ksi)/(u+c));
E3xksi=exp(-s*(x-ksi)/(u-c));
```

Reproduced with permission of the copyright owner. Further reproduction prohibited without permission.

```
e11=A11*E1xksi+B11*E2xksi+C11*E3xksi;
e12=A12*E1xksi+B12*E2xksi+C12*E3xksi;
e13=A13*E1xksi+B13*E2xksi+C13*E3xksi;
e21=A21*E1xksi+B21*E2xksi+C21*E3xksi;
e22=A22*E1xksi+B22*E2xksi+C22*E3xksi;
e23=A23*E1xksi+B23*E2xksi+C23*E3xksi;
e31=A31*E1xksi+B31*E2xksi+C31*E3xksi;
e32=A32*E1xksi+B32*E2xksi+C32*E3xksi;
e33=A33*E1xksi+B33*E2xksi+C33*E3xksi;
% Compute [Gt]
Gt11=e11-I13.*W31;
Gt12=e12-I13.*W32;
Gt13=e13-I13.*W33;
Gt21=e21-I23.*W31;
Gt22=e22-I23.*W32;
Gt23=e23-I23.*W33;
Gt31=e31-I33.*W31;
Gt32=e32-I33.*W32;
Gt33=e33-I33.*W33;
pressure=(g-1)*(.5*u*u*Gt13-u*Gt23+Gt33);
end   % of if loop
MAG=abs(pressure);
PHA=atan(imag(pressure)./real(pressure))*180/pi;
semilogx(f,20*log(MAG/MAG(1)))
title('Normalized Magnitude Response of Pressure')
xlabel('Frequency, Hz'), ylabel('MAGNITUDE, dB')
pause
semilogx(f,PHA)
title('Phase Response of Pressure')
xlabel('Frequency, Hz'), ylabel('PHASE')
pause
position=Z1.*pressure;
MAG=abs(position);
```

Reproduced with permission of the copyright owner. Further reproduction prohibited without permission.

```
PHA=atan(imag(position)./real(position))*180/pi;
semilogx(f,20*log(MAG/MAG(1)))
title('Magnitude Response of Shock Position')
xlabel('Frequency, Hz'), ylabel('MAGNITUDE, db')
pause
semilogx(f,PHA)
title('Phase Response of Shock Position')
xlabel('Frequency, Hz'), ylabel('PHASE')
end      % of program
```

Reproduced with permission of the copyright owner. Further reproduction prohibited without permission.

```
%   Program:        E_CW
%   Last update:    July 24, 1994
%   Source code:    Edu-Matlab

clear
echo off
casesen on
format short e
clc
subplot
hold off
N=600;   d1=-1;  d2=3;
L=5.8507; L1=3.1394; L2=L-L1;
AdA=.3;    % guess
Rc=1;      % guess
R=1716;    % gas constant
r1=6.5866e-4; ru1=0.9846; Energy1=1825.93; g1=1.4;
u1=1554.45; c1=936.38; M1=u1/c1; E1=Energy1/r1;
cT1=1170.99; Tt1=570.77;
r2=1.3492e-4; ru2=0.7880; Energy2=3368.94; g2=1.4;
u2=586.23; c2=1140.62; M2=u2/c2; E2=Energy2/r2;
cT2=1170.71; Tt2=570.50;
re=r2; ue=u2; ce=c2; Ee=E2; ge=g2; Me=M2;
% re=1.392e-3; ue=519.32; ce=1147.92; Ee=2.4879e6;
ge=1.4;Me=.4524;
% Define Fe matrix at exit (from C-W Data)
Fe1=-1;
Fe2=7/6;
Fe3=-1/6;
Wp=1/(ge-1);
% Define PHI matrix, The Cole-Willoh System Matrix
C1=7*(M1*M1-1)/(7*M1*M1-1);
C2=5*sqrt(1+0.2*M1*M1)*Rc/6/cT1/M1;
```

Reproduced with permission of the copyright owner. Further reproduction prohibited without permission.

```
C3=(M1^2-1)*Rc/cT1/M1/(1+.2*M1^2)^.5;
C4=(M1^2+5)/(7*M1^2-1);
C5=6*M1^2/(7*M1^2-1);
Cr=0.958;          % p.29 CW paper
CB=0.037;          % p.30 CW paper
F11=C4;
F12=C1/Cr;
F13=C1/7;
F21=0;
F22=1;
F23=0;
F31=6*C1/7;
F32=-C1/Cr;
F33=C5;
%  Define parameters needed for computation of H(s,x)
AB2=1/2/c2/c2;
At11=(1-u2*u2*(g2-1)/2/c2/c2);
At12=(g2-1)*u2/c2/c2;
At13=-(g2-1)/c2/c2;
At21=u2*(1-u2*u2*(g2-1)/2/c2/c2);
At22=u2*u2*(g2-1)/c2/c2;
At23=-(g2-1)*u2/c2/c2;
At31=u2*u2*(1-u2*u2*(g2-1)/2/c2/c2)/2;
At32=u2*u2*u2*(g2-1)/2/c2/c2;
At33=-u2*u2*(g2-1)/2/c2/c2;
Bt11=AB2*((g2-1)*u2*u2/2-u2*c2);
Bt12=AB2*(c2-(g2-1)*u2);
Bt13=AB2*(g2-1);
Bt21=(u2+c2)*AB2*((g2-1)*u2*u2/2-u2*c2);
Bt22=(u2+c2)*AB2*(c2-(g2-1)*u2);
Bt23=(u2+c2)*AB2*(g2-1);
Bt31=(.5*u2*u2+u2*c2+c2*c2/(g2-1))*AB2*((g2-1)*u2*u2/2-u2*c2);
Bt32=(.5*u2*u2+u2*c2+c2*c2/(g2-1))*AB2*(c2-(g2-1)*u2);
```

Reproduced with permission of the copyright owner. Further reproduction prohibited without permission.

```
Bt33=(.5*u2*u2+u2*c2+c2*c2/(g2-1))*AB2*(g2-1);
Ct11=AB2*((g2-1)*u2*u2/2+u2*c2);
Ct12=-AB2*(c2+(g2-1)*u2);
Ct13=AB2*(g2-1);
Ct21=(u2-c2)*AB2*((g2-1)*u2*u2/2+u2*c2);
Ct22=-(u2-c2)*AB2*(c2+(g2-1)*u2);
Ct23=(u2-c2)*AB2*(g2-1);
Ct31=(.5*u2*u2-u2*c2+c2*c2/(g2-1))*AB2*((g2-1)*u2*u2/2+u2*c2);
Ct32=-(.5*u2*u2-u2*c2+c2*c2/(g2-1))*AB2*(c2+(g2-1)*u2);
Ct33=(.5*u2*u2-u2*c2+c2*c2/(g2-1))*AB2*(g2-1);
%  Define Theta Transformation Matrix, QR
temp2=E2-u2*u2/2;
TEMP2=1+(g2-1)*M2*M2/2;
QR11=-g2*M2*u2*E2/2/r2/u2/temp2/TEMP2+u2*u2/2/r2/temp2;
QR12=g2*M2*E2/r2/u2/temp2/TEMP2-u2/r2/temp2;
QR13=1/r2/temp2/TEMP2-g2*M2*u2/2/r2/c2/temp2/TEMP2;
QR21=0;
QR22=1/r2/u2;
QR23=0;
QR31=g2*u2*u2*TEMP2/2/Tt2-M2*M2*E2*g2*(g2-
1)/2/Tt2+R*g2*M2*M2*E2/2/r2/temp2/TEMP2-
R*u2*u2/2/r2/temp2;
QR32=-g2*u2*TEMP2/Tt2+E2*M2*g2*(g2-1)/c2/Tt2-
R*g2*M2*E2/r2/c2/temp2/TEMP2+R*u2/r2/temp2;
QR33=g2*TEMP2/Tt2-M2*M2*g2*(g2-1)/2/Tt2-
R/r2/temp2+R*g2*M2*M2/2/r2/temp2/TEMP2;
%  Compute inverse of Theta matrix, QRi
QRdelta=QR22*(QR11*QR33-QR31*QR13);
QRi11=QR22*QR33/QRdelta;
QRi12=(QR13*QR32-QR12*QR33)/QRdelta;
QRi13=-QR13*QR22/QRdelta;
QRi21=0;
QRi22=(QR11*QR33-QR13*QR31)/QRdelta;
```

Reproduced with permission of the copyright owner. Further reproduction prohibited without permission.

```
QRi23=0;
QRi31=-QR22*QR31/QRdelta;
QRi32=(QR12*QR31-QR11*QR32)/QRdelta;
QRi33=QR11*QR22/QRdelta;
w=2*pi*logspace(d1,d2,N);          f=w/2/pi;
j=sqrt(-1);                        s=j*w;
% Compute H2(s,L)
Et1L=exp(-s*L/u2);
Et2L=exp(-s*L/(u2+c2));
Et3L=exp(-s*L/(u2-c2));
d11=At11*Et1L+Bt11*Et2L+Ct11*Et3L;
d12=At12*Et1L+Bt12*Et2L+Ct12*Et3L;
d13=At13*Et1L+Bt13*Et2L+Ct13*Et3L;
d21=At21*Et1L+Bt21*Et2L+Ct21*Et3L;
d22=At22*Et1L+Bt22*Et2L+Ct22*Et3L;
d23=At23*Et1L+Bt23*Et2L+Ct23*Et3L;
d31=At31*Et1L+Bt31*Et2L+Ct31*Et3L;
d32=At32*Et1L+Bt32*Et2L+Ct32*Et3L;
d33=At33*Et1L+Bt33*Et2L+Ct33*Et3L;
clear Et1L Et2L Et3L
% Compute Fe'H(s,L)
FH1=Fe1.*d11+Fe2.*d21+Fe3.*d31;
FH2=Fe1.*d12+Fe2.*d22+Fe3.*d32;
FH3=Fe1.*d13+Fe2.*d23+Fe3.*d33;
% Define elements of gamma matrix, The Cole-Willoh Input Matrices
gam1=-C1*(Rc*AdA*ones(s)+C2*s);
gam2=CB*ones(s)+Cr*C3.*s;
gam3=C1*(Rc*AdA*ones(s)-C3.*s);
% Define elements of auxilliary GAMMA_HAT matrix
GAM1=QRi11.*gam1+QRi12.*gam2+QRi13.*gam3;
GAM2=QRi21.*gam1+QRi22.*gam2+QRi23.*gam3;
GAM3=QRi31.*gam1+QRi32.*gam2+QRi33.*gam3;
% Compute denominator (1x1) matrix of transfer function
```

Reproduced with permission of the copyright owner. Further reproduction prohibited without permission.

```
FHG=FH1.*GAM1+FH2.*GAM2+FH3.*GAM3;
%  Compute response of Shock Position due to downstream pressure
input
D=Wp*ones(FHG)./FHG;
MAG=abs(D);
PHA=atan(imag(D)./real(D))*180/pi;
PHAu=unwrap(atan(imag(D)./real(D)))*180/pi;
semilogx(f,20*log(MAG/MAG(1)))
title('Magnitude Response of Xs due to dPdown')
xlabel('Frequency, Hz'), ylabel('MAGNITUDE, dB')
pause
semilogx(f,PHA)
title('Phase Response of Xs due to dPdown')
xlabel('Frequency, Hz'), ylabel('PHASE')
pause
semilogx(f,PHAu)
title('Phase Response of Xs due to dPdown')
xlabel('Frequency, Hz'), ylabel('UNWRAPPED PHASE')
end      % of program
```

Reproduced with permission of the copyright owner. Further reproduction prohibited without permission.

```
%   Program:        E_CW_mesh
%   Last update:    July 24, 1994
%   Source code:    Edu-Matlab

clear
echo off
casesen on
format short e
clc
subplot
hold off
j=sqrt(-1);
sc=-500:16:500;
ci=3*sc';
sigma=ones(length(ci),1)*sc;
w=ci*ones(length(sc),1)';
s=sigma+(j*w);
levels=50;
L=5.8507; L1=3.1394; L2=L-L1;
AdA=.3;     % guess
Rc=1;      % guess
R=1716;     % gas constant
r1=6.5866e-4; ru1=0.9846; Energy1=1825.93; g1=1.4;
u1=1554.45; c1=936.38; M1=u1/c1; E1=Energy1/r1;
cT1=1170.99; Tt1=570.77;
r2=1.3492e-4; ru2=0.7880; Energy2=3368.94; g2=1.4;
u2=586.23; c2=1140.62; M2=u2/c2; E2=Energy2/r2;
cT2=1170.71; Tt2=570.50;
re=r2; ue=u2; ce=c2; Ee=E2; ge=g2; Me=M2;
% re=1.392e-3; ue=519.32; ce=1147.92; Ee=2.4879e6;
ge=1.4;Me=.4524;
%  Define Fe matrix at exit (from C-W Data)
Fe1=-1;
```

Reproduced with permission of the copyright owner. Further reproduction prohibited without permission.

```
Fe2=7/6;
Fe3=-1/6;
Wp=1/(ge-1);
% Define PHI matrix, The Cole-Willoh System Matrix
C1=7*(M1*M1-1)/(7*M1*M1-1);
C2=5*sqrt(1+0.2*M1*M1)*Rc/6/cT1/M1;
C3=(M1^2-1)*Rc/cT1/M1/(1+.2*M1^2)^.5;
C4=(M1^2+5)/(7*M1^2-1);
C5=6*M1^2/(7*M1^2-1);
Cr=0.958;          % p.29 CW paper
CB=0.037;          % p.30 CW paper
F11=C4;
F12=C1/Cr;
F13=C1/7;
F21=0;
F22=1;
F23=0;
F31=6*C1/7;
F32=-C1/Cr;
F33=C5;
% Define parameters needed for computation of H(s,x)
AB2=1/2/c2/c2;
At11=(1-u2*u2*(g2-1)/2/c2/c2);
At12=(g2-1)*u2/c2/c2;
At13=-(g2-1)/c2/c2;
At21=u2*(1-u2*u2*(g2-1)/2/c2/c2);
At22=u2*u2*(g2-1)/c2/c2;
At23=-(g2-1)*u2/c2/c2;
At31=u2*u2*(1-u2*u2*(g2-1)/2/c2/c2)/2;
At32=u2*u2*u2*(g2-1)/2/c2/c2;
At33=-u2*u2*(g2-1)/2/c2/c2;
Bt11=AB2*((g2-1)*u2*u2/2-u2*c2);
Bt12=AB2*(c2-(g2-1)*u2);
```

Reproduced with permission of the copyright owner. Further reproduction prohibited without permission.

```
Bt13=AB2*(g2-1);
Bt21=(u2+c2)*AB2*((g2-1)*u2*u2/2-u2*c2);
Bt22=(u2+c2)*AB2*(c2-(g2-1)*u2);
Bt23=(u2+c2)*AB2*(g2-1);
Bt31=(.5*u2*u2+u2*c2+c2*c2/(g2-1))*AB2*((g2-1)*u2*u2/2-u2*c2);
Bt32=(.5*u2*u2+u2*c2+c2*c2/(g2-1))*AB2*(c2-(g2-1)*u2);
Bt33=(.5*u2*u2+u2*c2+c2*c2/(g2-1))*AB2*(g2-1);
Ct11=AB2*((g2-1)*u2*u2/2+u2*c2);
Ct12=-AB2*(c2+(g2-1)*u2);
Ct13=AB2*(g2-1);
Ct21=(u2-c2)*AB2*((g2-1)*u2*u2/2+u2*c2);
Ct22=-(u2-c2)*AB2*(c2+(g2-1)*u2);
Ct23=(u2-c2)*AB2*(g2-1);
Ct31=(.5*u2*u2-u2*c2+c2*c2/(g2-1))*AB2*((g2-1)*u2*u2/2+u2*c2);
Ct32=-(.5*u2*u2-u2*c2+c2*c2/(g2-1))*AB2*(c2+(g2-1)*u2);
Ct33=(.5*u2*u2-u2*c2+c2*c2/(g2-1))*AB2*(g2-1);
%  Define Theta Transformation Matrix, QR
temp2=E2-u2*u2/2;
TEMP2=1+(g2-1)*M2*M2/2;
QR11=-g2*M2*u2*E2/2/r2/u2/temp2/TEMP2+u2*u2/2/r2/temp2;
QR12=g2*M2*E2/r2/u2/temp2/TEMP2-u2/r2/temp2;
QR13=1/r2/temp2/TEMP2-g2*M2*u2/2/r2/c2/temp2/TEMP2;
QR21=0;
QR22=1/r2/u2;
QR23=0;
QR31=g2*u2*u2*TEMP2/2/Tt2-M2*M2*E2*g2*(g2-
1)/2/Tt2+R*g2*M2*M2*E2/2/r2/temp2/TEMP2-
R*u2*u2/2/r2/temp2;
QR32=-g2*u2*TEMP2/Tt2+E2*M2*g2*(g2-1)/c2/Tt2-
R*g2*M2*E2/r2/c2/temp2/TEMP2+R*u2/r2/temp2;
QR33=g2*TEMP2/Tt2-M2*M2*g2*(g2-1)/2/Tt2-
R/r2/temp2+R*g2*M2*M2/2/r2/temp2/TEMP2;
%  Compute inverse of Theta matrix, QRi
```

Reproduced with permission of the copyright owner. Further reproduction prohibited without permission.

```
QRdelta=QR22*(QR11*QR33-QR31*QR13);
QRi11=QR22*QR33/QRdelta;
QRi12=(QR13*QR32-QR12*QR33)/QRdelta;
QRi13=-QR13*QR22/QRdelta;
QRi21=0;
QRi22=(QR11*QR33-QR13*QR31)/QRdelta;
QRi23=0;
QRi31=-QR22*QR31/QRdelta;
QRi32=(QR12*QR31-QR11*QR32)/QRdelta;
QRi33=QR11*QR22/QRdelta;
% Compute H2(s,L)
Et1L=exp(-s*L/u2);
Et2L=exp(-s*L/(u2+c2));
Et3L=exp(-s*L/(u2-c2));
d11=At11*Et1L+Bt11*Et2L+Ct11*Et3L;
d12=At12*Et1L+Bt12*Et2L+Ct12*Et3L;
d13=At13*Et1L+Bt13*Et2L+Ct13*Et3L;
d21=At21*Et1L+Bt21*Et2L+Ct21*Et3L;
d22=At22*Et1L+Bt22*Et2L+Ct22*Et3L;
d23=At23*Et1L+Bt23*Et2L+Ct23*Et3L;
d31=At31*Et1L+Bt31*Et2L+Ct31*Et3L;
d32=At32*Et1L+Bt32*Et2L+Ct32*Et3L;
d33=At33*Et1L+Bt33*Et2L+Ct33*Et3L;
clear Et1L Et2L Et3L
% Compute Fe'H(s,L)
FH1=Fe1.*d11+Fe2.*d21+Fe3.*d31;
FH2=Fe1.*d12+Fe2.*d22+Fe3.*d32;
FH3=Fe1.*d13+Fe2.*d23+Fe3.*d33;
% Define elements of gamma matrix, The Cole-Willoh Input Matrices
gam1=-C1*(Rc*AdA*ones(s)+C2*s);
gam2=CB*ones(s)+Cr*C3.*s;
gam3=C1*(Rc*AdA*ones(s)-C3.*s);
% Define elements of auxilliary GAMMA_HAT matrix
```

Reproduced with permission of the copyright owner. Further reproduction prohibited without permission.

```
GAM1=QRi11.*gam1+QRi12.*gam2+QRi13.*gam3;
GAM2=QRi21.*gam1+QRi22.*gam2+QRi23.*gam3;
GAM3=QRi31.*gam1+QRi32.*gam2+QRi33.*gam3;
%  Compute denominator (1x1) matrix of transfer function
FHG=FH1.*GAM1+FH2.*GAM2+FH3.*GAM3;
%  Compute response of Shock Position due to downstream pressure
input
D=Wp*ones(FHG)./FHG;
MAG=abs(D);
MAGdb=20*log(MAG);
mesh(MAGdb),  pause
contour(MAGdb,levels,sc,3*sc)
xlabel('Real(s)'),  ylabel('Imag(s)')
title('Contours of Equal Magnitude of Shock Position')
end      % of all programs
```

Reproduced with permission of the copyright owner. Further reproduction prohibited without permission.

APPENDIX D

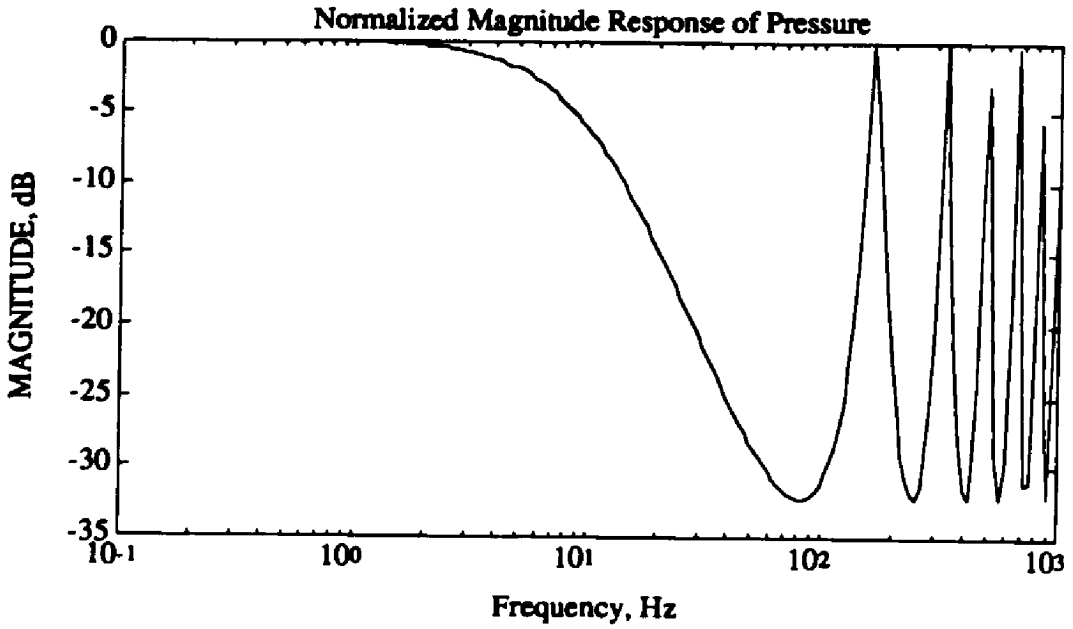
FREQUENCY RESPONSES

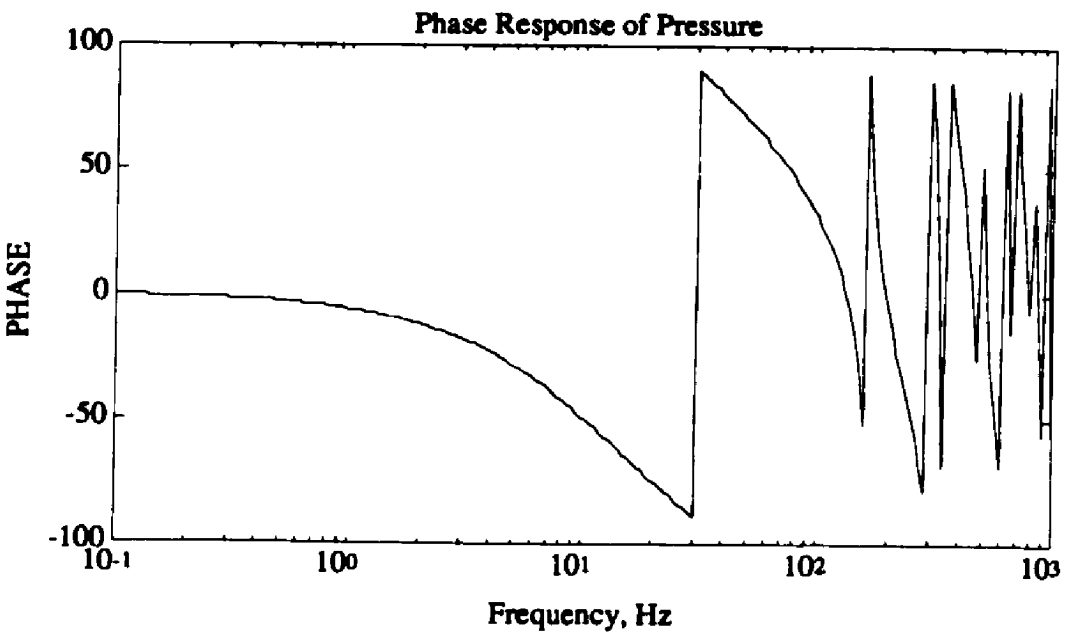
This appendix contains frequency responses computed at x=0 and generated using the programs of Appendix C. Each case contains a group of frequency responses that were generated by the same program. Finally, the conditions used to generated each response are stated.

Reproduced with permission of the copyright owner. Further reproduction prohibited without permission.

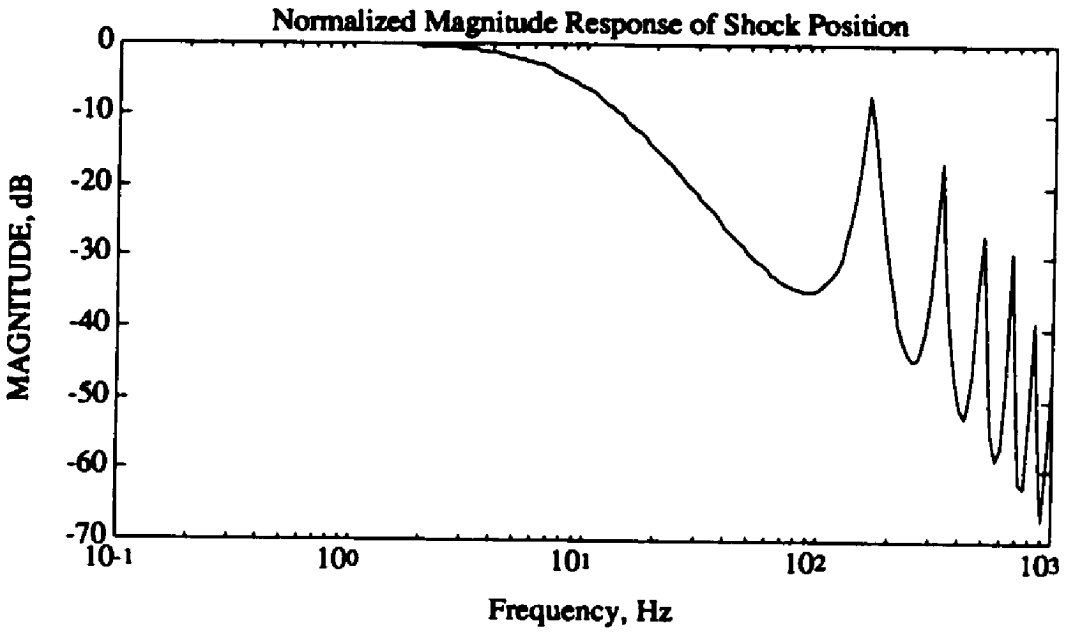
CASE	A-1
PROGRAM USED	**CONDITIONS**
A_two_wave	Ebar=3350 m=.78 L=2.57 R=6e-6 $Z_{us}(s) = \frac{1010}{s-1010}$

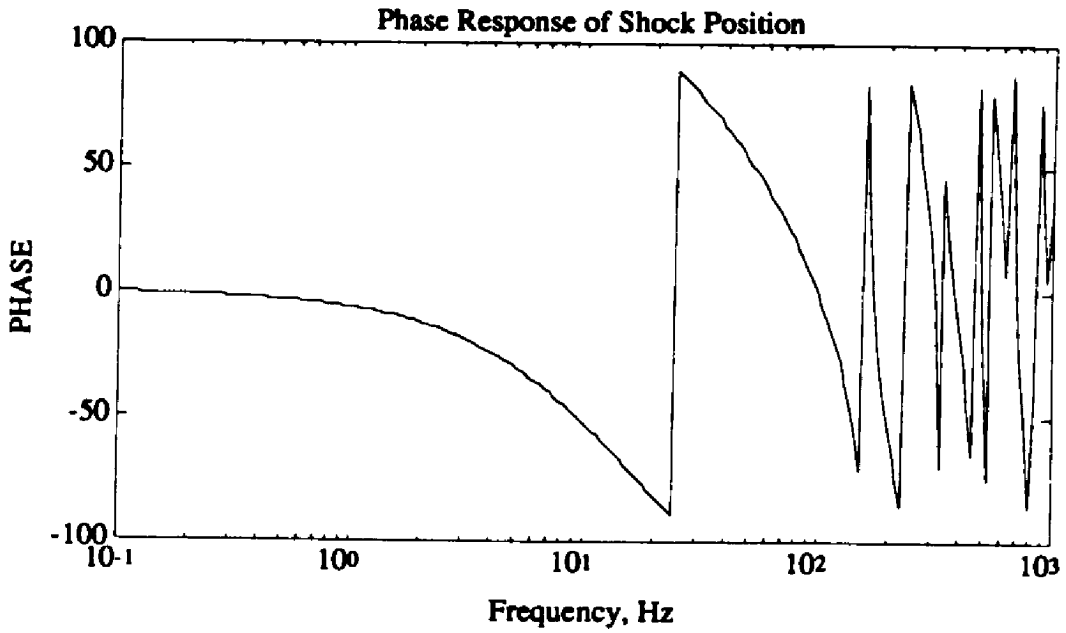
Reproduced with permission of the copyright owner. Further reproduction prohibited without permission.





Reproduced with permission of the copyright owner. Further reproduction prohibited without permission.



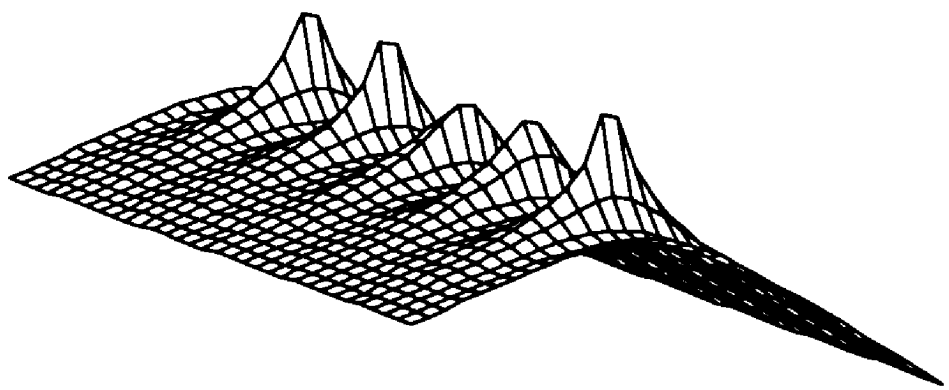


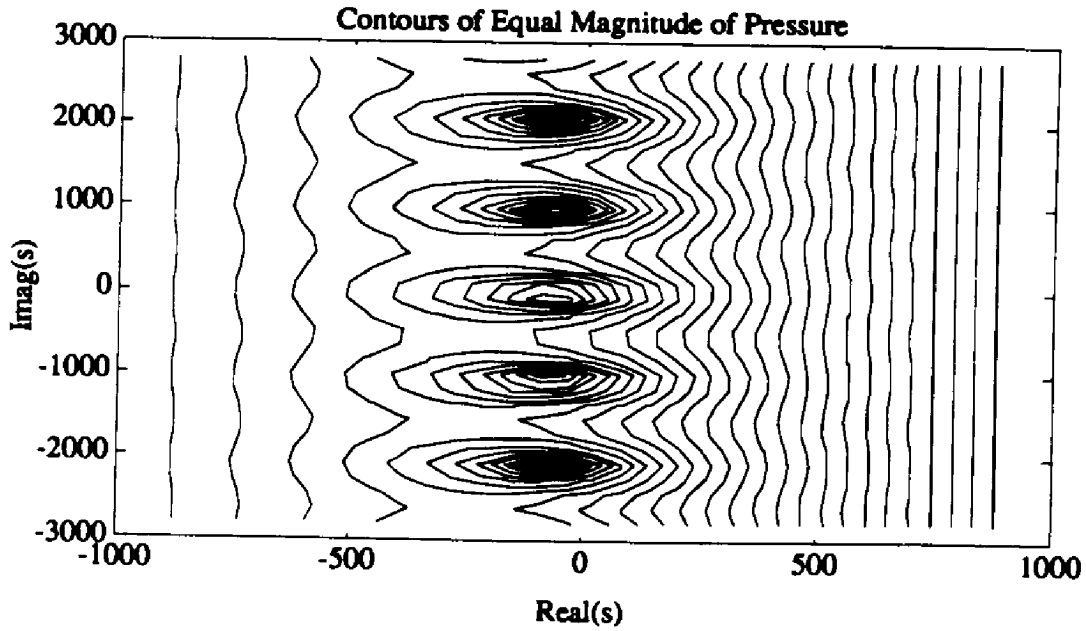
Reproduced with permission of the copyright owner. Further reproduction prohibited without permission.

CASE	A-2
PROGRAM USED	**CONDITIONS**
A_two_wave_mesh	Ebar=3350 m=.78 L=2.57 R=6e-6 $Z_{us}(s) = \frac{1010}{s-1010}$

Reproduced with permission of the copyright owner. Further reproduction prohibited without permission.

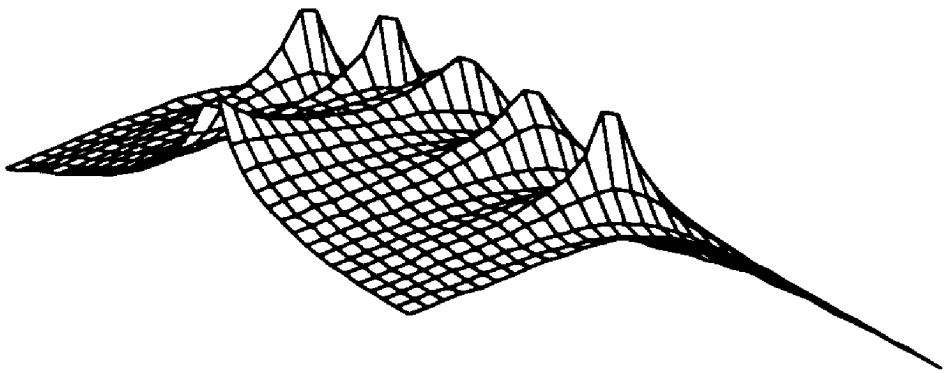
Mesh Plot of Pressure

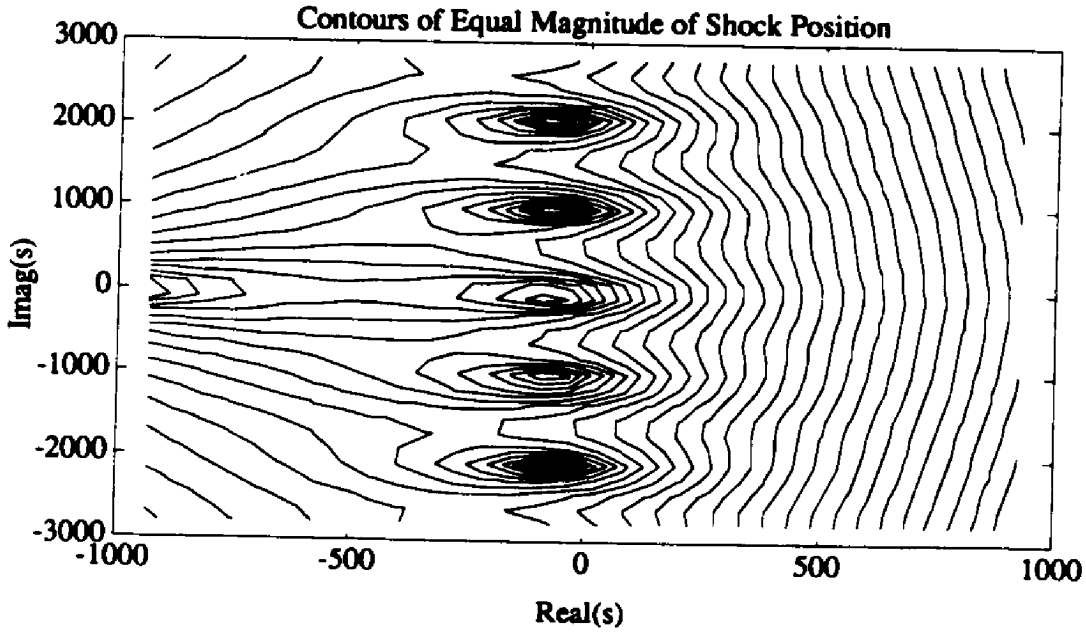




Reproduced with permission of the copyright owner. Further reproduction prohibited without permission.

Mesh Plot of Shock Position

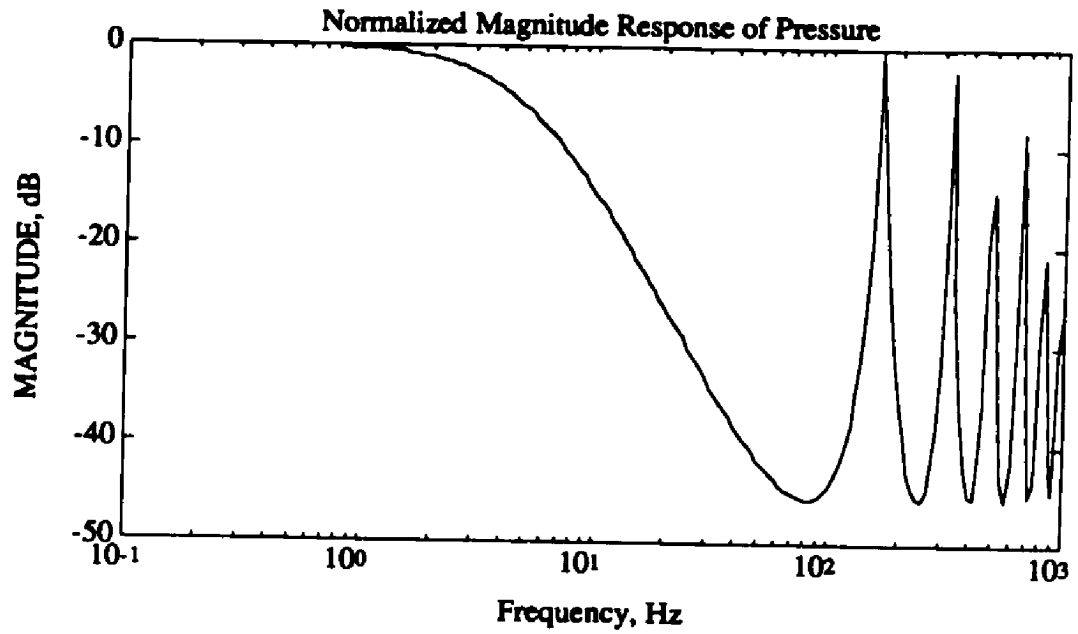


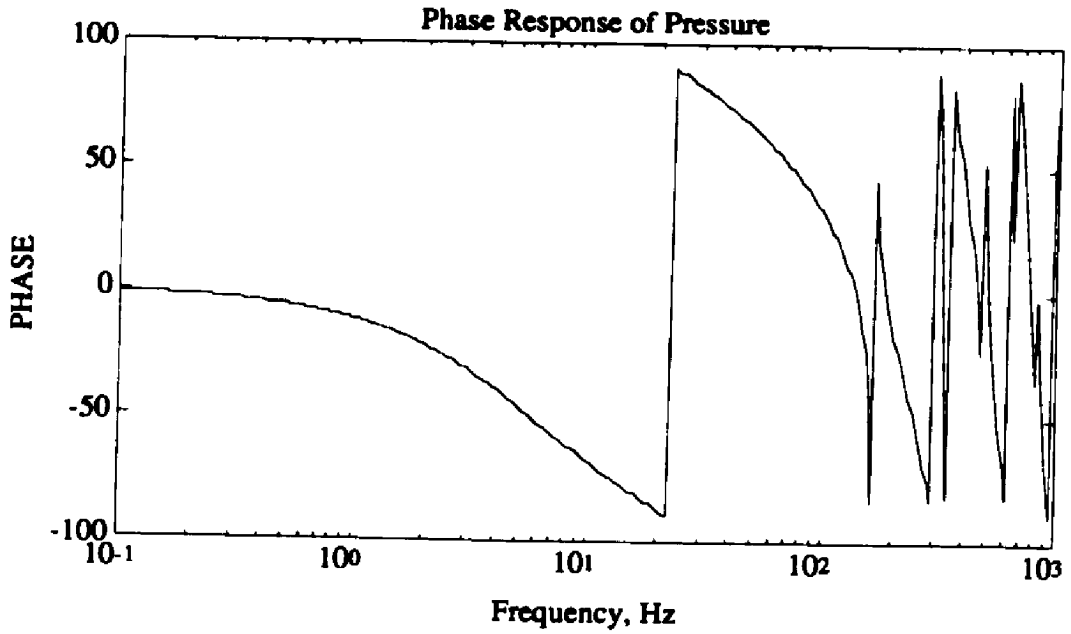


Reproduced with permission of the copyright owner. Further reproduction prohibited without permission.

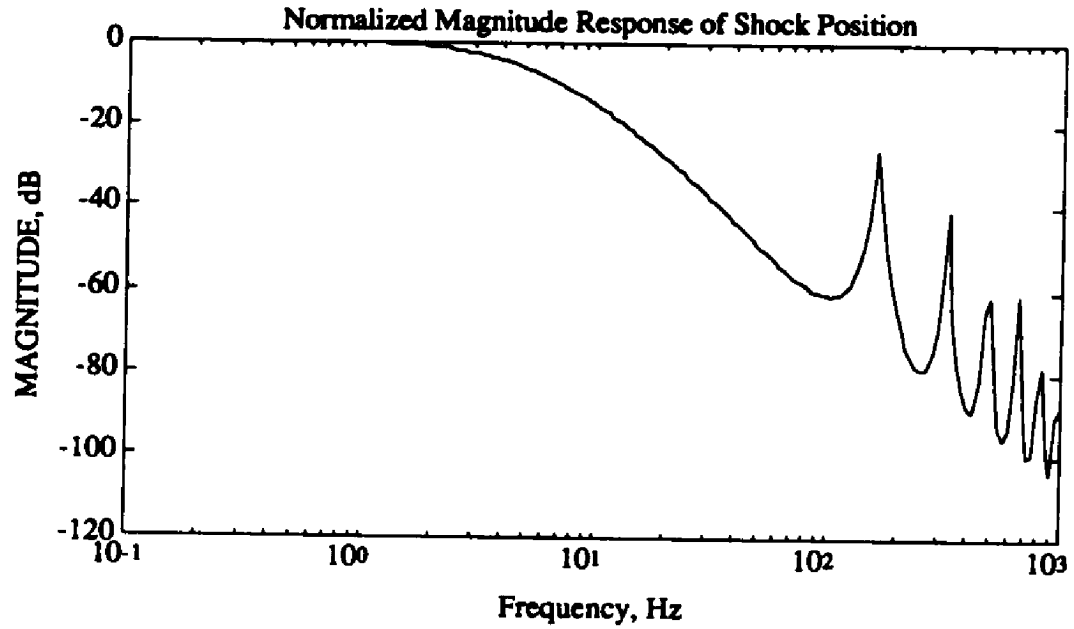
CASE	B-1
PROGRAM USED	**CONDITIONS**
B_three_wave	r=0.00136 L=3.61 m=0.78 Ebar=3350 u=586.23 c=1140.62 M=0.5144 $Z_1(s) = \frac{1010}{s-300}$ $Z_2(s) = \frac{1010}{s-1010}$

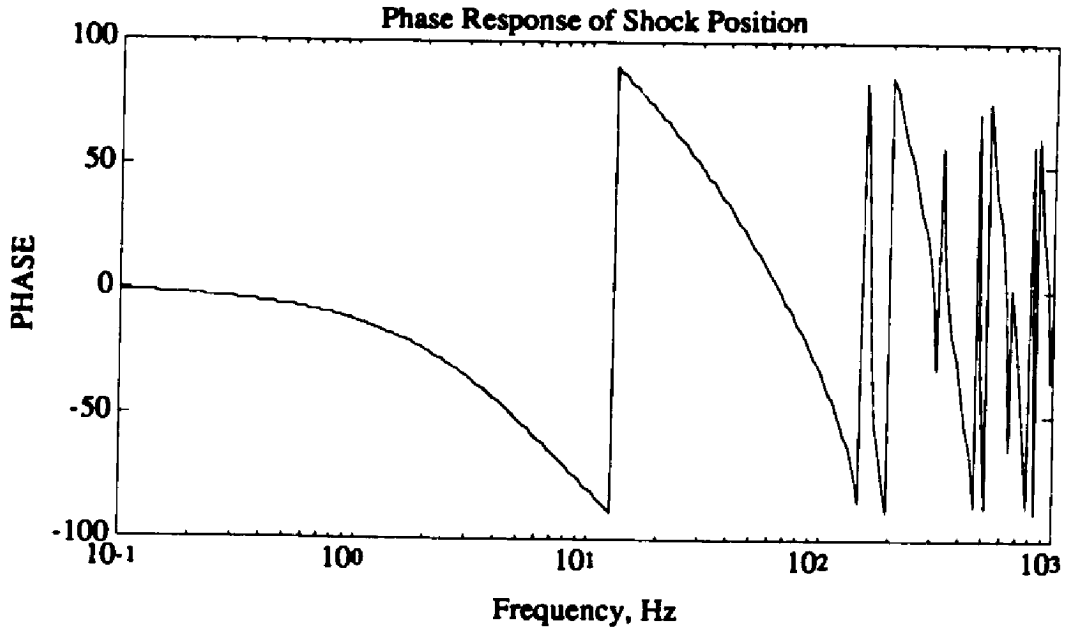
Reproduced with permission of the copyright owner. Further reproduction prohibited without permission.





Reproduced with permission of the copyright owner. Further reproduction prohibited without permission.



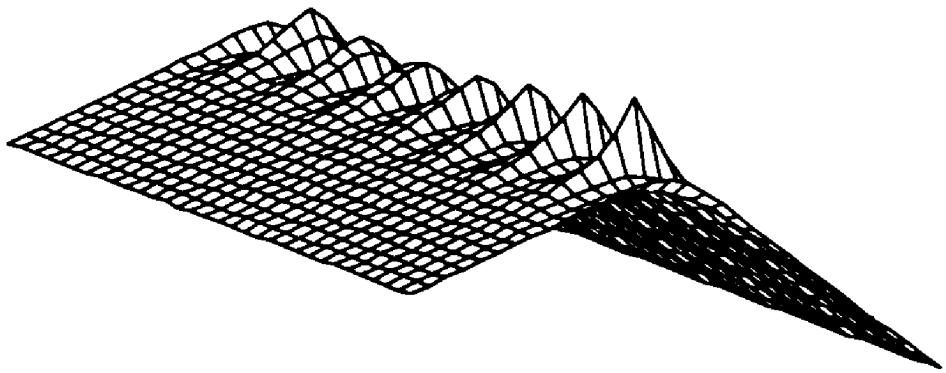


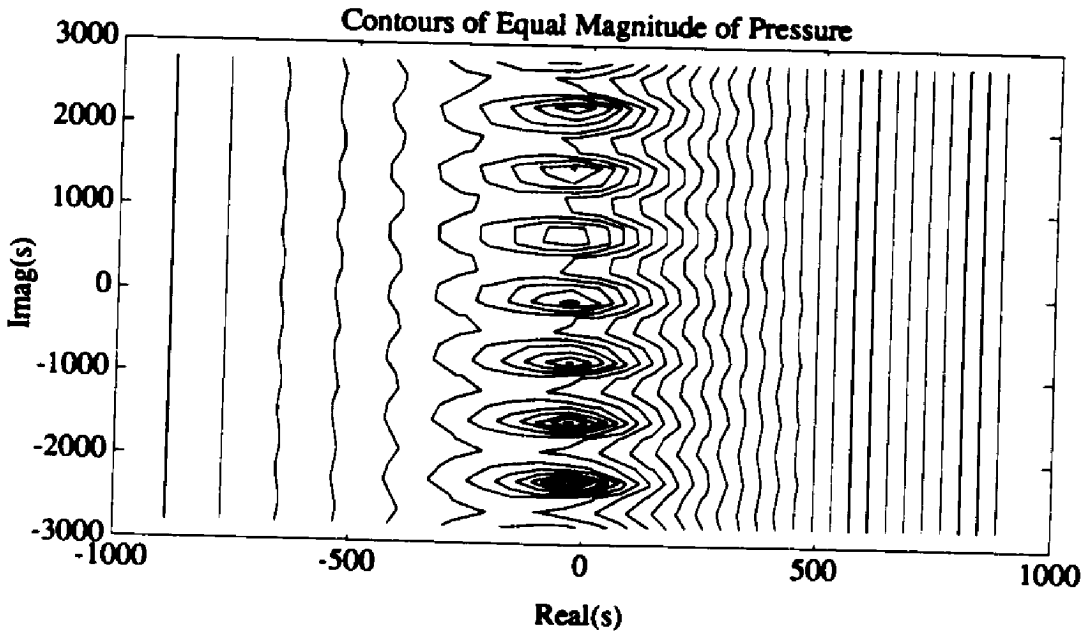
Reproduced with permission of the copyright owner. Further reproduction prohibited without permission.

CASE	B-2
PROGRAM USED	**CONDITIONS**
B_three_wave_mesh	r=0.00136 L=3.61 m=0.78 Ebar=3350 $Z_1(s) = \frac{1010}{s-1010}$ $Z_2(s) = \frac{1010}{s-1010}$

Reproduced with permission of the copyright owner. Further reproduction prohibited without permission.

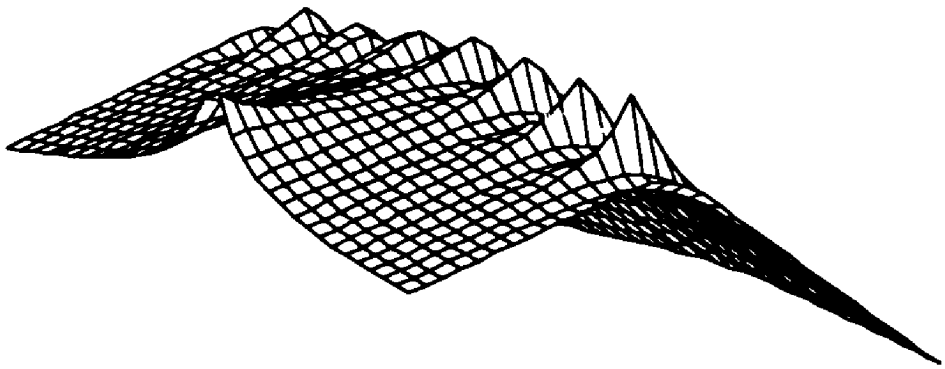
Mesh Plot of Pressure

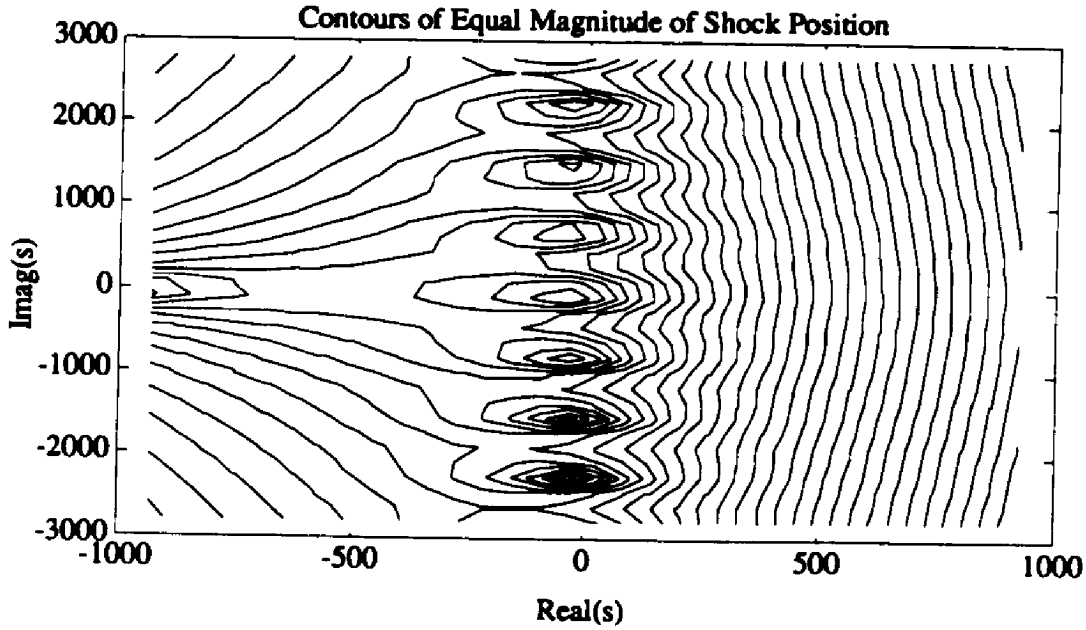




Reproduced with permission of the copyright owner. Further reproduction prohibited without permission.

Mesh Plot of Shock Position

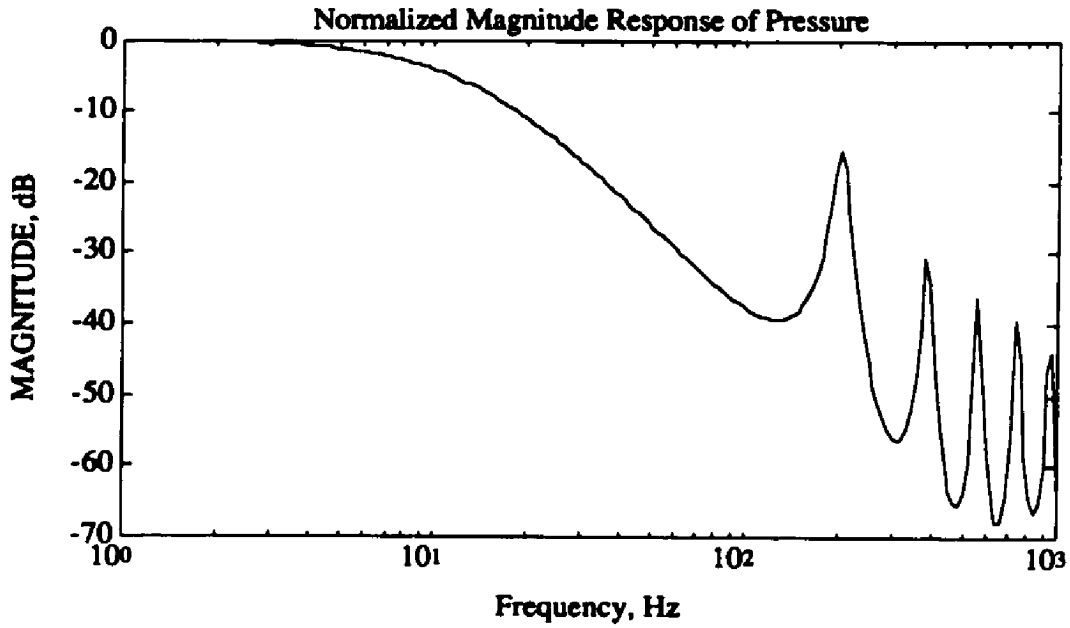


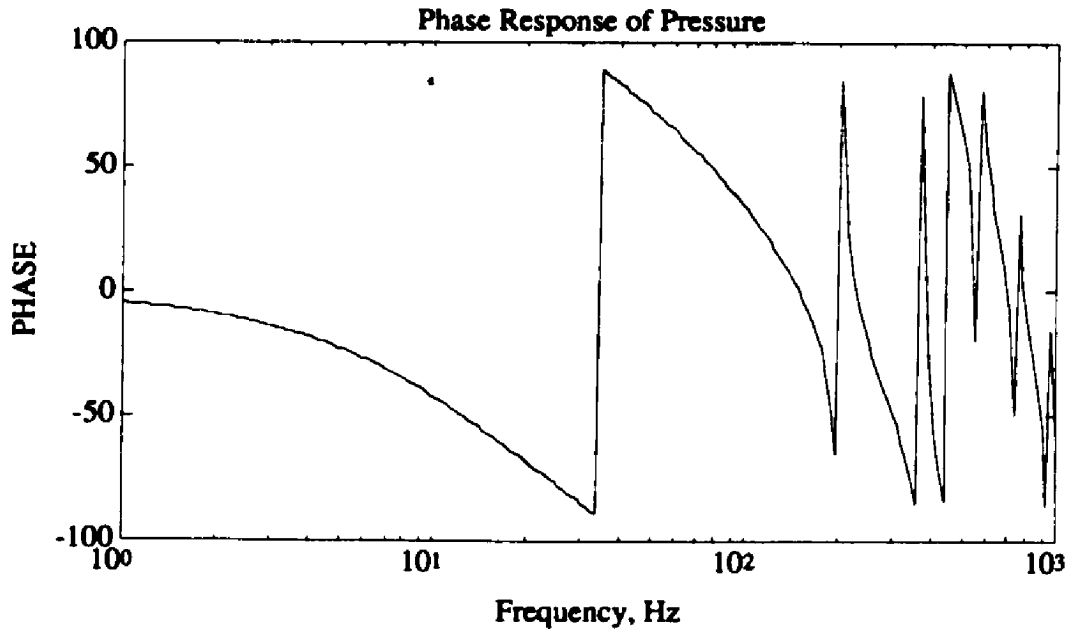


Reproduced with permission of the copyright owner. Further reproduction prohibited without permission.

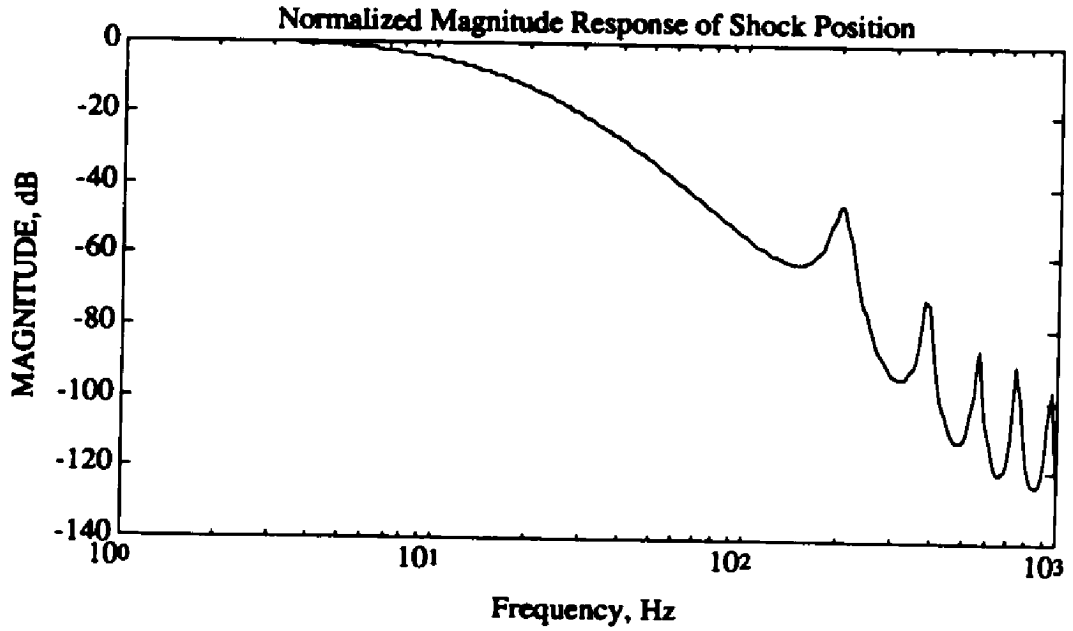
CASE	C-1
PROGRAM USED	**CONDITIONS**
C_two_wave_Blocks	u1=1554.45 r1=0.00065866 c1=936.38 g1=1.4 u2=586.23 r2=0.0013492 c2=1140.62 g2=1.4 L1=0.9186 L=3.61 R=6e-6 $Z_{us}(s) = \frac{10^6}{s-1010}$

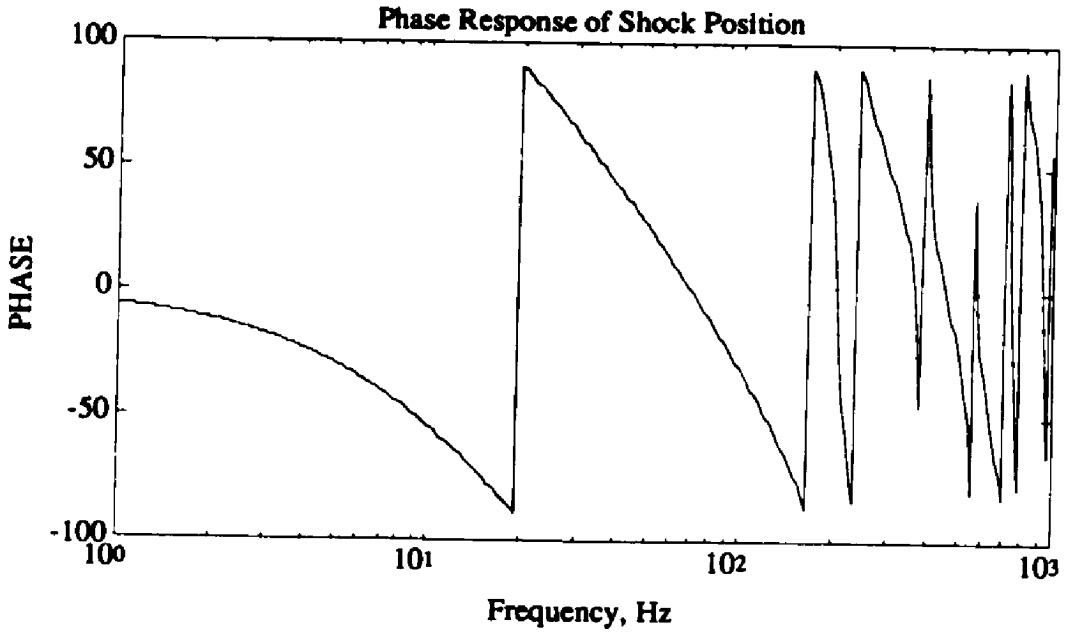
Reproduced with permission of the copyright owner. Further reproduction prohibited without permission.





Reproduced with permission of the copyright owner. Further reproduction prohibited without permission.

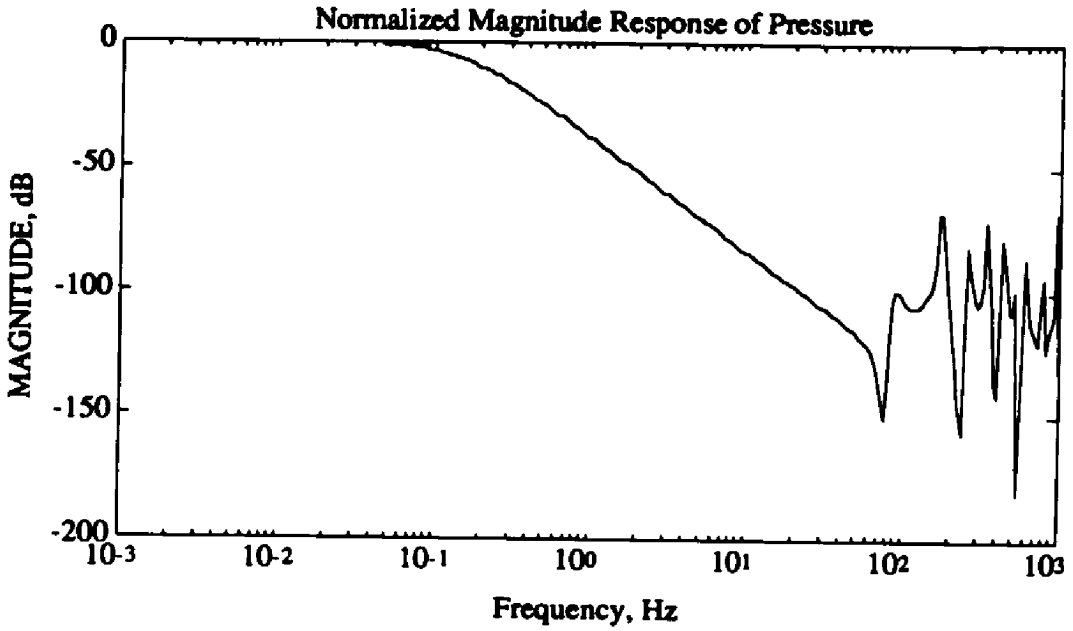


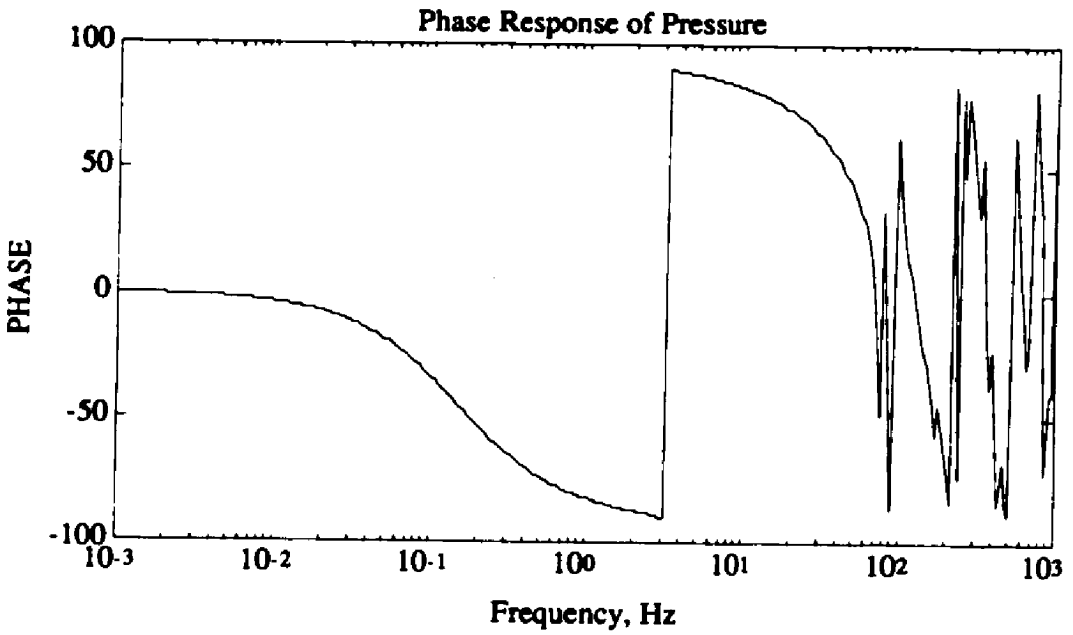


Reproduced with permission of the copyright owner. Further reproduction prohibited without permission.

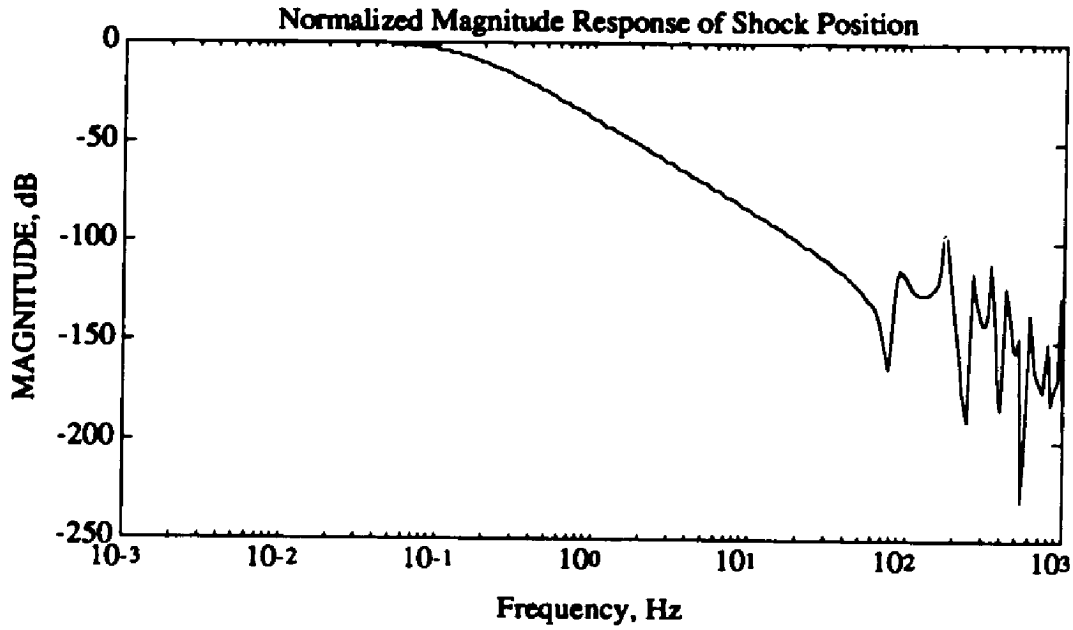
CASE	C-2
PROGRAM USED	**CONDITIONS**
C_three_wave_Blocks	u1=800 r1=0.002 c1=1000 g1=1.4 u2=586.23 r2=0.0013492 c2=1140.62 g2=1.4 L1=0.9186 L=3.61 $Z_1(s) = \frac{1}{s-300}$ $Z_2(s) = \frac{1}{s-1010}$ R1=-1e4 R2=500

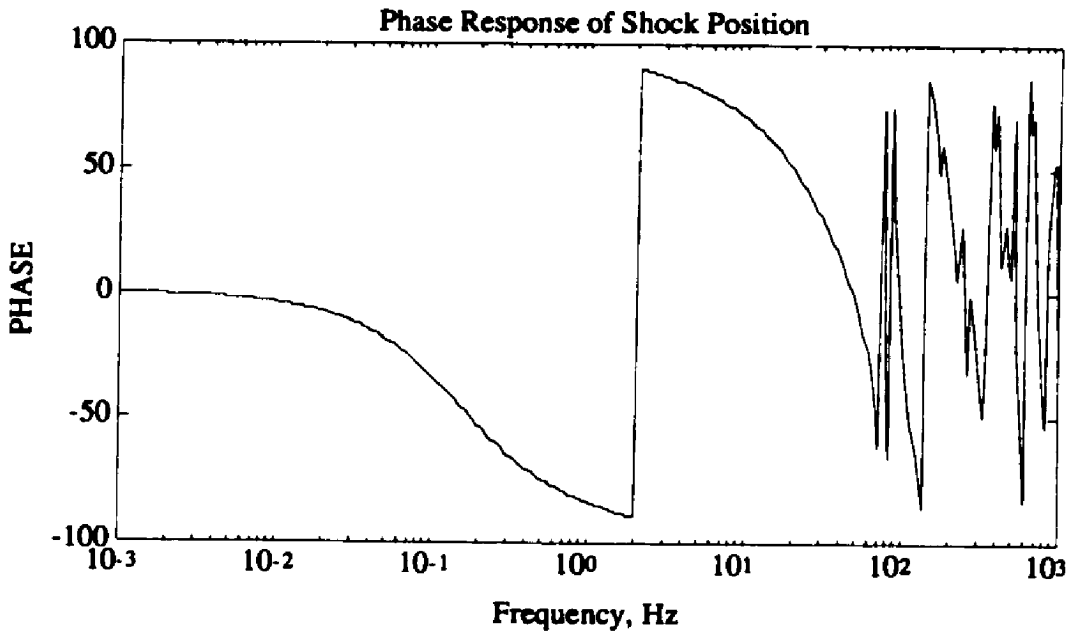
Reproduced with permission of the copyright owner. Further reproduction prohibited without permission.





Reproduced with permission of the copyright owner. Further reproduction prohibited without permission.

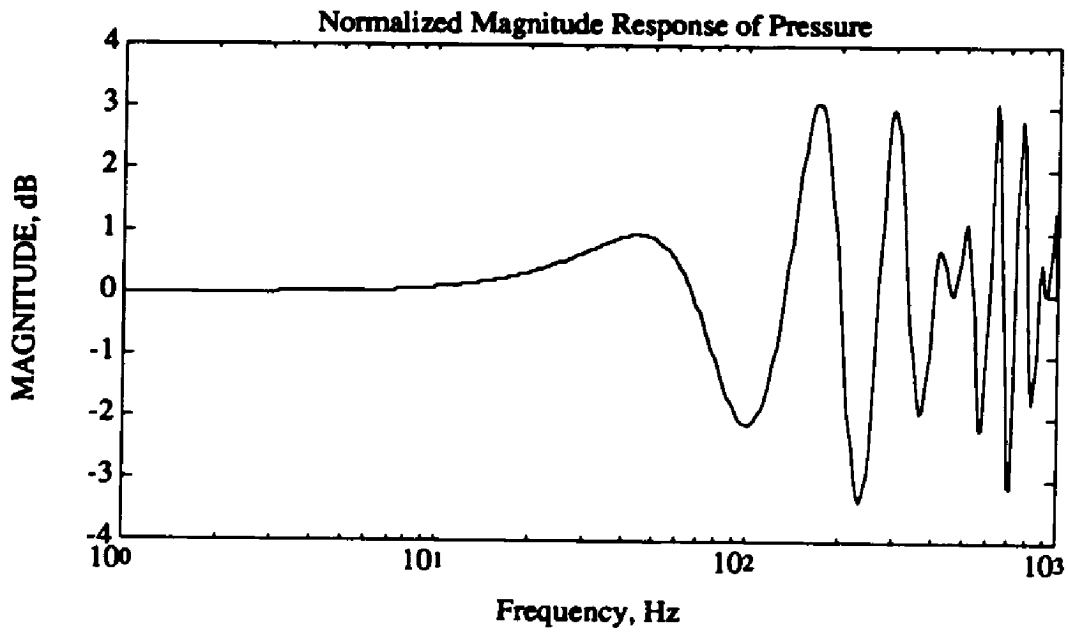


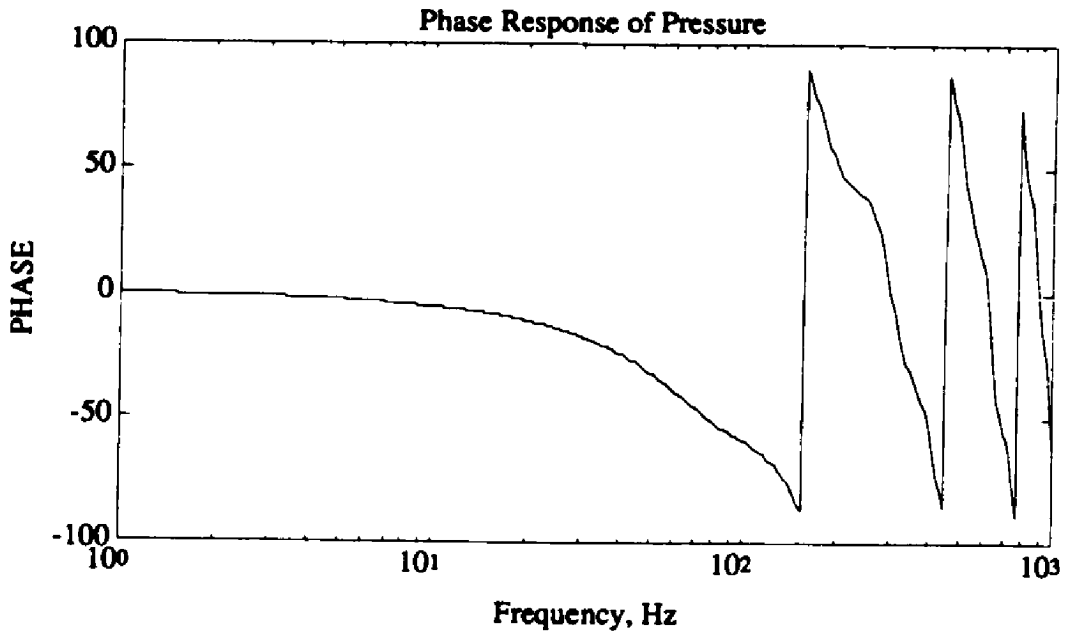


Reproduced with permission of the copyright owner. Further reproduction prohibited without permission.

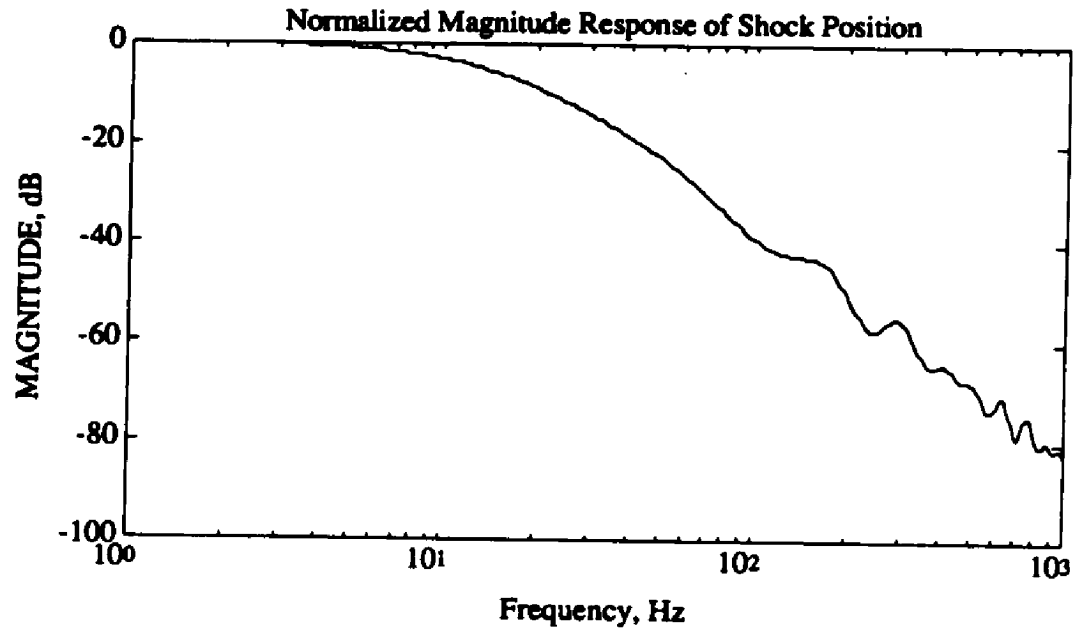
CASE	D-1
PROGRAM USED	**CONDITIONS**
D_two_wave_Green	u=586.23 r=0.0013492 c=1140.62 g2=1.4 ksi=0.9186 L=3.61 $Z_{us}(s) = \frac{1010}{s-300}$

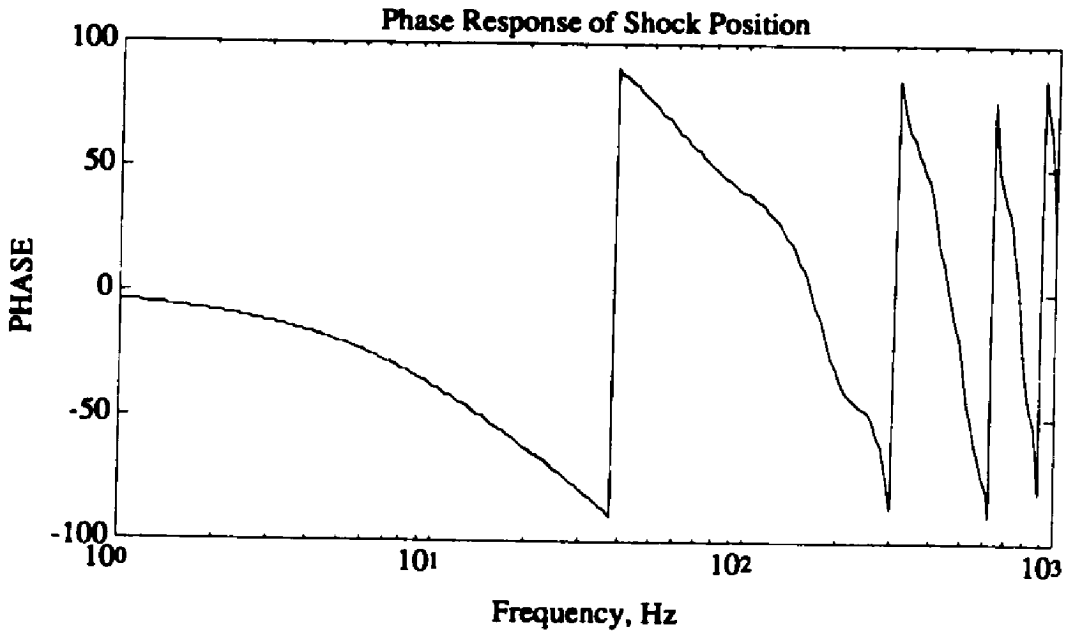
Reproduced with permission of the copyright owner. Further reproduction prohibited without permission.





Reproduced with permission of the copyright owner. Further reproduction prohibited without permission.

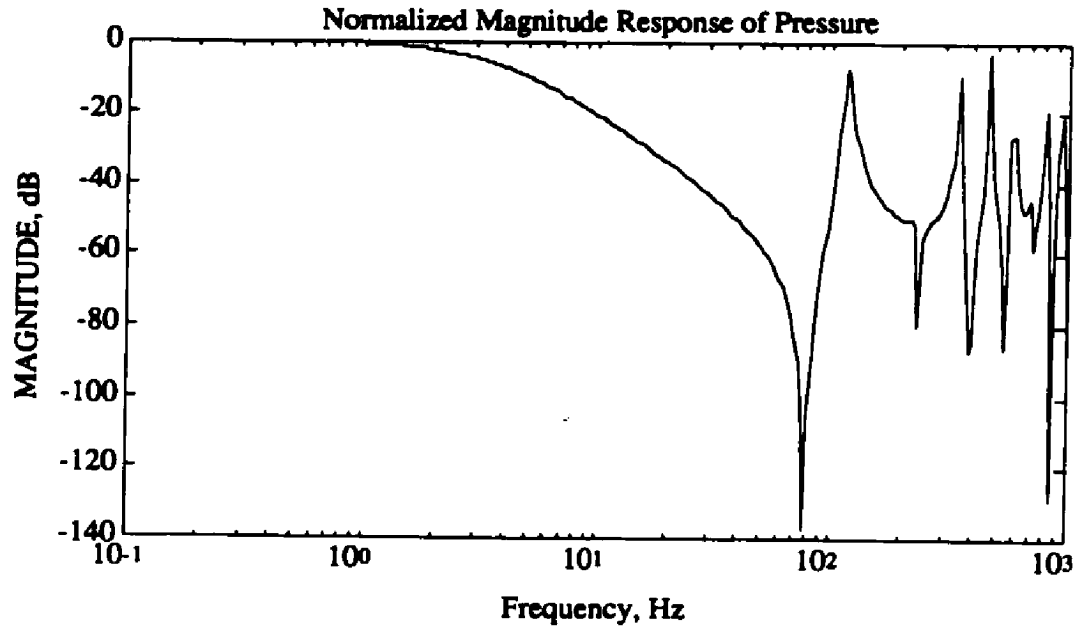


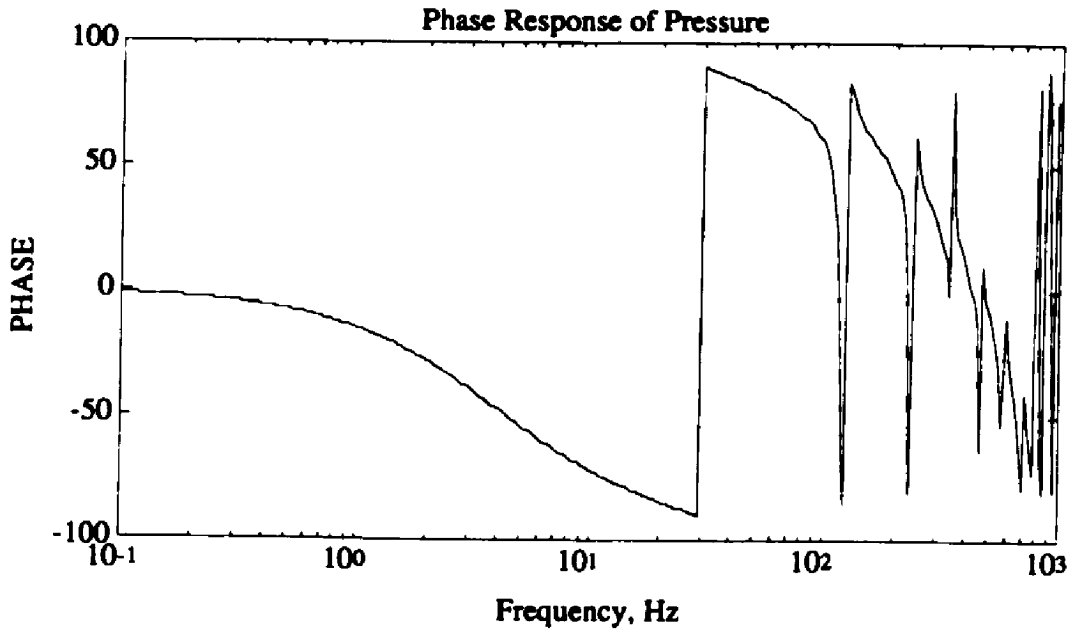


Reproduced with permission of the copyright owner. Further reproduction prohibited without permission.

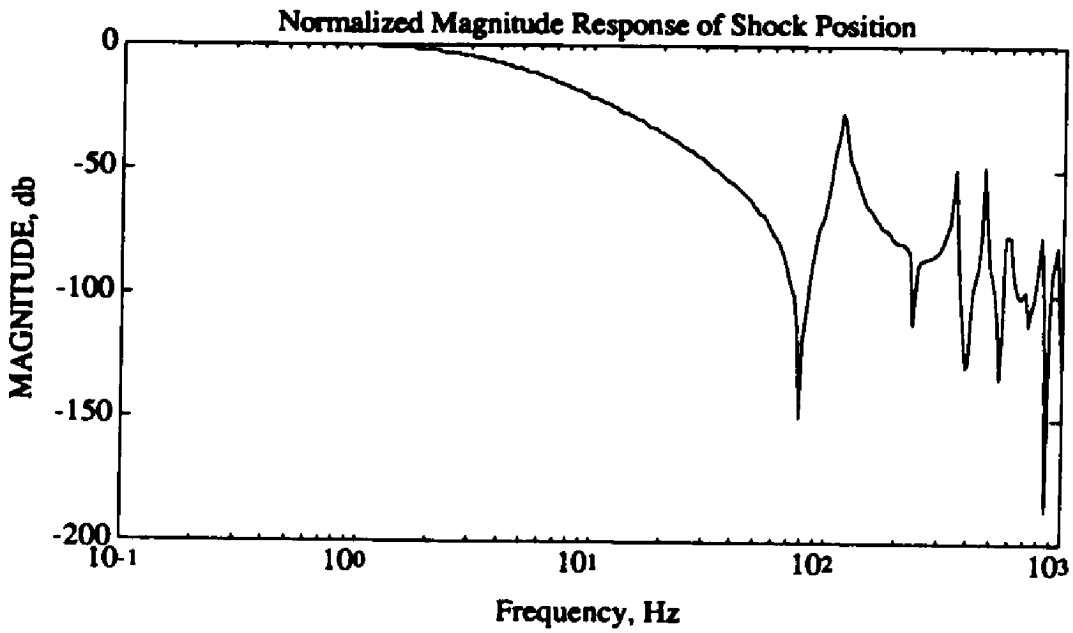
CASE	D-2
PROGRAM USED	**CONDITIONS**
D_three_wave_Green	u=586.23 r=0.0013492 c=1140.62 g2=1.4 ksi=0.9186 L=3.61 $Z_1(s) = \frac{1010}{s-300}$ $Z_2(s) = \frac{1010}{s-1010}$

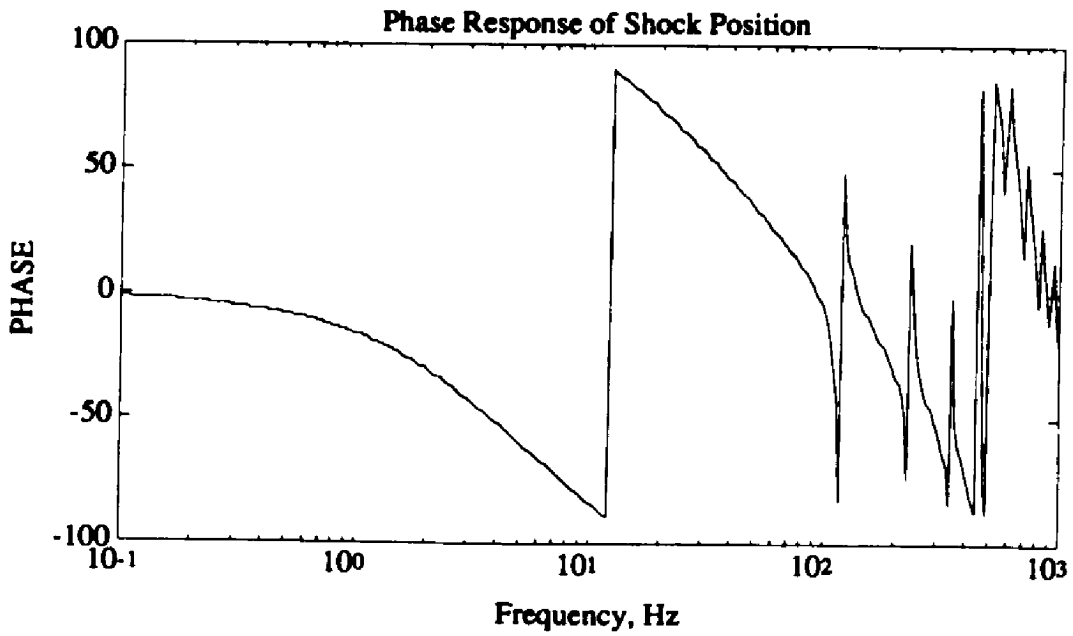
Reproduced with permission of the copyright owner. Further reproduction prohibited without permission.





Reproduced with permission of the copyright owner. Further reproduction prohibited without permission.

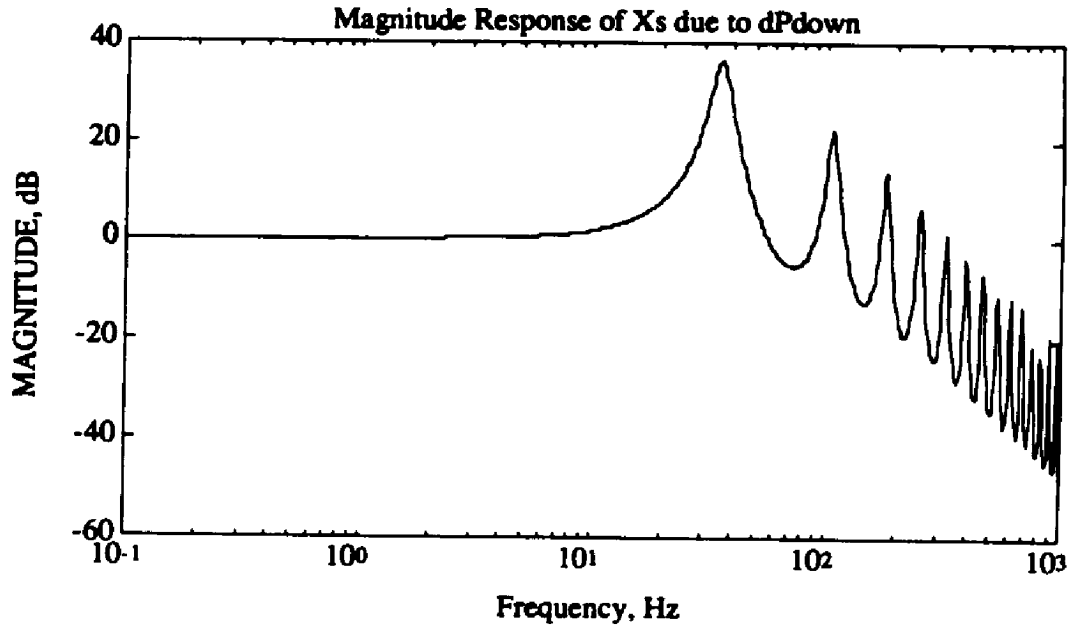


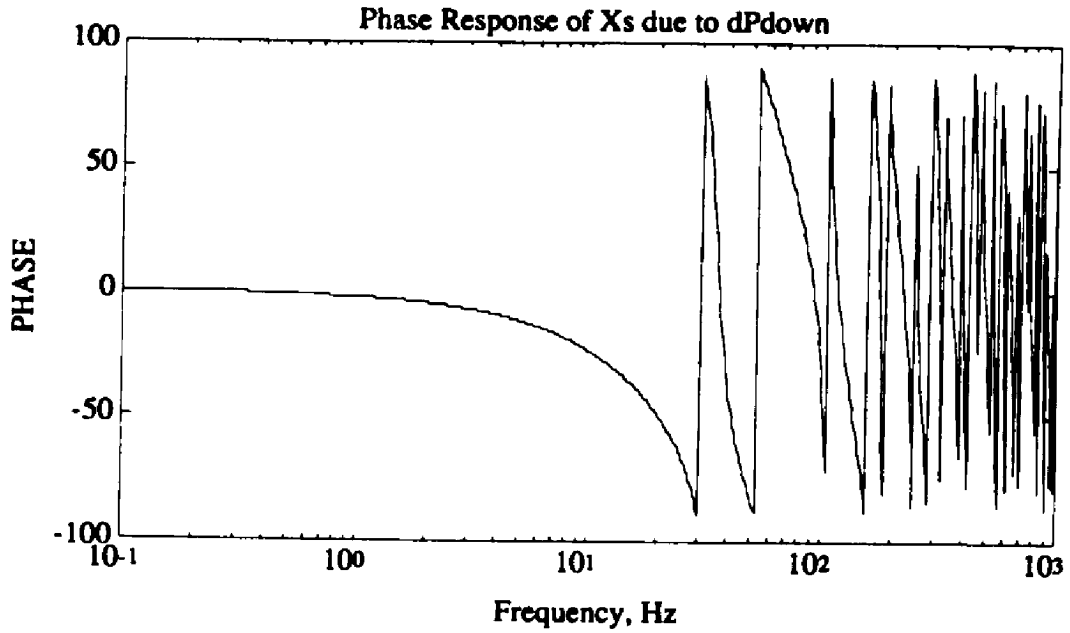


Reproduced with permission of the copyright owner. Further reproduction prohibited without permission.

CASE	E-1
PROGRAM USED	**CONDITIONS**
E-CW	L=5.8507 L1=3.1394 r1=6.5866e-4 ru1=0.9846 Energy1=1825.93 g1=1.4 u1=1554.45 c1=936.38 cT1=1170.99 Tt1=570.77 r2=1.3492e-4 ru2=0.7880 Energy2=3368.94 g2=1.4 u2=586.23 c2=1140.62 cT2=1170.71 Tt2=570.50 Fe1=-1 Fe2=7/6 Fe3=-1/6

Reproduced with permission of the copyright owner. Further reproduction prohibited without permission.



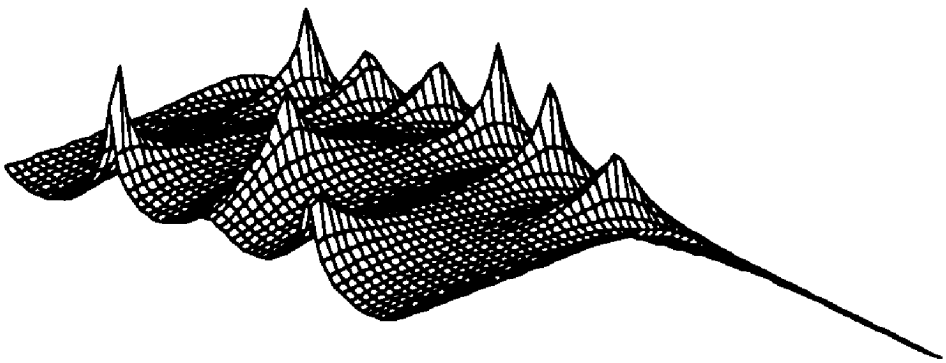


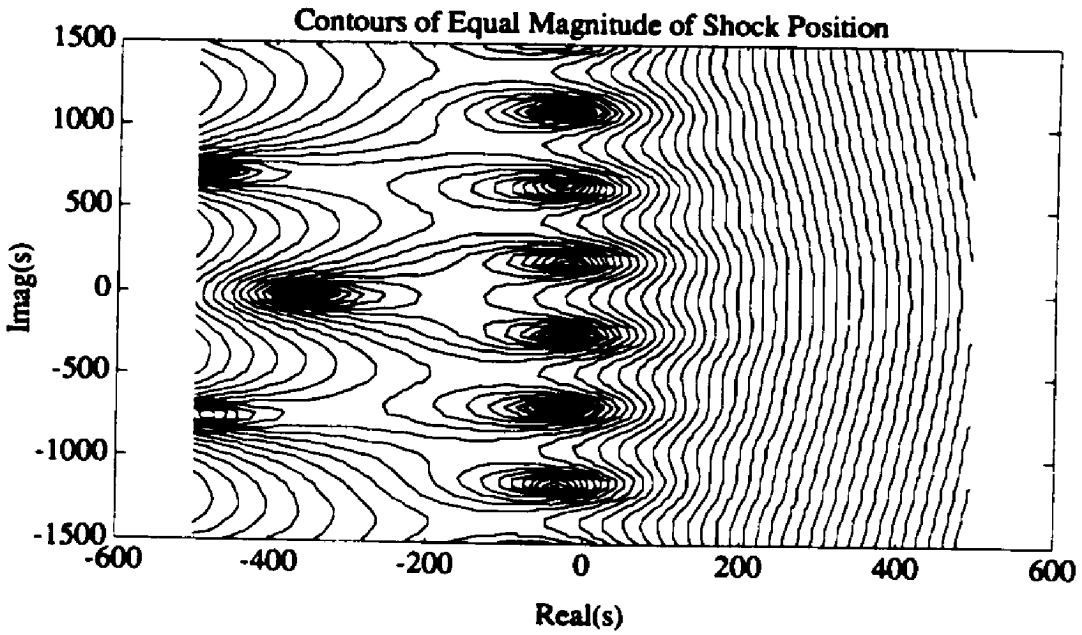
Reproduced with permission of the copyright owner. Further reproduction prohibited without permission.

CASE	E-2
PROGRAM USED	**CONDITIONS**
E_CW_mesh	L=5.8507 L1=3.1394 r1=6.5866e-4 ru1=0.9846 Energy1=1825.93 g1=1.4 u1=1554.45 c1=936.38 cT1=1170.99 Tt1=570.77 r2=1.3492e-4 ru2=0.7880 Energy2=3368.94 g2=1.4 u2=586.23 c2=1140.62 cT2=1170.71 Tt2=570.50 Fe1=-1 Fe2=7/6 Fe3=-1/6

Reproduced with permission of the copyright owner. Further reproduction prohibited without permission.

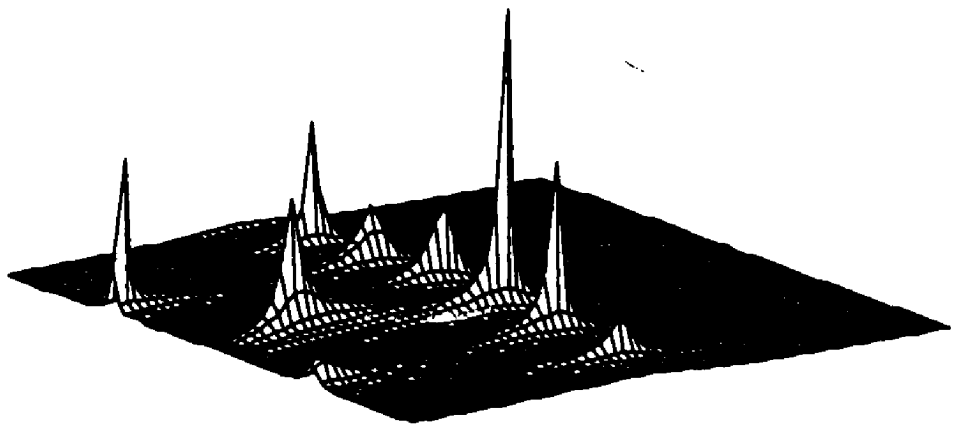
Mesh Plot of Shock Position

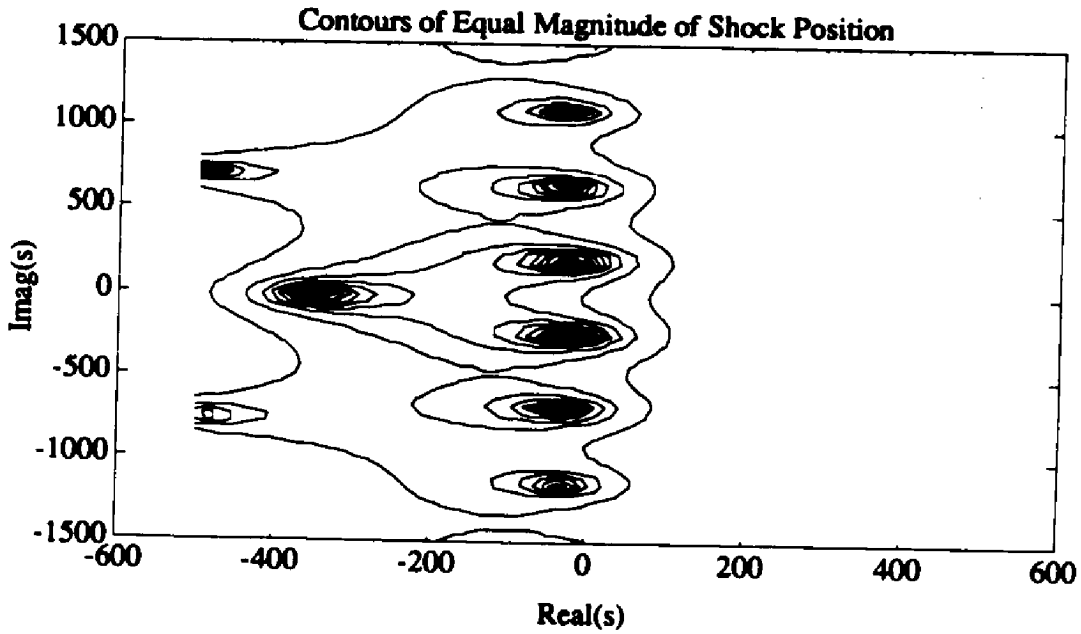




Reproduced with permission of the copyright owner. Further reproduction prohibited without permission.

Plain Log-Magnitude Mesh Plot of Shock Position





Reproduced with permission of the copyright owner. Further reproduction prohibited without permission.